



City Research Online

City, University of London Institutional Repository

Citation: Pinney, H. D. (1992). Modelling chromatic processes in human vision.
(Unpublished Doctoral thesis, City, University of London)

This is the accepted version of the paper.

This version of the publication may differ from the final published version.

Permanent repository link: <https://openaccess.city.ac.uk/id/eprint/29254/>

Link to published version:

Copyright: City Research Online aims to make research outputs of City, University of London available to a wider audience. Copyright and Moral Rights remain with the author(s) and/or copyright holders. URLs from City Research Online may be freely distributed and linked to.

Reuse: Copies of full items can be used for personal research or study, educational, or not-for-profit purposes without prior permission or charge. Provided that the authors, title and full bibliographic details are credited, a hyperlink and/or URL is given for the original metadata page and the content is not changed in any way.

MODELLING CHROMATIC PROCESSES IN HUMAN VISION

by

Huw David Pinney

Thesis submitted for the degree of
Doctor of Philosophy

to

THE CITY UNIVERSITY

Department of Optometry and Visual Science

September 1992

CONTENTS

	Page
LIST OF TABLES	5
LIST OF FIGURES	6
ACKNOWLEDGEMENTS	12
DECLARATION	13
ABSTRACT	14
CHAPTER 1. INTRODUCTION	15
1.1 General introduction	15
1.2 A review of the human visual system	16
1.2.1 The retina	16
1.2.2 Lateral geniculate nucleus	24
1.2.3 The visual cortex	25
1.3 Colour constancy	30
1.3.1 Models of colour constancy	32
1.3.2 Mechanisms of colour constancy	35
1.3.3 Quantitative studies of colour constancy	39
1.4 The pupil	45
1.4.1 The pupil light reflex	46
1.4.2 The near pupillary reflex	49
1.4.3 Pupillary responses to spatially structured stimuli	50
1.4.4 Pupillary responses to chromatic stimuli	51
1.4.5 Pupillary responses in amblyopia	56
CHAPTER 2. EQUIPMENT AND METHODS	64
2.1 Equipment used for colour constancy study	64
2.1.1 Display hardware	65
2.1.2 Monitor calibration	65

	Page
2.1.3 Reproduction of coloured samples	70
2.2 Equipment used in pupillometric study	71
2.2.1 Pupillometer hardware	71
2.2.2 Generation of visual stimuli	73
2.2.3 Pupillometer calibration & measurement accuracy	74
2.3 Measurement of increment thresholds during intense flashes of light	77
2.3.1 Equipment	77
2.3.2 Calibration of Maxwellian view system	79
2.3.3 Methods used in Maxwellian view experiments	84
 CHAPTER 3. A METHOD FOR THE QUANTITATIVE ASSESSMENT OF COLOUR CONSTANCY	 85
3.1 The effect of surround complexity and test target chromaticity on colour constancy	86
3.2 Spatio-temporal properties of colour constancy	93
3.3 Chromatic borders and colour constancy	100
3.4 The effect of scene saturation and chromaticity on colour constancy	102
3.5 The effect of object luminance on colour constancy	104
 CHAPTER 4. PUPILLOMETRIC STUDIES IN NORMAL AND AMBLYOPIC SUBJECTS	 109
4.1 Pupillary responses in normal subjects	109
4.1.1 The pupil light reflex	109
4.1.2 The pupil grating reflex	112
4.2 Pupillary responses in amblyopic subjects	115
4.3 Pupillary responses to chromatic stimuli	130
4.3.1 Preliminary experiments	130

	Page
4.3.2 Pupillary responses to chromatic gratings around isoluminance	133
4.3.3 The effect of chromatic contrast on pupillary responses	138
4.3.4 Pupillary responses to chromatic gratings, variation with spatial frequency	140
4.4 Measurements of accommodation for chromatic and achromatic stimuli	142
 CHAPTER 5. PSYCHOPHYSICAL AND PUPILLOMETRIC METHODS OF CHROMATIC DISCRIMINATION	 149
5.1 Psychophysical methods to determine chromatic discrimination thresholds	151
5.2 The chromatic pupil response and spatio-temporal luminance masking	158
 CHAPTER 6. SOME MEASUREMENTS ON THE CHANGES IN VISUAL SENSITIVITY CAUSED BY INTENSE FLASHES OF LIGHT	 161
 CHAPTER 7. SUMMARY AND CONCLUSIONS	 178
 APPENDIX. DESCRIPTION OF COLORIMETRIC TRANSFORMATIONS DEVELOPED FOR USE IN THE COLOUR CONSTANCY STUDY	 184
 REFERENCES AND BIBLIOGRAPHY	 189

LIST OF TABLES

	Page
1.1 Classification of primate ganglion cells.	21
2.1 Phosphor luminances and chromaticity co-ordinates for Mitsubishi monitor.	66
2.2 Variation of phosphor luminance with time.	69
2.3 Comparison of x,y chromaticity co-ordinates computed for Munsell samples with published data.	70
2.4 Channel retinal illuminances measured for Maxwellian view optical system.	80
3.1 Munsell chips used in Mondrian surround.	87
4.1 Clinical details of amblyopic subjects.	117
4.2 Isoluminant settings for a chromatic grating.	134
5.1 Best fit discrimination ellipse parameters.	154

LIST OF FIGURES

	Page or following page
1.1 Diagrammatic section through the human eye.	16
1.2 Transverse section through the retina.	16
1.3 Diagram of synaptic connections in the retina.	17
1.4 Absorbance spectra of cone and rod photopigments.	17
1.5 Receptor density in the human retina.	18
1.6 Cone flash response versus intensity curves.	18
1.7 Organisation of red-green opponent ganglion cell.	21
1.8 Action spectra of tonic ganglion cells.	21
1.9 The opponent model of colour vision.	23
1.10 The primate visual pathway.	24
1.11 Coronal section through the primate LGN.	24
1.12 Lateral view of the brain, and horizontal section through the prestriate cortex of the rhesus monkey.	25
1.13 The laminae and sublaminae of the striate cortex.	25
1.14 Ocular dominance columns, orientation columns and blob columns of the striate cortex.	26
1.15 Double opponent receptive field.	26
1.16 Functional segregation of primate visual system.	30
1.17 Chromaticity co-ordinates ($u'v'$) of a white paper under CIE Standard Illuminants D_{65} and A.	30
1.18 The pupil light reflex pathway.	46
1.19 The chromatic contrast sensitivity function.	54
2.1 Spectral power distributions for Mitsubishi monitor phosphors.	66
2.2 Relative spectral power distributions of CIE Standard Illuminants D_{65} and A.	66
2.3 Phosphor output for Mitsubishi monitor.	68
2.4 (A) Individual phosphor decay times.	69
(B) Decay times for combined output.	69
2.5 Munsell chip spectral reflectance functions.	70
2.6 Schematic drawing of P_SCAN 100 pupillometer.	71
2.7 Screen luminance versus look-up-table value.	71
2.8 Averaged trace recorded from artificial pupil.	75
2.9 Pupil response to low contrast grating stimuli.	75

	Page or following page
2.10 Extraction of pupil response parameters.	75
2.11 Schematic representation of Maxwellian system.	78
2.12 Calibration of filter wedge for (A) white light	81
(B) spectral light.	81
2.13 Rise and fall time of Uniblitz shutter.	82
2.14 Slider position signal versus displacement.	82
2.15 Slider velocity versus computer output voltage.	82
3.1 Definition of the C_{index} .	89
3.2 C_{index} versus test colour with Mondrian surround.	90
3.3 C_{index} versus test colour with uniform surround.	90
3.4 Averaged data for Mondrian and uniform surrounds.	92
3.5 Schematic diagram of stimulus configuration.	92
3.6 C_{index} as a function of surround duration.	96
3.7 C_{index} as a function of surround angular subtense:	
(A) viewing distance fixed;	96
(B) viewing distance varied.	96
3.8 C_{index} as a function of border angular subtense.	96
3.9 C_{index} as a function of test angular subtense:	
(A) viewing distance fixed;	96
(B) viewing distance varied.	96
3.10 Diagrammatic representation of surround configurations used in chromatic border experiment.	100
3.11 Results of chromatic border experiment.	100
3.12 C_{index} as a function of the white content of the surround.	103
3.13 C_{index} as a function of test luminance:	
(A) luminances from 6.3 - 50 cd/m ² ;	105
(B) luminances from 20 - 30 cd/m ² .	105
3.14 C_{index} as a function of test luminance for a green test target.	107
4.1 Pupil response amplitude versus luminance contrast.	110
4.2 Pupil response latency versus luminance contrast.	110

	Page or following page
4.3 (A) Pupil response amplitude as a function of the spatial frequency of an achromatic grating.	112
(B) Pupil response latency as a function of the spatial frequency of an achromatic grating.	112
(C) Contrast sensitivity for an achromatic grating plotted as a function of spatial frequency.	112
4.4 (A) Key to statistics table.	120
(B) Statistics of pupil light response data.	120
(C) Statistics of pupil grating response data.	120
4.5 Averaged pupil light reflex response amplitudes for amblyopic subgroups.	120
4.6 Typical pupil diameter traces: pupil light reflex.	120
4.7 Averaged pupil light reflex response amplitudes, comparison of amblyopes with normal group data.	120
4.8 Averaged pupil light reflex response latencies for amblyopic subgroups.	121
4.9 Pupil response amplitudes and latencies for selected strabismic amblyopes.	121
4.10 Pupil response amplitudes and latencies for selected anisometric amblyopes.	121
4.11 Averaged pupil grating response amplitudes for amblyopic subgroups.	122
4.12 Averaged pupil grating response amplitudes, comparison of amblyopes with normal group data.	122
4.13 Averaged pupil grating response latencies for amblyopic subgroups.	122
4.14 Averaged pupil grating response latencies, comparison of amblyopes with normal group data.	122
4.15 to 4.19 Psychophysical and pupillary deficits in amblyopia. Individual subject data.	123
4.20 Typical diameter traces: pupil grating reflex.	123
4.21 Averaged pre-stimulus pupil diameters.	124
4.22 Percentage pupil summation in amblyopes & normals.	124
4.23 Contrast sensitivity functions for 2 amblyopes.	127
4.24 Pupil grating response amplitude as a function of grating contrast and suprathreshold contrast.	127

	Page or following page
4.25 Contrast thresholds for detection of an isoluminant red-green grating.	131
4.26 Pupil diameter traces around isoluminance.	135
4.27 Pupil response latency versus green contrast.	135
4.28 Pupil responses for chromatic gratings presented in the periphery:	
(A) Response amplitude versus green contrast.	135
(B) Response latency versus green contrast.	135
4.29 Pupil diameter traces for achromatic gratings presented around isoluminance in a protanope:	
(A) 1 c/deg grating.	135
(B) 2 c/deg grating.	135
4.30 Pupil response versus chromatic contrast.	
(A) Amplitude.	139
(B) Latency.	139
4.31 Pupil response amplitude as a function of the spatial frequency of a chromatic grating.	
(A) Subject D.W..	140
(B) Subject M.K..	140
(C) Comparative data for an achromatic grating.	140
4.32 (A) Pupil response latency as a function of the spatial frequency of a chromatic grating.	141
(B) Comparative data for achromatic grating.	141
4.33 to 4.35 Pupil diameter traces and measurements of accommodation for achromatic gratings.	147
4.36 to 4.37 Pupil diameter traces and measurements of accommodation for uniform coloured targets.	147
4.38 Typical eye movements during attempted fixation.	147
5.1 Chromatic discrimination thresholds as a function of displacement angle.	153
5.2 The effect of random luminance modulation amplitude on chromatic discrimination in a normal trichromat.	153

	Page or following page
5.3 The effect of random luminance modulation amplitude on chromatic discrimination in	
(A) a deuteranope.	153
(B) a protanope.	153
(C) a tritanope.	153
5.4 Chromatic discrimination thresholds in anomalous trichromats.	
(A) a deuteranomalous subject.	153
(B) a protanomalous subject.	153
5.5 MacAdam's discrimination ellipses.	155
5.6 Chromatic discrimination in an amblyope.	155
5.7 Chromatic discrimination with and without an infra- red absorbing mirror, for 2 subjects (A) & (B).	158
5.8 Pupillary responses to a luminance-masked chromatic stimulus in a normal trichromat.	159
5.9 Pupillary responses to a luminance-masked chromatic stimulus in dichromats.	159
6.1 Representation of stimulus configuration employed in experiments using Maxwellian view.	163
6.2 Temporal profile of test and conditioning stimulus.	163
6.3 Test increment threshold versus onset asynchrony for a range of conditioning stimulus intensities	
(A) fovea	166
(B) periphery.	166
6.4 Comparison of fovea and periphery.	167
6.5 Test increment threshold versus eccentricity.	167
6.6 Test increment threshold versus onset asynchrony for a strabismic amblyope.	168
Test increment threshold versus onset asynchrony for a range of:	
6.7 conditioning stimulus durations	
(A) fovea	168
(B) periphery	168
6.8 conditioning stimulus diameters	
(A) fovea	169
(B) periphery.	169

6.9	Test increment threshold versus onset asynchrony for a range of background illuminance levels.	169
	Test increment threshold versus eccentricity with and without a conditioning stimulus for:	
6.10	foveal observations	169
6.11	observations made at an eccentricity of 6°.	169
6.12	Spectral sensitivity measurements for three values of stimulus onset asynchrony	
	(A) a normal trichromat	170
	(B) a protanope.	170
6.13	Late receptor potentials in the monkey retina.	174
6.14	Amacrine cell responses in the mudpuppy retina.	174
6.15	Ganglion cell responses in the cat retina.	174

ACKNOWLEDGEMENTS

I would like to thank my supervisor, Professor John Barbur, for the continual encouragement, advice and assistance that he has provided throughout this project.

I am grateful to the M.O.D. and R.A.R.D.E. for their financial support, and Dr. Ian Moorhead for his interest in the project.

Many people have given up much of their time to help me in the laboratory with experimental observations and technical difficulties. In particular I wish to thank Dr. David Thomson, Dr. Patrick Forsyth and Dr. Mairi Keenleyside with whom I have enjoyed many enthusiastic discussions. Thanks are also due to Mr. Alf Goodbody who taught me the art of electronics.

I would like to thank the following and acknowledge their help:

Dr. John Saunders for his advice and the loan of equipment for use in the colour constancy experiments;

Dr. Robert Hess for referring numerous amblyopes and for his helpful comments and suggestions relating to pupil function in amblyopia;

Dr. Vicki Barbur for helping with the statistical analysis of some of the data presented in Chapter 4.

Finally I am indebted to my parents, family and friends, all of whom have taken every opportunity to provide support and encouragement. I am particularly grateful to my wife, Helen, without whom none of this would have been possible.

DECLARATION

I grant powers of discretion to the University Librarian to allow this thesis to be copied in whole or in part without further reference to me. This permission covers only single copies made for study purposes, subject to normal conditions of acknowledgement.

ABSTRACT

This investigation programme has concentrated on a number of topics concerning visual function in humans, with particular emphasis on the processing of chromatic information.

The programme included an investigation of colour constancy which was carried out using a computer - controlled colour display. A new dynamic colour matching method was developed and the experimental conditions arranged so as to test the constancy of colour appearance. The technique makes possible the definition of an index of colour constancy which simplifies the interpretation of experimental results. Various spatial, temporal and chromatic parameters of the stimulus configuration were investigated and the results show the importance of the stimulus boundary and near surround in determining the magnitude of the constancy effects observed.

Pupillary function was investigated in normal and amblyopic observers. The results suggest that the pupil light reflex is essentially of normal amplitude in amblyopic eyes, although a latency anomaly does exist. Pupillary responses to achromatic, sinusoidal grating stimuli were anomalous in the affected eyes of many amblyopic subjects. Interestingly, certain response parameters were found to be anomalous in the normal eyes of amblyopic observers.

Pupillary responses in normal observers were measured following stimulation with isoluminant, red - green chromatic gratings. Responses were found to vary systematically with grating spatial frequency, and broadly reflect the way in which detection thresholds for the same stimuli vary with spatial frequency. Response latencies were approximately 80 ms longer than for equivalent responses to achromatic gratings. No responses were observed when the same experiments were carried out with a protanope.

Chromatic discrimination thresholds were measured using a spatio - temporal luminance masking technique. The technique is implemented on a carefully calibrated colour monitor and obviates the requirement of stimulus isoluminance. Preliminary experiments employing psychophysical and pupillometric procedures illustrate the use of the technique in the subjective and objective assessment of colour vision.

The rapid changes in visual sensitivity which occur following an intense flash of light were investigated by measuring increment thresholds for a small, brief test stimulus. Results are presented which show the dependence of the sensitivity changes on various spatial, temporal and chromatic parameters. An attempt is made to relate the experimental findings to the properties of retinal neurones.

CHAPTER 1

INTRODUCTION

1.1 GENERAL INTRODUCTION

The investigation of human vision, and the subsequent building of mathematical models of visual processes, not only aids our understanding of physiology, but also helps in the development of "machine vision" technology. Because of the obvious role of colour vision in artificial intelligence tasks, the modelling of chromatic processes, and more specifically, the modelling of colour constancy, has attracted a great deal of interest. The aim of the present study was to develop an experimental technique for quantifying colour constancy in human vision, and to use this technique to investigate how constancy changes with various stimulus parameters with a view to the assessment of some of the proposed models of colour constancy. Chapter 3 provides a description of the experiments undertaken, and the results of these experiments are discussed in relation to other findings in the literature.

Chromatic processes were investigated further by studying the response of the pupil to coloured stimuli. Chapter 4 recounts this investigation and also details experiments performed to determine the normality, or otherwise, of pupillary responses in a group of amblyopic subjects. The results of the experiments which employed chromatic stimuli suggested that pupillometric techniques were useful in the diagnosis of colour vision deficiency, but that generation of the appropriate stimulus could be difficult. In order to overcome the difficulties encountered, a new stimulus was developed and tested, and a preliminary report of the use of this type of stimulus in both psychophysical and pupillometric measurements is given in Chapter 5.

Whilst developing the equipment used in the colour constancy and pupillometry experiments outlined above, the opportunity arose to design and construct a Maxwellian view optical

system using components which were already available in the laboratory. A series of experiments were subsequently conducted to measure the spatial, temporal and chromatic properties of the threshold sensitivity changes which occur following exposure to intense flashes of light. Chapter 6 details the work undertaken.

The remaining sections of the present chapter examine briefly those stages of visual processing which are relevant to the experimental work carried out, and also provide a review of some of the pertinent literature published. The equipment, calibration procedures and experimental methods employed in each investigation are described in Chapter 2, though further information with respect to methodology is available in the relevant chapters. A summary of the principal results and conclusions of the work described in each of the experimental chapters (i.e., Chapters 3 - 6) is provided in Chapter 7.

1.2 A REVIEW OF THE HUMAN VISUAL SYSTEM

A horizontal section of the human eye is shown schematically in Figure 1.1. The gross anatomy of the eye is described in condensed form in many ophthalmic texts (e.g., Padgham and Saunders, 1975; Barlow and Mollon, 1982) but a more detailed account has been given by Wolff (1976). A detailed description of the neural pathways involved in the control of the pupil will be given later in this chapter and is therefore not discussed here. The optical components of the eye, namely the cornea, aqueous, lens, and vitreous, allow the image of an external object to be brought to focus on the retina, and it is here that the first stages of neural processing occur.

1.2.1 THE RETINA

The retina is a highly complex nervous structure composed of ten layers (Polyak, 1941) arranged as shown in Figure 1.2. In general, the retinal receptors, the rods and cones,

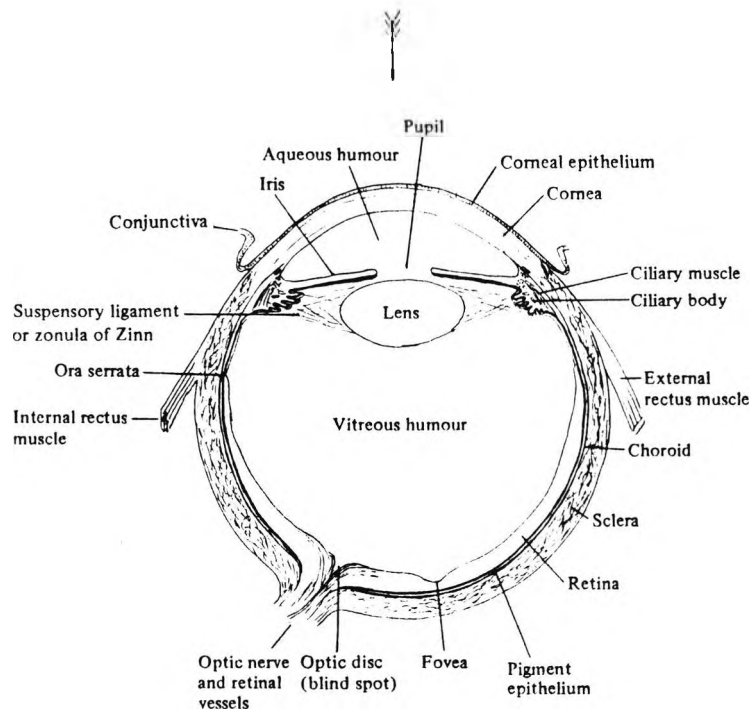


Figure 1.1. Diagrammatic section through the human eye (from Barlow and Mollon, 1982).

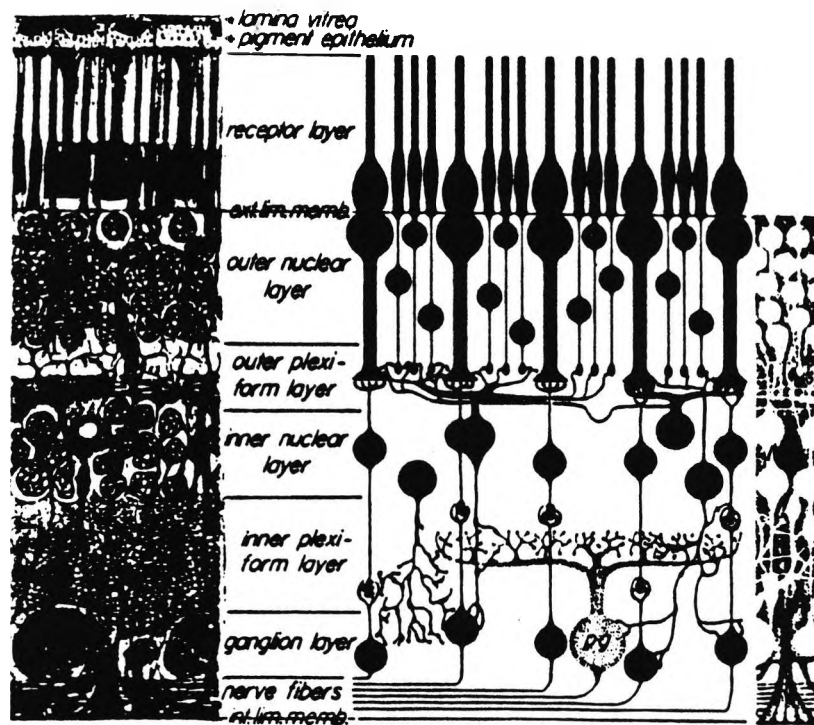


Figure 1.2. Transverse section through the retina (from Polyak, 1957).

synapse with the bipolar cells which in turn synapse with the ganglion cells. This vertical organisation is augmented by the numerous lateral interconnections of the horizontal cells and amacrine cells. A summary diagram illustrating some of the synaptic connections involved is shown in Figure 1.3. Comprehensive reviews of retinal anatomy may be found in several classical texts (e.g., Polyak, 1941; Dowling and Boycott, 1966; Boycott and Dowling, 1969) and will not be reproduced in this chapter.

There are three types of cone photoreceptor in the normal human retina, each type containing a different photosensitive pigment which is maximally sensitive in a specific part of the spectrum. The three cone types have been traditionally designated blue (B), green (G) and red (R) based upon their respective absorbance spectra, although Mollon (1982) has argued that a less misleading designation would be short - wavelength (S), middle - wavelength (M), and long wavelength (L). The interaction between the visual pigment and light, which occurs in the outer segment of the receptor, initiates the first stage in the visual process and involves the generation of an electrical potential. Several different techniques have been employed to measure cone and rod spectral sensitivities, including psychophysics (Vos and Walraven, 1971; Smith and Pokorny, 1975; Stiles, 1978) and, more recently, electrophysiology (Baylor et al., 1987; Schnapf et al., 1987). Similarly, microspectrophotometry has been used to measure directly the absorbance spectrum of individual photoreceptors (Brown and Wald, 1964; Bowmaker et al., 1980; Dartnall et al., 1983). The different methods are in good agreement over much of the spectrum though there are some discrepancies at short wavelengths (see Mollon, 1982; Lennie and D'Zmura, 1988). The absorbance spectra obtained from microspectrophotometric measurements are shown for the three types of cone in Figure 1.4, together with similar data for the rods. These data show that the peak sensitivity for the B cones occurs at approximately 420 nm, though due to the absorption characteristics of the crystalline lens (see Wyszecki and Stiles, 1982) this peak shifts to approximately

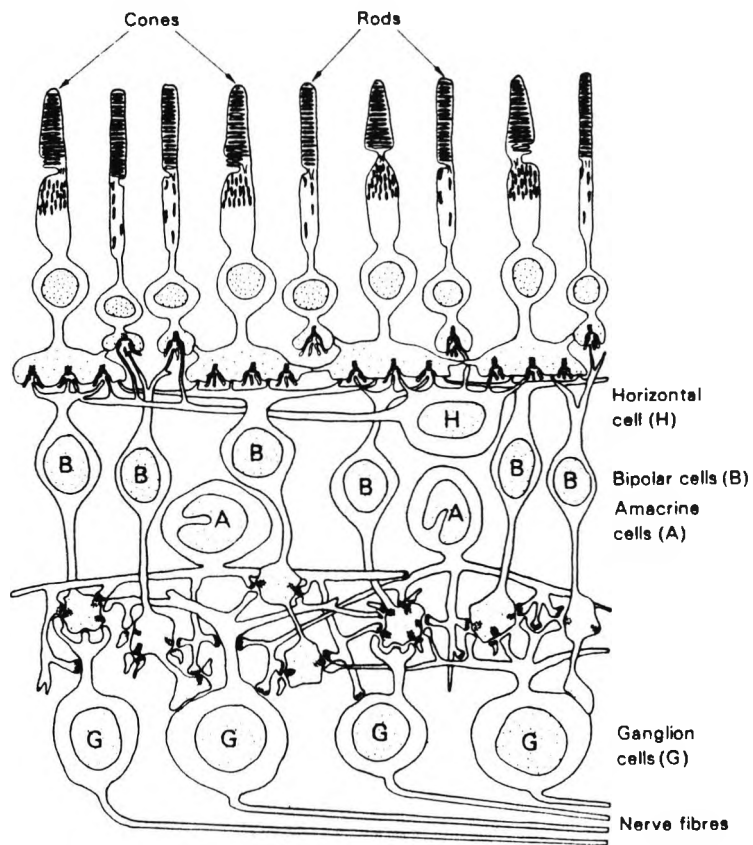


Figure 1.3. A summary diagram showing the synaptic connections in the retina (after Dowling and Boycott, 1966).

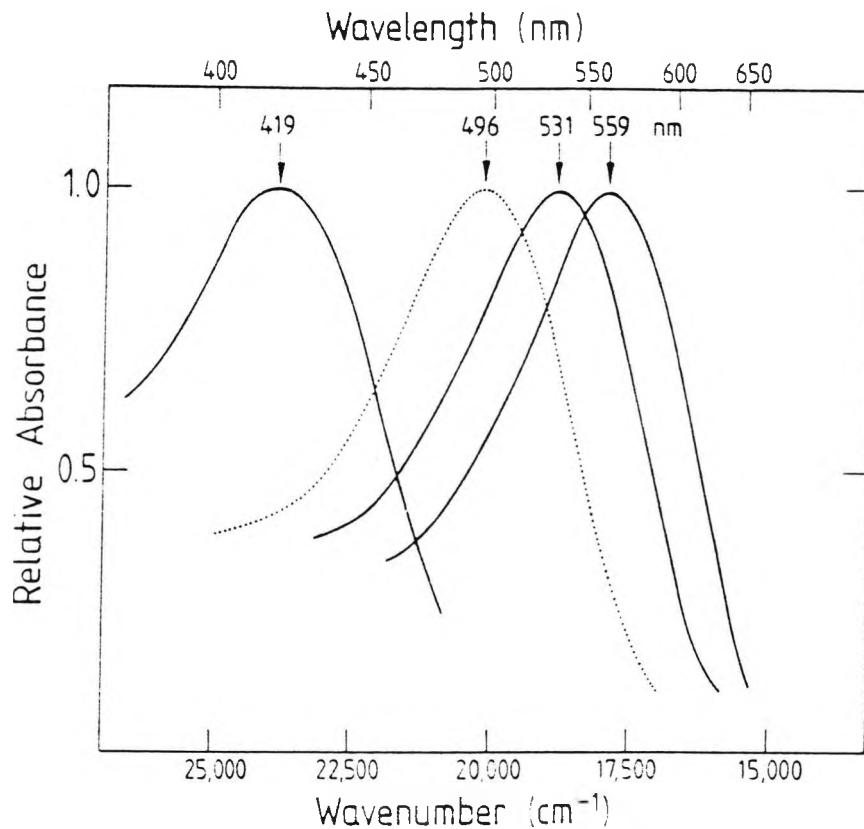


Figure 1.4. Absorbance spectra of the four photopigments of the normal human retina; solid curves are for the three cone types, dotted curve is for rods (from Mollon, 1982).

440 nm when measurements are made in terms of the radiance incident at the cornea. The rods function under low (scotopic) levels of illumination, whereas cones function at medium to high (photopic) levels of illumination usually greater than about 10 cd/m².

Isolated cones, when stimulated by small spots of light (i.e., less than about 100 μm in diameter), obey the "principle of univariance" in that their electrical responses vary only with the number of quanta absorbed. This means that a single cone mechanism is unable to distinguish between changes in quantum catch that arise from changes in light intensity, and those that arise from a change in the spectral composition of the light (Brindley, 1957, but see also Naka and Rushton, 1966). Only by a comparison of the rates of absorption in the three different classes of cone is the visual system able to discriminate between different parts of the spectrum. In fact, the concept of a trichromatic visual system was first clearly formulated by Young (1802), whose work on colour matching experiments was later supported by Helmholtz (1867). Whilst the principle of univariance holds for isolated receptors and small diameter stimuli, it is known that when larger diameter stimuli are used, spectral univariance breaks down due to coupling between cones (Fuortes et al., 1973; Baylor and Hodgkin, 1973).

There are approximately 4 - 7 million cones and 110 - 125 million rods in the human retina (Østerberg, 1935; Polyak, 1941). The cones are most heavily concentrated at the fovea (see Figure 1.5) where they are tightly packed together and are narrower and more elongated than elsewhere in the retina. Many of the retinal layers immediately in front of the foveal cones have a reduced representation to allow maximum light transmission. The ratio of foveal cones to ganglion cells is about 1, indicating that individual ganglion cells in this region are connected to a single cone (Polyak, 1941; Missotten, 1974; Perry and Cowey, 1985). The very centre of the fovea, the foveola, contains no rods and extends over a visual angle of approximately 1° (see Padgham

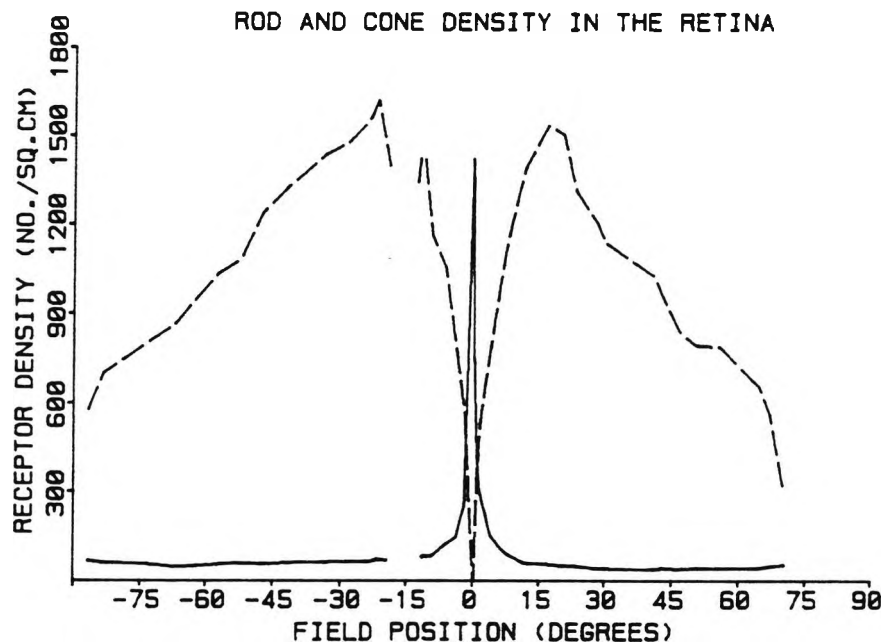


Figure 1.5. Receptor density as a function of eccentricity in the human retina. The solid line relates to the cone receptors whilst the broken line relates to rod receptors. (After østerberg, 1935).

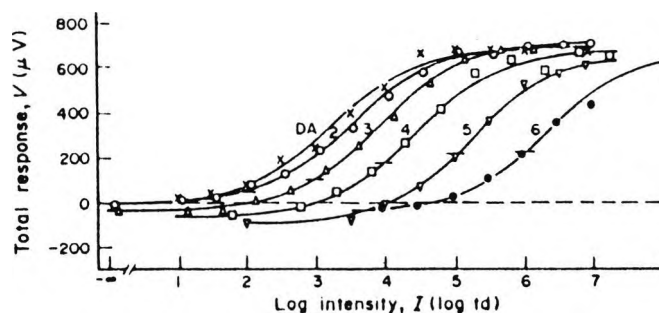


Figure 1.6. Cone flash response versus intensity curves in the presence of adapting background illumination. The background light intensity is indicated by the numbers next to the curves; DA is dark adapted. The small horizontal line in each curve represents the background response level. (After Valeton and van Norren, 1983).

and Saunders, 1975). Taken together, these properties explain the high spatial resolving power demonstrated by the fovea. R and G cones are found in the approximate ratio of 2 : 1, though B cones are known to be much rarer and are completely absent from the central 20 - 30', their frequency being greatest at an eccentricity of about 1°, where they account for approximately 16% of cones (see Mollon, 1982; Lennie, 1984).

Perry and Cowey (1985) have estimated that the number of ganglion cells in the primate retina is between 1.4 and 1.8 million. Since the axons of the ganglion cells form the optic nerve, then it is apparent that the information transmitted by the 120 or so million photoreceptors has been compressed by pre - ganglionic retinal mechanisms before it leaves the eye in the optic nerve. One mechanism that is partly responsible for this signal compression operates in the cones and is referred to as light adaptation. Although human vision is known to operate over a range of illumination levels of about $10^8:1$, the response range of the optic nerve fibres is only about 100:1. Light adaptation allows the operating range of the visual system to move with the level of ambient illumination and also to change its sensitivity such that as the level of illumination is raised, changes in illumination have to be progressively larger in order to be detectable (Valeton and van Norren, 1983). The response versus intensity curves shown in Figure 1.6 illustrate how cone sensitivity is maximised by adjustment of operating range for various background illumination levels.

The area of the retina over which a stimulus may evoke a response from a ganglion cell (or for that matter any cell at any level within in the visual pathway) is termed the receptive field, and physiological studies have basically involved the investigation of receptive field properties. Many of the pioneering studies in electrophysiology were carried out by Hartline using the invertebrate eye (e.g., Hartline, 1940), but it was Kuffler (1953) who gave the first systematic description of the receptive fields of

ganglion cells in the cat's retina. He found that they had a circular, centre - surround organisation, where the responses produced by stimulating the centre and surround were opposed such that stimulation of the centre excited the cell whilst stimulation of the surround inhibited the cell, or vice versa. Kuffler consequently designated these cells "on - centre" and "off - centre" cells. Following Kuffler's early classification of cat retinal ganglion cells, Enroth - Cugell and Robson (1966) proposed that ganglion cells in the cat could be subdivided into a further two groups on the basis of linearity of spatial summation: X - cells showing linear, and Y - cells showing non - linear, spatial summation. X - cells were found to respond best to fine spatial detail, whilst Y - cells were most responsive to coarse patterns and abrupt changes in diffuse illumination. Cleland et al. (1971; 1973) later offered another classification which was based on the time - course of response: cells were designated "sustained" and "transient" and were probably equivalent to X - and Y - cells respectively (although, as Lennie (1980) points out, this classification emphasises aspects of response that do not always distinguish X - cells from Y - cells).

Gouras (1968) identified two functionally distinct types of retinal ganglion cell in the macaque, namely the "tonic" and "phasic" ganglion cells. Both types of ganglion cell usually showed concentric, centre - surround receptive field organisation, but the receptive fields of tonic cells showed strong chromatic opponency (i.e., centre and surround had different spectral sensitivities), whereas those of phasic cells did not. Tonic cells were found to be much more numerous than phasic cells and to possess various arrangements and degrees of chromatic opponency (see Table 1.1 on following page).

Figure 1.7 shows a simplified schematic diagram of the likely retinal circuitry, receptive field structure, and responses of a red - green colour opponent cell. Red light projected on to the receptive field (RF) stimulates the R cones in the centre which subsequently causes excitation of

Type	Centre	Surround	Cone Opponency	Percent
Tonic	R on	G off	strong	8
Tonic	G on	R off	strong	6
Tonic	R off	G on	strong	1
Tonic	G off	R on	strong	1
Tonic	R on	G off	weak	15
Tonic	G on	R off	weak	9
Tonic	R off	G on	weak	7
Tonic	G off	R on	weak	6
Tonic	on		none	7
Tonic	off		none	4
Phasic	on		none	16
Phasic	off		none	10
Tonic	B on	Y off	strong	6
Unclassifiable				4

Table 1.1. Classification of primate ganglion cells
(after Gouras and Zrenner, 1982).

the ganglion cell (GC) via interneurons (IN_1), resulting in a tonic (i.e., sustained) increase in the cell's rate of discharge. Similarly green light stimulates the G cones in the surround which inhibit the ganglion cell through interneurons IN_2 and IN_3 (possibly horizontal and bipolar cells) causing a tonic period of inhibition in the ganglion cell response. Yellow light causes equal stimulation of centre and surround such that excitation and inhibition approximately cancel each other. Spectral sensitivity functions of the various types of tonic ganglion cell are shown in Figure 1.8 where the open symbols represent excitation, and the closed symbols represent inhibition. The broken lines in the upper diagram represent data generated by a linear subtraction of the R and G cone spectral sensitivity functions (see Figure 1.4), whilst the broken lines in the centre diagram describe a linear subtraction of the B cone function and an additive combination of the R and G cone functions. These latter type of ganglion cells, i.e., the blue - yellow opponent cells, have larger receptive field sizes and longer response latencies than the red - green opponent cells. The spectral sensitivity of the non - opponent phasic cell is similar to that shown for the non - antagonistic tonic cell, and resembles the photopic

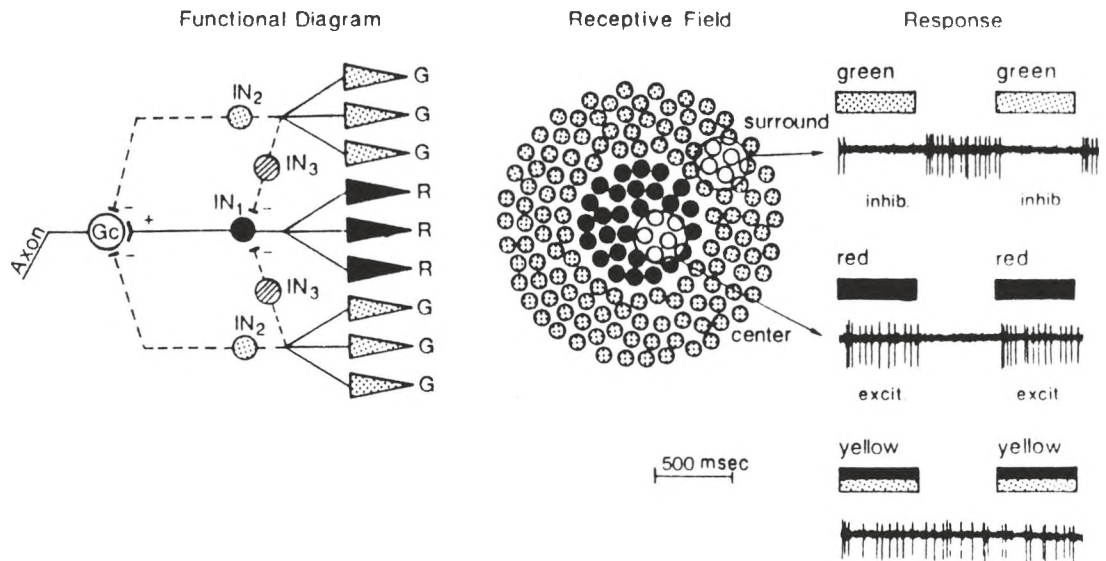


Figure 1.7. Schematic diagram of the organization and function of a red - green colour opponent ganglion cell (from Zrenner, 1983). See text for description.

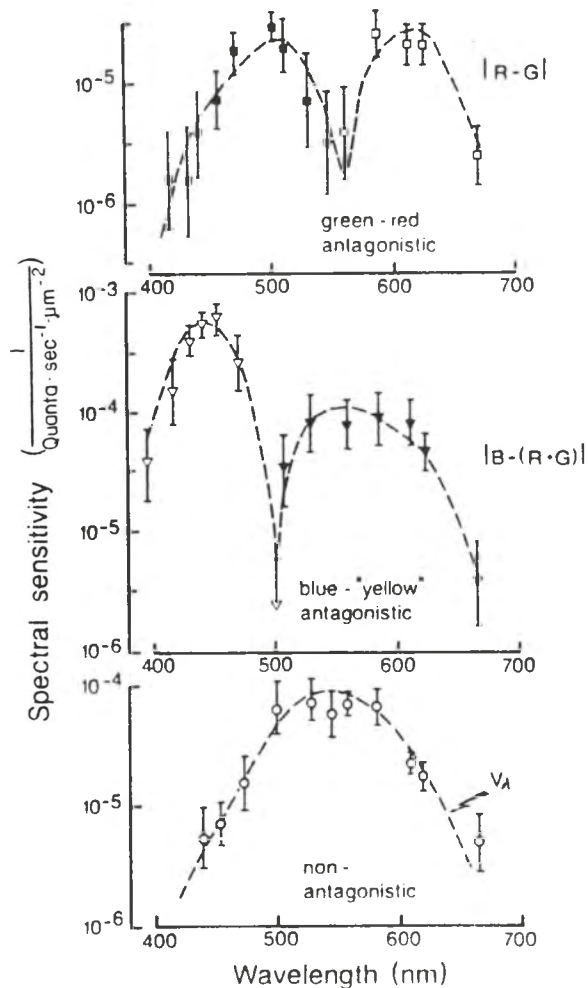


Figure 1.8. Action spectra of red-green opponent, blue-yellow opponent and non-antagonistic tonic ganglion cells. Open and closed symbols indicate thresholds of excitatory and inhibitory responses respectively. (From Zrenner, 1983).

luminosity ($V - \lambda$) function (the broken curve in the lower diagram of Figure 1.8). This latter type of non-opponent ganglion cell, which is more abundant in the retinal periphery, responds to luminance changes of any wavelength with a short, monotonic transient discharge and probably functions in the detection of changes in illumination level (Zrenner, 1983). Studies have shown that phasic cells possess larger receptive fields than tonic cells (de Monasterio and Gouras, 1975), and that the axons of phasic cells conduct impulses at a higher velocity than those of tonic cells (Schiller and Malpelli, 1977). Whilst in the present review, ganglion cells have been referred to as "tonic" and "phasic", it should be emphasized that there is, as yet, no universally accepted terminology or classification for ganglion cells. de Monasterio (1978), for example, confirmed that the responses of colour opponent ganglion cells are more sustained than non-opponent cells, but proposed that a more reliable distinction can be made on the basis of linearity of spatial summation, colour opponent cells being X-like, and non-opponent cells being Y-like. Shapley and Perry (1986) have presented evidence which suggests, however, that primate non-opponent ganglion cells are functionally similar to cat X-cells, whereas the chromatically opponent cells are functionally different from cat X-cells and probably represent a primate specialisation for colour vision. Lennie (1980) provides a detailed review of the various terminologies and classifications which have been used in the literature.

In summary, therefore, it appears that higher primates have two principal types of ganglion cell which are chromatically opponent, namely red-green and blue-yellow ganglion cells, and a third type of cell which is non-opponent. In fact as early as 1878, Hering had predicted that colour vision was mediated by mechanisms which were similar to those later demonstrated for ganglion cells in physiological experiments. Hering's opponent theory was partly based upon the observation that certain hues (blue, green, yellow and red) are unique and cannot coexist, for example, one can perceive a colour that is reddish-yellow or greenish-

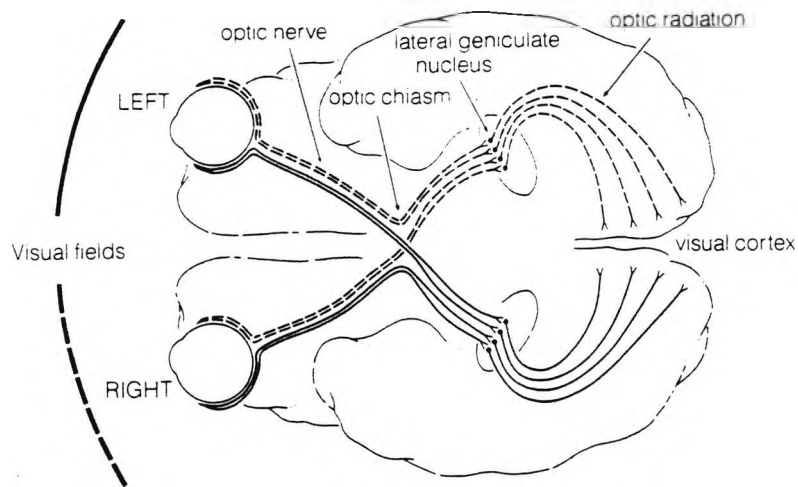


Figure 1.10. The primate visual pathway viewed from the underside of the brain (from Dowling, 1987).

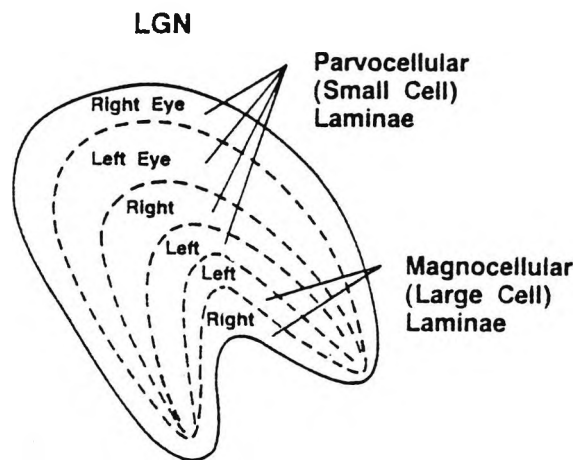


Figure 1.11. Diagram of a coronal section through the LGN in the left hemisphere of a primate. (From Lennie and D'Zmura, 1988).

yellow, but not one that is reddish - green. Hering's early work was later substantiated by a great deal of psychophysical experimentation (see Hurvich and Jameson, 1957) which also pointed towards the existence of two principal chromatically opponent mechanisms, and a single achromatic mechanism which receives a combined input from R, G and B cones (see Figure 1.9 below). The input from B cones, however, is too small to have much influence on the overall sensitivity of the achromatic mechanism. Because the spectral sensitivity curves of the different cones overlap considerably (see Figure 1.4), then the signals that they transmit will be highly correlated. Post - receptor processing, therefore, provides a means by which information from the photoreceptors is transformed to produce uncorrelated signals which are then transmitted through the optic nerve.

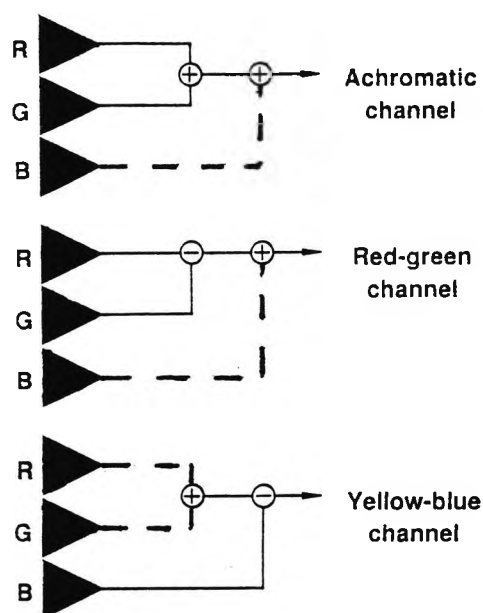


Figure 1.9. The opponent model of colour vision. Dashed lines indicate variable or uncertain input. (After Hurvich and Jameson, 1955).

Anatomical studies using the enzyme horseradish peroxidase have identified four morphologically distinct types of retinal ganglion cell in the macaque (Perry et al., 1984).

Only two of these, constituting some 90% of the total number of ganglion cells, project to the lateral geniculate nucleus (see below): P α (primate alpha) cells have larger cell bodies and dendritic fields than P β (primate beta) cells, but in both the dendritic tree is profusely branched. P α cells represent approximately 10%, and P β cells approximately 80%, of the ganglion cell population. The present consensus is that the P β cells correspond to the chromatically opponent ganglion cells identified by physiologists, whilst the P α cells correspond to the non-opponent cells (Lennie and D'Zmura, 1988).

1.2.2 THE LATERAL GENICULATE NUCLEUS

The ganglion cell axons leave the eye in the optic nerve and pass into the cranial cavity where the optic nerves from the two eyes meet at the optic chiasm (see Figure 1.10). A partial decussation of nerve fibres occurs at the chiasm whereby fibres from each nasal hemiretina cross over and pass into the contralateral optic tract, whilst fibres from each temporal hemiretina do not cross and pass into the ipsilateral optic tract. The majority of the optic tract fibres (approximately 90%) synapse in the lateral geniculate nucleus (LGN). In the primate, the LGN is a six-layered structure in which each layer receives projections alternately from ipsilateral and contralateral eyes (Figure 1.11). The four dorsal (parvocellular) laminae are made up of small cells and receive projections from P β ganglion cells, whilst the two ventral (magnocellular) laminae contain larger cells which receive projections from P α ganglion cells (Perry et al., 1984). There is a topographic representation of the visual field in each layer of the LGN such that each hemiretina is mapped three times onto each geniculate nucleus. Perry and Cowey (1985) have found that the fovea has a relatively greater representation in the LGN than the peripheral retina.

The functional characteristics of the colour opponent and non-opponent ganglion cells are maintained in the "parvo" and "magno" divisions of the LGN respectively.

Physiologically, the two divisions have been shown to differ in terms of colour processing, contrast sensitivity, and both spatial and temporal resolution (see Livingstone and Hubel, 1988). Thus, about 90% of the cells in the parvocellular layers have chromatically opponent receptive fields and are therefore sensitive to differences in wavelength; at a given eccentricity, magno cells have receptive fields which are 2 - 3 times larger than parvo cells; magno cells respond faster and more transiently than parvo cells; magno cells are much more sensitive than parvo cells to low - contrast stimuli, though parvo cell responses saturate at much higher contrasts.

Superficially, the magno system would appear to form the physiological basis of the putative achromatic pathway, and the parvo system that of the chromatic pathway. It is unlikely, however, that such a complete segregation of the two pathways exists at the level of the LGN. For example, the relatively large receptive field sizes of the cells in the magno system cannot support the high level of visual acuity normally associated with the achromatic system (Lennie, 1984; Lennie and D'Zmura, 1988). In an attempt to explain this, Ingling and Martinez - Uriegas (1983) have proposed that the red - green opponent cells signal chromatic contrast in stimuli of low spatial frequency, and luminance contrast in stimuli containing high spatial frequencies. In general, evidence suggests that the parvo system can carry a combination of chromatic and achromatic information, the relative strength of which depends upon the size and frequency (both spatial and temporal) of the stimulus in question.

1.2.3 THE VISUAL CORTEX

Fibres leave the LGN in the optic radiations which project to the striate cortex (visual area V1). The cortex is a highly convoluted, thin and layered sheet of tissue, the surface area of which is much greater than its thickness (Figure 1.12). By convention, the cortex is divided into six layers, with layer 1 being the outermost, and layer 6 the

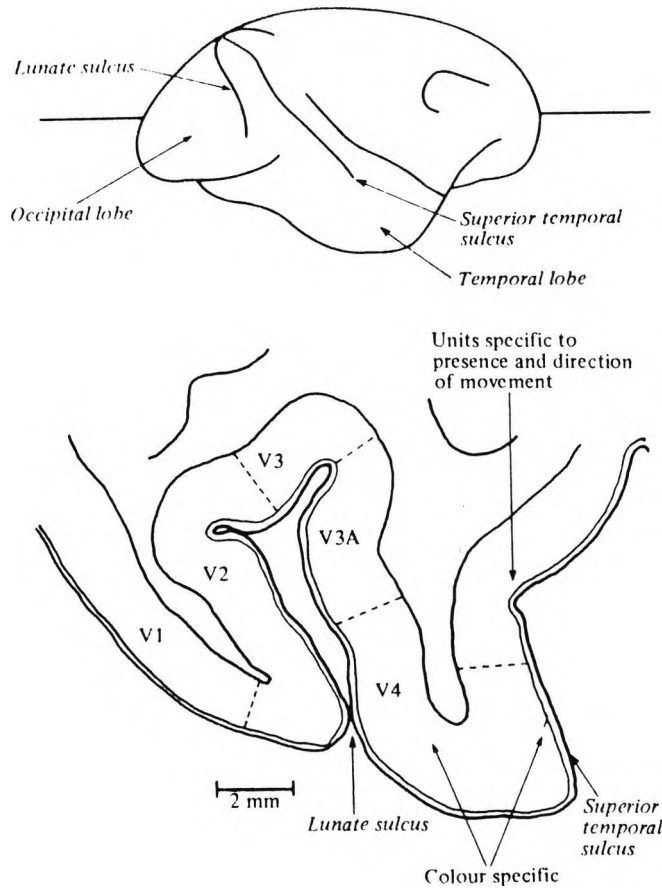


Figure 1.12. Upper diagram: lateral view of the brain of the rhesus monkey. Lower diagram: horizontal section through the prestriate cortex made at the level of the horizontal line shown in the upper diagram. (After Zeki, 1977).

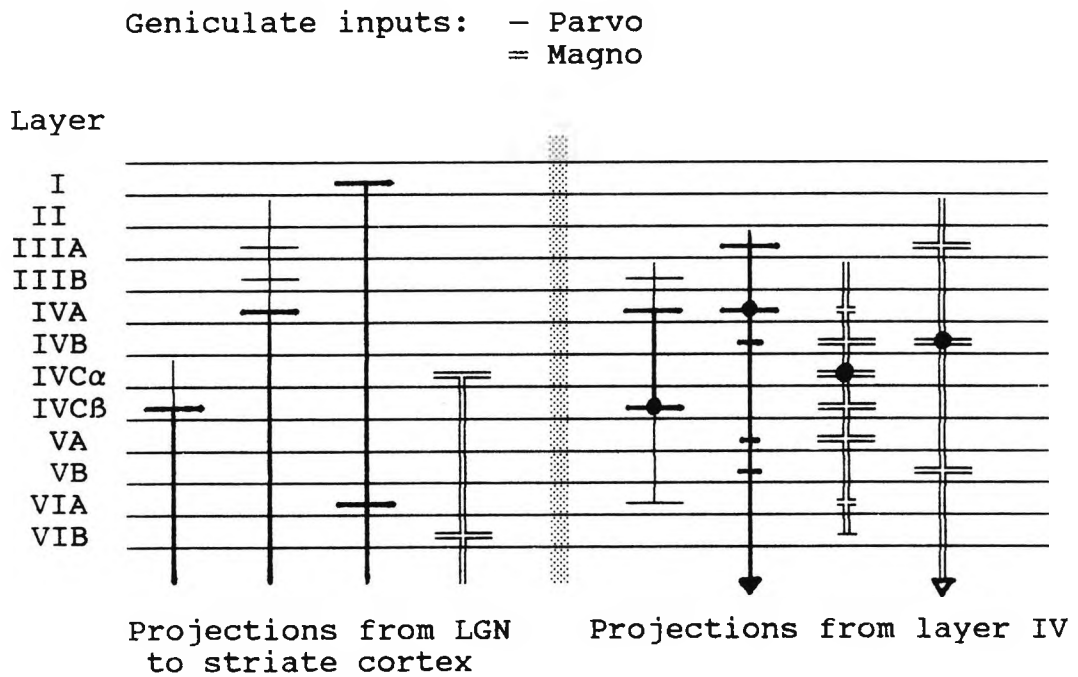


Figure 1.13. Representation of the laminae comprising the striate cortex showing the central projections of the magnocellular and parvocellular systems. (After Lennie and D'Zmura, 1988).

innermost. A schematic diagram of the various laminae and sublaminae of the striate cortex is shown, together with magno and parvo projections, in Figure 1.13. The segregation of the magno and parvo systems seen in the LGN is maintained in the primary visual cortex in that magnocellular neurones project almost exclusively to layer IVC α , whilst the majority of cells in the parvocellular geniculate project to layers IVC β and IVA. As in the LGN, the topographic representation of the retina on the striate cortex is non-uniform with much more area being devoted to central than peripheral retina (Daniel and Whitteridge, 1961). This overrepresentation of the central visual field arises partly in the retino-geniculate projection, and partly in the geniculo-cortical projection (Perry and Cowey, 1984). In addition to being organised on the basis of receptive field position, striate cells are also grouped according to eye dominance and receptive field orientation (Hubel and Wiesel, 1968). For both of the latter groupings, cells are arranged to form vertical slabs or "columns" which run perpendicular to the cortical surface (see Figure 1.14). Whilst cells in the retina and LGN (and for that matter in layer IVC of the striate cortex) respond best to spots of light and usually have concentric, centre-surround receptive fields, cortical cells in layers II, III, V, and VI were found to respond best to specifically orientated slits, bars, or edges of light. On the basis of their receptive field properties, three distinct types of cell were identified in the cat (Hubel and Wiesel, 1962) and monkey (Hubel and Wiesel, 1968), and were designated simple, complex and hypercomplex. Simple cells showed linear receptive fields with excitatory and inhibitory regions. Receptive fields of both simple and complex cells were orientation selective, but complex cells (which were found to be the most common cell type in the monkey) differed from simple cells in that their responses could not be predicted from a receptive field map made with circular spot stimuli. Receptive fields of complex cells, were also larger than those of simple cells. Hypercomplex (or end-stopped) cells had more complicated receptive fields than either simple or complex cells, and showed "end inhibition" whereby a stimulus longer

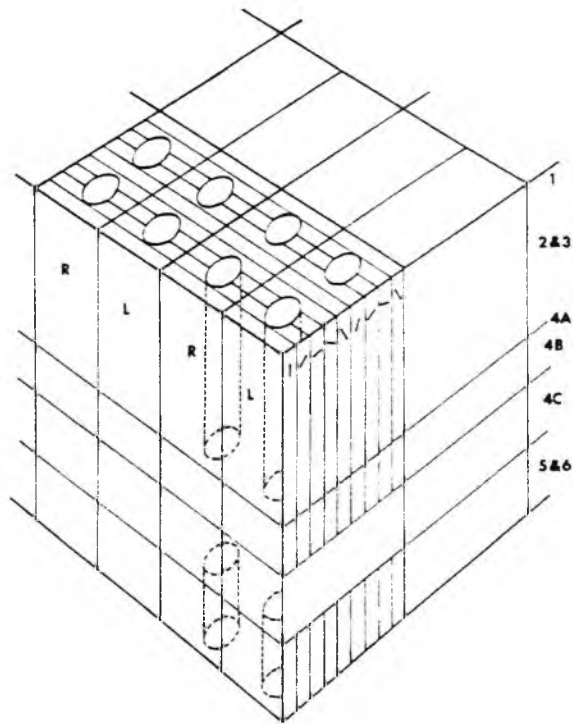


Figure 1.14. Diagrammatic representation of the striate cortex showing the relationship between the ocular dominance columns, orientation columns, and blob columns. (After Hubel and Livingstone, 1982).

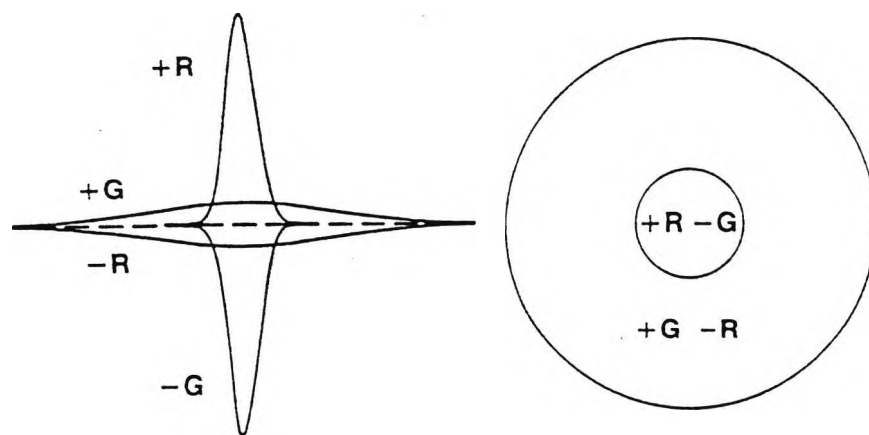


Figure 1.15. Schematic representation of a double opponent receptive field. The sensitivity profile is shown on the left, and a traditional receptive field map is drawn on the right. (After Lennie and D'Zmura, 1988).

than optimal evoked a reduced response. Since these early experiments of Hubel and Wiesel in the 1960's, advances in staining and recording techniques have allowed researchers to develop a more complete understanding of cortical structure and function. Some of the more recent advances are summarised in the following paragraphs.

All Neurones in layer IVC α have receptive fields which display orientation and sometimes direction, selectivity (Blasdel and Fitzpatrick, 1984; Livingstone and Hubel, 1984; Michael, 1985) but lack chromatic opponency (Lennie et al., 1985). Like the magnocellular neurones of the LGN, the neurones in this layer have high achromatic contrast sensitivities but relatively poor spatial resolution. The receptive fields of the cells in layer IVC β are concentrically organised but most, unlike the majority of cortical cells, are not orientation selective. Both colour opponent and non - opponent cells have been identified in this layer, though the relative number of each is uncertain (Blasdel and Fitzpatrick, 1984; Livingstone and Hubel, 1984; Michael, 1985). Livingstone and Hubel (1984) have found that all of the colour opponent cells have centre - surround receptive fields, whereas Michael (1985) reports that most have double - opponent receptive fields (see later). The general consensus with regard to this layer is that the chromatic and achromatic information carried in the parvocellular system becomes segregated and thus, some neurones are sensitive only to chromatic modulation, have low pass spatial characteristics and show no orientation selectivity, whilst others are most sensitive to achromatic modulation, have band - pass characteristics, and may show orientation selectivity (Lennie and D'Zmura, 1988). The precise function of the cells in layer IVA is uncertain, though evidence suggests that receptive fields are small and show both orientation and chromatic selectivity (Blasdel and Fitzpatrick, 1984).

Neurones in layer IVC α project principally to layer IVB but there are also smaller projections to layers II and III. Neurones in layer IVB have orientation selective receptive

fields and most also show directional selectivity (Livingstone and Hubel, 1984). Like the cells of layer IV α , they possess high contrast sensitivity (Blasdel and Fitzpatrick, 1984) but lack chromatic selectivity. Many are driven by both eyes (Lennie and D'Zmura, 1988).

Neurons in layer IV β mainly project to layers IVA and III, and then onwards to layer II. Anatomical studies using staining techniques for the mitochondrial enzyme cytochrome oxidase, have revealed an alternating pattern of light and dark regions which are particularly noticeable in layers II and III, the dark regions being round or oval in sections cut parallel to the surface (Horton and Hubel, 1980; Humphrey and Hendrickson, 1980). Livingstone and Hubel (1982) have termed these dark regions "blobs" because of their appearance in tangential section, and it seems that they are also faintly visible in layers V and VI (see Figure 1.14). The cells found within these blobs are not orientation selective but are either sensitive to chromatic or achromatic modulation. The non - opponent cells in the blobs have larger receptive fields than the non - opponent geniculate cells but are otherwise similar. The physiological properties of non - opponent blob cells indicate that they probably receive input from the magnocellular geniculate rather than the non - opponent division of the parvocellular system (Livingstone and Hubel, 1984). It seems probable that the colour opponent blob cells receive input from the colour opponent parvocellular geniculate cells, though blob receptive fields are larger and show double - opponent organisation (Hubel and Wiesel, 1968) in that the centre of the receptive field contains chromatically opponent mechanisms of one polarity (e.g., +R, -G) while the surround contains mechanisms of the opposite polarity (e.g., -R, +G). A schematic representation of a double - opponent receptive field is shown in Figure 1.15. Livingstone and Hubel (1984) found that over half the cells within the blobs show colour opponency, whereas cells outside the blobs tend to be non - opponent. Most interblob cells are orientation, but not direction, selective and have small receptive fields which respond well to achromatic

luminance borders. Approximately 15% of interblob cells are end - stopped responding to short line or edge stimuli. In consequence, it has been proposed that this layer may be responsible for high - resolution form perception (Livingstone and Hubel, 1988).

A number of distinct "visual association" areas, namely V2, V3, V4 and V5, have been identified in the prestriate cortex (see Figure 1.12, and Zeki and Shipp, 1988). Neurones from V1 project to V2, and when stained for cytochrome oxidase, V2 shows a pattern of alternating wide and narrow dense stripes which run perpendicular to the V1 / V2 border, and which are separated by paler interstripes (Livingstone and Hubel, 1984). The V1 blobs are reciprocally connected to the thin stripes, the interblobs to the interstripes, and layer IVB to the thick stripes (Livingstone and Hubel, 1987).

Livingstone and Hubel (see Livingstone and Hubel, 1988) have also examined the physiological properties of cells in V2. More than half the cells in the thin stripes were found to be colour - coded with double opponent receptive fields. These cells, like the blob cells in V1, showed no orientation selectivity, but differed from the blob cells in that they displayed larger receptive fields which were less selective for the position of a stimulus of optimal size. Cells in the interstripes were orientation, but not direction selective, and, like the interblob cells of V1, were not colour - coded. Over 50% were end - stopped and are therefore likely to be involved in coding shape. In the thick stripes also, cells show orientation selectivity, but the most marked response selectivity is to stereoscopic depth following binocular stimulation.

Area V4 receives input from the chromatically selective neurones in the thin stripes of V2 and also from the interstripes (Zeki and Shipp, 1988). Various studies have shown that the majority of V4 neurones are chromatically selective and have much larger receptive field sizes than neurones in V1 (see Lennie and D'Zmura, 1988). In spite of these large receptive field sizes it appears that V4

neurones, like those found in the striate cortex, show a high degree of selectivity for the spatial properties of stimuli (Zeki, 1983a). The likely involvement of area V4 in the mediation of colour constancy will be discussed later in this chapter.

The pattern that is emerging is one in which functional specialisation becomes more segregated at each successive cortical level. Thus, while area V4 is involved in the analysis of colour (and static form), the V3 complex (areas V3 and V3A) is involved in dynamic form analysis, and the V5 complex (areas V5 and V5A, also known as the middle temporal lobe or MT) is involved with motion. Most connections between areas in the cortex are reciprocal however (though forward and backward connections may not coincide), such that a certain amount of integrative processing is allowed. A diagram summarising the major connections and properties of the retino - cortical visual system is shown in Figure 1.16.

1.3. COLOUR CONSTANCY

Newton (1704) originally hypothesised that the colour of a specific object was determined by the relative amounts of red, green, and blue light that it reflects. In Newton's own words:

"Every Body reflects the Rays of its own Colour more copiously than the rest, and from their excess and predominance in the reflected Light has its Colour".

At least since the time of Helmholtz (1867), however, it has been known that this simple approach is only approximately correct in that objects can maintain a relatively constant hue despite large changes in the spectral composition of the light reflected from them into our eyes. For example, a sheet of paper which we perceive as being white in daylight still appears white when we view it under artificial tungsten light, even though the relative spectral composition of light reflected from it has changed markedly

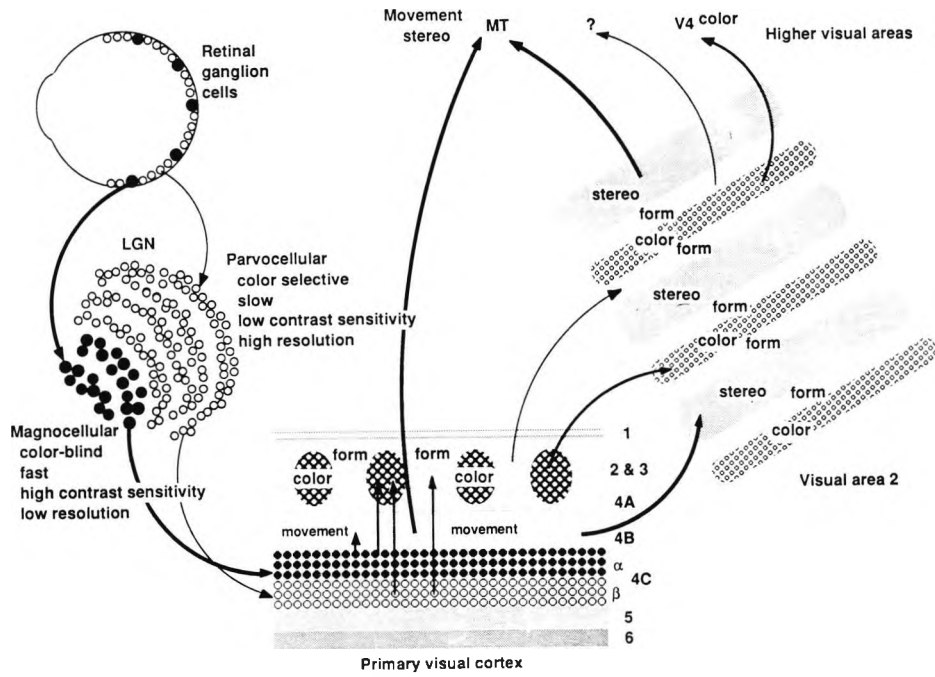


Figure 1.16. Summary diagram showing the functional segregation of the primate visual system (from Livingstone and Hubel, 1988).

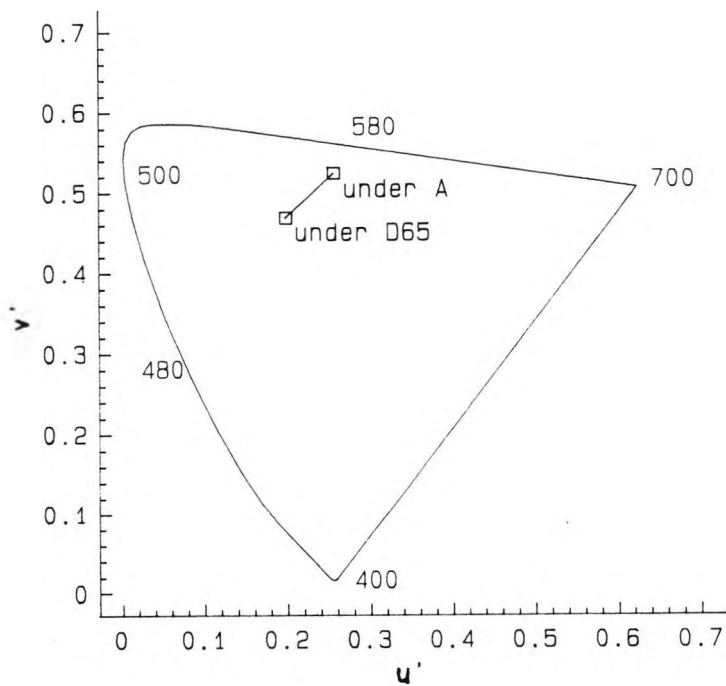


Figure 1.17. The approximately uniform CIE $u'v'$ chromaticity diagram showing the co-ordinates of an equal energy white paper illuminated by CIE Standard Illuminants D_{65} and A.

due to the change in illuminant. The change in the chromaticity of this "white" paper when viewed under the two illuminants may be seen by plotting the two conditions on a CIE (Commission Internationale de l'Eclairage) 1976 uniform chromaticity scale (or UCS) diagram as shown in Figure 1.17. The UCS diagram used here has the advantage over the commonly used x,y chromaticity diagram that equal distances on the diagram represent approximately equal perceptual colour differences (see Wyszecki and Stiles, 1982, or Hunt, 1987, for a review of the various CIE diagrams and their derivations). It would appear that the visual system displays an adaptive ability which tends to cancel physical colorimetric shifts caused by illuminant changes, though recent studies have indicated that human colour vision does not maintain perfect colour appearance under these conditions (McCann et al., 1976; Worthey, 1985). In general colour constancy may be defined as the invariance of perceived object colour despite variation in the spectral power distribution of the ambient light.

Some excellent demonstrations of object colour constancy have been given by Land (1959a, 1959b). Land took two or three colour separation photographs of a scene through long, medium and short wavelength filters and then projected them onto a screen in superimposition using three projectors. He showed that the perceived colours of the objects in the scene remained invariant when the wavelengths and intensities of the projectors were varied and even when one of the projectors was switched off, provided the long wavelength and the short wavelength photograph were projected using wavelengths longer and shorter than the medium wavelength photograph respectively. Land (1964, 1974) later went on to use Mondrian displays (so - called because of their resemblance to paintings by the artist Piet Mondrian) which consisted of about 100 coloured matt papers arranged arbitrarily so that no paper was surrounded by a single paper. The Mondrians were again illuminated by three, independently adjustable projectors, each with its own long, middle or short, narrow - band filter. The observers picked out two papers in the Mondrian, say a red one and white one,

and the experimenter used a photometer to measure separately the amounts of long, middle and short radiances from each paper. The experimenter then separately adjusted the projectors such that the triplet of radiances coming from the red paper were the same as those coming from the white paper. With all three projectors turned on the observer reported that the red paper still appeared red even though the radiance measurements indicated that the spectral composition of the light reaching the eye was the same as the white paper seen previously. Land performed this procedure for each paper in the display and showed that almost any colour sensation could be produced by a single triplet of radiance measurements.

1.3.1 MODELS OF COLOUR CONSTANCY

Helmholtz (1867) initially proposed that we form a correct idea of an object's "permanent" colour by unconsciously discounting the illuminant colour, suggesting that visual memory played an important part in this process. This early explanation of colour constancy was later disproved by Katz (1935) who showed that constancy could occur in situations where lack of prior experience meant that no colour memory had developed.

Though not originally conceived as a mechanism of colour constancy, the model of chromatic adaptation proposed by von Kries (1905) often represents the first stage in many current models of colour constancy (e.g., Land and McCann, 1971; West and Brill, 1982). The von Kries rule states that the eye has three receptor systems, which at the time was a supposition based on Young's (1802) theory, with different spectral - sensitivity functions which do not vary in shape under adaptation. The output of each of these receptor systems is weighted by a coefficient which is inversely related to the stimulation of each specific receptor type by the adapting light (Worthey, 1985; Worthey and Brill, 1986). Usually, the three coefficients are adjusted to keep the adapted appearance of a reference white surface constant. The von Kries transformation therefore, acts as a gain

control model that normalises each dimension of the colour signal to the maximum value of the signal over the visual field (Brill and West, 1986). Interestingly several authors point out that Ives (1912) should be credited with the idea of using this normalisation procedure to model colour constancy (e.g., Worthey, 1985; Brill and West, 1986).

An empirical model of colour constancy was formulated by Helson and Judd (Helson, 1938; Judd, 1940; Helson, 1943; Judd, 1960), and relied upon the idea that the space - averaged surface reflectance in scenes is constant across the visible spectrum and that the chromaticity of the illuminant can be determined from this averaged "adaptation" level. It was proposed that eye movements allow spatially localised retinal mechanisms to sample this averaged colour signal such that the colour of each object in the scene is perceived relative to this signal. Judd (1940) made a quantitative study of the above hypothesis by attempting to predict the hue, saturation and lightness of various colour samples (i.e., Munsell chips) under different illumination conditions and for surfaces uniformly illuminated Judd's empirical formula performs fairly well (Buchsbaum, 1980).

On the basis of his projection and Mondrian experiments, Land (1964) developed what appeared to be a novel theory of colour vision. Land proposed that colour sensations are dependent on three lightnesses calculated from the wavelength - radiance distribution on the retina, each lightness being computed from a single region of the spectrum such that, for example, information from the long - wave receptors for a particular area is compared with the information from all long - wave receptors over the whole visual field. Thus the information from each of the three cone types generates a separate lightness signal and that for each patch the subsequent comparison of these three lightnesses determines the colour sensation. Land designated his theory the Retinex theory because he was unsure whether the underlying physiological mechanisms were located in the retina or cortex, or in both. Land's Retinex model was the first attempt at developing a computational model for human

colour constancy and whilst it has been modified on several occasions since its first conception (McCann and Houston, 1983; Land, 1986a; Land, 1986b) it still forms the basis of many of the more recent colour constancy models (see Hurlbert, 1986 for a review).

The basic problem involved in the development of computational models of colour constancy is how the visual system can compute and keep invariant an object's colour when the cone signals generated from the object depend on both reflectance and illumination. In Land's early formulation of the Retinex model (Land and McCann, 1971; see also McCann et al., 1976), and in other von Kries type transformations, the unknown illuminant is effectively determined by using the brightest region in the Mondrian like a spectrally flat mirror which reflects the illuminant. This means however, that constancy would fail if there were no bright, white region in a scene. A second method for determining an unknown illuminant is by using the specular component of reflection (e.g., highlights) the reflectance of which is again normally flat across the visible spectrum (Lee, 1986). If this were the only mechanism operating it would mean that there would be no colour constancy for matt surfaces which we know, from Land's (1964) Mondrian studies, is not the case. A third method relies upon the fact that the space - averaged light in most natural scenes will bear a chromaticity that closely approximates that of the illuminant (see Judd, 1940 above). Buchsbaum (1980) also used this latter property in his "spatial processor" model of colour perception. This model is limited, however, in that it effectively requires a prior knowledge of the spectral reflectance functions of the objects in the scene (Lennie and D'Zmura, 1988). Maloney and Wandell (1986) have offered a solution to this particular problem by describing a method which allows the determination of surface spectral reflectance without any knowledge of the average spectral reflectance function. The improved model still has physical limitations, however, in that the illuminant must be spatio-chromatically homogeneous, and its spectral power distribution must be adequately represented by weights on a

particular set of three basis functions that characterise daylight (D'Zmura and Lennie, 1986).

1.3.2 MECHANISMS OF COLOUR CONSTANCY

It is supposed that exposure to a chromatic stimulus causes spectrally selective reductions in sensitivity i.e., adaptation (see Wyszecki and Stiles, 1982). Classical theories of colour constancy favoured the view that some type of adaptation within the visual system was responsible for removing the contribution of the illuminant. Ives (1912) was the first to suggest that the receptor - specific adaptation proposed by von Kries (1905) could contribute to the phenomenon of colour constancy, and his suggestion has gained the support of more recent research (e.g., Worthey, 1985; Worthey and Brill, 1986). It has been argued that in addition to receptor adaptation, adaptation at a second chromatically opponent site within the visual pathway may be necessary to achieve colour constancy (Buchsbaum and Gottschalk, 1983; D'Zmura and Lennie, 1986; Jameson and Hurvich, 1989). Adaptation mechanisms depend primarily on temporal interactions which cause the sensitivity of the chromatic channels of the visual system to change over time in response to an illuminant change. Simple adaptation mechanisms are largely independent of spatial interactions and hence field structure (see Arend and Reeves, 1986). Land (1959a, 1959b) initially believed that chromatic adaptation was not involved in colour constancy because it required prolonged viewing of a scene, and later he demonstrated (Land, 1962) that colour constancy effects could be observed when images were projected for only 6 ms. It is now known, however, that adaptation mechanisms can be extremely rapid (see McClaren, 1986) and therefore, Land's (1962) experiments cannot be used as evidence against the contribution of adaptation to colour constancy.

It is somewhat difficult to reconcile the concept of the Retinex theory with the modern view that chromatically opponent mechanisms subserve colour vision (Lennie and D'Zmura, 1988), though it has been suggested that the

Retinex algorithm may be made to work on colour opponent signals rather than on signals from independent cone mechanisms (Worthey, 1982; Livingstone and Hubel, 1984; Land, 1986b). A colour opponent physiological approach can be similarly correlated with other mathematical constancy models such as that proposed by Buchsbaum (1980) (D'Zmura and Lennie, 1986). Certainly cone adaptation mechanisms, such as that proposed by von Kries (1905), can go a long way towards explaining the maintenance of constant colour appearance, though it seems unlikely that adaptation alone can account for colour constancy (Worthey and Brill, 1986; Lennie and D'Zmura, 1988).

The rapid processes which are possibly involved in the mediation of colour constancy are normally ascribed to what have become known as simultaneous mechanisms. These mechanisms are defined primarily in terms of spatial interactions among chromatic channels in response to light at various locations in the retinal image and they depend only secondarily on temporal parameters (Arend and Reeves, 1986). Simultaneous colour contrast, for example, refers to the well - known phenomenon whereby a coloured target, when surrounded by an annulus of a different colour, will apparently change in appearance such that it takes on a hue complementary to that of the surround (Cornsweet, 1970). Walraven (1973) states, however, that the effect resulting from prolonged viewing of this type of stimulus pattern should be termed "lateral chromatic adaptation", or, when both instantaneous and long - term processes are involved in laterally evoked hue changes, "chromatic induction". Unfortunately, reviewing the literature, it seems that the terms simultaneous colour contrast and chromatic induction have become synonymous.

Whilst some workers in this field would disagree (e.g., Arend and Reeves, 1986; Arend et al., 1991), it seems probable that simultaneous mechanisms do contribute to colour constancy (Walraven et al., 1987; Tiplitz Blackwell and Buchsbaum, 1988a, 1988b ; Brenner et al., 1989). Classical theories of chromatic induction per se propose

that stimulation of cones of one class in one part of the retina desensitises cones of the same class in other parts of the retina (Evans, 1948; Alpern, 1964). A similar sort of lateral interaction has been proposed to occur between second - stage opponent mechanisms (Guth et al., 1980; Ware and Cowan, 1982). Recent psychophysical evidence seems to suggest, however, that chromatic induction may be mediated by higher - order cortical mechanisms (De Valois et al., 1986; Krauskopf et al., 1986).

Daw (1984) has suggested that simultaneous colour contrast and colour constancy can be explained by the activity of the double opponent cell. This type of cell was first identified by Hubel and Wiesel (1968) and is mainly found in the blobs of layers II and III of the striate cortex (Gouras, 1974; Michael, 1985; see also section 1.2). The double opponent cell has a centre - surround receptive field organisation with opposing responses for different wavelengths in both parts of the receptive field. Thus, as shown in Figure 1.15, the centre of the receptive field contains chromatically opponent mechanisms of one polarity (e.g., +R, -G) while the surround contains mechanisms of the opposite polarity (e.g., -R, +G). The cell will therefore respond when stimulated by, for example, a neutral spot in a short wavelength surround or by a long wavelength spot in a neutral surround, and moreover, if the cell activity signals redness in the centre of its receptive field, then both stimuli will result in the spot appearing reddish. In terms of colour constancy, it can be seen that the activity of the double opponent cell will tend to be independent of the wavelength composition of an illuminant, since the influence of the centre and surround will tend to cancel each other out as the illuminant changes (providing the object of interest is spatially co - extensive with, or larger than, the cell's receptive field).

Land et al.(1983) detail an experiment which again implicates the cortex in colour constancy. A subject with a clinically severed corpus callosum viewed a scene in which one hemifield was presented with a Mondrian array, and the other hemifield was presented with a structureless black

velvet field, the relative positions of each being reversible. The illumination of the Mondrian could be adjusted such that a target area positioned on, and just to the velvet side, of the vertical mid - line of the scene appeared either purple or white to a normal observer. The authors found that when the Mondrian was positioned to the right of the subject's fixation so that the verbal half of his brain (i.e., the left hemisphere) was dealing with the Mondrian plus target, he reported that the target area appeared "white" or "purple" in correspondence with a normal observer. When the verbal half of the subject's brain was dealing with the velvet plus target, however, he reported that the target only ever appeared "white". The authors concluded, therefore, that the cortex is required for colour constancy, and further that the necessary processing requires long - range interactions.

Further and more specific evidence that the cortex is involved with colour constancy has come from the physiological studies of Zeki (1980; 1983b). It had already been shown that certain cells in the V4 area of the monkey prestriate cortex were selective to narrow bands of the visible spectrum (average bandwidths at half maximum cell sensitivity, 20 nm) and that the responses of these non - opponent cells correlated well with perceptual "responses" to individual hues i.e., blue, green, purple and red (Gouras, 1974; Zeki, 1977). On the suggestion of Land, Zeki (1980) attempted to investigate the relationship between these V4 cells and the perceptual phenomena experienced in Land's (1964) Mondrian experiments. Zeki found that a specific cell would only respond to an area of the appropriate colour (i.e., one that fell within its own action spectrum) in the Mondrian when all three narrow band projectors were illuminating the whole scene. This finding corresponded to the experimenter's own observation that vivid colours were only perceived when all three projectors were simultaneously illuminating the Mondrian. Like the early experiments of Land (1964), Zeki equalised the triplets of radiances from each of the patches comprising the Mondrian and found that the responses of the V4 cells

were independent of overall light flux, the magnitude of the responses reflecting the colour of the patches as perceived by the experimenter. Zeki (1983b) later designated these cells colour - coded or "CO" cells to differentiate them from the wavelength - selective and wavelength opponent or "WL" and "WLO" cells found in the V1 area of the visual cortex.

Several studies have since been published which implicate the V4 complex in the mediation of colour constancy (Wild et al., 1985; Heywood and Cowey, 1987; Butler et al., 1988). In all of these studies, rhesus monkeys were trained in a colour constancy task in which they were found to perform well. Subsequently area V4 was removed bilaterally in some of the animals whilst the remainder served as controls. Post - operatively, the performance of the animals with the V4 lesions was shown to be deficient in the colour constancy task even though thresholds for hue and saturation discrimination remained unimpaired. Heywood and Cowey (1987) also reported, however, that the discrimination of pattern and orientation was severely disrupted in these post - operative animals suggesting that V4 may additionally be involved in spatial vision.

1.3.3 QUANTITATIVE STUDIES OF COLOUR CONSTANCY

Whilst there have been many theoretical studies involved with the formulation of improved algorithms for predicting colour constancy, until recently relatively few studies have managed to quantify how well colour constancy works in human vision.

Basing their study on the Mondrian experiments of Land (1964), McCann and his co - workers (McCann et al., 1976) attempted to quantify colour constancy and relate their findings to the Retinex model proposed by Land. A Mondrian pattern enclosed in a box was illuminated by three narrow - band lights (at wavelengths 450, 530 and 630 nm) from three, independently - adjustable projectors. A Munsell Book of Colour (see Hunt, 1987) in a second box was illuminated by

lights of identical wavelength but the intensity of each projector was fixed. The observer viewed the Mondrian with one eye and then the Munsell book with the other. For each of the 18 papers comprising the Mondrian, the observer matched as closely as possible the colour of the Mondrian paper with a paper from the Munsell book. This procedure was repeated for five different Mondrian illuminant conditions. One of the illuminants was identical to that used on the Munsell book, and this control experiment was designated the "grey" experiment. In each of the other four experiments, the variable illuminant was adjusted to give a selected coloured paper in the Mondrian the same spectral radiance as that of one of the neutral papers in the grey experiment. These experiments were then designated the red experiment, the yellow experiment, the green experiment and the blue experiment, according to the colour of each of the chosen papers. The results showed that colour constancy was almost perfect in the yellow and red experiments, although the magnitude of the constancy effects did vary with paper colour. Thus for these two conditions, the colour appearance of the paper in the Mondrian was relatively unaffected by illuminant change. Constancy worked less well in the green experiment, however, and in the blue experiment only minimal constancy effects were observed. In order to quantify their observations, McCann and his colleagues measured both the integrated radiance and integrated reflectance of a target paper in the Mondrian, and compared the values obtained with similar measurements made for the paper chosen by the observer from the Munsell book to match the target paper. To this end, and in order to simulate the proposed Retinex algorithm, they used a photometer in conjunction with filters chosen to approximate separately the spectral response of each of the three cone pigments (see Figure 1.4). Thus, spectral radiances weighted by the spectral responsivity of each of the three cone types were measured for each target paper in the Mondrian and its corresponding matching paper in the Munsell book. To describe the triplet of lightness values determined for each patch with respect to the lightness values measured for a standard reference white patch, the term integrated reflectance was introduced

and defined according to the following equation:

$$\Gamma_c = \frac{k \sum R_p(\lambda) E(\lambda) V_c(\lambda) d(\lambda)}{k \sum R_s(\lambda) E(\lambda) V_c(\lambda) d(\lambda)}$$

where $R_p(\lambda)$ is the spectral reflectance of the paper in question, $R_s(\lambda)$ is the spectral reflectance of the standard white, $E(\lambda)$ is the spectral irradiance, $V_c(\lambda)$ is the spectral sensitivity of the visual pigment c , and k is the conversion factor from irradiance to radiance (see Worthey, 1985). A comparison of the experimental data with that predicted on the basis of the Retinex theory, showed good correlation, and McCann and his colleagues (McCann et al., 1976) concluded that integrated reflectance was a much better predictor of colour sensation than integrated radiance. Whilst emphasising the importance of the retina and independent cone processing in the model, the authors do not rule out possible later interactions in the visual pathway, or even opponency. In fact Worthey (1985) later explains how an opponent colours approach (e.g., Guth et al., 1980) can describe the departures from perfect colour constancy observed in this experiment. Worthey notes from McCann's experiment that colour constancy works better for illuminant shifts in the blue - yellow direction than for those in the red - green direction and relates this finding to the overlap of receptor sensitivities. The blue - yellow channel compares the outputs of the red and blue receptors, and since the spectral sensitivity functions of these two receptor systems overlap little, then the integrated reflectance computation should work well. In the red - green channel, however, the outputs of the red and green receptors overlap comparatively more which means that illuminant compensation using this approach should be less satisfactory.

The first implementation of computer - controlled visual display units in the study of colour constancy was made by Arend and Reeves (1986). In their experiments observers were required to match corresponding patches in two displays presented simultaneously. The standard simulation was

presented on the left - hand display and corresponded to a scene under a 6 500 K illuminant, whilst the test simulation was presented on the right - hand display and consisted of the same scene under a 4 000 or 10 000 K illuminant. Both a Mondrian display made up of 32 simulated Munsell samples of equal value, and a simple centre - surround display employing a neutral grey surround, were used. The standard and test Mondrian scenes each subtended 5° square with their centres separated by a visual angle of 7° . The standard and test centre - surround scenes consisted of two 1° square patches again presented 7° apart (centre to centre) and each surrounded by a square annulus whose outer border subtended 3° . Observers were instructed to alternate between displays about once every second spending approximately the same amount of time viewing each display. Observers were required to match patches using two different criteria: (i) so that the test and standard patch were of equivalent hue and saturation (disregarding other areas of the screen as much as possible), and (ii) so that the test patch appeared as if it had been "cut from the same piece of paper" as the standard patch. Arend and Reeves found that whilst the "paper" matches were approximately colour constant (at least for two of the three observers), the hue - saturation matches showed little colour constancy. Furthermore they found that pattern complexity had little effect on the amount of colour constancy. They concluded that simultaneous mechanisms alone (e.g., simultaneous colour contrast) contribute little to colour constancy and that higher level cognitive processes are more influential. They later confirmed their conclusions in a second experiment (Arend et al., 1991) where they used chromatic arrays spanning a wider range of Munsell values to introduce achromatic contrast into the displayed scene.

Tiplitz Blackwell and Buchsbaum (1988a, 1988b) similarly investigated the role of simultaneous contrast mechanisms in colour constancy with the aid of a computer - controlled display. They used a centre - surround design with the centre square subtending 0.6° and presented with (i) no surround, (ii) an adjacent chromatic surround of width 0.6° ,

or (iii) a chromatic surround separated from the centre by an achromatic gap of 0.3° (Tiplitz Blackwell and Buchsbaum, 1988a). The centre colour was either blue - green (Munsell designation 2.5 BG 6/10) or yellow (2.5 Y 8/10) and the surround was either blue (10 B 7/8) or green (10 GY 7/10). Both centre and surround were presented under each of six simulated CIE standard illuminants. A number of comparison patches viewed under the same simulated illuminant were also presented on the display and were separated from the test pattern by 3° . Observers were required to choose a matching colour that most closely resembled the hue and saturation of the centre colour. Not unexpectedly they found that in the absence of a surround no colour constancy was demonstrated with the matched colours being physically identical to the centre colours. In the presence of a chromatic surround, however, both chromatic induction and colour constancy effects were observed, with both effects being greatest when the surround was adjacent to the centre. An association between chromatic induction and colour constancy was made in that when chromatic induction was weak (i.e., for the yellow centre separated from the surround by the achromatic gap) colour constancy was also weak. Whilst they conclude that simultaneous mechanisms contribute to colour constancy, they noted that colour constancy was not perfect in any of the experimental conditions since when the simulated illuminant of the central patch was changed, it was often matched to a significantly different comparison patch. Colour constancy worked well, however, when illuminants were only slightly different. This finding led them to conclude that "color constancy is strong enough to eliminate perceptual differences caused by slightly different illuminants but it can only partially remove perceptual differences caused by extremely different illuminants". Interestingly they comment on the experimental findings of Arend and Reeves (1986), pointing out that the data from the latter authors hue - saturation matches showed approximately the same magnitude of colour constancy as observed in their experiments. Thus there appears to be a disagreement in terms of data interpretation rather than in terms of quantitative results.

In a separate study, Tiplitz Blackwell and Buchsbaum (1988b) used a similar experimental paradigm to that described above to investigate the effect of certain spatial parameters on colour induction (and hence constancy). They found that the change in perceived colour of the centre decreased exponentially as the centre - surround separation increased. They also found an exponential relationship to exist between the size of the surround and the magnitude of the induced colour change. They conclude that chromatic induction is a local phenomenon and that virtually all fields that are more than 2° away from the focal area have little effect on colour appearance.

In their quantitative study of colour constancy, Valberg and Lange - Malecki (1990) used a projection system with narrow band interference filters similar to that employed by McCann and his co - workers (McCann et al., 1976). The Munsell book used in the comparison field by McCann et al. (1976) was, however, replaced by a projection colour mixture apparatus (Valberg, 1971) so that exact colour matches could be achieved for all combinations of samples and illuminants. Both a Mondrian surround and a uniform grey surround were used in the experiments. Again they report that the colour constancy effects observed in their investigation were relatively small when compared with the physical chromaticity shifts that occur under different illuminants. They also found that the magnitude of colour constancy varied with sample colour and with illuminant colour and showed that constancy is better for achromatic and white surfaces than for chromatic ones. Similar to Arend and Reeves (1986) they showed that constancy effects were comparable for uniform grey surrounds and Mondrian surrounds (providing that the grey represents the spatially weighted average of the Mondrian). Strong simultaneous contrast effects were observed by changing the immediate surround of the test patch so that a number of patches of the same colour surrounded the test field, thus emphasising the importance of the spatial structure and chromatic content of the near field. The authors emphasise that none of these

above effects are predicted by the Retinex algorithm (Land, 1964; Land and McCann, 1971; McCann et al., 1976).

In summary it would appear that colour constancy is a complicated visual process mediated by several perceptual mechanisms located at both central and peripheral sites. The results of many of the quantitative studies into the phenomenon are not always consistent and are not easily interpreted or explained by any of the algorithms that have been proposed to model this property of human vision.

1.4 THE PUPIL

The entrance pupil of the refracting system of the eye is the image of the iris (see Figure 1.1) which acts like a diaphragm, constricting or dilating as a result of the opposing actions of two muscles, the sphincter pupillae and the dilator pupillae. These two muscles are innervated by the autonomic nervous system, the sphincter pupillae predominantly by parasympathetic fibres, and the dilator pupillae predominantly by sympathetic fibres. At full mydriasis the human pupil can reach 7.5 to 8 mm in diameter, constricting to 1.5 to 2 mm at full miosis (Alexandridis, 1985). A detailed description of the anatomy of the iris has been given by Wolff (1976).

It is well known that changes in the diameter of the pupil may be elicited by changes in retinal illuminance or accommodation and convergence and also by certain psychosensory stimuli (Crawford, 1936; Alpern and Campbell, 1962; Lowenstein and Lowenfeld, 1969; Alexandridis, 1985). Lowenstein and Lowenfeld (1969) provide an historical review with regard to the characteristics and mechanisms of the pupillary reflex pathway. For the purpose of this study, however, only a brief review of relevant pupillary responses and their corresponding neural pathways involved will be given.

1.4.1 THE PUPIL LIGHT REFLEX

An increase in the level of light flux incident on one eye causes the pupil of that eye to constrict whilst, at the same time, the pupil of the other eye also constricts. If the change in light flux is only transitory, then the pupillary constriction is followed by a redilation. The response of the stimulated eye is termed the direct light reflex whereas the response of the unstimulated eye is known as the consensual reflex.

The pupil response amplitude and response latency are both known to vary as a function of stimulus luminance, with an increase in amplitude (Webster et al., 1968), and a decrease in latency (Lee et al., 1969), following an increase in stimulus luminance. The amplitude of the pupillary response is also dependent on other stimulus attributes including area (Schweitzer, 1956; Webster et al., 1968) and duration (Baker, 1963; Lowenstein and Lowenfeld, 1969), and also on the state of retinal adaptation (Lowenstein and Loewenfeld, 1959; Webster et al., 1968; Ohba and Alpern, 1972). The characteristics of the pupillary response in relation to these physical parameters (i.e., stimulus area, duration etc.), usually reflect the corresponding perceptual attributes. Whilst in general the response of the pupil is said to be consensual (Davson, 1980; Alexandridis, 1985), recent investigations have shown that stimulation of the nasal retina can produce a slightly larger direct than consensual response (Smith et al., 1979; Smith and Smith, 1980; Wyatt and Musselman, 1981; Cox and Parson - Drewes, 1984).

Figure 1.18 illustrates the probable pathway for the pupillary light reflex. Since the experiments of Hess in the early part of this century (see Wolff, 1976), it has been known that the receptors of the light reflex are the retinal rods and cones, and that it is unlikely that specific "pupillary" receptors exist. From these receptors, pupillomotor signals pass through the retina and probably relay at the ganglion cells before reaching the optic nerve.

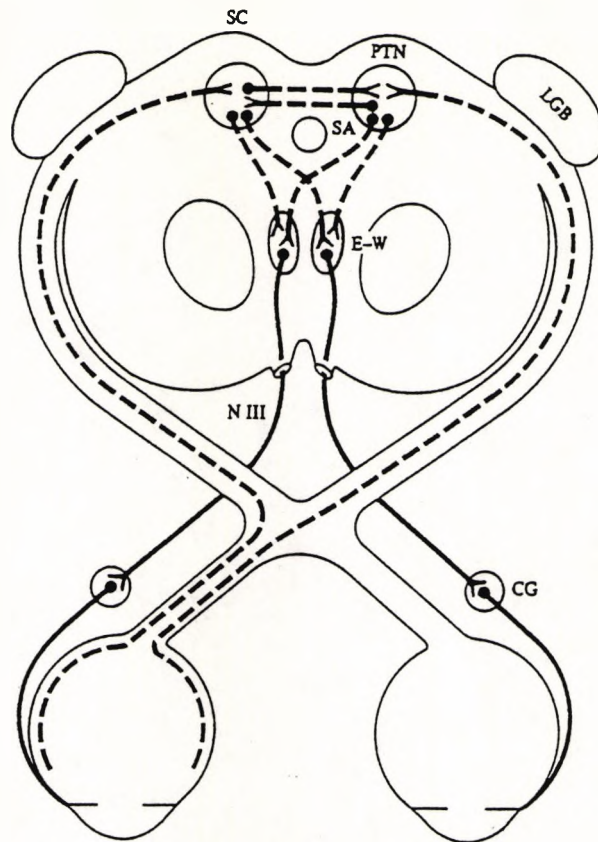


Figure 1.18. Simplified diagram showing the afferent and parasympathetic efferent pathways of the pupil light reflex. SC, superior colliculus; PTN, pretectal nucleus; LGB, lateral geniculate body; SA, sylvian aqueduct; E-W, Edinger-Westphal nuclei; CG, ciliary ganglion. (From Alexandridis, 1985).

It is most likely that the visual fibres and the pupillary fibres are different, but they both follow very similar pathways at this stage. It has been estimated that, in the monkey, no more than 10% of ganglion cells (namely the γ and ϵ cells) actually project to the midbrain (Perry and Cowey, 1984). The pupillary fibres run in the optic nerve and partially cross at the optic chiasm along with the visual fibres, before continuing into the optic tract. The pupillary fibres leave the optic tract in its posterior third, and enter the superior brachium. From here they pass into the midbrain lateral to the superior colliculus to reach the pretectal nucleus where they eventually synapse. The bilateral projections from the retina to the pretectal nuclei have been found to be approximately equal (Benevento et al., 1977).

The termination of retinal fibres in the midbrain is quite complex and several studies have attempted to clarify the issue. Scalia (1972) came to the conclusion that there were four pretectal nuclei receiving retinal input: the anterior and posterior pretectal nuclei; the nucleus of the optic tract; and the olivary pretectal nucleus. More recent studies seem to indicate a fifth nuclear mass, the medial pretectal nucleus (Hutchings and Weber, 1985; Benevento and Standage, 1983). The consensus of opinion seems to point towards the existence of a heavy retinal projection to both the nucleus of the optic tract and to the olivary nucleus (see also Pierson and Carpenter, 1974), though the posterior pretectal nucleus also receives a projection. The retinal projection to the anterior pretectal nucleus is uncertain (Hutchings and Weber, 1985), but may be species dependent (Scalia, 1972). The anatomical differences noted above would suggest a functional division of the pretectal nuclei, and certainly it is known that the fibres concerned with pupillary responses relay in a different nucleus from those mediating accommodation (Westheimer and Blair, 1973). It is interesting to note that, in addition to retinal projections, the pretectal nucleus also receives projections from the tectum and visual cortex (Benevento et al., 1977; Graham et al., 1979), and an influence of these areas on

pupil responsivity should not be overlooked.

From the pretectal nucleus, the pupillary fibres cross in the posterior commissure to reach the accessory oculomotor nucleus (Edinger - Westphal) of the same and opposite side via the medial longitudinal bundle. The Edinger - Westphal nucleus forms part of the oculomotor (III Nerve) complex and the majority of its component cells are, in fact, concerned with accommodation (Wolff, 1976). Similar to the projections from the retina to the pretectal nuclei, these bilateral projections to the Edinger - Westphal nuclei also seem to be approximately equal (Benevento et al., 1977). The equality of these bilateral projections can be correlated with the highly consensual nature of the pupillary response, though perhaps small asymmetries may be responsible for the differences between the direct and consensual responses observed pupillographically (e.g., Cox and Parson - Drewes, 1984).

The preganglionic, parasympathetic, efferent projections from the Edinger - Westphal nucleus extend into the oculomotor nerve and eventually leave it in its branch to the inferior oblique muscle. From here, the pupillomotor fibres form the short motor root of the ciliary ganglion. After synapsing in the ciliary ganglion, the postganglionic fibres pass in the short ciliary nerves and finally reach the sphincter pupillae. It is estimated that only 3 to 5% of the fibres in this efferent pathway are concerned with pupillomotor functions (see Wolff, 1976), the majority of fibres innervating the ciliary muscle.

The reciprocal (or antagonistic) nature of the autonomic nervous system is well known (see Day, 1979), and whilst the parasympathetic system and the sphincter pupillae play the dominant role in controlling pupillary activity, the sympathetic system and the dilator pupillae are also involved in the mediation of pupillary responses. Dilation of the pupil is often associated with emotional states, and therefore it is not surprising to find that the preganglionic sympathetic nerve fibres have their origin in

the hypothalamus. From here the fibres pass downwards, with partial decussation in the midbrain, into the lateral column of the spinal cord (the "dilator centre" of Budge and Waller (1852) is situated here). Again the pretectal nuclei are probably involved with this pathway (Benevento et al., 1977). The fibres leave the cord and travel upwards to synapse in the superior cervical ganglion, the postganglionic fibres passing through the carotid plexus to the trigeminal ganglion. From here they enter the orbit via the nasociliary nerve and reach the dilator pupillae in the long ciliary nerves.

1.4.2 THE NEAR PUPILLARY REFLEX

When visual attention is directed from a distant to a near object, then the pupils of both eyes constrict in synkinesis with an increase in accommodation and convergence. The physical stimulus for this "near triad" of events is thought to be blur or disparity, or a combination of both (Krishnan et al., 1977). Whilst the functional interactions of accommodation, convergence and pupillary miosis are well known, the neurological pathways which accomplish this synkinesis are less well understood (Myers and Stark, 1990).

The nervous pathway for the near pupillary response is almost certainly different to that for the light reflex. The clearest evidence for this comes from the examination of patients with Argyll Robertson pupil (see Ashworth and Isherwood, 1981). In such patients the pupil does not react to light, but reacts normally to convergence and accommodation. The pathway is thought to involve the cortex including Brodmann areas 17, 19 and 22 (e.g., Sakata et al., 1980) as well as midbrain structures including the pretectal nucleus and superior colliculus (e.g., Judge and Cumming, 1983). It seems likely that the near reflex and the light reflex share a common efferent pathway beyond the level of the oculomotor nucleus (see Benevento et al., 1977).

1.4.3 PUPILLARY RESPONSES TO SPATIALLY STRUCTURED STIMULI

In addition to the classical pupil light reflex and near reflex, more recent investigations have shown that the pupil responds systematically to spatially structured stimuli of constant space - averaged luminance. Several investigations have demonstrated pupillary constrictions to contrast reversal of chequerboard patterns (van der Kraats et al., 1977; Slooter and van Norren, 1980; Ukai, 1985), and all have found that the pupil responds selectively as a function of check size. It was also shown that the response of the pupil with check size bears a close resemblance to the corresponding perceptual function in which contrast thresholds for detection of the same type of stimulus are determined. Slooter (1985) has shown that whilst pupillometry correlates well with psychophysical measurements, the absolute contrast threshold for a pupillary response is about three times greater than for the corresponding psychophysical threshold. In addition, Ukai (1985) and Slooter (1985) have shown that the magnitude of the pupillary responses increases linearly with pattern contrast.

Studies using sinusoidal gratings also indicate a systematic pupillary constriction which is dependent upon the physical parameters of the stimulus (Barbur and Forsyth, 1986; Barbur et al., 1987a; 1987b; Barbur and Thomson; 1987; Barbur, 1991). The pupil response amplitude is seen to vary as a function of grating spatial frequency, the shape of the relationship resembling the psychophysical contrast sensitivity function. Barbur and Thomson (1987) went on to show the effects of defocus and retinal eccentricity on the pupil grating response (PGR), again highlighting the similarity with the perceptual correlates (see Hiltz and Cavonius, 1974; Green and Campbell, 1965). Furthermore, Barbur and Thomson (1987) have proposed that, since a good correlation exists between psychophysical grating acuity and grating acuity measured by means of pupillometry, then the PGR may be used as an objective measure of visual acuity. Slooter and van Norren (1980) similarly found a good

correlation between psychophysical chequerboard resolution thresholds and those obtained by extrapolation of pupil response data.

Several suggestions have been made with regard to the mechanisms mediating the PGR, including the triggering of small accommodative and convergence changes by the presentation of the grating stimulus (Ukai, 1985; Charman and Tucker, 1977), or a simple pupil light reflex response driven by local luminance changes in the grating pattern (Ukai, 1985; Sooter and van Norren, 1980). It has, however, been argued by Barbur and Forsyth (1986), and later by Keenleyside et al. (1988) that since a PGR cannot be evoked when the stimulus is restricted to cortically "blind" areas of the visual field, then it is likely that central mechanisms are involved in the mediation of the response.

1.4.4 PUPILLARY RESPONSES TO CHROMATIC STIMULI

Early experiments attempted to clarify that both rods and cones contributed to pupillary responses. Schweitzer (1956) illustrated rod involvement in pupillary activity by demonstrating a typical scotopic spectral sensitivity curve for pupillary responses, determined by measuring the stimulus intensity just sufficient to elicit a pupillary response as a function of wavelength. Alpern and Campbell (1962) were the first to obtain a photopic spectral sensitivity curve from measurements of pupillary responses. They found that even at high stimulus luminance levels the rods contributed to the pupil response, and it was only when the effects of the rods were excluded by using a blue background that they obtained a function of similar shape to the classic photopic spectral sensitivity curve. Alexandridis and Koepe (1969) later showed that pupillary responses can be used to demonstrate a Purkinje shift in wavelength sensitivity on passing from scotopic to photopic stimulation.

Kohn and Clynes (1969) were the first to show that pupillary responses may be elicited by changing only the colour of the

stimulus, having previously matched the intensity of the coloured stimuli used. Using a carefully calibrated Maxwellian view optical system to generate the chromatic stimuli, Young and Alpern (1980) verified the findings of Kohn and Clynes (1969), noting that the pupillary responses to equiluminant heterochromatic changes were bi-directional i.e., changes of stimulus wavelength from 490 to 650 nm or from 650 to 490 nm both produced a pupillary constriction of approximately equal amplitude. Furthermore they discovered that the amplitude of the pupillary response varied systematically with stimulus wavelength, and that the larger the wavelength difference between the two monochromatic stimuli used, the greater the amplitude of the constriction observed. Interestingly Young and Alpern also found that the pupil response latency was, on average, about 50 ms longer for equiluminant heterochromatic exchanges than for the equivalent homochromatic luminance increments which yield the same response amplitude. They were of the opinion that differences in conduction velocities between colour opponent ganglion cells and broad band (i.e., non - opponent) ganglion cells were not sufficient to account for such a large latency difference, and therefore proposed that the cortex may be involved in the mediation of chromatic pupillary responses. Furthermore, in terms of our present knowledge of the anatomical projections of colour opponent ganglion cells in the monkey, it would seem unlikely that such cells would be entirely accountable for the response of the pupil to chromatic stimuli since they are known to project only to the lateral geniculate nucleus (Shapley and Perry, 1986). Krastel et al. (1985) have, however, established the influence of postreceptoral colour opponent mechanisms on pupillary responses using stimuli which have been shown to isolate such mechanisms (King - Smith and Carden, 1976). This finding in itself may implicate the cortex in the mediation of chromatic pupillary responses.

More recently Barbur et al. (1987a) have shown that a pupillary response is also observed when the centre of a uniform white background field is replaced by a coloured stimulus, even when the luminance of the coloured target is

reduced significantly with respect to the background. Furthermore, this response is absent when the same stimuli are presented in cortically "blind" areas of the visual field in patients with geniculo - striate lesions (Keenleyside, 1989). These findings, therefore, add support to the hypothesis that central mechanisms are involved in the control of the pupil response.

The use of pupillometry as an objective method of assessing colour vision deficiencies has also been investigated. Protanopic observers may be distinguished from colour normal observers on the basis of the relatively reduced amplitude pupillary responses that they exhibit when stimulated with long wavelength light (Glansholm et al., 1974; Hedin and Glansholm, 1976; Cohen and Saini, 1978). In addition, Kohn and Clynes (1969), Saini and Cohen (1979) and Young and Alpern (1980) have shown that the pupillary responses of colour deficient subjects show consistently different patterns from those of colour normal subjects. Young et al. (1987) have taken this approach a step further by demonstrating the feasibility of using pupillary responses as a diagnostic tool in determining colour deficiencies in non-verbal patients. These authors used a colour monitor to generate their stimuli, which consisted of red to green or green to red, equiluminant chromatic exchanges (similar to the experiments of Young and Alpern, 1980 and Kohn and Clynes, 1969). They examined both anomalous trichromats and dichromats, and found that protan observers show little or no response to a green to red exchange but a large response to a red to green exchange, whereas deutan observers show smaller responses for both exchanges, particularly the red to green, when compared to colour normal observers. Interestingly, Young et al. (1987) extended their investigation to include a child (2.3 years old) and a neonate. They found that whilst the young child gave normal adult pupillary responses to the chromatic exchanges, the neonate (at both 12 and 16 days postnatally) failed to produce any consistent chromatic pupillary responses.

The spatial characteristics of human vision to achromatic gratings are well documented (see De Valois and De Valois, 1988; Barbur, 1988) but several authors have investigated the corresponding properties of sinusoidal chromatic gratings (van der Horst and Bouman, 1969; Granger and Heurtley, 1973; Mullen, 1985). When investigating pupillary activity it is important to ensure that there is no overall change in luminance on stimulus presentation, since otherwise the reponse elicited may be due simply to a component of the light reflex rather than due to the spatial structure or chromatic content of the stimulus. Similarly when measuring chromatic contrast sensitivity it is important to ensure that the gratings are isoluminant and vary only as a function of chromaticity. Figure 1.19 shows the contrast sensitivity function obtained for isoluminant red - green gratings.

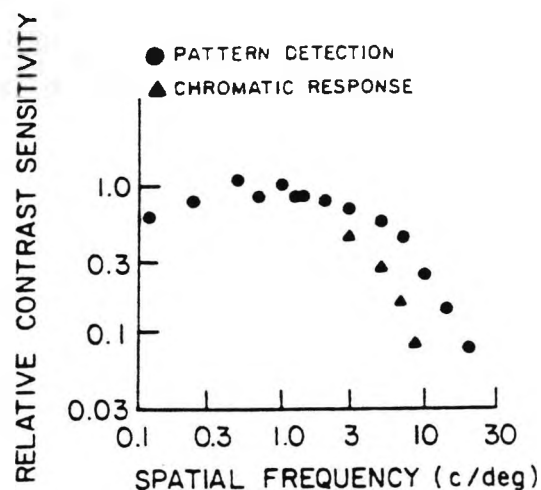


Figure 1.19. The chromatic contrast sensitivity function for isoluminant red - green patterns. The triangles represent data for the detection of colour differences, whilst the circles relate to pattern detection only. (After Granger and Heurtley, 1973).

When one compares the data shown in this figure with equivalent measurements for achromatic gratings then two distinct differences emerge. Firstly, sensitivity to the

chromatic grating falls off sooner at high spatial frequencies, and secondly, there is very little attenuation of sensitivity for the chromatic grating at low spatial frequencies. The results for blue - yellow gratings are similar, though most reports indicate that the high frequency attenuation occurs at lower spatial frequencies than for the equivalent red - green grating, presumably due to the sparse retinal distribution of B cones (De Valois and De Valois, 1988). Mullen (1985), however, reports no difference in the high frequency cut - off for red - green and blue - yellow gratings, and attributes reported differences to uncorrected chromatic aberration effects. Colour contrast sensitivity has recently been used for clinical diagnostic purposes (Arden et al., 1988a, 1988b), and initial results suggest that it may provide a very sensitive method of detecting early changes in visual function in patients with diabetes, ocular hypertension and glaucoma (Gündüz et al., 1988a, 1988b).

The psychophysical evidence given above shows that the chromatic contrast sensitivity function has low - pass characteristics, whereas the achromatic contrast sensitivity function has band - pass characteristics. Physiological studies support the hypothesis that the underlying mechanisms responsible for these spatio - chromatic properties are mediated via the parvocellular pathway (Lee et al., 1990). De Valois and De Valois (1988) have shown that the responses of colour opponent LGN cells to luminance and chromatic gratings are very similar to those observed psychophysically. Physiological recordings from the primate visual cortex also confirm the broad spatial tuning properties of chromatic mechanisms (Livingstone and Hubel, 1984; Thorell et al., 1985).

Bearing in mind the relationship between the response characteristics of the pupil to achromatic gratings and the psychophysical contrast sensitivity function, it would be of interest to investigate whether the pupil behaves in a manner which correlates with perceptual studies for chromatic gratings.

1.4.5 PUPILLARY RESPONSES IN AMBLYOPIA

It would appear, therefore, that the activity of the pupil provides us with a readily accessible way of exploring some of the mechanisms underlying visual processes in human vision. In addition to the use of pupillometry in the diagnosis of colour vision deficiencies, pupillary measurements have also been used to aid the investigation of certain neuro - ophthalmological diseases such as diabetic autonomic neuropathy (Smith and Smith, 1983), optic neuritis (Miller and Thompson, 1978), and lesions of the optic nerve (Alexandridis, 1985), as well as in retinal disorders such as macular degeneration (Newsome et al., 1981). Several studies have also attempted to ascertain the "normality" of the pupil light reflex in amblyopia (Harms, 1938; Drews, 1962; Thompson, 1966; Brenner et al., 1969; Greenwald and Folk, 1983; Portnoy et al., 1983; Kase et al., 1984), but the results from these studies are equivocal.

Functional amblyopia is currently defined as a unilateral lack of vision for which no obvious cause can be detected by physical examination of the eye, and which, in appropriate cases, is correctable by therapeutic measures (Burian, 1956). The condition is normally associated with a strabismus (strabismic amblyopia), anisometropia (anisometropic amblyopia) or a combination of strabismus and anisometropia (mixed amblyopia) occurring during the sensitive period of visual development in early life (Hubel and Wiesel, 1970). Estimates of the incidence of amblyopia in the general population vary between 1% and 6% (Cole, 1959; Oliver and Nawratski, 1971).

It has been established that amblyopia is a defect of form perception rather than light perception since detection thresholds are normal in amblyopic subjects for both rod and cone vision (Wald and Burian, 1944). Characteristically amblyopia results in a reduction of visual acuity and, not unexpectedly, a depression of the threshold contrast sensitivity function (Hess and Howell, 1977; Bradley and

Freeman, 1981), though the relationship between these two measures of visual performance in amblyopia is not clear cut with strabismic amblyopes exhibiting a more marked visual acuity deficit relative to the contrast sensitivity loss (Abrahamsson and Sjöstrand, 1988). Numerous studies have explored the visual deficit in amblyopia and abnormalities have been shown to exist in terms of, for example, eye movements (Hess, 1977a; Ciuffreda et al., 1980), accommodation (Wood and Tomlinson, 1975), reaction times (Hamasaki and Flynn, 1981), spatial filtering and pattern discrimination (Bromley et al., 1987) and other aspects of spatial vision (Hess et al., 1978; Bedell and Flom, 1981), stereopsis (Harwerth, 1982), and spectral sensitivity and colour vision (Harwerth and Levi, 1977; Marré and Marré, 1979).

The site of the primary dysfunction in the visual pathway in human amblyopia has been controversial. Anatomical and physiological investigations have, for obvious reasons, been restricted to animals, most commonly the cat and monkey. These animals have been made artificially amblyopic by extra - ocular muscle surgery (inducing a strabismus), or by unilateral removal of the crystalline lens or chronic monocular instillation of a cycloplegic (producing anisometropia). Studies using monkeys have shown that, in both strabismic and anisometropic amblyopia, there is a reduction in the number of striate cortical cells which can be driven by the amblyopic eye (Baker et al., 1974; von Noorden and Crawford, 1977) and furthermore that there is a shift in ocular dominance in favour of the normal eye (Crawford and von Noorden, 1979; Crawford, 1978). Again for both strabismic and anisometropic amblyopia, histological investigations of the LGN have found a reduction in cell size in layers receiving input from the amblyopic eye (von Noorden, 1973), which is restricted to binocularly innervated portions of the LGN for strabismic amblyopia (von Noorden and Middleditch, 1975). The retina appears to be histologically normal in both strabismic and anisometropic amblyopia (von Noorden, 1973; Crawford, 1978).

Normally 80% of cells in the striate cortex can be driven binocularly by the stimulation of either of the two eyes (Wiesel and Hubel, 1963). Wiesel and Hubel (1963) found, however, that the proportion of these binocularly driven cells was reduced to less than 1% in newborn kittens which had been deprived monocularly for two or more months during the sensitive period of visual development. It was subsequently proposed that amblyopia may be caused by an absence of binocular vision, resulting in a lack of competition for synaptic connections on binocularly driven cortical cells (Hubel and Wiesel, 1965; von Noorden, 1973; Cynader, 1982) or possibly LGN cells (Headon and Powell, 1973). Ikeda and her co-workers (Ikeda and Wright 1972, 1974; Ikeda and Tremain, 1978) further proposed that amblyopia is the result of an arrest of development caused by the habitual exposure of the fovea to defocussed images during the sensitive period. More specifically these authors suggest that it is the sustained retinal ganglion cells (X-cells) and LGN cells which are affected in amblyopia (Ikeda and Wright, 1974; Ikeda and Tremain, 1978). Physiological evidence for a primary afferent deficit in amblyopia has been provided by several authors who have shown that there is a reduction in retinal ganglion cell and LGN cell acuity in the cat (Ikeda and Wright, 1976; Ikeda and Tremain, 1979; Chino et al., 1980). These findings have been questioned by others who have shown that the retinal deficits depend critically on the techniques used to produce the amblyopia, it generally being necessary to cause immobilisation of one eye, as well as to disturb normal binocular interaction, before retinal abnormalities can be detected (Cleland et al., 1980, 1982; Crewther et al., 1982, 1985). Strong evidence for binocular interactions has been presented by several authors (e.g., von Noorden et al., 1976; Guillery, 1972; Kratz and Spear, 1976) but most studies have involved animals with stimulus deprivation amblyopia (but see also Eggers and Blakemore, 1978; Cynader, 1982).

In spite of the many similar characteristics exhibited by strabismic and anisometropic amblyopes, psychophysical studies in human amblyopia indicate that the two forms do

not always have identical properties. For example, Hess and his co-workers (Hess and Howell, 1978; Hess et al., 1980), extending the research of von Noorden and Burian (1959a, 1959b), demonstrated the effect of luminance on the contrast sensitivity function of strabismic amblyopes. They noted that the deficit that exists between the amblyopic eye and its fellow normal eye at photopic levels becomes negligible at scotopic luminance levels, whereas no similar effect was seen to occur in anisometric amblyopia. Furthermore Hess and Bradley (1980) showed that the difference between strabismic and anisometric amblyopes still exists at supra-threshold contrasts. Hess and Pointer (1985) measured contrast sensitivity as a function of visual field eccentricity, and again found differences between the two types of amblyopia; in strabismus the peripheral region of one or both hemifields is unaffected, whereas in anisometropia the sensitivity loss is distributed uniformly across the visual field. Hess and his colleagues suggest that these psychophysical differences may reflect differences in the neural basis of strabismic and anisometric amblyopia in humans. Other workers have also found differences between strabismic and anisometric amblyopes in terms of spatial properties of vision (Levi and Klein, 1982a, 1982b; Bedell and Flom, 1981, 1983; Flom et al., 1982).

Electrophysiological methods have also been used to investigate the extent of the deficit in amblyopia. Some studies measuring the visual evoked potential (VEP) using flashing, unpatterned stimuli have found anomalies in the response amplitude and latency for the amblyopic eye (Nawratski et al., 1966; Lawwill, 1973), whereas other studies have shown that the amblyopic eye seems to be normal in this respect (Fishman and Copenhaver, 1959; Levi, 1975). Further studies using pattern reversal chequerboard stimuli seem to indicate a reduction in the VEP from the amblyopic eye (Sokol and Nadler, 1979; Portnoy et al., 1983). The results of these VEP studies cannot provide exact information as to the site of the deficit in amblyopia, since the VEP signals mainly reflect electrical activity in

the striate cortex and do not, therefore, represent a specific localised response. A more useful electrophysiological approach in terms of localising the site of the deficit in human amblyopia involves the use of the electroretinogram (ERG). Again, however, the results are equivocal, with some workers reporting that many severe and untreatable amblyopes have a reduced pattern ERG (Sokol and Nadler, 1979; Arden et al., 1980a, 1980b; Arden, 1985; Arden and Wooding, 1985), whereas other workers report no evidence of any ERG abnormality (Nawratski et al., 1966; Burian and Lawwill, 1966; Hess and Baker, 1984; Hess et al., 1985).

Pupillomotor activity in amblyopia is of interest for two main reasons. Firstly, in view of the traditional belief that the pupil light reflex reflects the activity of the retino - pretectal pathway, the characteristics of the pupillary response may be used to localise the site of the abnormality in amblyopia. Secondly, from the clinical viewpoint, it is important to establish the normality or otherwise of the pupillary response to light in order to help differentiate a benign amblyopia from a more serious neuro - ophthalmological condition such as an optic nerve lesion. Harms (1938) was the first to investigate pupil responsiveness in amblyopic subjects. Using a telescopic observation system and perimetric light stimulation, he confirmed that in normal subjects stimulation of the central retina elicits a larger amplitude pupillary response than for equal stimulation of the peripheral retina, whereas for amblyopic subjects, stimulation of the central retina did not always elicit larger response amplitudes. Krüger (1961) reported that out of a total of 100 amblyopic subjects, 93 displayed anomalous pupillary responses when examined using a clinical testing procedure sensitive to pupillomotor asymmetry (the "pseudo - anisocoria test" of Kestenbaum). Drews (1962) on the contrary, using a similar clinical procedure with bright illumination (the "Gunn pupil test"), could find no evidence of pupillary defects in patients with amblyopia ex anopsia. Thompson (1966) recorded the pupillary responses of profoundly strabismic subjects (with surgically straightened eyes) using Lowenstein and Loewenfeld's

electronic pupillograph (see Lowenstein and Loewenfeld, 1958). He reported that such subjects displayed only minor pupillary response asymmetries which he felt were probably related to poor fixation of the amblyopic eyes. Soon after, ten Doesschate and Alpern (1967) reported that the pupillary constriction to light stimulation was dependent on which eye was fixing (or attending to) the stimulus. They used photographic methods to show that, in two strabismic subjects, the amplitude of the pupillary constriction was more marked when light stimulated the fixing eye than the non - fixing eye, irrespective of whether the fixing eye had the poorer visual acuity. Brenner et al. (1969) examined the responses of sixteen subjects (nine amblyopic and seven normal) to light stimuli of high luminance (ranging from about 140 cd/m² to 14 000 cd/m² on a 14 cd/m² background). Using Lowenstein's pupillograph combined with a haploscope, they confirmed Doesschate and Alpern's finding that stimulation of the fixing eye causes a greater constriction of both pupils than equal stimulation of the the non - fixing or suppressed eye. They found that this effect was greater for amblyopic subjects than for normal subjects, but was dependent on the level of illumination, and also on the depth of amblyopia (or suppression). They also noted that as suppression in amblyopia deepens (one assumes with more severe types of amblyopia), the pupillary response to light in the affected eye diminishes when compared to its fellow normal eye. On average (i.e., across all amblyopic subjects and for all luminance levels), the response amplitude of the amblyopic eyes were about 0.45 mm less than for their fellow normal eyes.

The "swinging flashlight test" involves the use of a bright light source which is projected on to one eye for about 5 seconds until the pupil stabilises, and then moved rapidly to the other eye. The light source is then swung from one eye to the other so that the duration of illumination of each eye is approximately equal. An afferent pupillary defect is said to be present when the initial pupillary constriction is reduced or absent and the redilation (or pupillary escape) rapid (see Levatin, 1959; Ashworth and

Isherwood, 1981). More recently, two studies have used the swinging flashlight test to investigate pupillary behaviour in amblyopic subjects and quantitatively they report very different results. Greenwald and Folk (1983) report that only 4 out of a total of 45 amblyopic subjects were diagnosed as having "probable" afferent pupillary defects and no subject was judged to have a "definite" defect (responses were grouped into five categories ranging from definitely normal to definitely abnormal). They found that there was no relationship between either the severity or the type (i.e., whether anisometropic or strabismic) of amblyopia and the likelihood of an abnormal pupillary response. Portnoy et al. (1983) on the other hand found that 45 out of 55 amblyopic subjects displayed an afferent pupillary defect. In this study they utilised neutral density filters to quantify any observed pupillary deficit, placing a filter over the better eye until pupillary responses were equalised. In this way they determined that the mean afferent pupillary deficit for the entire group was equal to 0.26 log units. This figure is obviously quite small in terms of the clinical nature of the test, but the authors point out that 29 subjects had clearly visible pupillary defects of 0.3 log units or greater. Again they could find no correlation between either the depth or the type of the amblyopia and the magnitude of the defect.

Whilst several studies have attempted to measure the amplitude of the pupillary response in amblyopia, fewer have presented data on the latency of the response. Dolének (1960) used a cinematographic pupillography technique, and found that the latencies of contraction and dilation for the pupillary response to light were longer for amblyopic eyes. More recently Kase and his colleagues (Kase et al., 1984) recorded pupillary responses to low intensity stimuli of diffuse light using an infrared electropupillogram. They found that whilst the response amplitude and constriction velocity were not significantly different in amblyopic and normal eyes for the majority of the fifteen subjects studied, longer response latencies were recorded for the amblyopic eyes of ten subjects. In accordance with other

studies they could find no significant correlation between the latency difference and the subjective visual acuity.

Under conditions of steady - state illumination, pupil diameter is smaller for binocular viewing when both eyes are illuminated than when only one eye is illuminated and the other occluded. Binocular luminance summation may therefore be defined as the increase in pupil diameter from a binocular viewing condition to a monocular viewing condition. Sireteanu (1987) has found that subjects with no functional binocularity (i.e., amblyopes) show much less binocular summation of the pupillary response than normal subjects. Her findings indicate that binocular summation of the pupil can be used as a test for the simultaneous use of the two eyes, i.e., an index of suppression.

It can be seen therefore that the evidence for a pupillary anomaly in amblyopia is equivocal. Unfortunately, many of the studies to date have used methods which have not been quantitative in either stimulus administration or in pupillary measurement and analysis. In the main, studies have been based on informal clinical observation and there appears to be a great deal of variability in the incidence of any pupil response abnormality detected (Krüger, 1961; Portnoy et al., 1983; Greenwald and Folk, 1983). Clearly further quantitative investigation is required to resolve the issue of whether there are anomalies in the amplitude of the pupillary response to unpatterned light stimulation in amblyopic eyes. Furthermore, since it has been shown that a contrast sensitivity deficit exists in amblyopic eyes (Hess and Howell, 1977; Bradley and Freeman, 1981), it would be of interest to determine if this deficit is reflected in the response of the "amblyopic pupil" to suprathreshold grating stimuli of fixed luminance.

CHAPTER 2

EQUIPMENT AND METHODS

2.1 EQUIPMENT USED FOR COLOUR CONSTANCY STUDY

Computer - controlled colour monitors have become a convenient way of producing the stimulus configurations required for experiments in visual psychophysics (Cowan, 1983; Rodieck, 1983; MacLeod, 1986; Arden et al., 1988a; 1988b; Brainard, 1989; Post and Calhoun 1989). They provide a relatively versatile way of varying the spatial, temporal and chromatic properties of a stimulus, without the need for construction of specific mechanical and optical components associated with more traditional methods.

Any technology, however, has limitations and specific calibration problems which must be investigated thoroughly before it can be used with confidence. Accurate control of the stimulus is possible only if the relation between the specified luminance value and the corresponding output of the monitor is known. Because of the large number of stimulus configurations that may be displayed, direct measurement of this relation is not practically possible, and therefore it is necessary to make assumptions about the monitor's performance. Common assumptions include those of spatial independence (Brainard, 1989), those of phosphor constancy, and those of phosphor independence (Cowan and Rowell, 1986). The assumption of spatial independence is that the monitor's output at a location depends only on the input values for that location. The assumption of phosphor constancy is that the relative spectral power distribution of the light emitted by a phosphor does not vary with the intensity of stimulation of the phosphor. The assumption of phosphor independence is that the intensity of stimulation of a phosphor is determined by the input value for that phosphor, and is independent of the input values of the other two. These three assumptions allow the spectral power distribution of the monitor's output at a single location to be predicted from the input values, measurements of the

three phosphor spectral power distributions, and measurements of the three phosphor input - output relations.

The following sub - sections describe the equipment and calibration procedures employed in the study of colour constancy described in Chapter 3.

2.1.1 DISPLAY HARDWARE

The visual display unit employed in the study was a Mitsubishi 14" high resolution RGB monitor (model C-3419SP) operating at a vertical frequency of 80 Hz. The monitor incorporates a short persistence P22 phosphor. The unit was driven by a Vectrix colour graphics adaptor controlled by an IBM AT computer. The Vectrix adaptor provided a screen resolution of 672 x 480 pixels. The graphics memory on the Vectrix board is organised as nine bit planes, and each pixel's colour is determined by combinations of the nine bits. Therefore, since there are 2^9 combinations possible, up to 512 colours can be stored in the colour look-up-table at any given time. When a colour look-up-table entry is referenced, three, eight bit values are output to the RGB monitor i.e., the red, green and blue signals. These three values control the intensities of each of the three colour guns in the monitor, and hence the phosphor intensities. Thus, with 0 - 255 intensities available for each gun, a possible 16.8 million colours can be generated.

For most of the experiments, the subject viewed the monitor from a distance of 55 cm with his head positioned in a chin and forehead rest. At this distance the screen subtended a visual angle of $23.1 \times 17.1^\circ$ in the horizontal and vertical direction, respectively. For the sake of symmetry however, the screen dimensions were restricted to 480 x 480 pixels which equates to a visual angle of $17.1 \times 17.1^\circ$.

2.1.2 MONITOR CALIBRATION

A telespectroradiometer was used to obtain a measure of the spectral power distributions of the monitor phosphors. This

consisted of an Applied Photo - Physics monochromator, Gamma Scientific high efficiency photometric telescope (model 2020-31), digital radiometer (model 2009) and photomultiplier. The device had previously been interfaced with a PC XT and the available software allowed for the computation of various photometric quantities, including the CIE chromaticity co - ordinates and luminances. The radiometer output was calibrated against a GEC standard lamp run at 25 Amps, for which NPL spectral radiance data were available.

After some preliminary adjustments, the monitor gain control was secured so that no accidental alterations could be made. A target area of 100 pixels square was chosen and the telescope focused on this from a distance of 1 m using a 1° aperture. An arbitrary look-up-table value of 100 was output to the monitor over the test area to set the phosphor intensity. The room was darkened and radiometric readings were taken at 5 nm intervals throughout the visible spectrum (380 - 775 nm) for each phosphor separately. Table 2.1 shows the luminances and chromaticity co - ordinates computed from each radiometric scan, and Figure 2.1 plots the spectral power distribution for each phosphor. A further radiometric scan showed the ambient screen luminance to be 0.4 cd/m².

PHOSPHOR	LUMINANCE(cd/m ²)	CHROMATICITY CO-ORDINATES		
		x	y	z
Red	2.86	0.6262	0.3448	0.0290
Green	6.90	0.2089	0.7037	0.0874
Blue	1.69	0.1467	0.0677	0.7856

Table 2.1. Phosphor luminances and chromaticity co-ordinates for Mitsubishi monitor.

In order to verify the independence of each phosphor, a scan was also carried out for all three phosphors emitting together (thus producing a "white" test area), again with look-up-table values of 100 for each phosphor. The luminance measured in this way was 11.55 cd/m², which represents a difference of less than 1% when compared with the summated luminance obtained when the luminances for each phosphor were measured separately (see Table 2.1). To test the assumption of phosphor constancy, the phosphor spectral

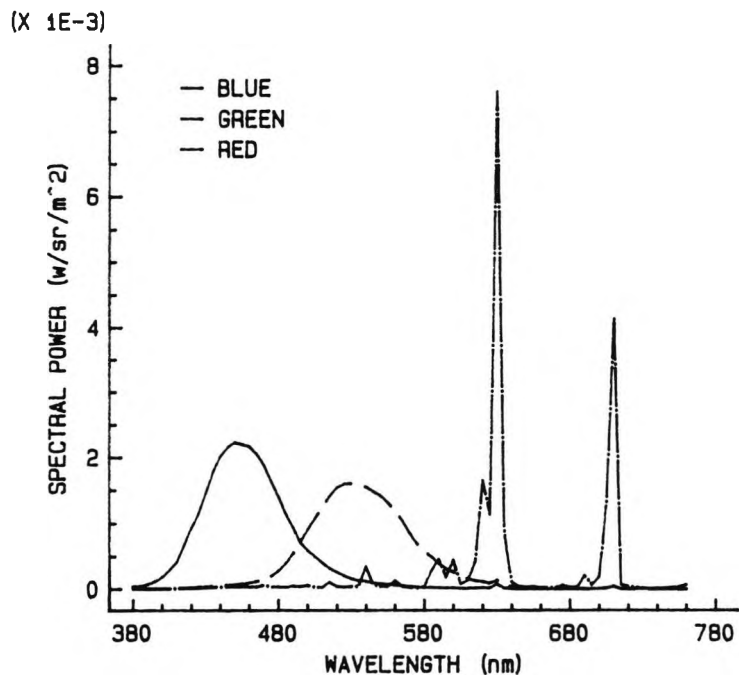


Figure 2.1. Spectral power distributions measured for the three phosphors in the Mitsubishi monitor.

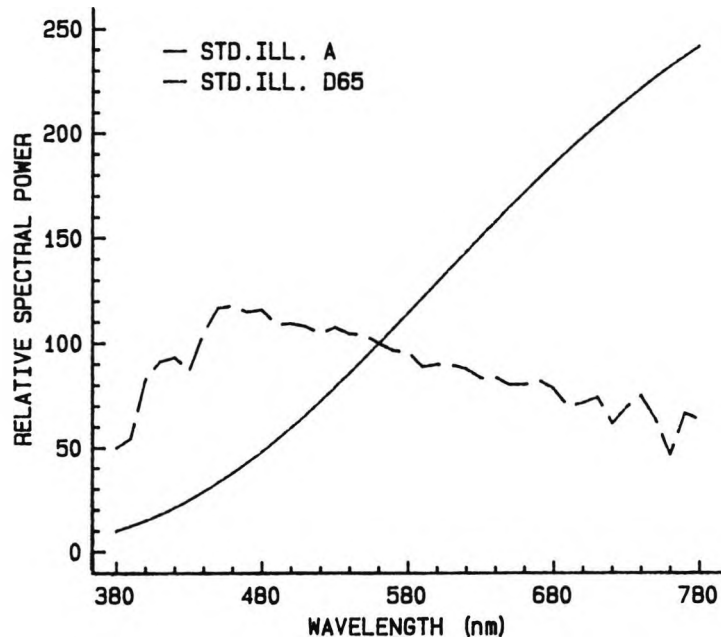


Figure 2.2. Relative spectral power distributions of CIE Standard Illuminants D₆₅ and A.

power distributions were remeasured at a higher intensity corresponding to a look-up-table value of 200. Regression analysis showed a root mean squared error in fit of less than 1% for each of the three phosphors when the low intensity and high intensity measurements were compared at each wavelength. Similarly there was little change in the chromaticity co - ordinates of each phosphor in the test area when the latter was presented with a white surround.

The time taken to run a scan using the telespectroradiometer (approximately 4 minutes) was prohibitively long for the daily monitor calibrations which proved to be necessary. In addition, the equipment was often required elsewhere within the laboratory, and it also proved somewhat cumbersome in the limited space available. Consequently an Oriel radiometer (Model 7072) and UDT photopic response photodiode were calibrated with the GEC standard lamp and used to make screen luminance measurements by positioning the photodiode directly against the screen. Conversion factors were computed by comparing the photometer's readings with integrated luminance values measured with the telespectroradiometer.

In order to be able to determine the output of each phosphor for a particular look-up-table value, photometric measurements were taken for a range of look-up-table values using the Oriel detector. Preliminary measurements allowed the simulation of a surround to the 100 pixel square test area which approximated to either CIE Standard Illuminant D₆₅ or CIE Standard Illuminant A (see Figure 2.2), thereby replicating scene parameters to be used in the study (see Chapter 3). The relationship between look-up-table value and phosphor output is often said to approximate a power function (Post and Calhoun, 1989), such that an equation of the form $\log Y = a + b \times \log D$ should fit the data, where Y is the light intensity, a and b are constants, and D is the voltage. Figure 2.3 shows the logarithm of the detector response plotted as a function of the logarithm of the look-up-table value for a surround approximating Standard Illuminant A.

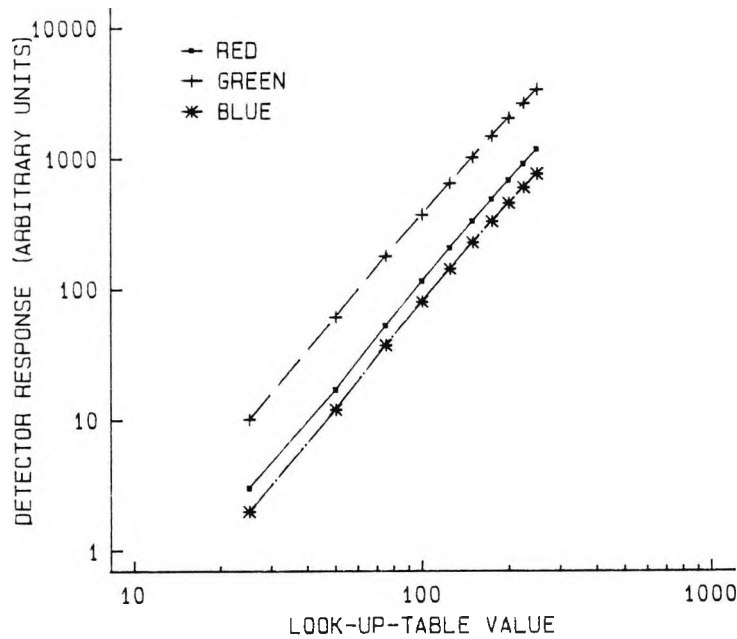


Figure 2.3. UDT photodiode response (i.e., phosphor output) as a function of look-up-table value measured for each of the three Mitsubishi monitor phosphors.

Regression analysis allowed the determination of equations which best fit the data for each phosphor. The gradient and intercept of each straight line were then used in a power law relationship in order to determine the phosphor luminance relating to the look-up-table values input. Thus, for example, the green phosphor luminance (LG) is given by:

$$LG = GI \times Q^{GG}$$

where GI is the intercept, Q is the look-up-table value and GG is the gradient.

The temporal stability of the monitor was also investigated by measuring the output of each phosphor on different days, and at different times on the same day. Relatively large variations in phosphor luminance were noted from day to day and during the initial warm - up period. In particular it was the green phosphor which demonstrated the greatest variability, with changes in phosphor luminance of up to 15% occurring on separate days and during the warm - up period.

The luminance of the other two phosphors varied by no more than 5%. Table 2.2 shows luminance measurements for each of the phosphors for a look-up-table value of 200, taken at various intervals after the warm - up period on the same day. As can be seen from this table, the luminance variations noted over this time course were small, and furthermore could be considered to be negligible over the duration of a single experiment (i.e., approximately half an

<u>TIME AFTER WARM - UP</u> (HOURS)	<u>PHOSPHOR LUMINANCE (cd/m²)</u>		
	RED	GREEN	BLUE
0	15.16	33.01	9.04
1	15.37	33.30	9.12
1.5	15.34	33.36	9.14
2	15.29	33.33	9.10
3	15.15	33.27	9.14
4	15.21	33.40	9.11
5	15.18	33.25	9.09

TABLE 2.2. Phosphor luminance variation with time.

hour). Consequently the monitor was calibrated immediately before each experiment using a shortened version of the calibration program described above.

It was a requirement that the physical characteristics of the scene generated on the monitor should be changeable both spatially and temporally (see details in Chapter 3). In order to determine the actual time taken for each phosphor to change from one luminance level to another it was necessary to measure the phosphor decay times. For this purpose, a Nicolet digital storage oscilloscope (Model 3091) and fast response photodiode (UDT) were used. Tracings of the isolated phosphor decay times are shown in Figure 2.4 (A), from which it can be seen that the green phosphor has the longest decay time of about 12 ms. In addition, measurements of the decay time were taken for the combined output of the three phosphors and these are reproduced in Figure 2.4 (B). In this case, however, the chromaticity and luminance of the test area were modified as the output was monitored so as to simulate a change from Standard Illuminant D₆₅ to Standard Illuminant A. It can be seen that the output increases accordingly within the space of one cycle (which is equivalent to about 11 ms).

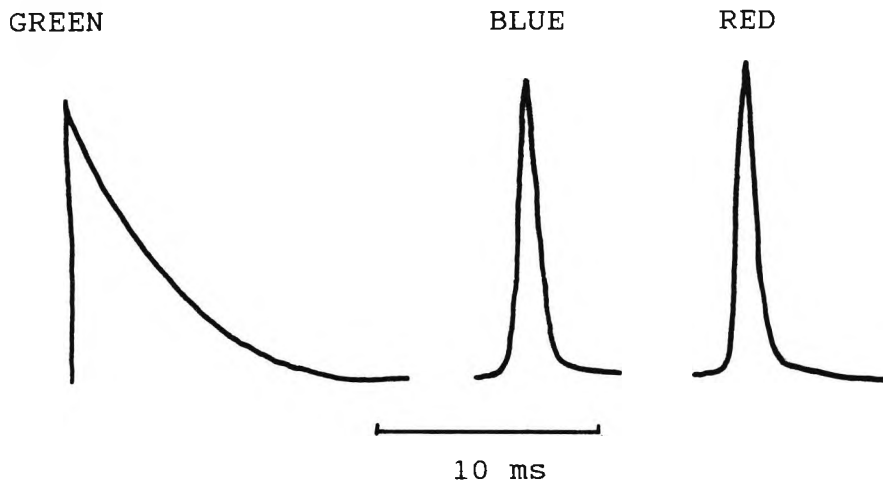


Figure 2.4 (A). Phosphor decay times recorded using the Nicolet oscilloscope and UDT fast response photodiode.

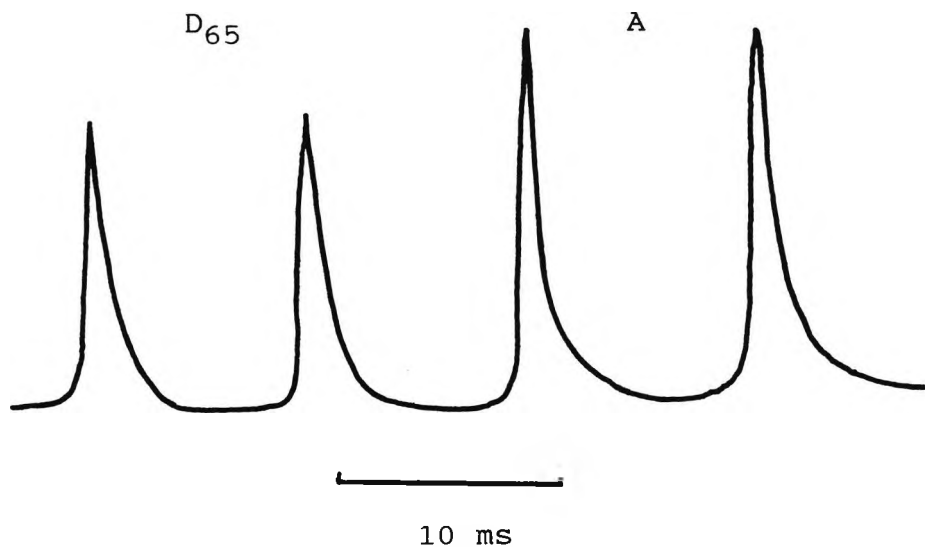


Figure 2.4 (B). Decay times for the combined output of the three phosphors when changing from Standard Illuminant D₆₅ to Standard Illuminant A.

2.1.3 REPRODUCTION OF COLOURED SAMPLES

It was desirable that the chromaticity of any specified colour sample could be accurately reproduced on the monitor. As a basis for describing the colour samples, the Munsell colour order system was chosen, as this has been most widely used in comparable studies. The colour samples are painted paper chips which are arranged to form an atlas, the Munsell Book of Color (for description see Hunt, 1987). Ten, matt chips were chosen which were distributed fairly uniformly throughout colour space. The spectral reflectance of each chip was determined using the Perkin Elmer spectrophotometer and the resulting curves are displayed, together with the corresponding Munsell Notation in Figure 2.5.

An algorithm was developed to allow the simulation of any colour object under any illuminant (see Appendix). In order to verify this algorithm and the measured spectral reflectance functions, the computed x and y chromaticity co-ordinates for the ten Munsell chips were compared with those given by Wyszecki and Stiles (1982) for Standard Illuminant C. The comparative data are listed in the following table (Table 2.3) and show remarkably small differences. Note that for four of the chips the Munsell

MUNSELL NOTATION	CHROMATICITY CO-ORDINATES(x,y)			
	WYSZECKI & STILES		COMPUTED	
5B6/6	0.2320	0.2789	0.2330	0.2761
5BG6/6	0.2441	0.3290	0.2493	0.3285
5G7/6	0.2801	0.3721	0.2839	0.3693
5GY7/6	0.3581	0.4291	0.3568	0.4267
5Y7/6	0.4009	0.4198	0.3978	0.4132
5YR7/6	0.4091	0.3701	0.4152	0.3658
5R6/6	0.3921	0.3244	0.3737	0.3165
5P6/6	0.2950	0.2585	0.2930	0.2476
5PB6/6	0.2533	0.2558	0.2547	0.2566
5RP6/6	0.3520	0.2904	0.3458	0.2883

Table 2.3. Comparison of computed chromaticity co-ordinates for selected Munsell chips, with equivalent data from Wyszecki and Stiles (1982) for Standard Illuminant C.

Value is 7, and not the 6 used to measure the spectral reflectance. However, since Munsell Value refers to the

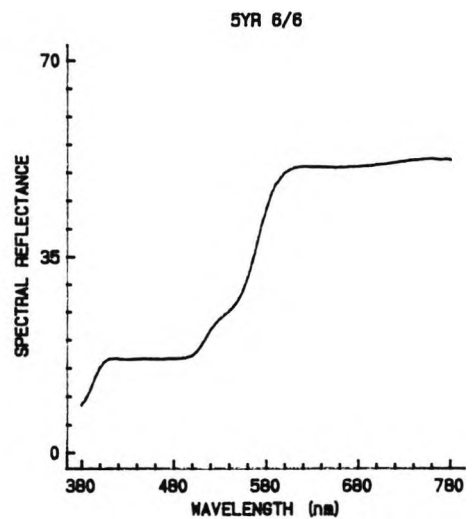
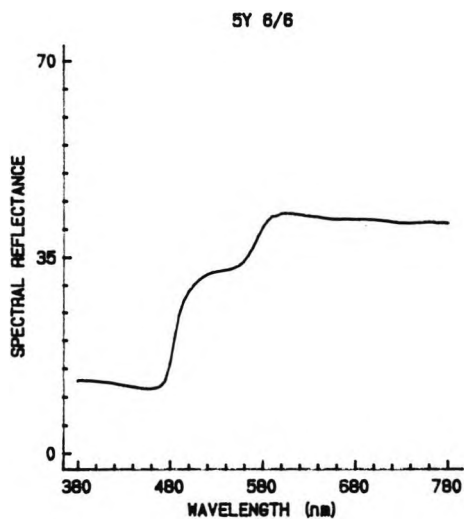
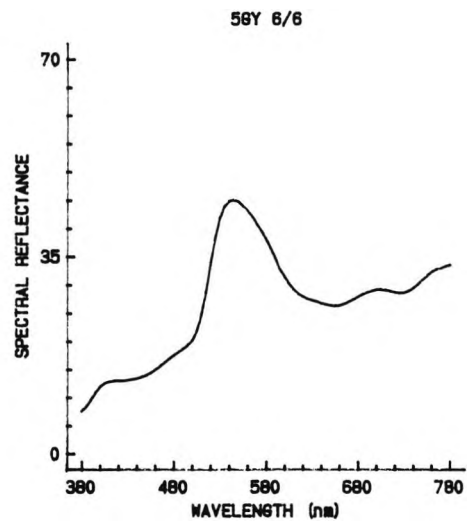
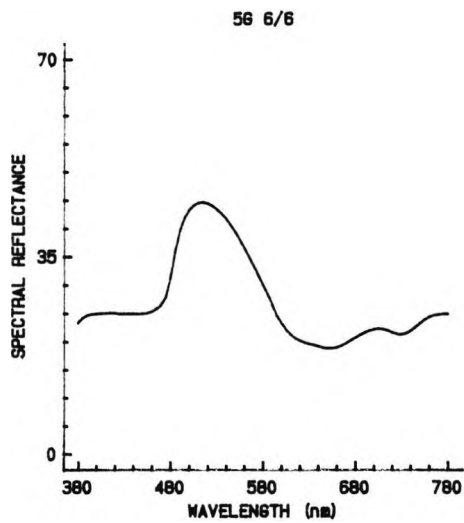
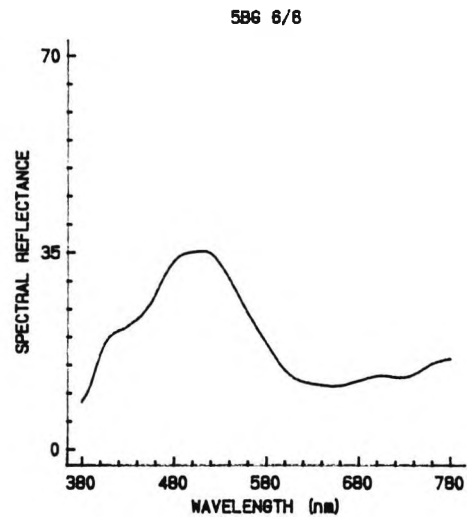
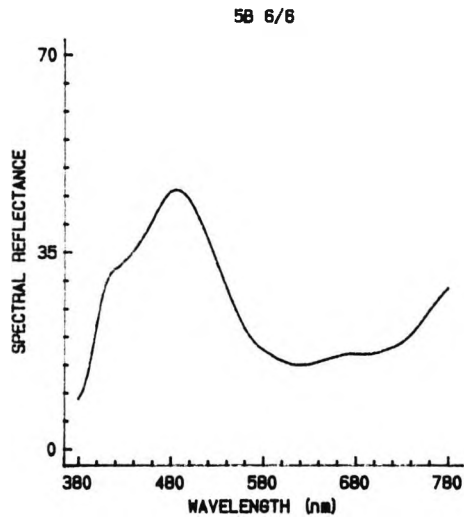


Figure 2.5. The spectral reflectance functions of the Munsell chips used as the basis for the colour samples reproduced in the colour constancy experiment. Measurements were made with the Perkin Elmer spectrophotometer. Contd....

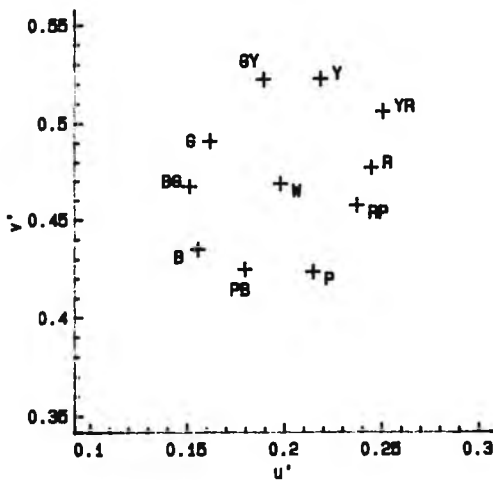
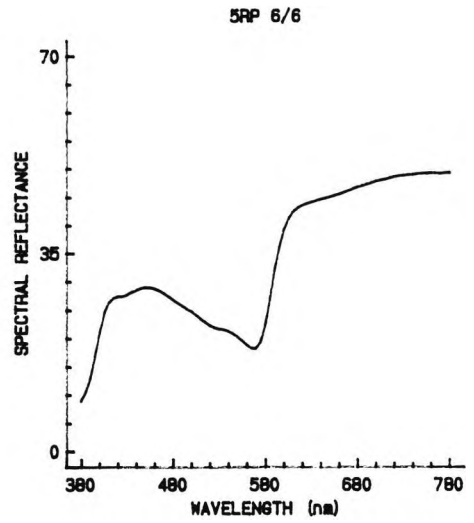
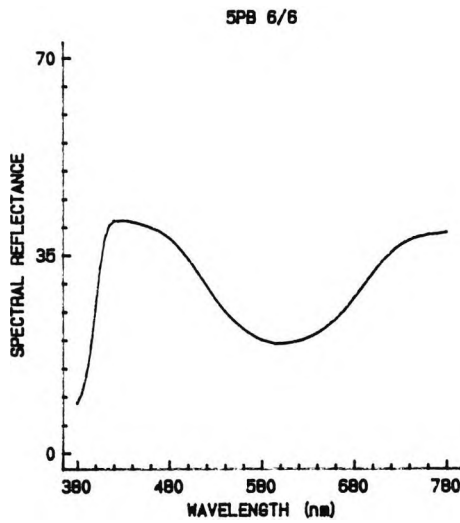
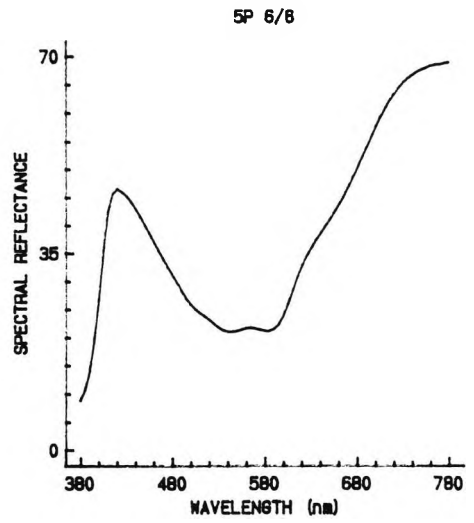
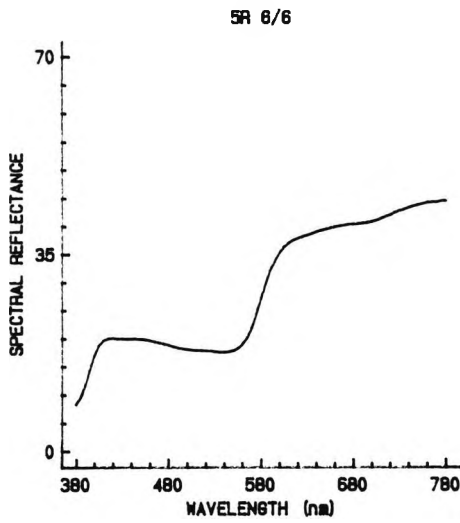


Figure 2.5 contd. The Munsell Notation is given above each diagram. The lower diagram above shows the position of each of the chips, together with a white, w, on a CIE UCS diagram.

degree of lightness of a sample, then this does not affect the chromaticity co - ordinates which describe that sample.

2.2 EQUIPMENT USED IN PUPILLOMETRY STUDY

Several techniques for measuring pupil size have been developed and early techniques involved subjective assessment, e.g., the Haab Scale, or even subjective self - assessment, e.g., using the Scheiner disc principle (for a review see Alexandridis, 1985). The two most popular techniques used today are based on either: (a) principles of infra - red reflex photometry (Mathes, 1941; Cuepers, 1951); or (b) the principle of video - image processing (Lowenstein and Loewenfeld, 1958). An example of an instrument employing the former technique is the Heidelberg Pupillograph (Alexandridis, 1968). The device has a high temporal resolution, and has therefore proven to be ideal for analysing the temporal characteristics of the pupil light reflex. An example of a device using the second principle which makes use of digital processing of video images has been developed by Barbur et al. (1987b) and recently updated (see Alexandridis et al., 1991). The P_SCAN 100 system designed by these authors was the system used in the present study and it allows for the simultaneous binocular measurement of pupil size and two - dimensional eye movements.

2.2.1 PUPILLOMETER HARDWARE

Figure 2.6 shows a schematic diagram of the basic apparatus. The subject sits on a height - adjustable chair with the head positioned on chin and forehead rests, and immobilised by adjustable head - clamps. The infra - red (IR) iris illumination system, IR - sensitive CCD sensors (EEV) and camera lenses are all mounted on a twin instrument base unit. This base unit, adapted from a Zeiss instrument table, allows the necessary adjustment required for interpupillary distance, height and image focus. Light emitting diodes (LED's) provide uniform, IR illumination of the iris with

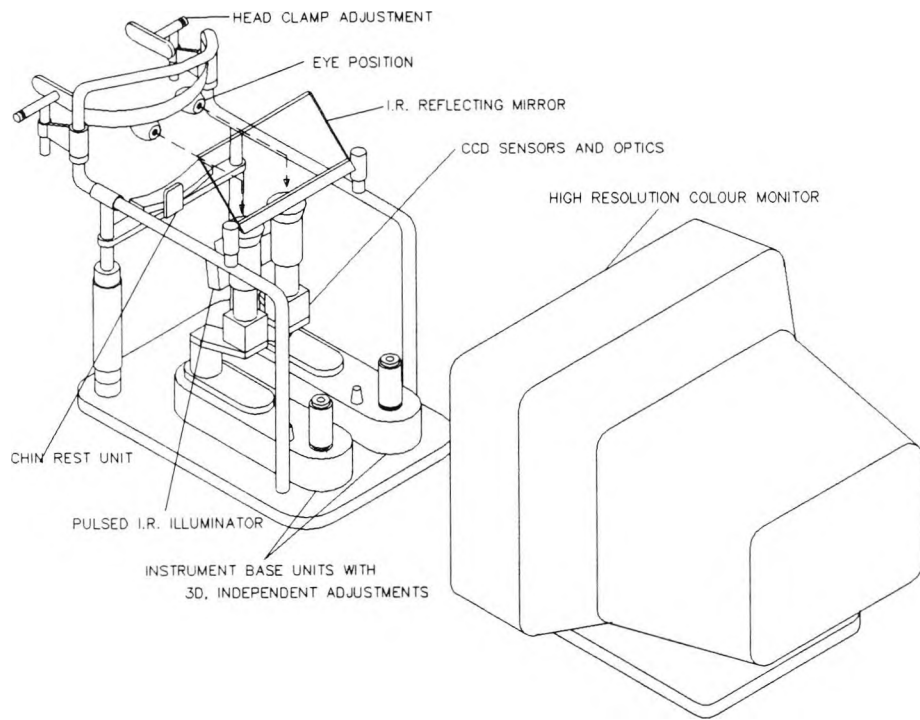


Figure 2.6. Schematic drawing of the P_SCAN 100 system which allows the simultaneous binocular measurement of pupil size and eye movements. See text for detailed description of apparatus. (From Barbur, Hess and Pinney, in preparation).

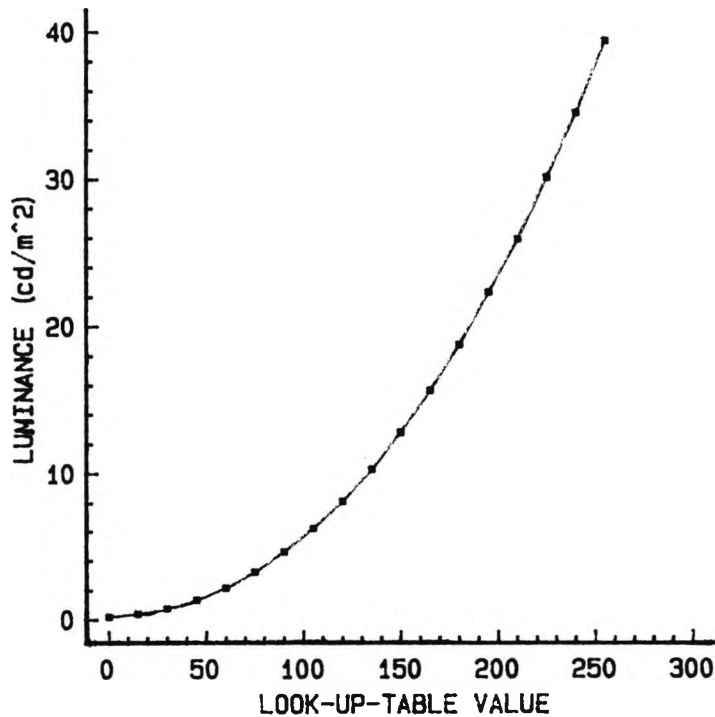


Figure 2.7. Screen luminance level plotted as a function of grey level look-up-table value for the Ayadin monitor used in the pupillometry experiments.

specular images outside the pupil area. This illumination system is pulsed for 4 ms within each image frame so as to minimise image smear caused by rapid eye movements. An IR - reflecting mirror which transmits about 95% of visible light is positioned in front of the subject and at 45° to the horizontal. This mirror provides the reflected image of the pupils for the CCD sensors whilst allowing the subject a clear field of view.

Reduced, non - interlaced video signals are produced every 20 ms and are relayed to two specialised adapter boards in a standard IBM AT computer. The signals are processed and a series of pre - selected, equidistant scan lines generated (see Barbur et al., 1987b). The intersection co - ordinates between the pupil / iris border and these scan lines can then be extracted and stored for later analysis. The number of scan lines employed is variable, and can be set to 16, 32 or 64, but for the purpose of this study only the 32 - line setting was used. This setting gave a sufficient degree of accuracy and reduced the amount of raw data to be processed. The analysis algorithm fits the best circle to each set of raw data points and extracts the pupil diameter and its centre spatial co - ordinates. This algorithm and the errors involved in computing the relevant parameters have been described elsewhere (Barbur et al., 1987b).

Separate images of each eye were displayed on two Hitachi (VM 1220) monochrome monitors. This allowed for the correct positioning of the subject at the beginning of each experiment, and also to monitor alignment and focus throughout the course of each experiment. In addition they were used to set the optimum threshold level for edge detection, which was found to vary from subject to subject depending on iris pigmentation. When set correctly, a circular array of dots appeared to be superimposed on the pupil margin in the video image.

For monocular presentation of the stimulus and binocular recording of pupil responses, an IR - transmitting filter (Kodak type 88A) which blocks all visible light may be

mounted in a modified spectacle frame and used to occlude one eye. Observer refractive errors may be corrected either with soft contact lenses or with spectacles, though with the latter unwanted specular reflections can sometimes be a problem.

2.2.2 GENERATION OF VISUAL STIMULI

In previous studies using this system (Barbur et al., 1987b), Maxwellian stimulation has been used, but complex stimuli are more easily generated with the aid of a visual display unit. For the purpose of this study therefore, stimuli were generated on one of two monitors: an Ayadin 8886 high resolution colour monitor and a Tektronix 608 CRT.

The 19" Ayadin monitor operated at a frame rate of 60 Hz, and was driven by a Pennant graphics card in conjunction with the IBM computer. Screen resolution was 1024 x 768 pixels in the horizontal and vertical respectively and, with approximately 0.33 mm per pixel, provided an angular subtense of $18.7 \times 14.2^\circ$ when viewed at a distance of 1 m. The graphics adaptor gave 8 bits of intensity i.e., 256 levels, for each colour primary allowing the generation of a possible 16.8 million colours. The spectral power distribution and chromaticity co-ordinates of the screen phosphors were determined using a Gamma Scientific telespectroradiometer (see section 2.1.2). Screen luminance measurements were made with the aid of a LMT (L1003) photometer. Figure 2.7 plots screen luminance as a function of grey level look-up-table number. The monitor was recalibrated at regular intervals and allowed at least a half an hour "warm-up" period before any experiments were conducted.

For certain experiments it was desirable to produce achromatic grating stimuli with high spatial frequencies (see Chapter 4 section 1.2). For this purpose a Picasso pattern generator linked to a Tektronix monitor was used, and this combination provided a higher spatial resolution than could be obtained accurately with the Ayadin monitor.

The visual display subtended $7.0 \times 5.4^\circ$ when viewed at a distance of 1m. The necessary contrast calibration was performed with the aid of the LMT photometer and Nicolet storage oscilloscope. The maximum contrast obtainable without introducing significant luminance components was 0.6.

For both of the monitors used, the space - averaged luminance of the grating stimuli presented differed from the luminance of the background by less than 1%.

2.2.3 PUPILLOMETER CALIBRATION AND MEASUREMENT ACCURACY

The diameter of a circular, artificial pupil was measured using a travelling microscope. The artificial pupil, consisting simply of a black disc on a white surround, was placed in the pupillometer system and the appropriate calibration constant derived for each eye. Figure 2.8 overpage shows the averaged diameter trace for 15 separate recordings with an artificial pupil of diameter 7.46 mm. The high frequency component visible in this figure illustrates the inherent electronic noise in the system which can cause typical measurement errors of up to 0.01 mm. Other practical sources of error, such as slight image defocus and non - uniformities of illumination over the iris, can cause additional errors of no more than 0.01 mm. The spatial coordinates of the pupil centre are computed with a similar accuracy, which translates to a maximum eye movement error of some 2 min of arc (see Barbur et al., 1987b).

The temporal resolution of the system is limited by the frame rate of the video signals (i.e., 50 Hz). However, Barbur (1989) has shown that normal video rates are sufficient to reproduce all the information present in the pupil response, and an increase in sampling frequency would not in any way improve measurement accuracy.

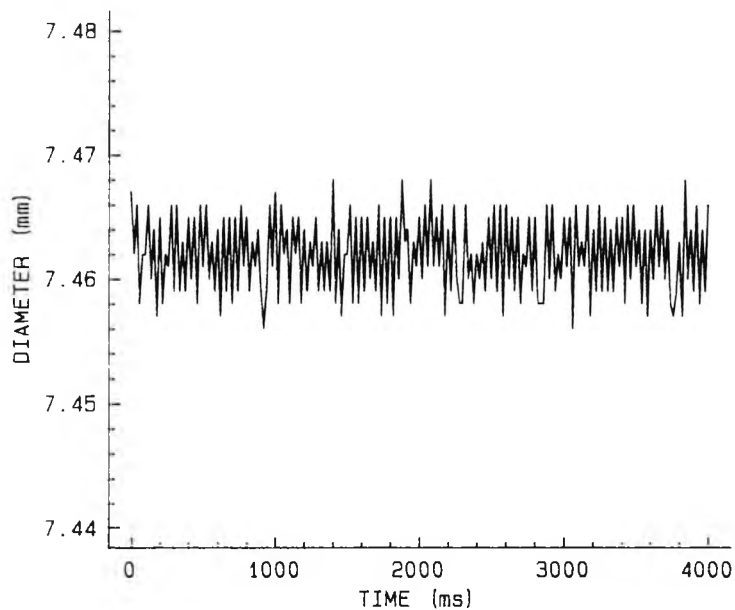


Figure 2.8. Averaged diameter trace for 15 separate recordings of a 7.46 mm artificial pupil over a time period of 4 seconds.

Figure 2.9 shows measurements of pupil diameter for a real eye in response to a low contrast grating stimulus. The smooth line represents the average of 64 traces, the first eight of which are also shown. The single recording traces show random pupillary fluctuations which tend to mask the smaller amplitude, stimulus - specific pupil response. However, these random pupillary fluctuations are eliminated by the averaging process, which effectively increases the signal to noise ratio for the stimulus - specific responses. This is the case because the noise part of each trace is statistically uncorrelated. The signal to noise level may be defined as the ratio of the signal and root mean square noise amplitudes, and therefore the averaging of n traces will increase the signal level (i.e., the stimulus - specific pupil response) by a factor n , and the root mean square noise deviation by the square root of n . Hence the signal to noise ratio will increase by the square root of n (Dawson, 1951).

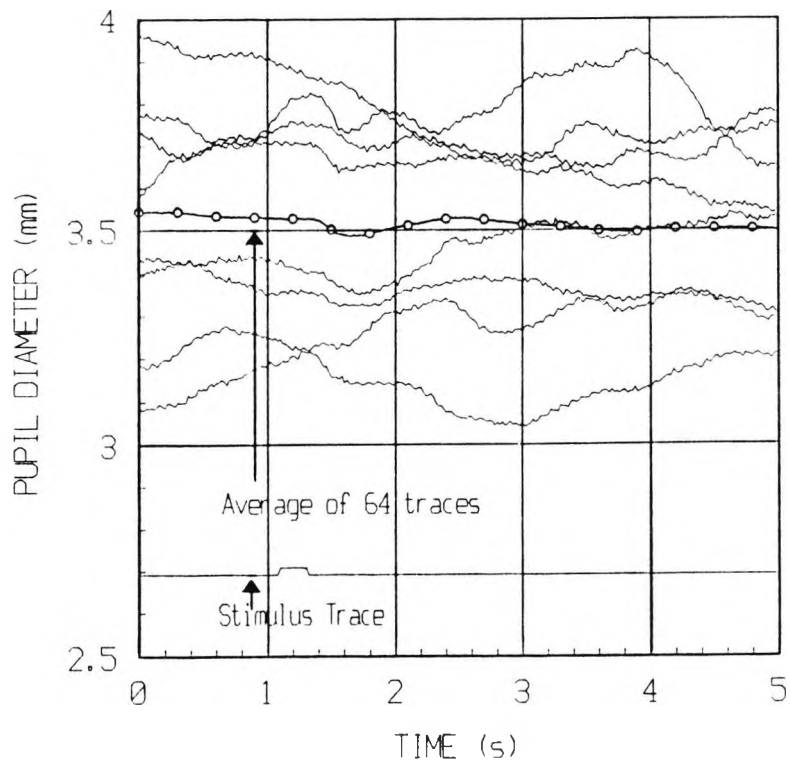


Figure 2.9. Eight single traces showing the response of the pupil to a low contrast (4%) sinusoidal grating of spatial frequency 1.2 c/deg. Note the normal drift in the steady state pupil size. The smooth curve represents the average of 64 traces. Response amplitude was 0.38 mm and latency 280 ms.

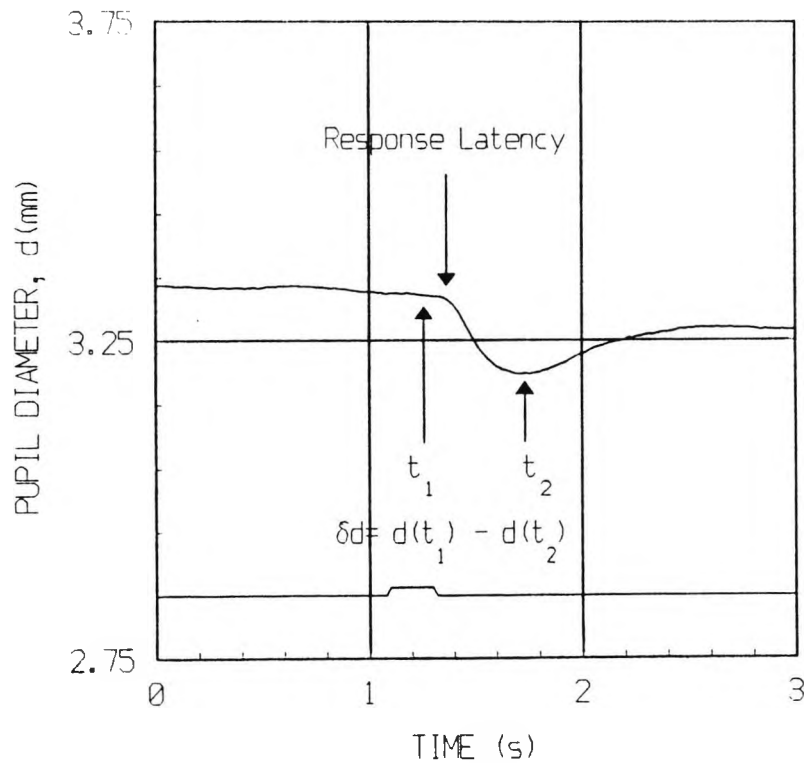


Figure 2.10. Diagram showing the extraction of the response amplitude and response latency from an averaged pupil trace. The response amplitude represents the difference between the pupil diameters (δd) recorded at times t_1 and t_2 . The response latency refers to the time taken for the pupil to respond i.e., constrict following the onset of the stimulus.

Two parameters are of particular interest when analysing pupil traces, namely, the response amplitude and the response latency (see Figure 2.10). The response amplitude refers to the transient change in pupil diameter produced by the stimulus and may be measured either as a percentage change, or as a difference in pupil diameter or area. It has been shown that the change in pupil diameter associated with a stimulus is approximately independent of the pre - stimulus pupil diameter. Hence this measure should be used in preference to percentage changes to quantify the amplitude of pupillary responses (Alexandridis et al., 1991; Lowenfeld and Newsome, 1971).

The response latency gives a measure of pupil responsivity as a function of time in relation to a particular stimulus. The use of the averaged trace in latency determination has been justified by Lee et al. (1969) and later by Keenleyside (1989). These authors pointed out that if there was no increase in the standard deviation associated with the average trace around the point of the maximal rate of constriction, then the average trace was a reliable predictor of the response latency. This fact has been confirmed by my own observations, and therefore in this study, the average trace has been used to extract the latency parameter. In order to measure the pupil response latency accurately, the averaged trace was viewed under high magnification and the latency determined using graphical cursor methods. This method proved to be consistent with an accuracy of 20 ms. Other methods of latency extraction, e.g., by calculation of velocity or acceleration changes, fail to yield significantly more accurate results (Keenleyside, 1989).

A description of the statistical approach employed when analysing the data from experiments with normal and amblyopic subjects is given in Chapter 4.

The software developed for use with this system allowed for extensive analysis of data with library functions provided for the extraction of the parameters outlined above i.e.,

averaged response amplitude and latency. Functions are also provided for the elimination of blinks, digital filtering of high frequency noise, the measurement of noise variance, and various other parameters of interest may be extracted from the processed data files.

2.3 MEASUREMENT OF INCREMENT THRESHOLDS DURING INTENSE FLASHES OF LIGHT

In order to measure the change in threshold sensitivity caused by intense flashes of light directed towards the eye (see Chapter 6), a monocular Maxwellian view optical arrangement was designed and constructed. This type of system, first described by James Clerk Maxwell in 1860, involves imaging a light source in the eye's pupil instead of viewing it directly (Westheimer, 1966). The technique has several distinct advantages over ordinary viewing, the main being that there is a more efficient use of light available from the source such that high retinal illuminances are attainable over larger fields of view. In addition, the focus of such a system may be adjusted to compensate for observer refractive error, and the use of an artificial pupil eliminates the variation of retinal illuminance with pupil size.

As this series of experiments progressed a number of modifications were made to the original optical system. The following section describes the completed arrangement of the three channel Maxwellian view system.

2.3.1 EQUIPMENT

All optical components were mounted in holders and secured onto optical benches. The optical benches were fixed firmly to a large black sheet of wood which was in turn secured to the top of a heavy table. A height - adjustable observation chair was positioned at one end of the table. A dental bite attachment was secured to the table in front of the chair and allowed for both vertical and horizontal positioning of

the observer relative to the system's optical axis. The observer bites on a dental impression which immobilises the head. All experiments were performed in a darkened room and the observer and apparatus enclosed by black curtains.

A schematic representation of the optical apparatus is shown in Figure 2.11. The source, S, was a 100 W tungsten halogen lamp of colour temperature 3340 K, driven by a stabilised 12V DC supply and cooled by a small electric fan positioned directly above. The lamp was switched on for at least 15 minutes before any measurements were taken. This single light source produced a rectangular image (2.5 x 1.5 mm) in an artificial pupil, AP, of 4 mm diameter. The artificial pupil provided a fixed frontal plane for positioning of the observer's head. Infra - red absorbing filters, IRF, were positioned on either side of the lamp. CL1 and CL2 are collimating lenses. A combination of 50 mm and 135 mm, large aperture (f2.8), multi - element photographic lenses were used (L1 - L9). All employed multilayer anti - reflection coatings and were well corrected for aberrations. Since their focusing mechanisms were not required, and in order to utilise space more efficiently, most of these lenses were stripped before mounting. A permanent, central fixation spot was incorporated on the field lens, L5. High reflection, flat mirrors (M1 - M5) and cube beamsplitters (BS1 - BS3) were used to split the source into three channels and then recombine it for viewing. A circular, laser - bored aperture, OP1, mounted on a modified microscope slide carrier provided the limiting field diameter for the test channel, BEAM 1. This aperture, which provided the test target, could be moved both manually and under computer control via a bi - directional DC servo motor. The background field was provided by BEAM 2 and its angular subtense was limited by an iris diaphragm at OP2. Either laser - bored or mechanically - drilled apertures (OP3) were used to set the angular subtense of the third, or conditioning channel. Brief presentation of the test target and conditioning flash were achieved by means of fast electromagnetic shutters (SH1 and SH2). Light intensity for stimulus beam 1 was controlled by a motor - driven neutral density filter wheel (NDF) and a

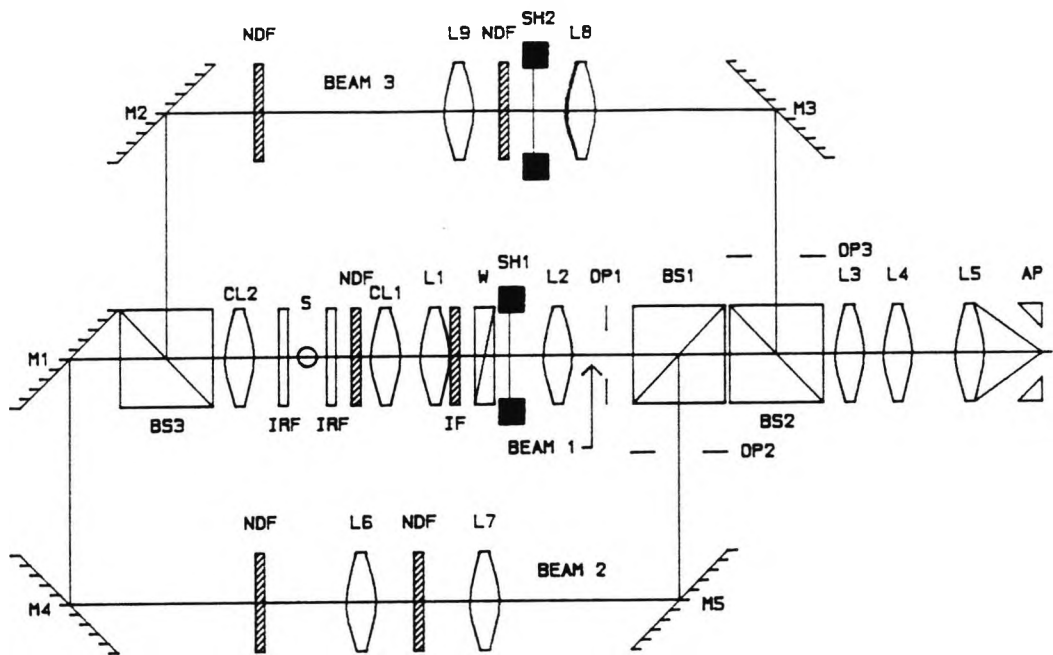


Figure 2.11. Schematic representation of the three channel Maxwellian view optical arrangement used for the experiments detailed in Chapter 6. BEAM 1 provided the test channel, BEAM 2 the background channel, and BEAM 3 the conditioning channel. S, source; IRF, infra-red absorbing filters; NDF, neutral density filter wheel; CL1-CL2, collimating lenses; L1-L9, multi-element lenses; IF, interference filter wheel; W, neutral density wedge; SH1-SH2, shutters; OP1-OP3, apertures; BS1-BS3, cube beamsplitters; M1-M5, flat mirrors.

3.0 log unit neutral density wedge (W). The light intensities for beams 2 and 3 were controlled by mechanical insertion of neutral density filters (NDF), either mounted on a wheel or singly in a slide - holder. The three neutral density filter wheels used each gave optical densities ranging from 0.1 to 3.0 log units. The spectral composition of the test beam could be altered by means of 19, narrow - band interference filters (average bandwidth = 8 nm) mounted on a motor - driven wheel.

An Analogue Devices Macsym 2 Computer System was used to control the test target retinal illuminance level, spectral content, and movement, and also the triggering of the test and conditioning channel shutters (the latter via a digital timer). The computer also recorded observer responses via a response button box placed near the observer's right hand.

2.3.2 CALIBRATION OF MAXWELLIAN VIEW SYSTEM

The equations and constants to follow relate to the most recent calibration of the Maxwellian view system. Complete re - calibration of the system was undertaken at regular intervals.

FIELD OF VIEW

The field of view was calibrated by placing a graticule in the object plane, and recording its projected image on a screen 333 mm from the exit pupil plane. A distance of 15 mm in the object plane corresponds to 110 mm on the screen. Hence 1 mm in the object plane represents a visual field angle of 1.25° . The total field of view subtended an angle of 44° in diameter. Numerous apertures of varying diameters were used in the apparatus, all of which were accurately measured using a travelling microscope. The corresponding angular subtenses were then calculated.

RETINAL ILLUMINANCE

In a Maxwellian view system, all the light flux imaged in

the eye's pupil reaches the retina (with the exception of transmission losses in the ocular media). Therefore retinal illuminance may be determined simply by measuring the luminous intensity of the aerial image of the source.

Calibration of the retinal illuminance level of each channel was carried out in situ using an Oriel radiometer (see section 2.1.2) connected to a UDT photopic response detector. The photocell was positioned 68.5 mm from the imaged lamp filament and the luminous intensity calculated according to the following equation:

$$\text{Luminous intensity (I)} = \frac{P \times 465 \times 68.5^2}{1.285 \times 10^{-5} \times 1000^2} \quad \text{candelas}$$

where P = photometer reading. Therefore the retinal illuminance is $I \times 10^6$ trolands (see Westheimer, 1966). Subsequently the retinal illuminances may be calculated for each channel, and are given in the following table (Table 2.4).

CHANNEL	PHOTOMETER UNITS	RETINAL ILLUMINANCE (LOG TROLANDS)
Test (beam 1)	0.527×10^{-5}	5.950
Background (beam 2)	0.718×10^{-6}	5.085
Conditioning (beam 3)	0.504×10^{-5}	5.931

Table 2.4. Maxwellian view channel retinal illuminances.

In the above table (Table 2.4) retinal illuminance has been expressed in log trolands. When working with optical filters and wedges, optical densities are usually expressed in terms of log units, and therefore using the log troland as the unit of retinal illuminance facilitates calculations. The amount of ambient light measured was negligible, giving a photometer reading of only 0.012×10^{-9} units.

NEUTRAL DENSITY WEDGE

The neutral density wedge used in the system was circular and linear, with its relative optical density being an

accurate linear function of angle as measured from a reference radius. The wedge was coated over a sector of 300° , the remainder being clear. It was mounted on a stepper - motor, such that it could be driven round one step at a time using TTL pulses from the Macsym computer.

Calibration of the wedge was again carried out in situ using the photodiode / Oriel combination. It was found that the relative optical density varied linearly from approximately 0 to 3.3 log units over 332 steps. Measurements of optical density were taken with unfiltered white light (see Figure 2.12 A) and for each of three wavelengths by interposing narrow band interference filters in the test beam (see next sub - section). Although neutral density wedges are, by definition, "neutral", small differences in optical density as a function of wavelength are often found. This was indeed the case as shown in Figure 2.12 (B), where optical density as a function of step number is plotted for three wavelengths of 433 nm, 548 nm, and 621 nm. Linear regression analysis was used to fit the best straight line to these data in order to determine the optimum relationship between optical density (D) and step number. The four equations obtained were as follows:

white light	$D = 0.01026 \times (\text{step no.}) + 0.01151$
433 nm	$D = 0.01054 \times (\text{step no.}) - 0.04415$
548 nm	$D = 0.01027 \times (\text{step no.}) - 0.01747$
621 nm	$D = 0.00991 \times (\text{step no.}) + 0.00643$

Correlation coefficients for the above equations were all greater than 0.999.

Since the optical density of a wedge may vary slightly as a function of radius, it was important to ensure that the source was always imaged at the centre of the neutral density coating. The wedge was always positioned in exactly the same place at the beginning of each experiment. In this way its position, and hence optical density, was known relative to the starting point throughout the experiment.

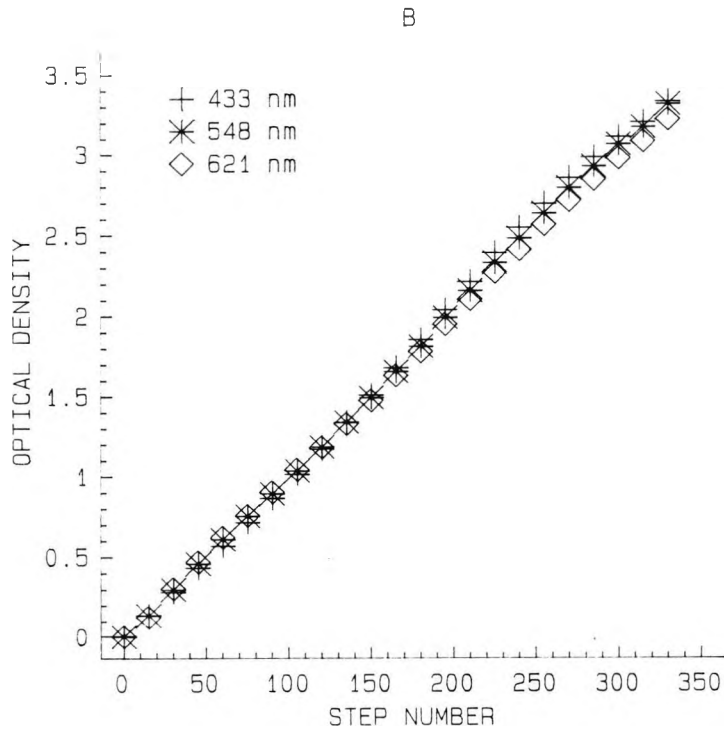
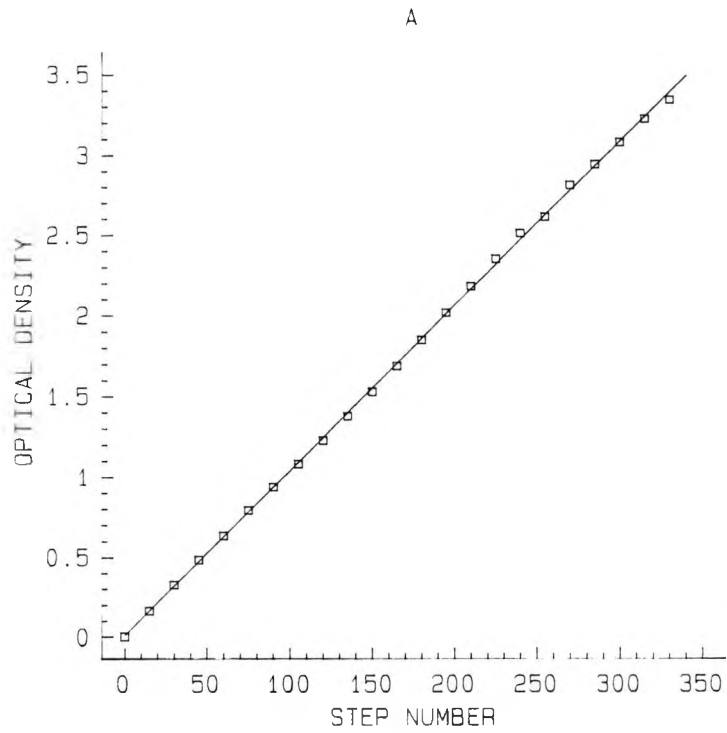


Figure 2.12. (A) Calibration of the neutral density filter wedge for unfiltered white light. (B) Calibration of the same wedge for three wavelengths using narrow band interference filters. In both diagrams, wedge optical density is plotted as a function of the step number.

NEUTRAL DENSITY AND INTERFERENCE FILTERS

All discrete neutral density filters used in the various channels were calibrated appropriately using the photodiode/Oriel combination.

Interference filters had been previously scanned using a Perkin Elmer spectrophotometer in order to determine individual transmission characteristics i.e., peak transmission and bandwidth. Altogether nineteen filters were used in the wheel, spanning wavelengths from 400 to 668 nm. The irradiance of the aerial image of the source with a specific interference filter in position was also determined. To this end, a UDT flat response photodiode in conjunction with the Oriel radiometer was used, and the combination itself calibrated against a GEC standard lamp (No. A453). The photodiode used was, in fact, not quite "flat", and correction factors supplied by the manufacturer were applied to the measured values.

SHUTTER CALIBRATION

In order to measure the changes in visual sensitivity of the eye at discrete points in time, a fast shutter was required to provide a short duration test stimulus in the test channel. A Uniblitz electromagnetic shutter was chosen and its opening and closing times measured with the aid of the Nicolet oscilloscope, photodiode and amplifier combination. Figure 2.13 illustrates the time course of this shutter for a 10 ms pulse from a digital timer. It can be seen that the rise time is only 1.6 ms, though the total fall time is of a somewhat longer duration i.e., 4ms. For the conditioning channel, a Vickers electromagnetic shutter was used with a measured rise and fall time of less than 4 ms.

Both shutters required electronic driver circuits for their operation. Fortunately, these had already been designed and constructed in the laboratory. However, it was decided that a third shutter may be of use for future experimentation and consequently a third drive circuit was built to accompany a

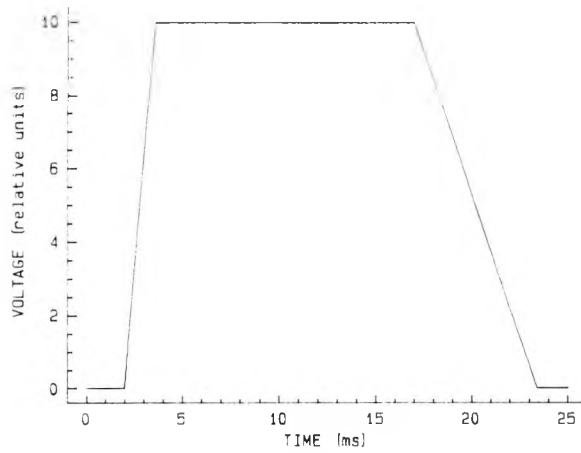


Figure 2.13. The photocurrent versus time trace showing the rise and fall time of the Uniblitz electromagnetic shutter.

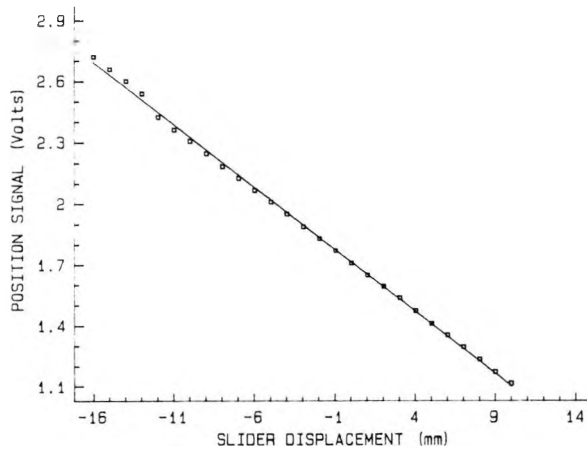


Figure 2.14. Slider calibration showing analogue position signal as a function of displacement in the object plane.

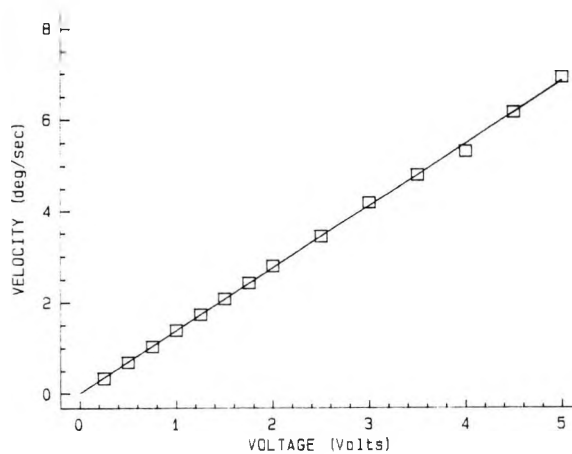


Figure 2.15. Slider velocity is plotted as a function of the analogue output voltage from the computer.

Uniblitz shutter. This latter circuit was designed to be more versatile than the existing units allowing both manual, and computer control of the shutter. The basic design involved the generation of a short duration, 60V spike to open the shutter rapidly, and a 5V DC holding voltage to keep the shutter open.

SERVO SLIDER CALIBRATION

In order to measure the state of retinal adaptation at various eccentricities, it was necessary to be able to move the test stimulus along the horizontal meridian. This was achieved with the aid of a bi - directional DC servo motor and slider. The analogue voltage signal from the slider provided a measure of its position and Figure 2.14 illustrates the position signal as a function of test target (i.e., slider) displacement in the object plane. Linear regression analysis was used to fit the best straight line to these data, and the following equation derived:

$$\text{Position signal (volts)} = - 0.06098 \times D + 1.71627$$

where D is equal to the linear displacement (in mm). The correlation coefficient was 0.9992.

An analogue output voltage from the Macsym computer to the servo motor controlled the velocity of the slider and hence that of the test target. Velocity calibration was carried out by using the Macsym timer function to measure the time taken for the test target to travel a set displacement with a series of applied voltages. Figure 2.15 plots test target velocity against the Macsym output voltage. The equation of the straight line which best fit these data was as follows:

$$\text{Velocity (deg/sec)} = 1.3682 \times V + 0.012898$$

where V is equal to the analogue output voltage (in Volts). The correlation coefficient was 0.9996.

2.3.3 METHODS USED IN MAXWELLIAN VIEW EXPERIMENTS

A detailed discussion of the procedure adopted for individual experiments will be undertaken in Chapter 6. In general, however, it was necessary to measure the detection thresholds of a small test target for various stimulus configurations. To this end, there are basically three types of psychophysical method available (Blackwell, 1952):

1. the method of adjustment, in which the subject adjusts the stimulus parameter in question (in this case the test target retinal illuminance) until he judges it to be just at threshold i.e., just visible;
2. the method of constant stimuli, in which a series of stimuli at several discrete levels are presented, and the subject responds with a "yes" or "no" answer as to whether the particular stimulus was detected;
3. the two - alternative forced choice method, in which the subject has to choose in which of two periods of time the stimulus presentation occurred.

For this series of experiments it was considered that the most convenient measurements of detection thresholds would be achieved using the method of constant stimuli. The parameter in question was randomly interleaved with test retinal illuminance in a simultaneous multiple staircase procedure in which step sizes were adjusted according to a decaying exponential curve. Generally about 12 steps were required to arrive at an accurate threshold. An erroneous subject response could be corrected within the following two steps since step direction was reversible. To obtain more accurate results, some subjects underwent a pilot experimental run, with fewer steps, to determine approximate thresholds. These thresholds could then be incorporated into the experimental program and used as the starting values in a new staircase procedure with smaller step sizes.

A METHOD FOR THE QUANTITATIVE ASSESSMENT OF COLOUR CONSTANCY

Some of the proposed mechanisms and models of colour constancy were reviewed in Chapter 1, and from this brief review it is apparent that we still lack a full understanding of the processes involved in this phenomenon. More recently there has been renewed interest in colour constancy because of its potentially important role in the artificial intelligence task of object recognition. Certainly if colour is to be used to identify a particular object then it is desirable that the recognition system should be able to make illuminant - invariant judgements.

Many of the studies in the field of colour constancy have been theoretical, involving the development of algorithms capable of maintaining colour constancy. Several studies have, however, attempted to quantify the colour constancy effects observed experimentally (e.g., Arend and Reeves, 1986; Tiplitz Blackwell and Buchsbaum, 1988a; Valberg and Lange - Malecki, 1990), but the results and subsequent interpretations have often been at odds. Many of these previous investigations have employed a technique based on that developed by McCann and his colleagues (McCann et al., 1976; and see also Chapter 1), but the technique involves dichoptic presentation of test and matching fields and is difficult to use.

The purpose of the study described in this chapter was to develop and assess a quantitative, experimental method of investigating colour constancy using a computer - controlled colour display. The technique developed yields an index of colour constancy which is relatively easy to measure and simple to interpret, and is based on colour matching a selected test object in sequential presentation of a surrounding field illuminated with one of two illuminants (Pinney et al., 1989). Results are presented which illustrate the importance of chromatic border information and many other characteristics of the surround and test

fields in determining the magnitude of the constancy effects observed.

3.1 THE EFFECT OF SURROUND COMPLEXITY AND TEST TARGET CHROMATICITY ON COLOUR CONSTANCY

PROCEDURE

The equipment and technical details related to this particular study have been described previously in Chapter 2 section 1. Each experimental session consisted of a series of forced response colour matching trials using a centre - surround stimulus configuration presented on a high resolution display. At a viewing distance of 55 cm, the central test object subtended a visual angle of $3.5 \times 3.5^\circ$, whilst the rectangular surround subtended $17 \times 17^\circ$. The contiguous surround consisted of a Mondrian type array of numerous overlapping rectangles of varying dimensions, each of which were randomly assigned one of eleven possible colours. The chromaticity of each coloured patch in the array was computed on the basis of the measured spectral reflectance curves of ten chips taken from the Munsell Book of Colour (Matte Finish Collection, 1976) and an additional patch which was based on the reflectance data of an Eastman Kodak White sample (EKW). The chromaticity co - ordinates of each of the patches comprising the Mondrian surround were changed sequentially to simulate illumination by CIE Standard Illuminant D_{65} (i.e., daylight, $x = 0.3128$ $y = 0.3291$), and CIE Standard Illuminant A (i.e., tungsten, $x = 0.4474$ $y = 0.4075$) (see Figure 2.2 and also Hunt, 1987). The Munsell Notation for each of the colours used in the surround is given in Table 3.1 overpage, together with the corresponding x, y - chromaticity co - ordinates computed for each illuminant simulation.

In a second experiment, the importance of surround complexity was investigated by replacing the Mondrian surround with a homogeneous "white" surround with the same chromaticity co - ordinates as those of the EKW sample given in Table 3.1. The simulated illuminance of the surround was

MUNSELL NOTATION	CHROMATICITY CO-ORDINATES			
	D ₆₅		A	
	x	y	x	y
5B 6/6	0.2346	0.2911	0.3548	0.3982
5BG 6/6	0.2504	0.3439	0.3622	0.4390
5G 6/6	0.2848	0.3839	0.3989	0.4554
5GY 6/6	0.3568	0.4378	0.4585	0.4657
5Y 6/6	0.3979	0.4226	0.5044	0.4336
5YR 6/6	0.4175	0.3745	0.5299	0.4043
5R 6/6	0.3773	0.3269	0.5149	0.3837
5P 6/6	0.2968	0.2602	0.4552	0.3586
5PB 6/6	0.2573	0.2706	0.3940	0.3785
5RP 6/6	0.3497	0.2997	0.5016	0.3699
EKW	0.3128	0.3291	0.4474	0.4075

Table 3.1. Munsell chips used in Mondrian surround.

such that the measured screen luminance of the white (EKW) was 38 cd/m² for both illuminant conditions. Consequently the luminance of each patch comprising the Mondrian surround varied depending on its integrated spectral reflectance. The luminance of the central white (grey) test area was 22.6 cd/m². On the basis of some preliminary measurements, a surround duration of 800 ms was chosen for each illuminant condition, and this was kept constant throughout the course of a single experiment (but see also following section).

If the perceived colour of the test object was determined entirely by its own wavelength - radiance distribution, then changing the illuminant in the surround field should have absolutely no effect on its perceived colour. During the experiments, however, the colour of the test appeared to change when the surround illuminant changed so that, for example, a neutral grey test object was perceived to be more "reddish" with the daylight - illuminated surround, and more "bluish" with the tungsten - illuminated surround. The experimental program allowed the observer to adjust the red, green and blue content of the test object using the computer keyboard until the perceived colour of the test was the same (or as nearly identical as possible) with both surrounds. The observer was only allowed to adjust the spectral composition of the test object when it appeared with the tungsten surround and to facilitate this adjustment the test object with the tungsten surround was always presented with

a small, central marker. The program was designed so that the luminance of the test was maintained at a constant level despite any adjustments in target chromaticity made by the observer. The observer could, however, vary the "white" content of the test with the tungsten surround if he wished to do so, thereby modifying the overall luminance of the test. Once happy with the match, a key press enabled the matching chromaticity to be recorded and then the next stimulus condition was presented.

The chromaticity of the uniform test object was varied randomly under experimental control with each test chromaticity being chosen from those listed in Table 3.1. In the course of a single experiment, each chromaticity test was presented five times in random sequence. In all, therefore, the number of trials totalled 55, and a typical experiment lasted about 20 minutes. The final matching chromaticity recorded was the mean of the five independent settings. In order to avoid excessive afterimages, the observer was instructed to scan the test object at all times rather than maintain accurate fixation. All experiments were carried out in a darkened room and each observer performed a trial run in order to become familiarised with the procedure. In order to achieve a steady - state of light adaptation, subjects viewed a uniform background field of luminance 38 cd/m^2 , for a 2 minute period before each experiment was performed.

DATA ANALYSIS

As mentioned in Chapter 1, the interpretation of results in quantitative colour constancy experiments is often difficult and is confused by the mode of presentation. In order to simplify the data analysis and interpretation such that a single scalar quantity would act as a descriptor of the magnitude of colour constancy for a given set of experimental parameters, an index of colour constancy was derived. This index was designated the C_{index} , and it was defined as the ratio of the experimentally observed shift in CIE 1976 uniform colour space corresponding to an observer's

mean colour match, to the expected shift in chromaticity when the test patch is illuminated with daylight and tungsten illuminants respectively (see Figure 3.1). The index denominator is therefore simply determined from the physical change in the chromaticity co - ordinates of the test which occurs when the illuminant changes from daylight to tungsten (i.e., "e" in Figure 3.1). Thus, the Euclidean distance is given by:

$$e = [(u'_1 - u'_2)^2 + (v'_1 - v'_2)^2]^{\frac{1}{2}}$$

where u'_1, v'_1 (T_D in Figure 3.1) and u'_2, v'_2 (T_A in Figure 3.1) are the chromaticity co - ordinates of the test object under the daylight and tungsten illuminants respectively. The index numerator is the measured difference between the initial $u'v'$ co - ordinates of the test object with the daylight surround and the co - ordinates to which the observer sets the test for equal colour appearance with the tungsten surround (i.e., "c" in Figure 3.1). Thus, the Euclidean distance is given by:

$$c = [(u'_1 - u'_3)^2 + (v'_1 - v'_3)^2]^{\frac{1}{2}}$$

where u'_3, v'_3 are the chromaticity co - ordinates for which the test target colour appears invariant for the two surround illuminant conditions (T_M in Figure 3.1). The C_{index} can therefore be written as:

$$C_{index} = c / e$$

According to this definition, perfect colour constancy corresponds to a C_{index} value equal to unity (since "c" and "e" in Figure 3.1 would have the same magnitude), whereas for no colour constancy, the C_{index} would be equal to zero.

Certain assumptions have been made in defining the above index. Firstly, the CIE 1976 UCS is not a Euclidean vector space, but the assumption is made that within small subspaces, distance is an accurate measure of colour difference. In fact an earlier version of the C_{index} was

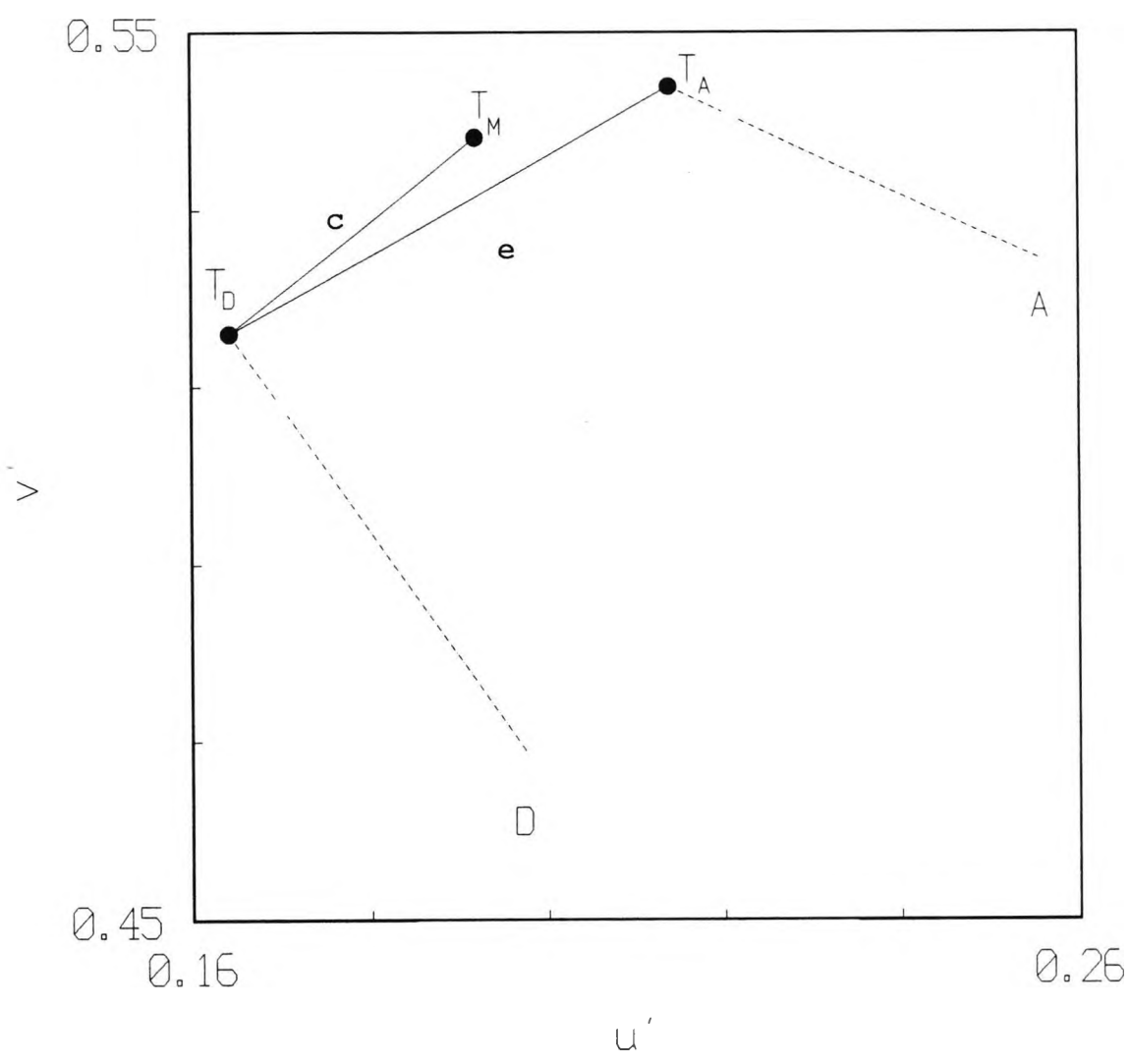


Figure 3.1. Definition of the C_{index} . The above figure represents a portion of the CIE 1976 u', v' diagram. T_D and T_A indicate the chromaticity co-ordinates of a test object illuminated by CIE Standard Illuminants D_{65} (D) and A (A) respectively. T_M indicates the chromaticity co-ordinates for which the test object colour appears invariant when the surround is illuminated alternately by these two illuminants. e represents the chromaticity difference between T_D and T_A , and c represents the difference between T_D and T_M . The C_{index} is given by c / e .

defined in which the observed test chromaticity shift was related to the physical chromaticity shift of the surround, but it was found that the non - uniformity of the CIE 1976 UCS diagram led to inaccuracies in the computed index when test and surround chromaticity were markedly different. Secondly, the angle between the vectors c and e in Figure 3.1 is assumed to be negligible. The results of preliminary experiments have shown that observer colour matches are invariably along similar directions in colour space as the illuminant change. In the light of these findings therefore, this second assumption also seems justified.

OBSERVERS

In all, seven experienced observers participated in the experiments described in this chapter, though not all took part in each individual experiment. Usually at least one of the participating observers was naive about the purpose of the experiments. Six of the subjects were colour normal as determined by the Farnsworth - Munsell 100 - hue and Ishihara tests (see Birch, 1985), and each wore the appropriate refractive correction. One subject, H.P., was a protanope.

RESULTS

Figure 3.2 displays the results of the experiment incorporating the Mondrian surround for three colour normal subjects and one protanopic subject. C_{index} is plotted for each of the test targets used in the experiment. The targets are designated using the Munsell Notation of each test object. Each data point represents the mean of five colour matches. For clarity, error bars have not be drawn, but typically one standard error amounted to about 0.04 for the colour normal subjects and about 0.02 for the protanope. Considering first the colour normal subjects, it may be seen that the C_{index} ranges between values of about 0.24 and 0.53. Analysis of variance indicates that there were significant differences in the value of the C_{index} with

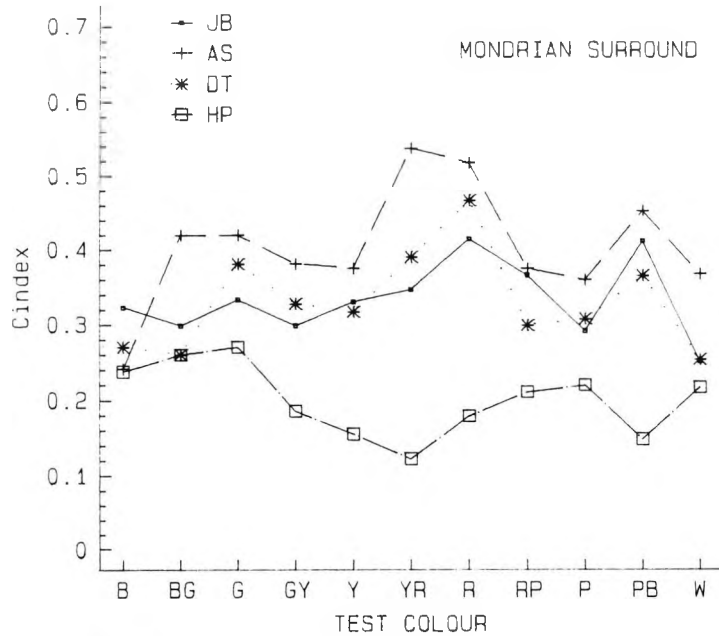


Figure 3.2. C_{index} is plotted for each test object colour, the latter designated on the abscissa according to Munsell Notation. The test surround consisted of a Mondrian-type pattern illuminated sequentially by D_{65} and A. JB, AS, and DT are normal trichromats, HP is a protanope. Each symbol represents the mean of 5 trials, 1 se approximately 0.04.

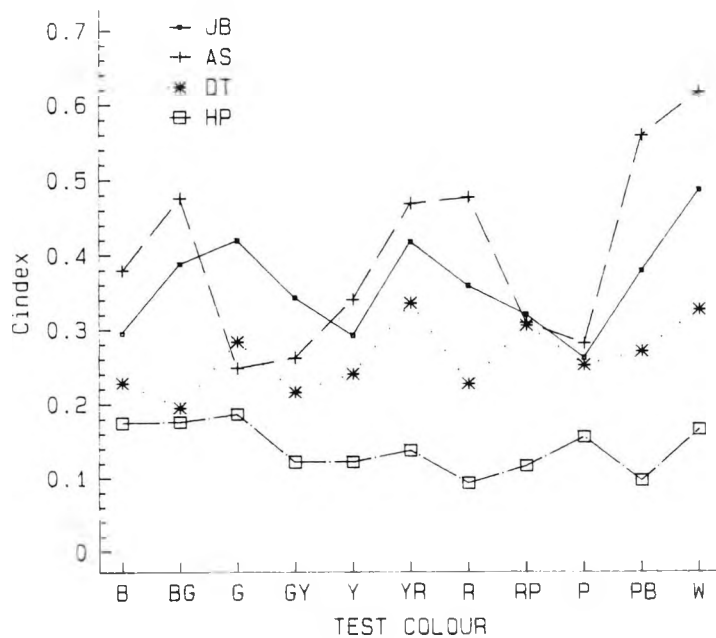


Figure 3.3. C_{index} is plotted for each test object colour as in Figure 3.2 above, but in this case the surround was a uniform white, again illuminated sequentially by D_{65} and A. 1 se approximately 0.04.

respect to the colour of the test object ($p < 0.02$) and furthermore that differences between subjects were also significant ($p < 0.03$). The values of the C_{index} computed for the colour defective observer were consistently below those measured for the colour normal observers.

Figure 3.3 shows the results obtained with the same observers when the Mondrian surround was replaced with the uniform surround. Standard errors were of a similar magnitude to those recorded in the previous experiment. Again it may be seen that the C_{index} varies with the choice of test target chromaticity and also varies between those subjects with normal colour vision. Similarly, the indices measured for the colour defective subject were significantly smaller than for those measured with colour normal subjects. An analysis of data averaged across all subjects indicates that any differences between the results obtained with Mondrian surrounds and those obtained with uniform surrounds are not significant ($p = 0.24$). These averaged data are displayed in Figure 3.4.

DISCUSSION AND CONCLUSIONS

The range of C_{index} values obtained in both of the preceding experiments indicates that immediate colour constancy is far from perfect. The magnitude of the effects observed in the present study are in general agreement with those reported in other quantitative investigations of colour constancy (Arend and Reeves, 1986; Buchsbaum, 1988a; Arend et al., 1991). It seems likely that simultaneous mechanisms (e.g., simultaneous colour contrast) are primarily responsible for the observed constancy effects, since any long term adaptation was minimised by the relatively rapid interchange of illuminants. This is supported by the subjective comments made throughout the experiments that the colour change observed when the illuminant changed occurred in phase with the illuminant change. In order to investigate this observation more systematically, an experiment was carried out to measure the C_{index} as a function of illuminant presentation time and the results are reported in the

following section. The aim of the present experiments was to quantify immediate colour constancy, but when viewing time is unlimited, it is possible that long term adaptation and memory may also play a part in colour constancy, and if this is so, then it is conceivable that the measured C_{index} would be greater.

In the past it has been argued that a complex Mondrian pattern is more favourable for colour constancy than a less complex one (Daw, 1984; Brill and West, 1986), in spite of the fact that the effects of simultaneous contrast are minimised with such patterns since no area in the pattern is surrounded by a single colour. The results obtained in the present study indicate, however, that pattern complexity does not influence colour constancy to any great extent. A similar finding has been reported by Arend and Reeves (1986) and more recently by Valberg and Lange - Malecki (1991). As the latter authors point out, Land's most recent Retinex algorithm (1986b) fails to predict the similar magnitudes of constancy observed with the Mondrian and uniform surrounds. In terms of illuminant identification, however, Mondrian patterns must provide the visual system with less ambiguous information, since the physical chromaticity shifts between patches in Mondrians viewed under different illuminants are correlated. Whatever the degree of pattern complexity, the results suggest that it is the space - averaged chromaticity of the scene which is important in determining the magnitude of the colour constancy effects.

The somewhat reduced C_{index} observed for the protanopic subject raises the interesting question of whether colour defectives demonstrate less colour constancy than normal trichromats. If one considers the difference in the overall hue signal produced by an illuminant change, then for certain illuminant shifts, smaller differences would be recorded for a colour defective observer than for a colour normal observer. This in turn means that object colour appearance is less influenced by illuminant changes in colour defective observers, so that colour constancy need not function to the same extent as in normal observers.

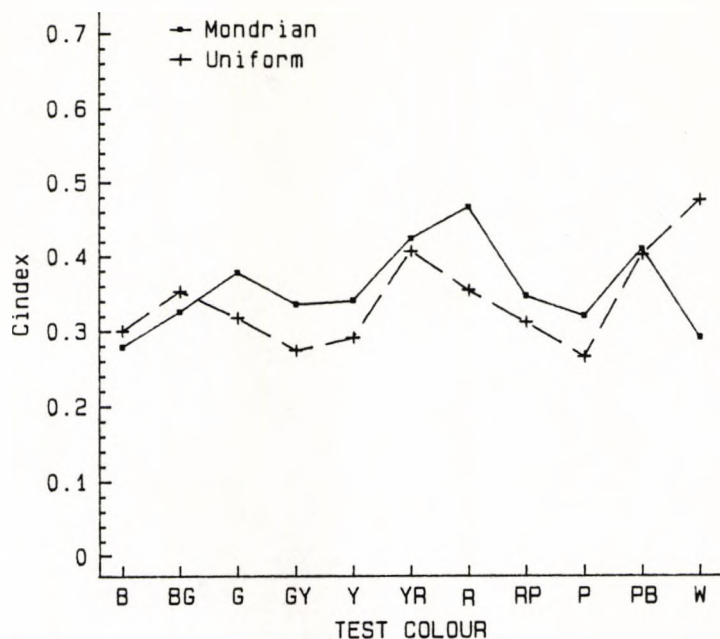


Figure 3.4. C_{index} plotted for each test object colour with Mondrian and uniform surrounds. Symbols represent the average data for three normal trichromats.

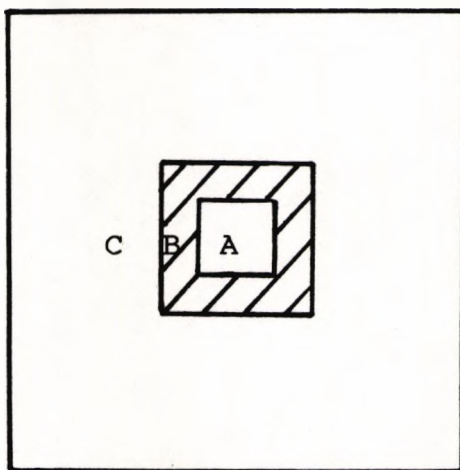


Figure 3.5. Centre - surround configuration used to investigate spatial properties of colour constancy. A represents the central test object, and B the dark border which could be interposed between the test and surround (C). In Experiment 2, B was equal to zero and C was varied; in Experiment 3, B was varied and C varied proportionally; in Experiment 4, B was equal to zero and A was varied while C varied proportionally. See text for details.

Somewhat surprisingly, the standard errors associated with the measured C_{index} were smaller for the protanope than for the colour normal subjects. This may in part be explained by the fact that the protanope is the author, and consequently performed the experiments many more times and with greater interest than the other, colour normal observers.

Interestingly, the results show that inter - subject differences amongst colour normal observers can be quite large. The most likely explanation for these differences is that subjects tend to use slightly different criteria or procedures for matching the test area with the two illuminant simulations. As mentioned in Chapter 1 (section 2.3), Arend and Reeves (1986) found that the magnitude of the constancy effects observed were directly related to the instructions given to the subject i.e., whether the subjects were required to make direct hue - saturation matches (ignoring the test surround), or "paper" matches where subjects were instructed to make the test patch look as if it were cut from the same piece of paper as the standard patch. An inspection of their published results (Arend and Reeves, 1986; Arend et al., 1991) indicates, however, that inter - subject differences are still present even when the instructions given were the same. In the present study, it was noted that by restricting one's fixation to the very centre of the test object, the amount of colour constancy measured could be reduced. This suggests, therefore, that test object size could be an important parameter, which in turn suggests that other spatial parameters of the scene may be important in determining the C_{index} and hence the level of colour constancy achieved.

3.2 SPATIO - TEMPORAL PROPERTIES OF COLOUR CONSTANCY

In view of some of the comments made above, it was of interest to investigate the influence of certain spatial and temporal parameters on the magnitude of the C_{index} . Since surround complexity appears to have little effect on the

magnitude of the C_{index} , the following experiments were restricted to a simple centre - surround configuration employing a uniform white surround (luminance = 38 cd/m²) and a grey test target (luminance = 22.6 cd/m²). Unless otherwise stated, the experimental procedure and stimulus configuration used were identical to those described in the previous experiments (i.e., section 3.1). Four basic experiments were carried out as follows:

EXPERIMENT 1

The C_{index} was measured as a function of the tungsten / daylight cycle presentation time. In the previous experiment a fixed surround duration of 800 ms was employed where the time refers to the duration of each simulated illuminant rather than to a complete cycle of the two illuminants. In this experiment, surround duration was varied randomly under experimental control from 100 to 1400 ms.

EXPERIMENT 2

The C_{index} was measured as a function of surround angular subtense. The surround remained square but was varied randomly in size, under experimental control, between 0.28° and 13.3° (see Figure 3.5). A fixed viewing distance of 55 cm was used, and the angular subtense of the test remained constant at 3.5° throughout the experiment. In a separate experiment, the effect of varying the surround angular subtense over a greater range was investigated. To this end, four different viewing distances of 12.5, 25, 50, and 100 cm were employed providing surrounds of 64, 32, 16, and 8° respectively. In order to keep the angular subtense of the test constant, its physical screen dimensions were modified to compensate for the different viewing distances used.

EXPERIMENT 3

The C_{index} was measured for a series of scene configurations in which a dark border was superposed between the test area

and the uniform surround (see Figure 3.5). The border completely encompassed the test, and its angular subtense was varied randomly under experimental control from a minimum of 0° (i.e., no border) to a maximum of 13.2° . The area of the surround was inversely proportional to the area of the border.

EXPERIMENT 4

The magnitude of the C_{index} was determined for a series of test object sizes ranging between 0.85° and 10.53° (see Figure 3.5). The test object was presented in a randomised sequence of sizes. Subjects were always instructed to scan the test area rather than concentrate on the fixation marker. In a second experiment, observations were made at four viewing distances of 12.5, 25, 50, and 100 cm. The test object was of constant physical size and consequently its angular subtense varied with the viewing distance from 0.85° to 6.7° . The physical size of the surround was adjusted such that its angular subtense remained constant at 8° .

RESULTS

The results from the above experiments are displayed in Figures 3.6 - 3.9. In general, the format for each of the figures is the same in that the value of the C_{index} is plotted as a function of the variable relevant to one of the above experiments. In all the figures that follow, individual data are presented for several colour normal subjects and one colour defective subject (H.P.). The solid line drawn represents the mean values for the colour normal subjects as a group whilst the discontinuous line is drawn for the colour defective subject alone. Each data point drawn represents the mean of five measurements of the C_{index} (see details of procedure above). For clarity of presentation, error bars have not been reproduced in the figures, but as an indication one standard error rarely exceeded 0.04 (and was generally below 0.03) for any of the subjects in any of the experiments.

The results of experiment 1 are displayed in Figure 3.6 for three colour normal subjects (J.B., A.S., and D.D.) and one colour defective subject (the protanope H.P.). C_{index} has been plotted as a function of surround duration. It may be seen that the value of the C_{index} increases monotonically with surround duration for durations up to about 400 ms. For presentation times longer than 400 ms, the value of the C_{index} appears to be relatively independent of surround duration for all observers. Once again the colour defective subject shows relatively reduced C_{index} values when compared with the colour normal subjects.

Figures 3.7 (A) and (B) show the results from experiment 2. In Figure 3.7 (A), C_{index} is plotted as a function of surround angular subtense for two colour normal observers (J.B. and A.S.) and one colour defective subject (H.P.). Basically the results indicate that the value of the C_{index} increases as the angular subtense of the surround increases. An initial rapid rise in the value of the C_{index} occurs as the surround is increased to approximately 2° to 3° , but as surround size increases beyond 3° , the C_{index} appears to rise more slowly. The results obtained with subject J.S. for the larger surround angular subtense are shown in Figure 3.7 (B) (in which, for comparison purposes, the same scale as that in Figure 3.7 (A) has been used). The data indicate that the slow rise in the value of the C_{index} continues as the size of the surround is increased up to approximately 16° . It may be seen, for this subject, that when the angular subtense of the surround is increased beyond 16° , the value of the C_{index} appears to fall again slightly.

The results from experiment 3 are reproduced in Figure 3.8 in which C_{index} is plotted as a function of the angular subtense of the border for three normal trichromats (J.B., A.S. and M.K.) and one colour defective subject (H.P.). The angular subtense of the border as displayed in this figure was calculated by subtracting the subtense of the test from the total subtense of the outer limit of the border. It may be seen that the interposition of a dark border between the test and the surround causes a reduction in the value of the

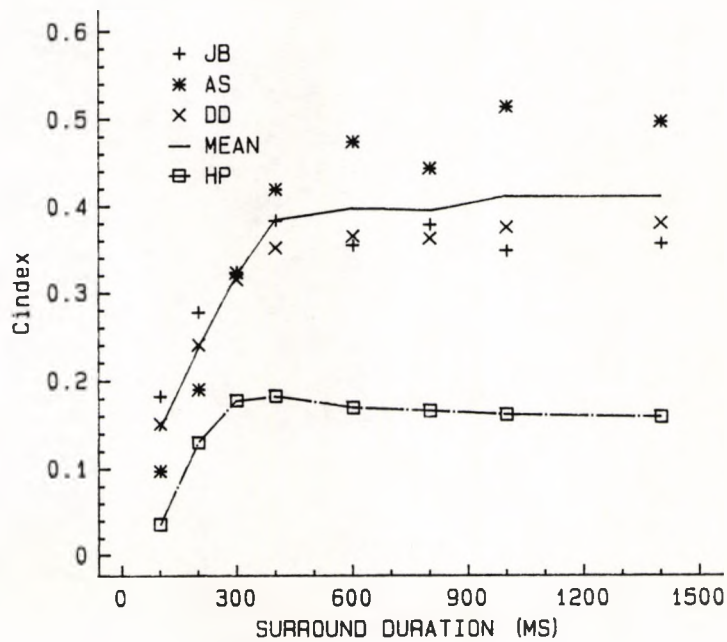


Figure 3.6. C_{index} plotted as a function of the duration of the uniform white surround. Each symbol indicates the mean of 5 trials for each subject, 1 se equals approximately 0.03. The solid line represents the averaged C_{index} for the colour normal observers (JB, AS and DD). Data is also shown for protanope HP.

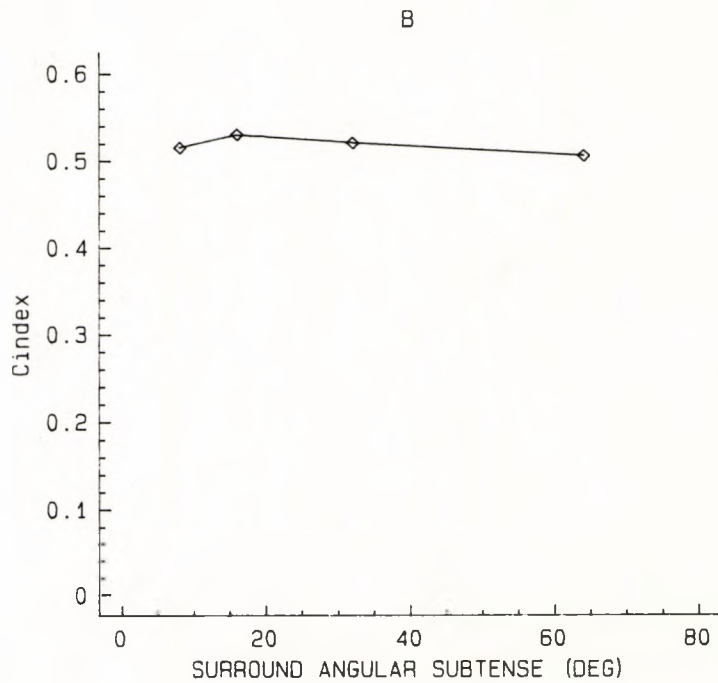
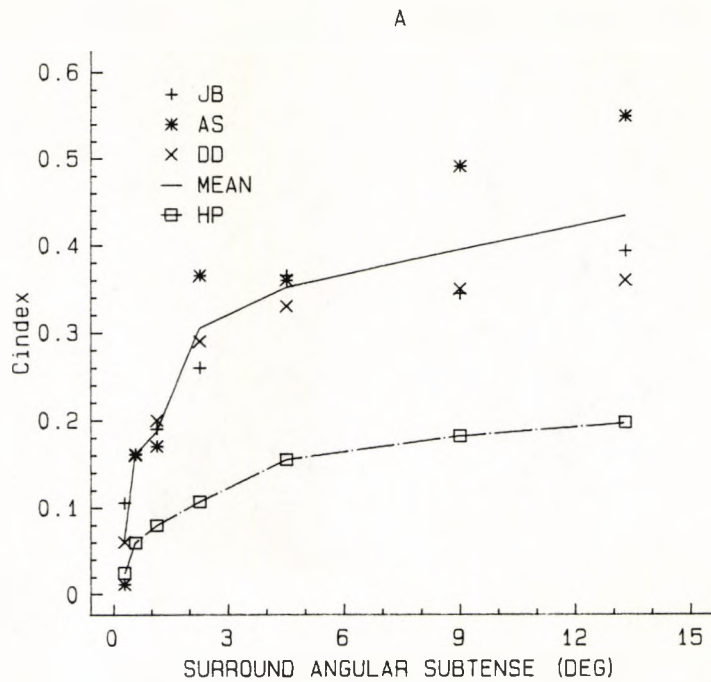


Figure 3.7. Data from Experiment 2 showing C_{index} as a function of surround angular subtense. In (A) measurements were made at a fixed viewing distance of 55cm and data are presented for three normal trichromats (JB, AS and DD) and one protanope HP. The solid line represents the average data for the colour normals. In (B) measurements were made at several viewing distances in order to provide a greater range of surround subtenses (see text). Data is plotted for one subject (JS). Each symbol represents the mean of 5 observations.

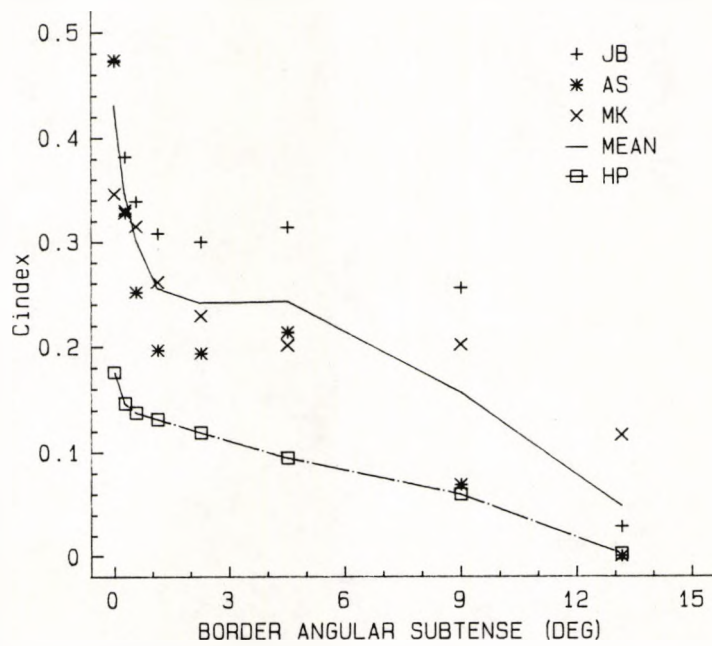


Figure 3.8. Data from Experiment 3 in which a dark border was interposed between the central test object and surround. C_{index} is plotted as a function of the border angular subtense for three normal trichromats (JB, AS and MK) and one protanope HP. The solid line represents the average data for the colour normal subjects.

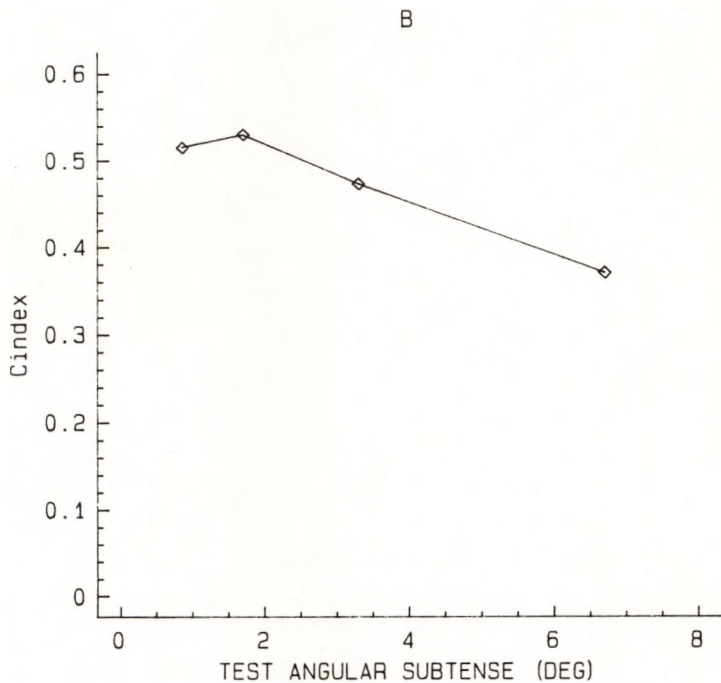
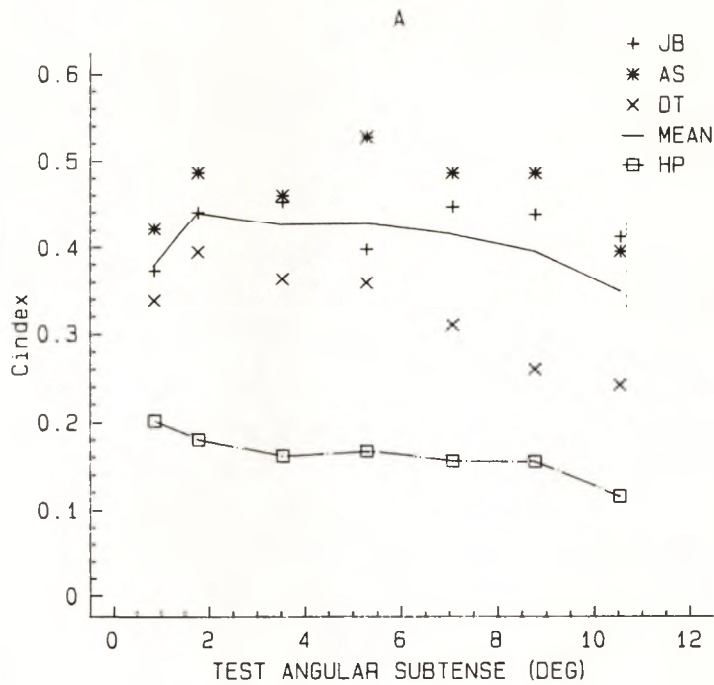


Figure 3.9. Data from Experiment 4 showing C_{index} as a function of the angular subtense of the central test object. In (A) the viewing distance was fixed at 55cm and the angular subtense of the surround decreased proportionally as test subtense increased. Data are presented for three colour normal observers (JB, AS and DT) and one protanope HP. In (B) the test object was of a constant screen dimension, and the viewing distance was varied to provide a range of test subtenses. The screen dimensions of the surround were adjusted so as to maintain a constant surround subtense of 8° . Data is presented for one colour normal subject JS. In both diagrams each symbol represents the mean of 5 trials.

C_{index} , even when the border is extremely narrow i.e., 17 minutes of arc. The C_{index} continues to fall rapidly as the width of the dark border increases to between $2^\circ - 3^\circ$, but thereafter the fall is more gradual. Interestingly, in two of the normal subjects (J.B. and M.K.), it seems that the colour appearance of the test object is still influenced by the surround even when it is separated from the test by as much as 13° . This finding is all the more astounding when one remembers that at this eccentricity the surround is very narrow (less than 10 minutes of arc). Similar results were found when the dark border was replaced with various chromatic borders (the chromaticity of these chromatic borders remained invariant as the simulated illuminant changed).

Figures 3.9 (A) and (B) show the results obtained from experiment 4. In Figure 3.9 (A), C_{index} is plotted as a function of the angular subtense of the test area for three colour normal subjects (J.B., A.S. and D.T.) and one colour defective subject (H.P.). The data for two of the colour normal subjects (J.B. and J.S.) indicate that the value of the C_{index} is relatively independent of the angular subtense of the test, except, that is, for particularly small or particularly large test dimensions (i.e., less than about 1° , or greater than about 9°). The results obtained with subject D.T. are somewhat different to those for the other two colour normal subjects in that the C_{index} appears to fall for test objects with an angular subtense greater than only 5° (or possibly even 2°). Whilst in general the results for the colour defective subject show a relative independence on test object size, it may be seen that the value of the C_{index} increases very slightly for test objects of smaller dimensions. The data plotted in Figure 3.9 (B) for subject J.S. (using a constant surround angular subtense) are similar to those obtained previously for subject D.T. in that the value of the C_{index} appears to fall for test objects larger than approximately 2° . It was again noted that if subjects did not scan the test area, then the resulting values of the C_{index} were relatively reduced, especially for those configurations employing the larger

test dimensions.

DISCUSSION AND CONCLUSIONS

The results of experiment 1 (Figure 3.6) indicate that colour constancy effects can occur fairly rapidly, with surround presentations of 400 ms producing high C_{index} values. This finding suggests that any long term adaptational effects are relatively small (or at least relatively short - lived) and that more immediate mechanisms may be responsible for the observed colour changes. In an analogous study, De Valois and his colleagues (De Valois et al., 1986) reported similar findings for the temporal properties of colour induction. They found that colour induction was reduced markedly when the chromaticity of the surround was oscillated at frequencies greater than about 2 Hz. These authors felt that the observed temporal effects were, in fact, quite slow, and this led them to conclude that chromatic induction effects are mediated via a cortical, or even a late - cortical site. De Valois and his colleagues support their argument by pointing out that LGN cells will respond to receptive field surround modulation up to very high temporal frequencies. A similar argument for cortical involvement could be applied to the data presented in the current study.

It is clear from the results of experiments 2 and 3 (Figures 3.7 and 3.8) that the near surround of a test object is most important in determining the colour appearance of that object. Using a conventional optical arrangement, Walraven (1973) has shown that similar spatial characteristics apply to chromatic induction. Employing a nulling paradigm with simultaneously flashed centre and surround, he showed that the effect of the surround on the centre increased exponentially with increasing surround diameter, and decreased exponentially with increasing centre - surround separation, the most rapid changes occurring over the first one degree of surround diameter or surround separation. More recently similar results have been obtained using computer - controlled visual displays (Tiplitz Blackwell and Buchsbaum,

1988b; Brenner et al., 1989). The results of the present study (especially those reproduced in Figure 3.7 A) indicate, however, that the most influential region around a particular object may extend over a slightly larger area than previously reported i.e., an area somewhere between 1 and 3°. Although eye movements were not restricted, the limited spatial extent of the main contribution to colour constancy would seem to indicate that the mechanism involved is unrelated to adaptation. The results are consistent with the hypothesis that cortical double opponent cells (see Chapter 1) may be involved in the mediation of colour constancy.

A close examination of Walraven's (1973) data shows that, in addition to the large effects produced by the immediate surround, smaller effects are also produced by a spatially remote surround up to 6° away from the central test object. Similar long - range interactions were observed in the present study where surrounds as far as 13° away from the central test object influenced the latter's colour appearance (see Figure 3.8). Studies with hemianopic subjects have indicated that similar long - range interactions may be mediated at either the retinal (Pöppel, 1986) or cortical (Land et al., 1983) level.

Considering next the influence of object size on colour constancy, one would predict that if fixation was rigidly maintained on the centre of the test object, then as object size is increased, a decrease in the measured constancy index should be seen (since the surround becomes progressively more remote as test size is increased). On the other hand, if the subject were instructed to scan around the object, then perhaps such a decrease in the constancy index would be less evident. An inspection of the results of the present study (Figures 3.9 A and B) reveals certain inter - subject differences with regard to the variation of test object size. For two of the colour normal subjects (J.B. and A.S.), test size appears to have little effect on the value of the C_{index} , whereas for the other two normal subjects (D.T. and J.S.), the C_{index} decreases as the size

of the test is increased above 2° . In spite of the fact that each subject was given instructions to avoid steady central fixation, it is possible that these observed inter - subject differences arise from differences in the subjects' mode of fixation.

3.3 CHROMATIC BORDERS AND COLOUR CONSTANCY

The finding that a centre - surround separation of as little as 17 minutes of arc can significantly inhibit colour constancy suggests that the presence of a physical border between a test and its surround is necessary for colour constancy to function optimally. An experiment was therefore designed which enabled the direct assessment of the importance of the extent of the chromatic border on the magnitude of the C_{index} .

PROCEDURE

The basic procedure employed was similar to that detailed for the experiments above. The angular subtense of the central test object was increased to $5.7 \times 5.7^\circ$ (at 55 cm) and the surround consisted of one of seven possible spatial configurations. The various surround configurations are drawn in Figure 3.10. In the control condition (diagram 1 in Figure 3.10), the test object is presented with a contiguous uniform surround, and as before, the chromaticity of the surround changes sequentially as if illuminated by daylight or tungsten. In the other conditions the surround consists of either one, two, or four rectangles, each with dimensions identical to those of the central test target. The rectangles comprising the surround were positioned such that: (i) their inner borders were either directly contiguous with the test object (diagrams 2, 3 and 4 in Figure 3.10); or (ii) such that only their inner corners were touching the test object (diagrams 5, 6 and 7 in Figure 3.10). Surround conditions were presented in random sequence and the C_{index} determined for each. The chromaticities and luminance of the test and surround were

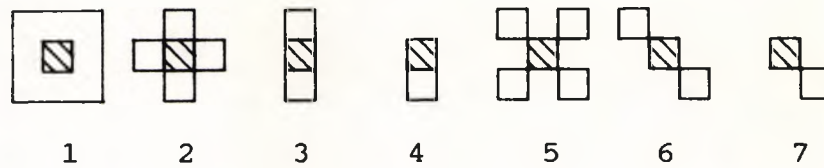


Figure 3.10. The seven surround configurations employed in the experiment designed to investigate the importance of border information. Diagram 1 represents the control condition in which the surround completely encloses the test object. In diagrams 2 - 4, the rectangles comprising the surround are positioned such that their inner borders are contiguous with the test. In diagrams 5 - 7, the surround rectangles are positioned such that only their inner borders are in contact with the test. See text and Figure 3.11 below

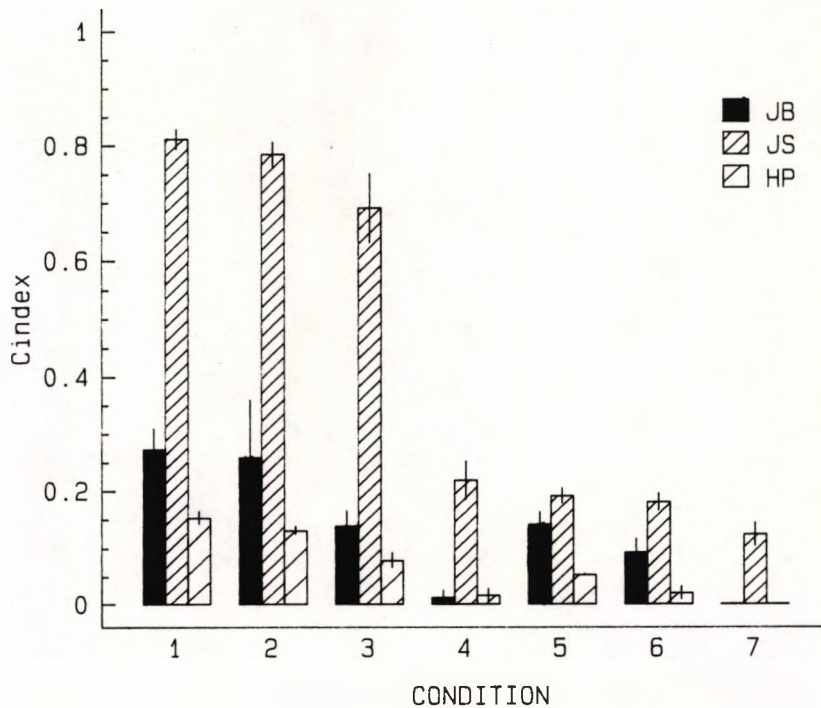


Figure 3.11. C_{index} is plotted for the surround conditions shown in Figure 3.10 above. Data is shown for two colour normal observers (JB and JS) and one protanope (HP). The values plotted represent the mean of 5 observations for each subject and the error bars show ± 1 standard error.

identical to those detailed in section 7.1 of this chapter. A surround duration of 800 ms was employed.

RESULTS

Figure 3.11 shows the results of the above experiment in bar chart form for two colour normal subjects (J.B., solid fill; J.S., diagonal lines) and one colour defective subject (H.P., wide separation diagonal lines). The numbers used along the abscissa refer to the various surround configurations and correspond with the diagram numbers used in Figure 3.10. The error bars drawn represent ± 1 standard error computed from five C_{index} measurements for each surround condition.

An interesting feature of Figure 3.11 is the similarity in the values of the C_{index} recorded for surround conditions 1 and 2. Even though the area of the surround is halved in the second of these two conditions, the C_{index} remains relatively unchanged for each of the subjects. A comparison of conditions 2 and 5, however, shows that the C_{index} is markedly reduced for the second surround configuration even though the area of the surround in the two conditions is identical. Furthermore, if all the conditions for which the surround area is equal, but the configuration is different, are compared (i.e., a comparison of the contiguous and non-contiguous surround conditions), then it is clear that the value of the C_{index} is always significantly greater for each subject when the surround is contiguous with the test.

Another notable feature of this figure (but one that does not bear upon the particular topic in question) is the relatively large magnitude of colour constancy measured for subject J.S.. In the full surround condition this subject records a C_{index} of about 0.8, whereas all other colour normal subjects generally record a C_{index} in the range 0.25 - 0.5. Informal measurements involving some of the experiments detailed previously, indicate that this subject yields consistently much higher C_{index} values than any of the other subjects investigated. As mentioned previously,

Arend and Reeves (1986; 1991) similarly report large inter - subject variations.

CONCLUSIONS

The results of the above experiment show that the presence of a chromatic border between an object of interest and its surroundings plays an important role in determining the magnitude of colour constancy effects. The area occupied by the surround is only of secondary importance. This finding again favours the view that adaptation contributes only secondarily to colour constancy.

The picture that is emerging is one in which the proximal surround and associated border information play a crucial part in the colour constancy effects observed experimentally. If colour appearance algorithms are to accurately model human colour constancy, then these spatial properties should be adequately compensated by appropriate weighting factors. Most currently advocated algorithms, however, attach equal significance to all parts of the visual field. Interestingly, Land (1986a) has proposed a modification to his earlier Retinex algorithm (Land, 1964) which results in more contiguous areas (up to 2° away from the object of concern) carrying a greater weight. In the light of the evidence presented here, this integral weighting procedure seems a highly desirable feature of the proposed algorithm.

3.4 THE EFFECT OF SCENE SATURATION AND CHROMATICITY ON COLOUR CONSTANCY

Many von Kries type algorithms locate the area in a scene which generates the largest signal in each of the three receptor types. By scaling all receptor signals of a given type with respect to the maximum, then a triplet of normalised responses may be generated for each patch in the scene. This triplet is then assumed to determine the perceived colour of the target of interest. If this were the

case, then colour constancy should fail if there was no bright, white region in a scene (D'Zmura and Lennie, 1986). In order to investigate this further, experiments were carried out in which the surround consisted of saturated coloured patches which changed in spectral radiance so as to emulate changes between illuminant A and D₆₅.

PROCEDURE

The central test object subtended 5.7 x 5.7° and was surrounded by eight rectangles of identical spatial dimensions. The chromaticity co - ordinates of the test were as before, but each of the surround rectangles was a saturated red, green, or blue with "daylight" chromaticity co - ordinates of $x = 0.4535$ $y = 0.3232$, $x = 0.2190$ $y = 0.4123$, $x = 0.1919$ $y = 0.1887$ or "tungsten" chromaticity co - ordinates of $x = 0.5828$ $y = 0.3512$, $x = 0.3057$ $y = 0.4932$, $x = 0.2915$ $y = 0.3086$, respectively. The surround was therefore composed of three rectangles of red, three rectangles of green, and two rectangles of blue, arranged such that each was separated by a rectangle of different colour. The luminances of each of these coloured rectangles were such that they were in the same ratio as for the previously used uniform surround, and hence the average chromaticity of the surround was also as before. Varying numbers of rectangles with chromaticity equal to the uniform white surround, were randomly substituted for the coloured rectangles. Thus, for any one particular measurement of the C_{index} , the surround could consist of anywhere between zero and eight neutral (grey) rectangles, or zero and eight coloured rectangles. Five measurements of the C_{index} were recorded for each experimental condition and (in view of the results obtained for the previous experiment) the spatial position of the white rectangles substituted was randomised.

RESULTS

Figure 3.12 plots the C_{index} as a function of the number of "white" rectangles comprising the test target surround. Results are presented for two colour normal observers (J.B.

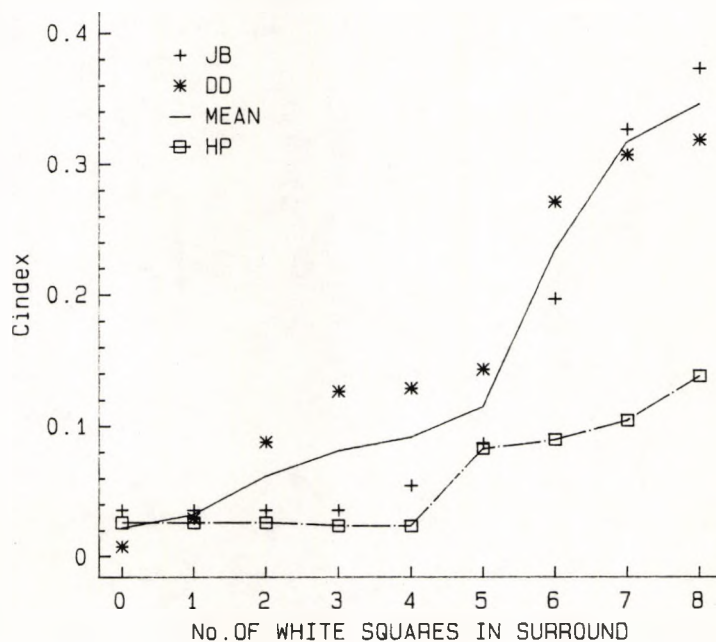


Figure 3.12. C_{index} is plotted as a function of the number of white squares comprising the surround. In condition 0, the surround consisted of three rectangles of red, three rectangles of green, and two rectangles of blue, each rectangle having the same angular subtense as the central test object (5.7°), and each changing in chromaticity sequentially as if illuminated by D_{65} and A. The space-averaged chromaticity of the surround was the same as for the uniform white surround used previously. Varying numbers of "white" rectangles were substituted randomly for the coloured rectangles. Data is presented for two colour normal observers (JB and DD) and one protanope (HP) and each symbol represents the mean of five observations. The solid line shows the averaged data for the colour normal observers.

and A.S.) and one colour defective observer (H.P.). Each data point represents the mean of five measurements with one standard error usually less than 0.03. The solid line represents the C_{index} values averaged for the two colour normal observers and the broken line joins the data points obtained with the colour defective observer. It may be seen that the values of the C_{index} are extremely low (and close to zero) for all observers when the surround is made up of only saturated coloured rectangles. As more white rectangles were substituted into the surround, the values of the C_{index} obtained with the normal observers increased gradually. A large rise in the value of the C_{index} is seen to occur when the number of white rectangles comprising the surround increases from five to six.

CONCLUSIONS

The results (Figure 3.12) suggest that the immediate colour constancy measured in these experiments is only possible when the surround field consists of patches with broad spectral reflectance functions. It would seem that the presence of patches of saturated colours makes the perception of colour more dependent on the wavelength - radiance distribution at a given point on the retina and therefore minimises colour constancy. The saturated coloured patches may actively inhibit colour constancy, since it is apparent that the C_{index} is reduced even when a single saturated patch is in the surround. This finding also highlights the importance of the white component of the surround in determining the magnitude of the observed constancy.

3.5 THE EFFECT OF OBJECT LUMINANCE ON COLOUR CONSTANCY

Most of the experiments described in this chapter so far have employed a fixed centre - to - surround luminance ratio. The effect of varying this ratio on the induced hue and saturation in a central test field have been studied extensively in analogous chromatic induction experiments.

Early studies indicated that maximum induced hue and saturation occurred when the luminances of the test and inducing fields were equal (Kirschmann, 1890). More recent experimenters have reported either that chromatic induction is not effected by the relative luminance of the test and inducing fields (Valberg, 1974), or that induction is greatest when the test field luminance is below that of the surround (e.g., Troscianko, 1977; 1982). In order to investigate the effect of test field luminance on the value of the C_{index} , the experiments described below were carried out.

EXPERIMENT 1

The spatial configuration of the scene was identical to the uniform centre - surround scene described in section 1 of this chapter. The chromaticity of the central test object was the same as that of the surround simulating illumination with illuminant D_{65} (i.e., $x = 0.3128$, $y = 0.3291$). The luminance of the surround was fixed at 25 cd/m^2 whilst that of the test was varied randomly between 6.3 and 50 cd/m^2 .

RESULTS

The results of the above experiment are reproduced in Figure 3.13 (A) where the C_{index} is plotted as a function of test field luminance. Data are presented for two colour normal observers (J.B. and J.S.) and the protanope (H.P.). Each data point represents the mean of five measurements and the computed standard errors were always less than 0.03 . As the luminance of the test object is increased towards that of the surround, the value of the C_{index} rises rapidly for subject J.S. and less rapidly for subject J.B.. There appears to be no systematic effect of test luminance on the value of C_{index} for subject H.P. For all subjects, however, the value of the C_{index} falls markedly when the luminance of the test object is equal to that of the surround (i.e., 25 cd/m^2). As the test luminance rises above that of the surround, the C_{index} initially increases again (at least for subjects J.B. and H.P.), and then decreases when the test

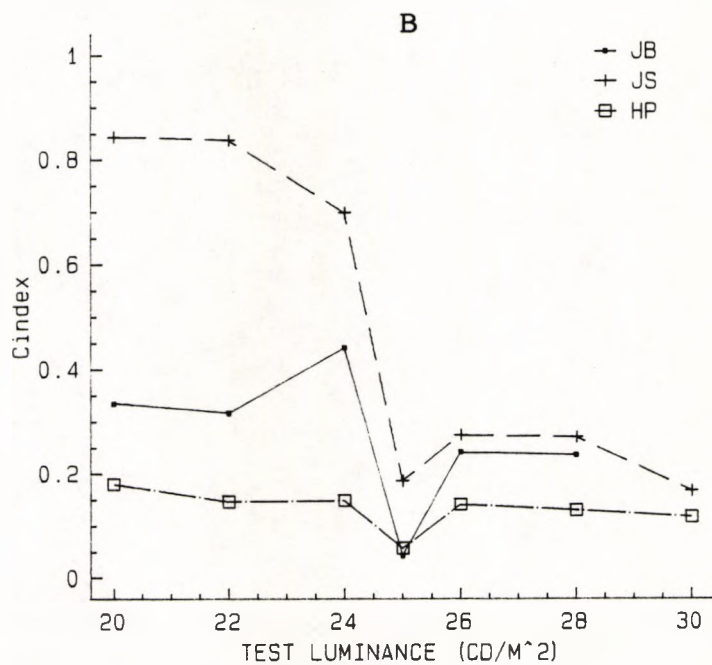
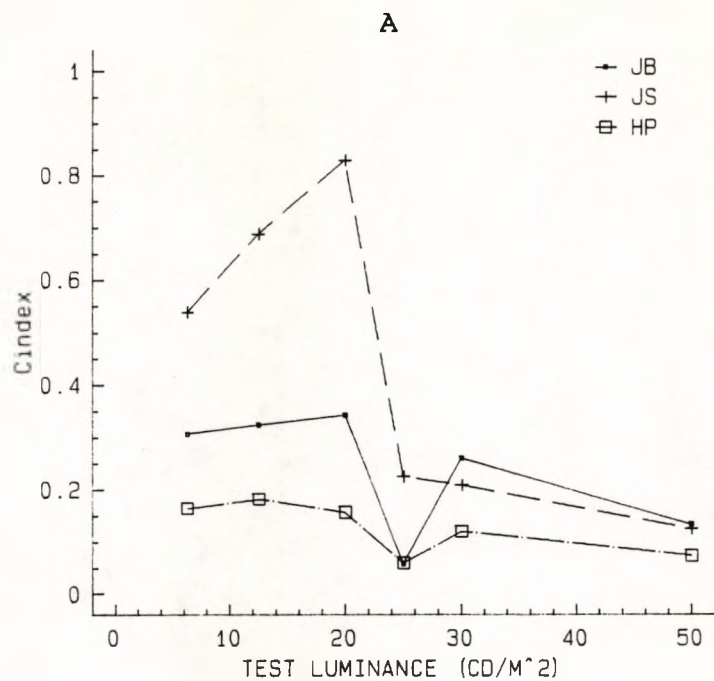


Figure 3.13. (A) C_{index} is plotted as a function of test object luminance for a simple centre-surround configuration. The surround was a uniform white of constant luminance 25 cd/m^2 . (B) The same experiment was repeated using test luminances covering a smaller range of values nearer to the luminance of the surround. Data is shown for two colour normal subjects (JB and JS) and one protanope (HP). Each data point shows the mean of five observations. Standard errors were < 0.03 for each data point and each subject.

luminance is raised to a value which is twice that of the surround.

In order to determine more precisely the test luminances for which the C_{index} was a minimum, the experiment was repeated using a series of test object luminances spanning a smaller range. The surround luminance was again constant at 25 cd/m^2 whilst the luminance of the test was varied in random sequence from 20 to 30 cd/m^2 . Figure 3.13 (B) displays the results of the experiment for the same three observers. It may be seen that the fall in C_{index} occurs specifically when the luminance of the test object is equal to that of the surround (or at least within 1 cd/m^2 of it).

COMMENTS

The data obtained for the two colour normal observers suggests that the effects of colour constancy increase as the test luminance approaches that of the surround, with maximal effects observed when the test luminance is just below that of the surround. Although experimental procedures differ widely, the results are in accordance with analogous chromatic induction experiments where the amount of induced saturation was measured (Pitt and Winter, 1974; Troscianko, 1977; Bartleson, 1979). Furthermore, the reduction in constancy observed when the test luminance exceeds that of the surround, is similar to the results reported in other induction experiments (Evans and Swenholt, 1967; 1969; Troscianko, 1982).

The results of the experiments reported in this section would seem to suggest that colour constancy should fail under certain conditions of isoluminance. Interestingly, a recent colour constancy algorithm tentatively proposed by Buchsbaum (1989) has the property of predicting zero constancy at isoluminance ! In the "real world", however, isoluminant conditions such as those produced artificially in the above experiments, occur very rarely and furthermore the experimental conditions are particularly "artificial" in that, at isoluminance, the test object and the surround

simulating the daylight condition were indistinguishable from one another (since the chromaticities, as well as luminances, were identical). In view of the loss of the border information in this situation (which has already been shown to be of great importance in determining the magnitude of colour constancy effects), it is perhaps not so surprising to find that the C_{index} measured at isoluminance was virtually zero.

EXPERIMENT 2

In order to produce a situation, therefore, in which chromatic borders would still be present at isoluminance, the chromaticity of the test object was modified in a second experiment to simulate a green Munsell chip (5G 6/6) with daylight chromaticity co - ordinates of $x = 0.2848$ and $y = 0.3839$. In a preliminary experiment, the luminances for which this test object and its surround were isoluminant, were determined using a procedure known as the minimum distinct border technique (Boynton and Kaiser, 1968). This technique relies on the fact that the observed border between two half - fields of differing chromaticity becomes less distinct as the luminance of the two half - fields approaches equality (for a comparison of different methods of heterochromatic photometry, see Wagner and Boynton, 1972). Having established the isoluminant point for a surround of 30 cd/m^2 , the value of the C_{index} was determined at isoluminance, and also for a range of test luminances around isoluminance.

CONCLUSIONS

Figure 3.14 displays the results of the experiment for two subjects, J.S. (colour normal) and H.P. (protanope). Error bars represent ± 1 standard error for five measurements. The results do not show the large reduction in the value of the C_{index} that was observed at isoluminance in the previous experiments. The relatively small reduction for subject J.S. seems to be part of a more gradual reduction in C_{index} occurring with increase in test luminance, and is probably

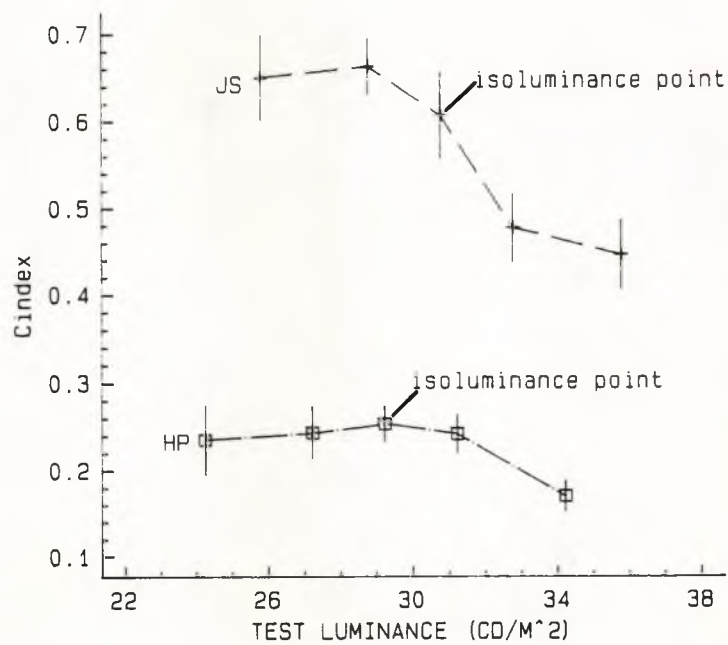


Figure 3.14. C_{index} is plotted against the luminance of a green test object (D_{65} chromaticity of $x=0.2848$, $y=0.3839$) viewed within a uniform white surround. The luminance of the test object and surround were equated using the minimum distinct border technique. The surround luminance was fixed at 30 cd/m^2 . Data is presented for one colour normal observer (JS) and one protanope (HP). Each data point indicates the mean of five observations and the error bars drawn represent ± 1 standard error.

unrelated to the condition of isoluminance per se. Using similar "disk - annulus" patterns presented simultaneously under two illuminants, Arend and Reeves (1991) have examined colour constancy for two luminance conditions, the first in which the luminance of the disk was below that of the surround, and the second in which disk luminance was greater than that of the surround. For the majority of their subjects, they found that larger constancy effects were observed when the annulus luminance was greater than that of the disk. The results presented here confirm Arend and Reeves' findings that object colour constancy is greatest when object luminance is below that of its surround, and also show that constancy effects diminish as object luminance rises significantly above that of the surround.

CHAPTER 4

PUPILLOMETRIC STUDIES IN NORMAL AND AMBLYOPIC SUBJECTS

In order to appreciate fully the properties of pupillary responses to chromatic stimuli, it is useful to consider first some of the basic responses to achromatic stimuli. This chapter will therefore detail experiments undertaken to examine the pupil light reflex (PLR) and the pupil grating response (PGR) in normal subjects. Whilst performing these preliminary studies, the opportunity arose to investigate these same pupillary responses in subjects with functional amblyopia (see Chapter 1). The results of these additional experiments are also reported in this chapter. The equipment used for all pupil response measurements has been described in Chapter 2, section 2.

4.1 PUPILIARY RESPONSES IN NORMAL SUBJECTS

4.1.1 THE PUPIL LIGHT REFLEX

The response of the pupil to a light flux change on the retina is probably the most well researched and documented of all the types of pupillary response. Previous investigations show that the magnitude of the PLR varies with stimulus intensity, area, and duration, and is also dependent on the state of retinal adaptation (see Chapter 1). For the purpose of this study, however, the PLR was investigated only as a function of stimulus intensity.

PROCEDURE

Stimuli for this experiment were generated on the Ayadin monitor and consisted of three achromatic luminance increments. The background subtended $18.7 \times 14.2^\circ$ at a viewing distance of 1 m, and was set at a fixed luminance of 9.4 cd/m^2 . The stimulus subtended $4.8 \times 4.8^\circ$ and was presented foveally for a duration of 300 ms. Pupil size was recorded for each eye continuously over a period of not less than 2 seconds, and commenced 300 ms prior to stimulus

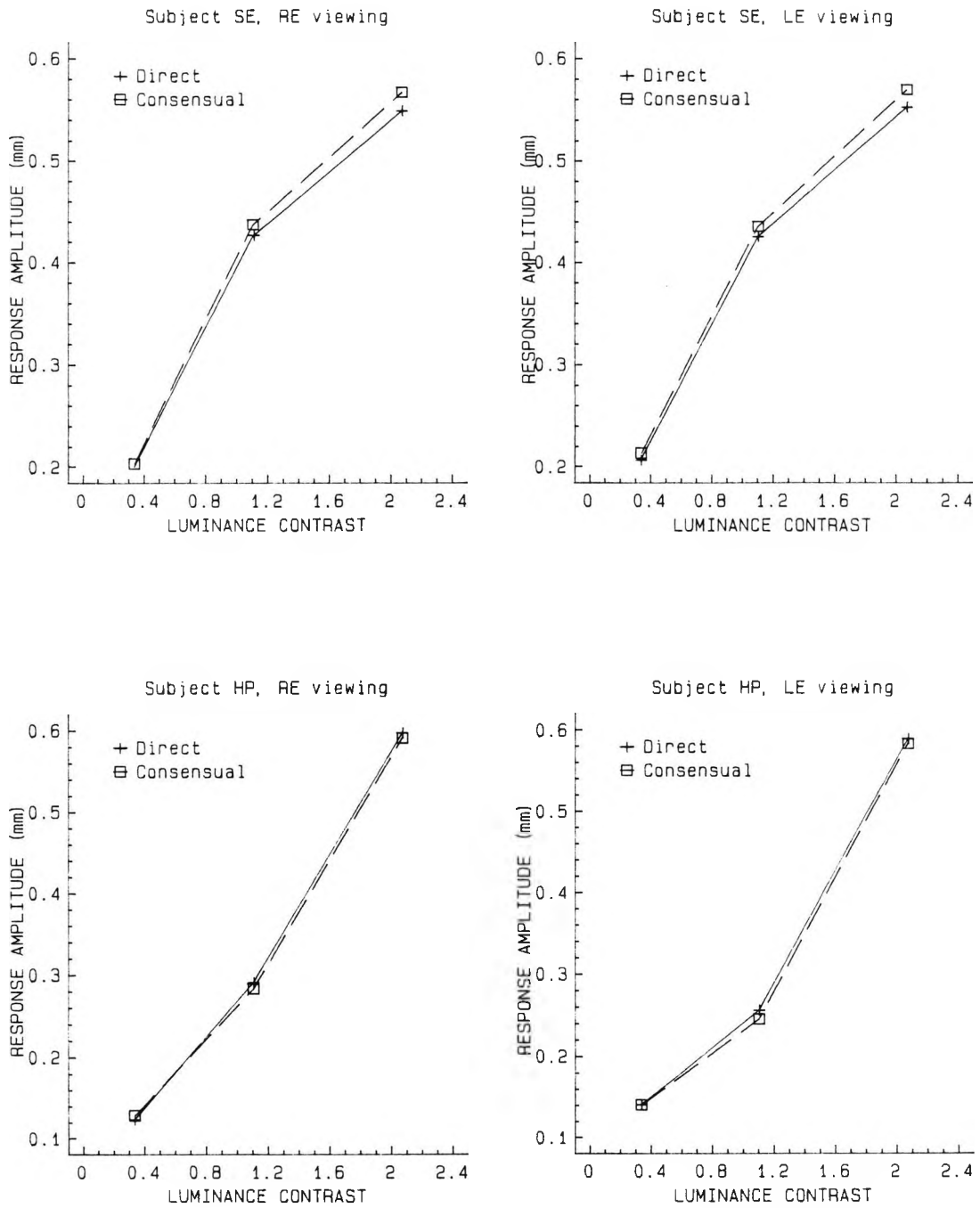


Figure 4.1. Pupil response amplitude plotted for three levels of luminance contrast for two subjects. The data shows the highly consensual nature of the pupil light reflex, and the equality of responses following monocular stimulation of right and left eyes.

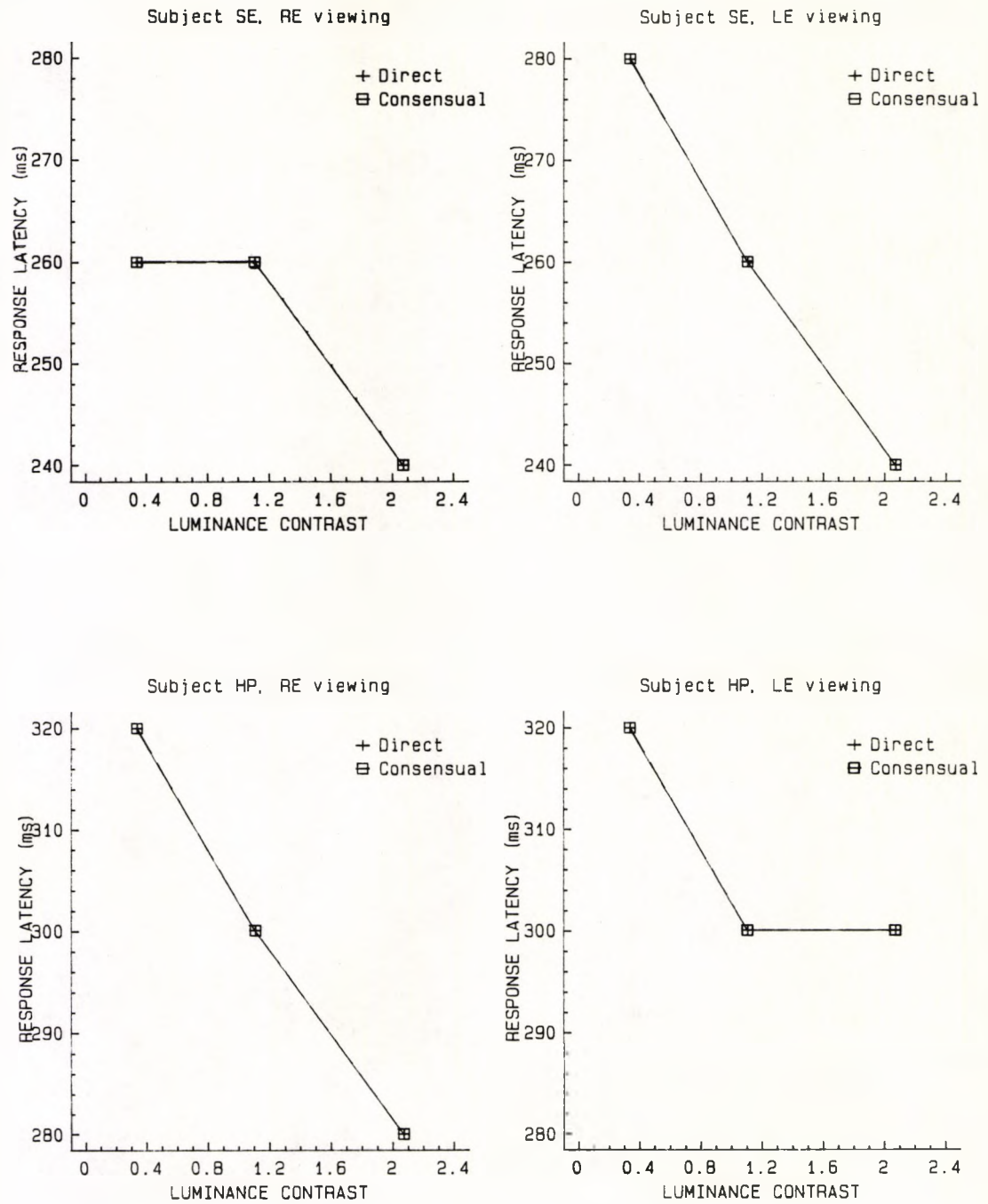


Figure 4.2. Pupil response latency plotted for three levels of luminance contrast for two subjects. The data shows the highly consensual nature of the pupil light reflex, and the similarity of response latencies following monocular stimulation of right and left eyes.

onset. Each stimulus condition was presented 15 times in random order, with about 4 seconds between each trial to allow for blinking. Viewing conditions were monocular with each eye being tested separately in two successive experiments. Throughout the course of the experiment the subject was instructed to fixate a small, central fixation target and to endeavour not to blink during recording periods (the beginning and end of which were marked by auditory stimuli). Each participating subject had normal visual acuity in each eye of 6/6 (Snellen) or better, and any refractive error was corrected. The subject viewed the uniform background for three minutes before any stimuli were presented so as to reach a steady state of light adaptation.

RESULTS

Results from the above experiment are shown in Figures 4.1 and 4.2. In Figure 4.1 pupil response amplitude has been plotted as a function of the stimulus luminance contrast for each subject. To clarify, the pupil response amplitude refers to the difference (in millimetres) between the pre-stimulus pupil size, and the pupil size recorded at the time of maximum constriction (see Figure 2.10). The stimulus luminance contrast may be defined as:

$$\frac{\text{LUMINANCE}_{\text{stimulus}} - \text{LUMINANCE}_{\text{background}}}{\text{LUMINANCE}_{\text{background}}}$$

It may be seen that the pupil response amplitude increases as the luminance of the stimulus increases, and that the response amplitudes for the direct and consensual reflexes are virtually identical. Similarly there was no significant difference in response amplitude between right and left eyes for stimuli of the same luminance. Figure 4.2 shows pupil response latency plotted as a function of luminance contrast for each subject. Data are presented for the direct and consensual responses of both the right and left eyes. The results show that there is a decrease in response latency with increasing luminance contrast. Again, differences

between direct and consensual, and between right and left eyes were not found to be significant.

Although the data presented here are only for two subjects, several other normal subjects have participated in the experiment. The inter - subject differences with respect to the absolute amplitude and latency of the pupillary responses were found to be large, although the trends are similar in all cases.

In summary, an increase in stimulus luminance level results in an increase in the pupil response amplitude which is usually associated with a corresponding decrease in response latency. The pupillary responses show a high degree of consensuality and symmetry. The results of this experiment are in general agreement with those obtained by other researchers. For example, Webster et al. (1968), using a conventional optical system to generate their stimuli, demonstrated a similar increase in the amplitude of the pupillary response with target luminance. Likewise, Lee et al. (1969) found a decrease in pupil response latency with an increase in stimulus intensity.

The rapid constriction of the pupil following a sudden increase in retinal illuminance level may have a functional role to play in protecting the visual pigments of the retina from extensive bleaching (Barlow, 1972; Alpern et al., 1974). In a similar way, the constriction of the pupil at high light levels reduces the retinal illumination and facilitates a subsequent return to dark adaptation (Alpern and Campbell, 1962; Woodhouse and Campbell, 1975). The pupil makes only a small contribution towards the range of light levels to which the eye responds. The total area change when the pupil constricts from 8 mm to 2 mm is 16 times, whereas the range of luminance levels required to change the pupil size by this same amount is 10^6 times (Reeves, 1918; Crawford, 1936). It has also been shown that the pupil acts to optimise visual resolution in all lighting conditions (Campbell and Gregory, 1960; Woodhouse, 1975).

4.1.2 THE PUPIL GRATING REFLEX

In addition to the PLR, recent investigations have shown that systematic pupillary responses can be induced by changes in the spatial structure of a stimulus (see Chapter 1). The following experiment illustrates the response of the pupil to achromatic, sinusoidal grating stimuli of fixed space - averaged luminance.

PROCEDURE

The grating stimuli required for this experiment were generated using the Picasso pattern generator and Tektronix monitor described in Chapter 2, section 2. The monitor was positioned at a viewing distance of 1.37 m, at which distance the angular subtense of the screen measured $5.2 \times 4.2^\circ$. The stimulus consisted of a circular, achromatic sinusoidal grating presented foveally for 330 ms at a contrast of 60% and subtending a visual angle of approximately 4° . Here contrast is defined as the Michelson contrast, or $L_{\max} - L_{\min} / L_{\max} + L_{\min}$ (*100). The mean luminance of the grating pattern was 11.9 cd/m^2 and this remained constant for all spatial frequencies tested. In all, 10 grating spatial frequencies were presented in random order ranging from 0.5 cycles per degree (c/deg) to 24 c/deg. The procedure for determining the pupillary responses to these grating stimuli was the same as that used in the preceding experiment to measure the PLR. It was also of interest to compare pupillometric measurements with the corresponding psychophysical contrast sensitivity function. Consequently the behavioural contrast sensitivity was determined for each subject using identical stimulus configuration and parameters to that detailed above. An adaptive staircase procedure with three reversals was employed in the contrast threshold measurement.

RESULTS

Data from the above experiments are presented for two subjects in Figure 4.3. In (A), pupil response amplitude is

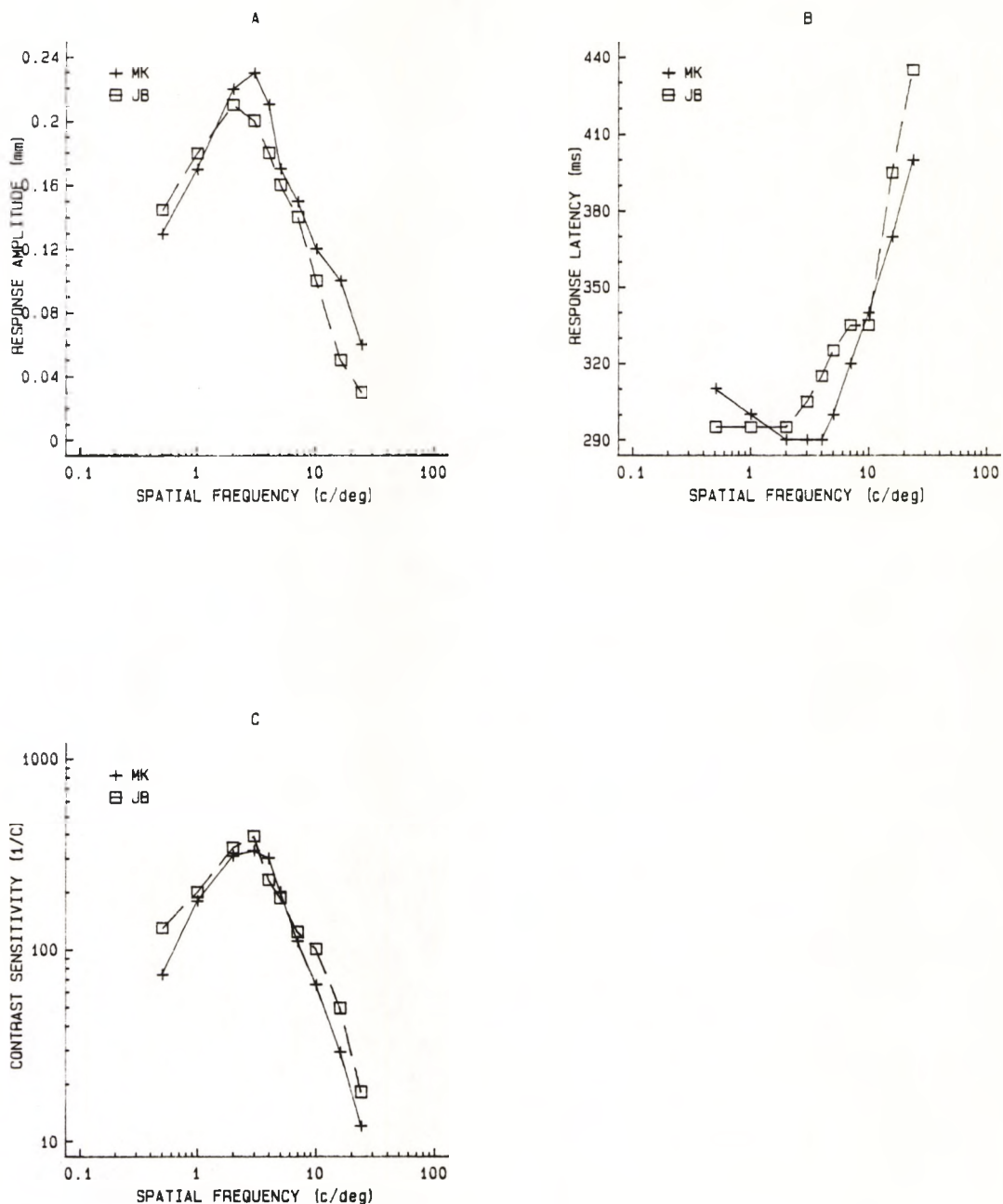


Figure 4.3. (A) Pupil response amplitude and (B) pupil response latency are plotted as a function of the spatial frequency of a sinusoidal grating of 60% contrast. The circular grating subtended a visual angle of 3.6° and was presented foveally for a duration of 330 ms. The space-averaged luminance of the grating was equal to that of the background (11.9 cd/m^2). Each symbol represents the mean of the direct and consensual response for monocular viewing (the response averaged for 15 presentations). The psychophysical contrast thresholds for detection of the same stimulus are shown in (C). Data are presented for two subjects (MK and JB).

plotted as a function of grating spatial frequency, whilst in (B) the corresponding response latencies are displayed. The contrast sensitivity function for the same subject is presented in (C), and is plotted in the conventional manner with the reciprocal of the threshold contrast for detection as ordinate, and spatial frequency as abscissa. The pupil responses were again found to be highly consensual in terms of both the response amplitude and response latency, and therefore the data are presented for the mean of the direct and consensual responses. Similarly analysis of variance showed that there were no significant differences between the responses obtained with the right or the left eye viewing independently.

It may be seen that the transient constriction of the pupil which follows the stimulus, varies systematically in both amplitude and latency as a function of grating spatial frequency. It is interesting to note that the pupil response amplitude and the behavioural contrast sensitivity appear to have a similar relationship with respect to the spatial frequency of the grating stimulus. The data show an increase in response latency for grating frequencies in the high spatial frequency range. Pupil response latencies following stimulation with gratings of all spatial frequencies were found to be longer than those following stimulation with unpatterned fields (i.e., for the PLR).

The small, but systematic changes observed in pupil response amplitude with grating spatial frequency confirm the reports of similar experiments by Barbur and Thomson (1987) and Barbur et al. (1987a; 1987b). The similarity of the contrast sensitivity functions and the PGR data suggest that both types of measurement may involve similar mechanisms. Further support to this statement is given by the fact that both measurements are similarly affected by defocus and eccentric viewing (see Barbur, 1988). Since both contrast sensitivity and PGR data show similar high spatial frequency cut - off properties (see Figures 4.3 A-C), it has also been proposed that pupillometry may be used as an objective measure of visual acuity (Barbur and Thomson, 1987; Slooter, 1985).

The increase in pupil response latency observed with increasing spatial frequency gratings correlates with similar findings for visual evoked potentials (Parker and Salzen, 1977) and reaction time experiments (Breitmeyer, 1975; Tolhurst, 1975; Vassilev and Mitov, 1976). It has been suggested (Vassilev and Mitov, 1976) that the increase in reaction times observed for high spatial frequency stimuli is related to a change in the visual channels used in the detection of grating stimuli, from sustained at low frequencies, to transient at higher frequencies. It is also possible that longer latencies simply reflect a longer visual pathway, and Breitmeyer (1975) has postulated that there may be a transfer of processing from the superior colliculus to the striate cortex.

What is the origin of the PGR ? The PLR is usually attributed to retinal afferent signals to the pre - tectal nuclei (Brindley et al., 1969), yet studies in patients with damaged central visual pathways suggest that the PLR is reduced in amplitude when the stimulus is restricted to blind areas of the visual field (Cibis et al., 1975; Zihl, 1980; Alexandridis et al., 1983; Keenleyside et al., 1988). These studies suggest that, contrary to classical theories (see Alexandridis, 1985 and also Davson, 1980), geniculostriate projections may play some role in the mediation of the PLR. Further evidence for this comes from the work of Jampel (1959), who found that miosis and accommodation changes could be induced by electrical stimulation of pre - striate areas. More recent investigations with hemianopic subjects and subjects with occipital lesions have shown that the PGR is absent when grating stimuli are restricted to perimetrically blind areas of the visual field (Barbur et al., 1987a; Keenleyside et al., 1988). It seems highly likely, therefore, that central mechanisms are involved in the mediation of the PGR.

4.2 PUPILLARY RESPONSES IN AMBLYOPIC SUBJECTS

As stated in chapter 1, the study of pupillary responses in amblyopic subjects is of interest for two main reasons: (i) as a possible aid to the localisation of the site of the deficit in such subjects; and (ii) as an aid in the clinical differential diagnosis of amblyopia from other more serious pathological conditions.

CLINICAL INVESTIGATION OF AMBLYOPIC SUBJECTS

In all, 22 amblyopic subjects participated in this study, and it was important to ascertain the type and extent of the visual deficit present in each. The University Optometry Clinic was suitably equipped for this purpose, and each of the subjects underwent a thorough orthoptic and ophthalmic examination.

A clinical history was first taken in order to determine the age of onset of the amblyopia, any previous occlusion or other treatment, and details of spectacle usage. Retinoscopy was performed and followed by a careful subjective refraction. Visual acuities for amblyopic eyes were measured in three ways:

- (i) morphoscopic or line acuity, where the subject is required to read the smallest line from a standard (Snellen) chart of letters;
- (ii) angular or letter acuity, where the subject identifies an isolated letter;
- (iii) the acuity with a neutral density filter (ND 2) in front of the eye.

These three methods of visual acuity measurement can, in themselves, give more information concerning the nature of the amblyopia. Angular acuity in the amblyopic eyes of strabismic subjects, is usually better than the morphoscopic acuity because of the phenomenon of "separation difficulty" (Bangertter, 1950; Rubinstein, 1984). It is therefore a useful measure in the differential diagnosis of

anisometropic and strabismic amblyopia (Amos, 1978). Similarly, a neutral density filter placed before the amblyopic eye of a strabismic subject can result in an improvement of the visual acuity (von Noorden and Burian 1959a, 1959b), whereas in normal eyes, or eyes with anisometropic amblyopia, the visual acuity is reduced (Pickwell, 1984). A cover test was performed for distance and near fixation in order to evaluate the magnitude of any heterotropia (strabismus) or heterophoria (latent strabismus) present (see Bennett and Rabbetts, 1984). In certain amblyopic subjects where the depth of the anomaly is not too severe, a quasi - binocularity may develop and allow a degree of stereopsis (Pickwell, 1980a, 1980b; Mallett, 1970). Stereopsis was measured using the Frisby, Titmus and Mallett tests (for a review of stereopsis tests see Hall, 1982) and the mean result recorded. The absence or presence and magnitude of eccentric fixation was investigated with the aid of a visuoscope and with transfer after - image techniques (Brock and Givnor, 1952; Mallett, 1975), again with the mean result of both methods being recorded. In strabismic amblyopia it is often the case that the magnitude of eccentric fixation correlates with the visual acuity, though Hess (1977) has shown that this is not always the case. In some cases, Amsler Chart No.1 (Amsler, 1949) was also used to aid differential diagnosis. The subject views a white grid on a black background and reports any loss or distortion of the grid pattern, the position and size of the scotoma observed (if any) being diagnostic of the nature of the amblyopia (Pickwell, 1984).

Table 4.1 overpage shows the results of the above tests for the amblyopic subjects who participated in this study. The criteria described in this section, together with the known ocular history, provided sufficient information to classify the subjects into strabismic and anisometropic categories. The initial aim of the study was to investigate pupillary responses in purely strabismic or purely anisometropic amblyopes, but an additional 3 mixed strabismic - anisometropic amblyopes were also found and participated in the project. As can be seen from Table 4.1, the depth of the

CLINICAL DETAILS OF AMBLYOPIC SUBJECTS

Subject	Age	Refraction	MVA	AVA	VA(2ND)	OMB	Stps	Fixation	Class	History	
1. T.O.	20	R.Plano L.+3.50/-1.25 x 30	6/5 6/60	6/18	6/60		Ortho	Nil	Central	Aniso	Occlusion at 7yrs for 1yr. No Rx.
2. S.R.	26	R.+0.25/-0.50 x 180 L.+1.00/-1.25 x 15	6/6 6/60	6/24	6/60		6°LSOT	Nil	Central	Strab	No treatment. No Rx.
3. F.W.	68	R.+4.00/-1.50 x 100 L.+7.00/-2.00 x 65	6/5 6/18	6/18	6/24		Ortho	475"	Central	Aniso	No treatment. Rx worn since child.
4. J.N.	65	R.Plano/-2.00 x 100 L -1.00/-3.00 x 85	6/6 6/60	6/24	6/36		1°LSOT 1 LHOT	510"	15' N	Strab	No treatment. Rx worn since child.
5. N.L.	26	R +3.00/-1.00 x 180 L +0.50/-0.25 x 170	6/18 6/4				Ortho	Nil	Central	Aniso	No treatment. No Rx.
6. D.P.	18	R +2.50/-1.25 x 90 L +2.25/-1.75 x 80	6/4 6/9	6/9	6/9		2°LSOT 2 LHET	800"	Central	Strab	Occlusion at 5yrs for 2yr. Rx at 2yr.
7. S.N.	17	R -1.00/-0.75 x 120 L -1.75/-1.25 x 80	6/5 6/18	6/9	6/18		4°LSOT	Nil	Central	Strab	Occlusion at 5yrs for 1yr. Rx at 13yr.
8. R.T.	37	R +0.25 DS L +7.50/-3.50 x 30	6/5 6/60	6/36	6/60		Ortho	Nil	Central, unsteady	Aniso	Rx worn 7-14yrs. Occlusion 7-14yrs.
9. C.L.	50	R +4.50/-2.00 x 20 L +0.25/-1.00 x 5	1/60 6/5				17°RSOT	Nil	Unsteady	Mixed	No treatment. No Rx.
10.R.S.	41	R -1.00 DS L -1.00 DS	6/6 6/18				11°LSOT	Nil	15' N	Strab	Occlusion at 6yrs for 3 months.
11.C.G.	22	R.Plano/-0.25 x 180 L +4.00/-3.00 x 5	6/4 5/60	5/60	4/60		Ortho	Nil	Central	Aniso	Occlusion at 8yr for 1-2yrs Rx at 6yrs.
12.S.M.	24	R.Plano L +3.50 DS	6/4 6/24				1°LSOT	Nil	15' N	Mixed	No treatment.
13.K.W.	29	R +1.50 DS L +0.75/-0.25 x 90	6/18 6/4	6/6	6/18		1°RSOT	115"	45' N	Strab	No treatment.
14.A.Y.	22	R +1.25/-0.25 x 45 L +0.50 DS	6/9 6/3	6/6	6/9		1°RSOT	100"	Central	Strab	Occlusion at 8yrs for 3yrs.
15.P.M.	21	R +0.50 DS L +2.00 DS	6/3 6/24				8°LSOT	Nil	Central	Strab	Occlusion & surgery at 7yrs.
16.H.P.	21	R -1.50/-1.75 x 170 L -2.00/-1.50 x 70	6/6 6/36	6/18	6/18		2°LSOT	Nil	1° N	Strab	No treatment.
17.J.A.	18	R +7.25/-0.50 x 100 L +7.25/-1.00 x 65	6/12 6/5	6/6	6/9		4°RSOT	Nil	15' N	Strab	Rx since 3yrs. Occlusion until 7yrs
18.S.T.	55	R -0.25/-0.50 x 65 L +0.50 DS	6/4 1/60				10°LSOT	Nil	1° N	Strab	Rx at 5yrs. Occlusion as child.
19.J.S.	46	R -5.00 DS L +1.50/-0.50 x 20	2/60 6/5				15°RXOT	Nil	Central	Mixed	No treatment.
20.P.C.	19	R +0.50/-0.50 x 40 L +3.75/-0.75 x 40	6/4 6/9	6/6	6/9		Ortho	Nil	Central	Aniso	No treatment. Rx since 5yrs.
21.P.S.	43	R +3.25/-3.00 x 10 L -0.50 DS	6/12 6/5				Ortho	Nil	Central, unsteady	Aniso	No treatment or Rx.
22.A.P.	58	R +1.00 DS L +0.75 DS	6/6 6/24	6/9	6/24		2°LSOT	Nil	Central	Strab	Occlusion at 2yrs for 4rs. Orthoptic treatment at 12yrs.

Abbreviations used in table:

MVA morphoscopic visual acuity; AVA angular visual acuity; VA(2ND) morphoscopic visual acuity with 2 log unit neutral density filter; OMB oculomotor balance; Stps stereopsis; Ortho orthophoric; SOT esotropia; XOT exotropia; HOT hypotropia; HET hypertropia; Aniso anisometropic; Strab strabismic; Rx spectacle correction.

Table 4.1. Clinical details of amblyopic subjects.

amblyopic anomaly varied over a wide range, with visual acuities from 6/9 to 1/60 (Snellen). For comparison purposes a group of 6 subjects with normal binocular vision and visual acuity were also included in the study. Again each of the normal subjects underwent an ophthalmic examination to confirm visual acuity, binocular status etc. prior to the pupillometric investigation. All subjects wore their optimum optical correction, as determined at the time of their examination, during the experimental sessions.

PROCEDURE

The experimental procedure and stimulus generation were basically the same as that previously described in section 1.1 of this chapter, when measurements of the pupil light response were made for normal subjects. Stimulus luminance levels were 8.4, 13.3, and 19.4 cd/m^2 with each presented on a uniform background of luminance 6.2 cd/m^2 . For some subjects however (see following results section), pupillary responses to larger luminance contrasts were also measured, and where this was the case stimulus luminances of 26.8 and 35.1 cd/m^2 were used on the same background.

In a separate experimental session, achromatic, sinusoidal grating stimuli were presented at a fixed contrast of 80% over a rectangular area subtending $4.8 \times 4.8^\circ$. The space-averaged luminance of the gratings was constant and equal to the luminance of the uniform background (i.e., 11.9 cd/m^2). Gratings of three spatial frequencies were used: 1.2; 3; and 6 c/deg. In some subjects pupillary responses were also measured over a larger range of grating spatial frequencies i.e., from 0.5 to 24 c/deg. In this instance stimuli were generated using the Tektronix monitor and presented at a contrast of 60% over a circular area subtending approximately 4° at a viewing distance of 1.37 m (i.e., the stimulus parameters were identical to those described in section 1.2 when grating responses were investigated in normal subjects).

For both the luminance and grating experiments each stimulus condition was presented 15 times in random order. Measurements were taken with either the normal eye or the amblyopic eye occluded. Whilst viewing conditions were monocular, measurements of pupil size were always made binocularly so that both the direct and the consensual response were recorded. The eye occluded first was randomised between subjects. For the more severely amblyopic eyes it was often found necessary to increase the size of the central fixation target to facilitate fixation.

In addition to the stimulus conditions described above, measurements of the resting state pupil diameter under conditions of monocular and binocular view were also made specifically in several subjects (4 subjects from each of the strabismic, anisometropic and normal groups). In this case the subject simply viewed the uniform field (luminance 6.2 cd/m^2) with occlusion of each eye in turn, and then with no occlusion, the viewing conditions being randomised between subjects. Measurements of pupil diameter were recorded over a period of 13.5 seconds for each condition and were usually made after performing the luminance modulation and grating experiments.

Where possible contrast sensitivity measurements were made for the amblyopic eye and the normal eye using the procedure described in section 1.2 of this chapter.

RESULTS

The data for each individual subject were grouped according to the type of amblyopia. In this way data were averaged separately for strabismic, anisometropic, and mixed strabismic - anisometropic amblyopes. Furthermore, a statistical analysis of the data showed no significant differences between the direct and the consensual responses (p always > 0.9) following stimulation of either the amblyopic or the normal eye. Since this was the case for both grating and luminance stimuli, the responses in the two eyes were always averaged. A statistical analysis of the

data is shown in Figure 4.4. A multi - way analysis of variance for a mixed model has been used to analyse the data - sets for each group and for each stimulus condition. The mixed model employed assumes that the subjects have been selected randomly for each group i.e., small, random samples of normal subjects and amblyopic subjects taken from larger populations. The remaining factors, namely the stimulus characteristics (i.e., luminance contrast, grating spatial frequency, background luminance level, eye to which stimulus is presented etc.), have been taken as fixed since they were chosen specifically and remained unaltered throughout the investigation. The expected mean squares play an important part in the analysis of variance table for a model of this kind and have been used to develop the appropriate statistic for testing hypotheses about any model parameter.

Figure 4.5 displays the averaged pupil response amplitude as a function of stimulus luminance contrast for the three amblyopic subgroups, and Figure 4.6 shows some typical traces from which the data was extracted. In Figure 4.5, the averaged response amplitude following stimulation of the amblyopic eyes (crosses) is compared with that following stimulation of the fellow normal eyes (discs). It can be seen that the response amplitudes for amblyopic eyes are reduced only minimally with respect to the fellow normal eyes for the anisometropic and strabismic groups, but the reduction is somewhat greater for the mixed group. The reduced response amplitudes however, were not found to be statistically significant for any of the three amblyopic subgroups (see Figure 4.4). One noticeable feature is that the absolute response amplitudes for the mixed amblyope subgroup are depressed compared with those of the other two. Moreover, if response amplitudes for the normal eyes of each amblyopic group are compared with the normal eyes of normal observers (see Figure 4.7), then the data show reduced amplitude responses in all amblyopic groups by comparison with normal subjects, though these differences were only found to be statistically significant for the strabismic and mixed group. No significant differences were

GROUPS OF SUBJECTS AND NOTATIONS USED

NORMALS	NORM,	Right Eye	NORM_R,	Left Eye	NORM_L
ANISOMETROPIC	REF,	Amblyopic Eye	REF_A,	Good Eye	REF_G
STRABISMIC	STRAB,	Amblyopic Eye	STRAB_A,	Good Eye	STRAB_G
MIXED	MIXED,	Amblyopic Eye	MIXED_A,	Good Eye	MIXED_G

SUMMARY OF ABBREVIATED NAMES

NORM_AV Averaged result following left and right eye stimulation in the normal group.

REF_AV Averaged result following good and amblyopic eye stimulation in the group of anisometropic amblyopes.

STRAB_AV Averaged result following good and amblyopic eye stimulation in the group of strabismic amblyopes.

MIXED_AV Averaged result following good and amblyopic eye stimulation in the group of mixed amblyopes.

TYPE OF MEASUREMENT CARRIED OUT AND NOTATION USED

INITIAL	Pupil Diameter (pre-stimulus)	INIT_D
Dynamic Response	AMPLITUDE	AMPL
Response	LATENCY	LAT
SPATIAL FREQUENCY	of grating pattern	S_FREQ

SYMBOLS USED TO DESCRIBE SIGNIFICANCE LEVEL

NS Difference not significant at the 10% level ($p > 0.1$)

***** Difference is significant at the 5% level ($p < 0.05$)

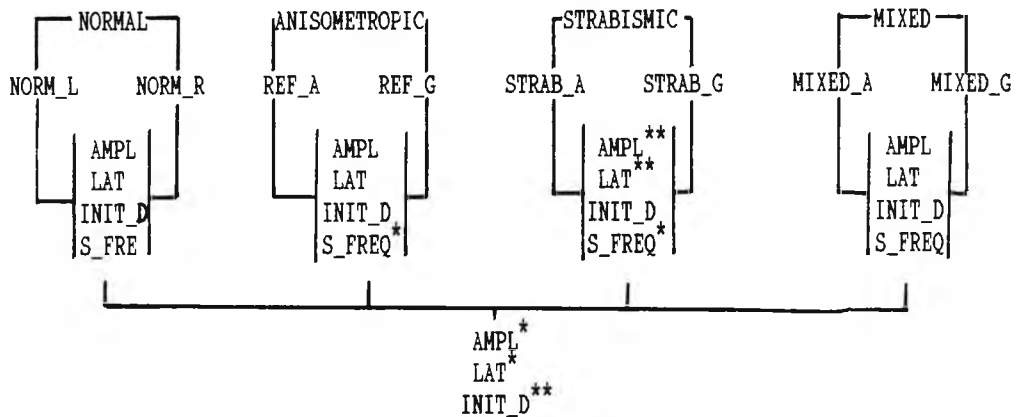
****** Difference is significant at the 1% level ($p < 0.01$)

******* Difference is significant at the 0.1% level ($p < 0.001$)

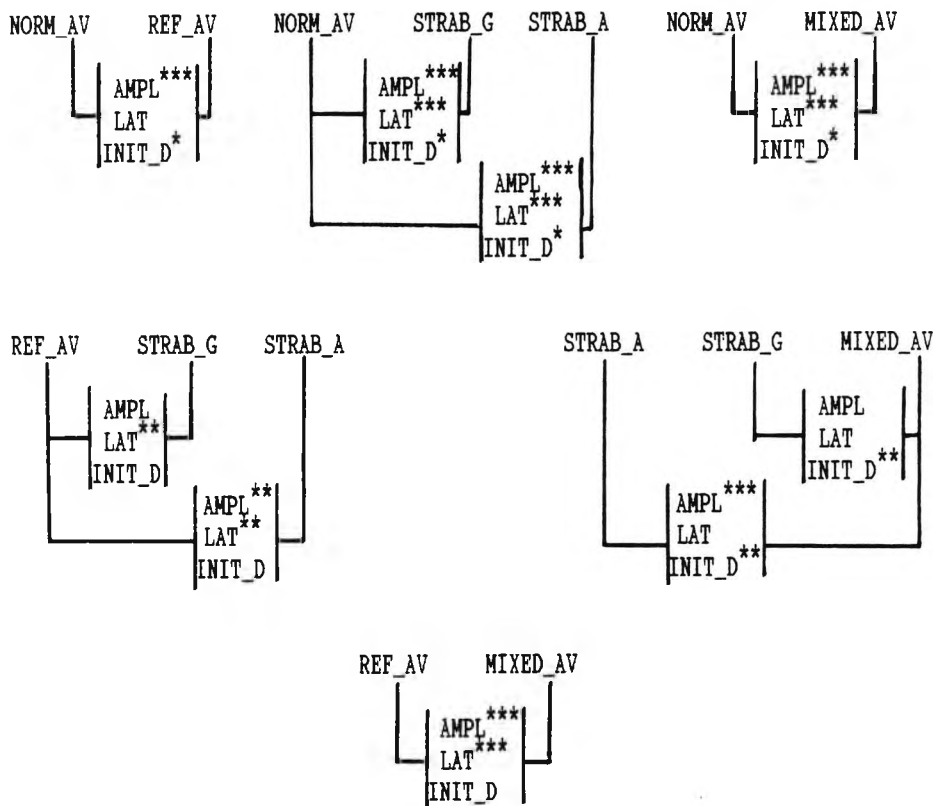
Figure 4.4 (A). Key to statistics table presented overpage
contd....

ANALYSIS OF INITIAL PUPIL DIAMETER AND RESPONSES TO ACHROMATIC GRATINGS

Significance of differences in response to fixed parameters within each group



Significance of differences in response to fixed parameters across all groups



Significance of differences in response to fixed parameters in separate comparisons of two selected groups

Figure 4.4 (C). Statistical analysis of pupillary responses to achromatic gratings (see text for description of tests employed).

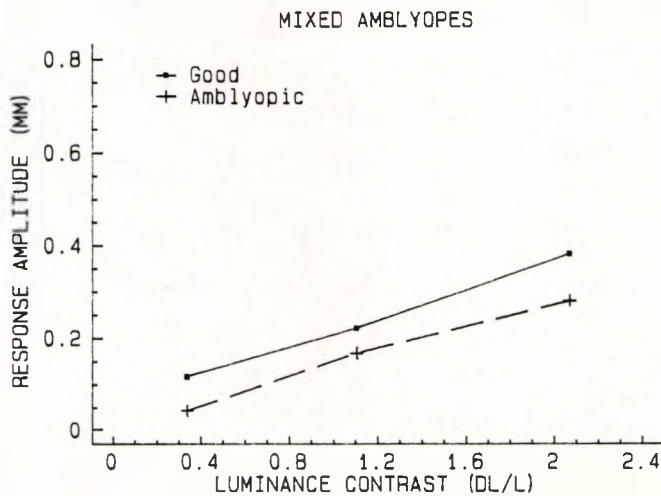
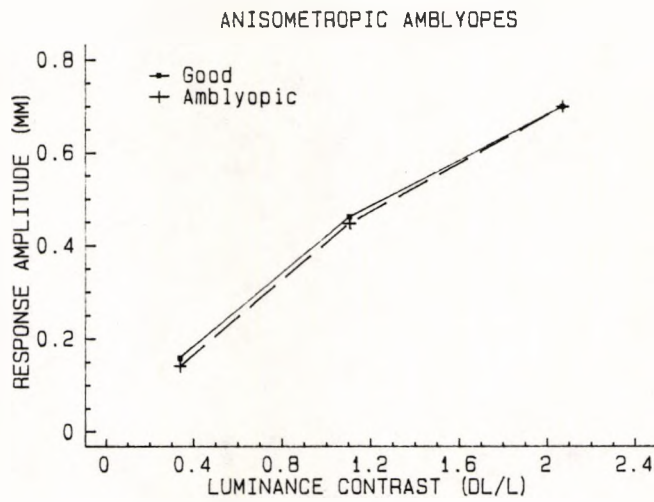
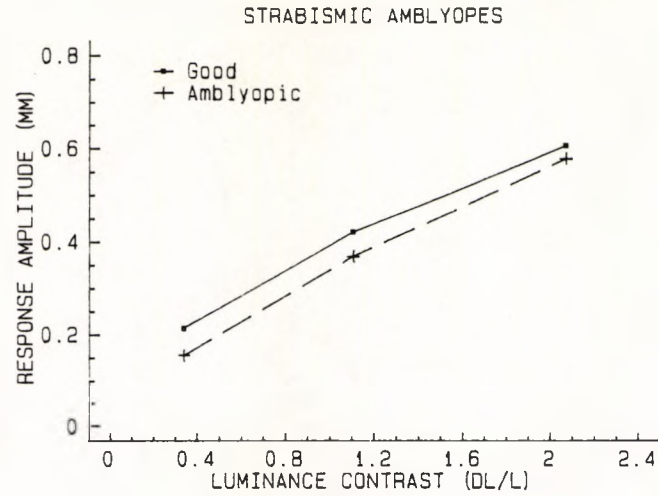


Figure 4.5. The average response amplitude for the pupil light reflex measured in each subgroup of amblyopes, following monocular stimulation of either the normal or the amblyopic eye, is plotted against stimulus luminance contrast. Pupillary responses were recorded binocularly, but since no significant differences were found between the direct and consensual responses following stimulation of either eye, these responses were always averaged. The results do not show any statistically significant difference in response amplitude following stimulation of the normal or the fellow amblyopic eye within each group (see Figure 4.4).

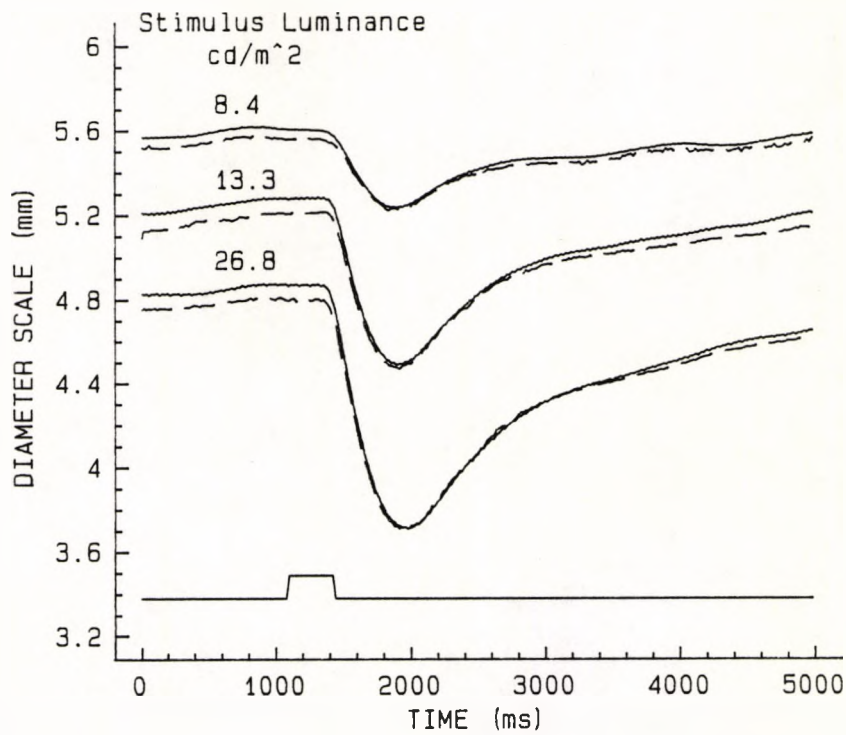
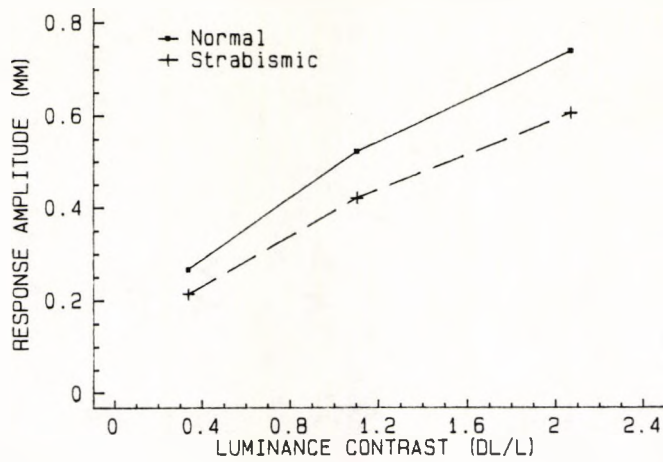
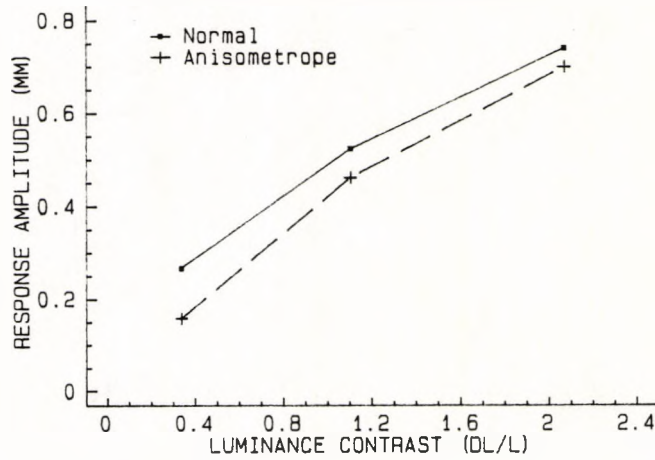


Figure 4.6. Some typical pupil diameter traces from which the response parameters were extracted. Data is shown for an anisometropic amblyope, the dotted line refers to the normal eye, and the solid line refers to the amblyopic eye (the mean of the direct and consensual response is drawn). The stimulus profile is shown just above the abscissa.

NORMAL EYES COMPARED WITH THE GOOD EYES
OF STRABISMIC AMBLYOPES



NORMAL EYES COMPARED WITH THE GOOD EYES
OF ANISOMETROPIC AMBLYOPES



NORMAL EYES COMPARED WITH THE GOOD EYES
OF MIXED AMBLYOPES

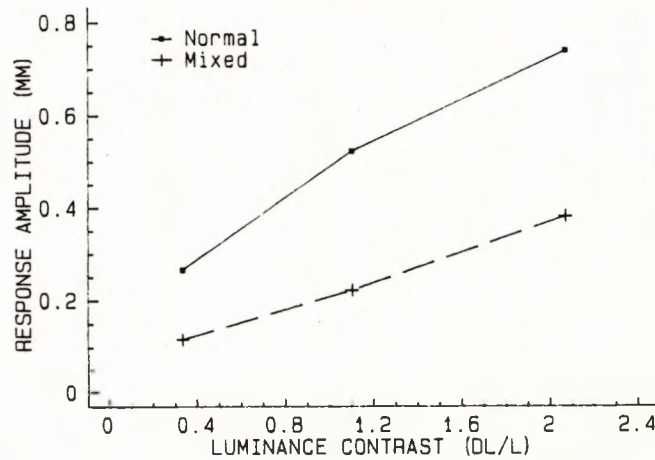


Figure 4.7. Average response amplitude of the pupil light reflex is plotted against the stimulus luminance contrast for the normal fellow eyes of each amblyopic subgroup (crosses and broken lines), and the normal eyes of a group of normal observers (dots and solid lines). The differences were only statistically significant for the strabismic and mixed amblyopes (see Figure 4.4).

found between right and left eyes of normal observers and consequently the mean response has been plotted.

Figure 4.8 displays the averaged pupil response latency as a function of stimulus luminance contrast for the three amblyopic groups. Again responses are compared for amblyopic eyes and fellow normal eyes within each group. The latencies for the amblyopic eyes in all groups were significantly longer than for the good eyes in the same group. This is especially clear for the lowest luminance contrast, where the mean increase in latency averaged over the three groups was about 50 ms (there were no significant differences between the amblyopic eyes of each group). Inspection of these data shows that, at least for the strabismic and anisometropic groups, the latency deficit for amblyopic eyes decreases with an increase in stimulus luminance contrast; at a luminance contrast of just over 2, the latency deficit is of the order of only 10 ms. At higher luminance contrasts therefore, would the response latencies of the amblyopic eye and its fellow normal eye become the same? To investigate this possibility, several representative amblyopes participated in a further experiment in which higher stimulus luminance contrasts were used. Figures 4.9 and 4.10 show the results of this experiment for each of three strabismic and three anisometropic amblyopes. Interestingly the amblyopic latency deficit is maintained at about 10 ms for the anisometropic subjects, but for the strabismic subjects the deficit is abolished, with in fact two subjects demonstrating shorter response latencies for the amblyopic eye.

Is this observed latency deficit for the light reflex of amblyopic eyes related to stimulus visibility? To examine this possibility, the pupil latency deficit for each subject was compared with any low spatial frequency contrast sensitivity deficit demonstrated by the subject. No correlation ($c = 0.1$) was found to exist. Similarly there was no correlation ($c = 0.3$) between subject visual acuity and pupil response latency. No significant differences in

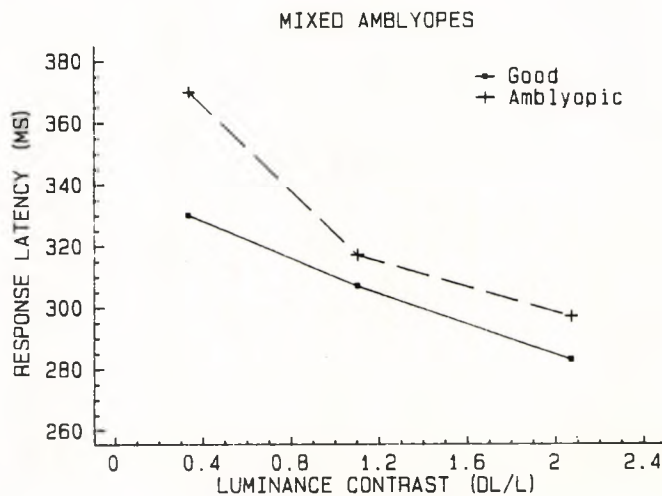
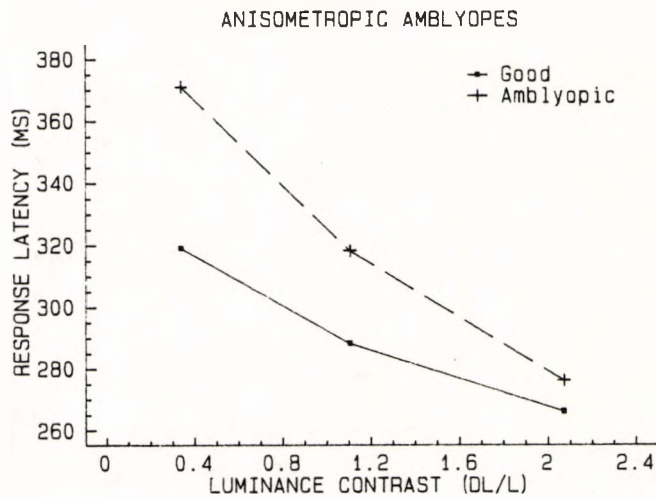
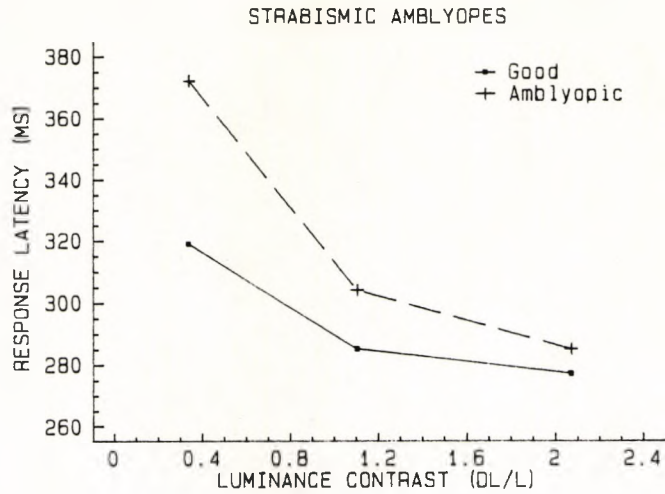


Figure 4.8. Average response latency of the pupil light reflex is plotted against the stimulus luminance contrast for the normal and fellow amblyopic eyes of each amblyopic subgroup. Analysis of variance shows statistically significant differences between the normal and fellow amblyopic eyes within each of these subgroups (see Figure 4.4).

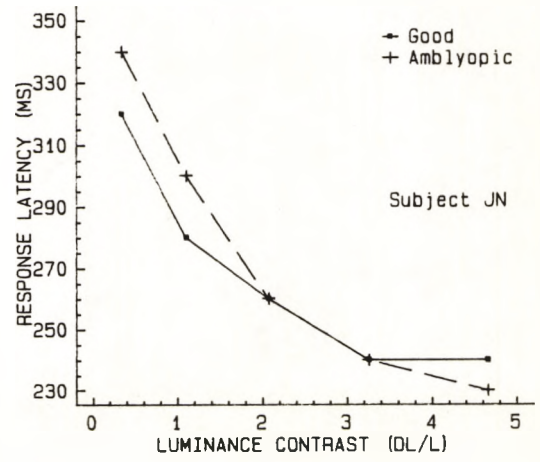
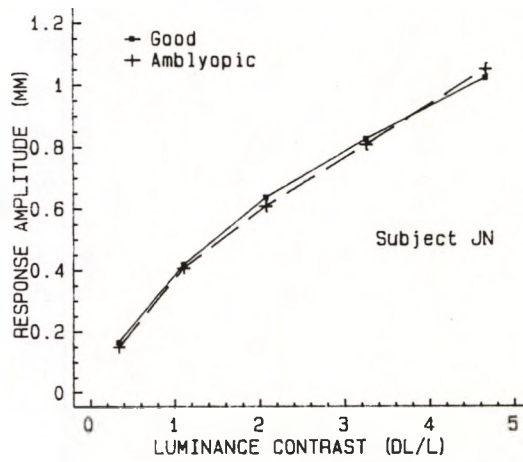
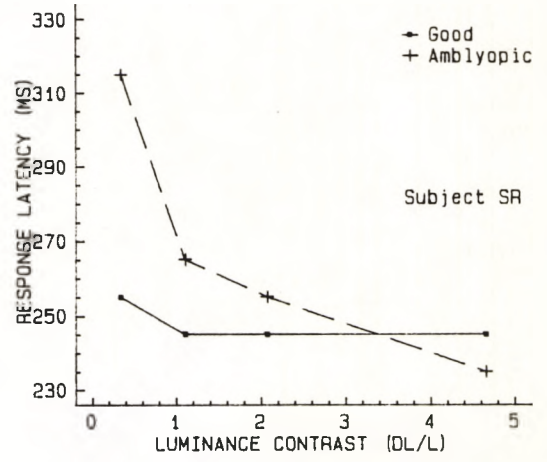
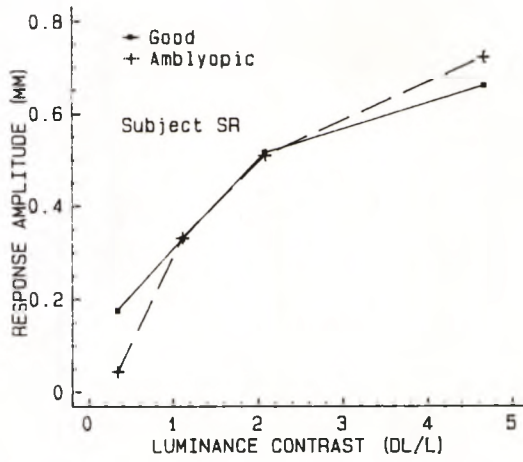
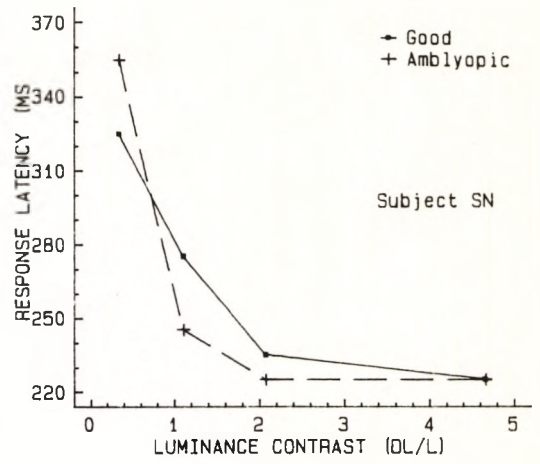
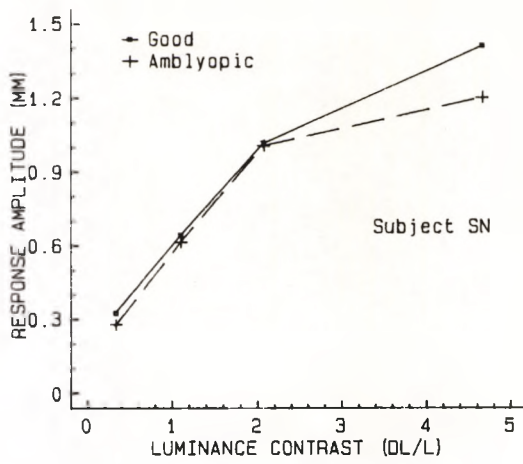


Figure 4.9. Pupil response amplitude (on the left), and pupil response latency (on the right), plotted as a function of stimulus luminance contrast. Data is shown for three individual strabismic amblyopes. Each data point represents the mean of the direct and consensual response.

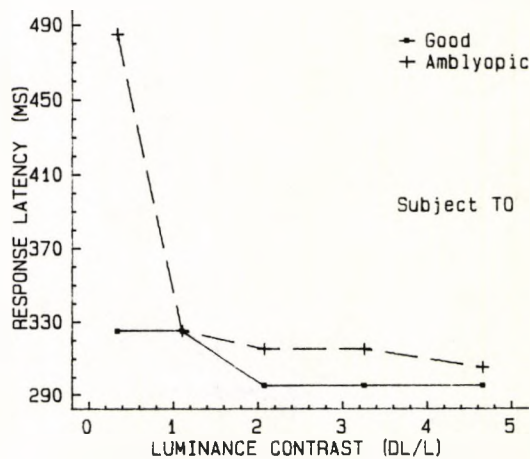
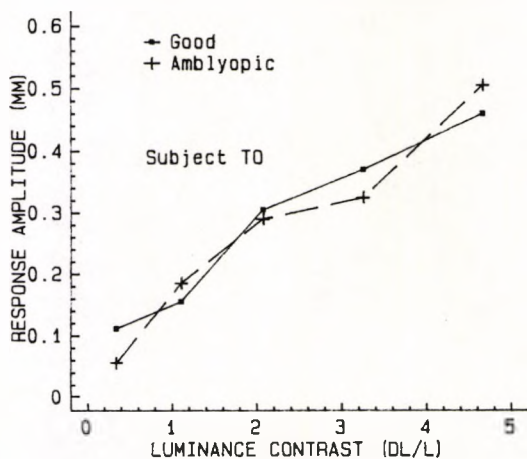
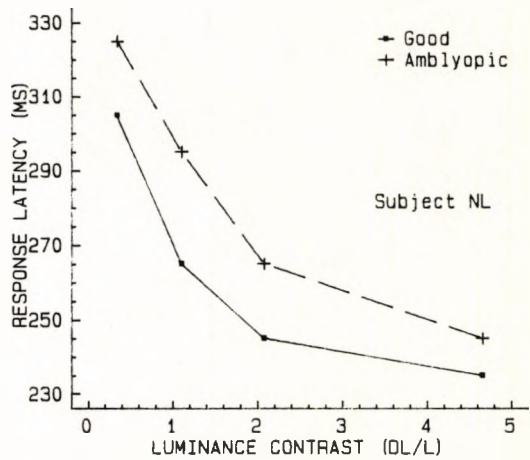
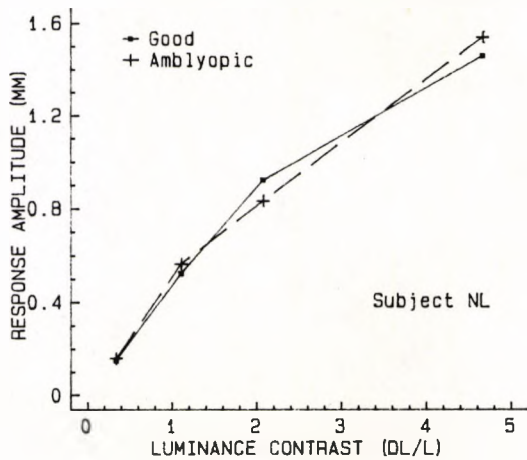
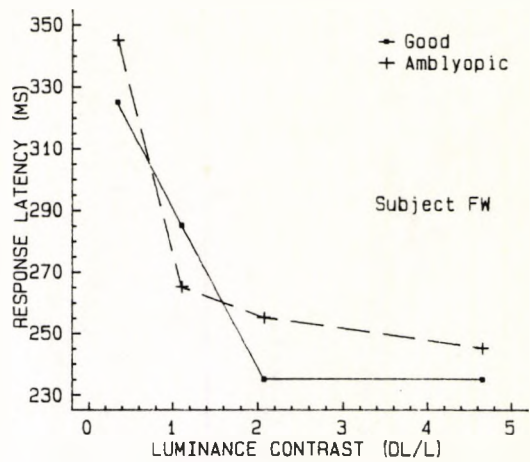
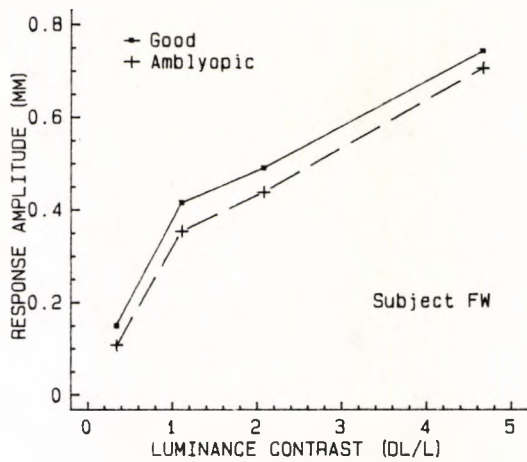


Figure 4.10. Pupil response amplitude (on the left), and pupil response latency (on the right), plotted as a function of stimulus luminance contrast. Data is shown for three individual anisometric amblyopes. Each data point represents the mean of the direct and consensual response.

response latency were measured between the normal eyes of amblyopic observers and the normal eyes of normal observers.

The results of the experiments to measure pupillary responses to sinusoidal grating stimuli are presented in Figures 4.11 to 4.14. The responses have been averaged for each amblyopic group and are plotted for the normal and fellow amblyopic eye as a function of grating spatial frequency (see Figure 4.11). The data show reduced amplitude responses for amblyopic eyes compared to their fellow normal eyes across all three amblyopic groups, the magnitude of the deficit increasing as grating spatial frequency increases. Analysis of these data show, however, that these reduced amplitude responses are only statistically significant for each spatial frequency in the strabismic group, though the results for the anisometric amblyopes, while not being significantly reduced across all frequencies do become significant ($p < 0.05$) at the highest spatial frequency tested (i.e., 6 c/deg). The absence of a significant difference in pupil grating response amplitude between the normal and affected eyes in the mixed group of amblyopes may not be representative of the mixed amblyope population as a whole because of the small number of subjects in this group. If pupil grating response amplitudes for the normal eyes of each amblyopic group are compared with the mean responses measured in the normal eyes of normal observers (see Figure 4.12), then significantly smaller amplitude responses are found for each amblyopic subgroup (see also Figure 4.4). No correlation ($r = 0.14$) was found between subject visual acuity and pupil grating response amplitude.

Figure 4.13 displays the averaged pupil response latency as a function of grating spatial frequency for the three amblyopic groups. Examination of these data shows that longer response latencies are recorded for the amblyopic eyes of both the strabismic and mixed subject categories at all spatial frequencies tested, and for the anisometric category only at the highest spatial frequency. A statistical analysis of these data reveals a similar pattern to that observed when analysing the corresponding response

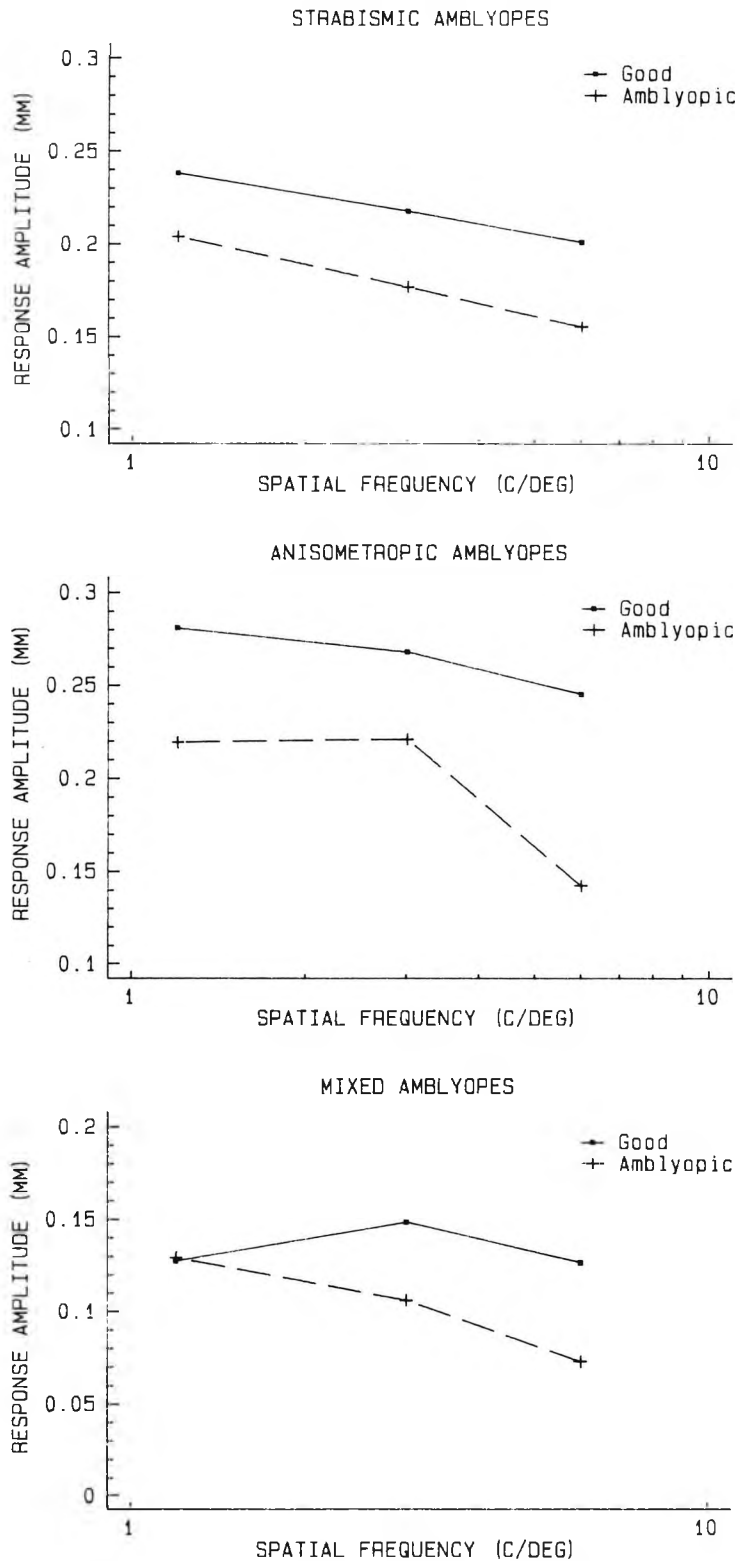


Figure 4.11. The average amplitude for the pupil grating response measured in each subgroup of amblyopes, following stimulation of either the normal or the amblyopic eye, plotted as a function of the spatial frequency of the sinusoidal grating. Statistical analysis shows that there is a significant difference between the normal and fellow amblyopic eye within each of these subgroups at the highest spatial frequency, and for the strabismic group at all spatial frequencies (see text and Figure 4.4).

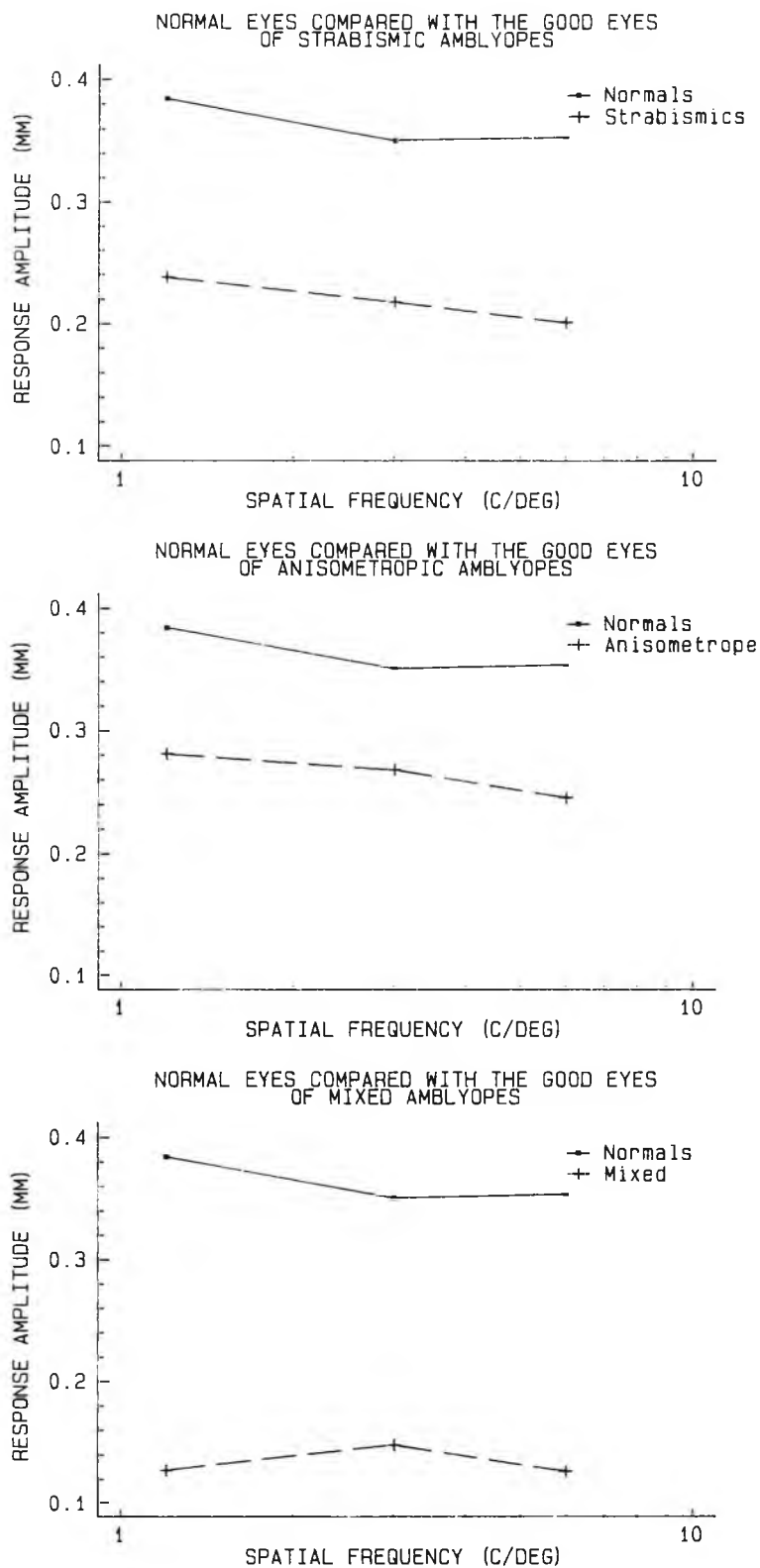


Figure 4.12. Average pupil grating response amplitude plotted against grating spatial frequency for the normal fellow eyes of each subgroup of amblyopes, and the normal eyes of a group of normal observers. The analysis shows a statistically significant difference between response amplitudes measured in the normal group, and those measured following stimulation of the normal eyes of each amblyopic subgroup (see Figure 4.4).

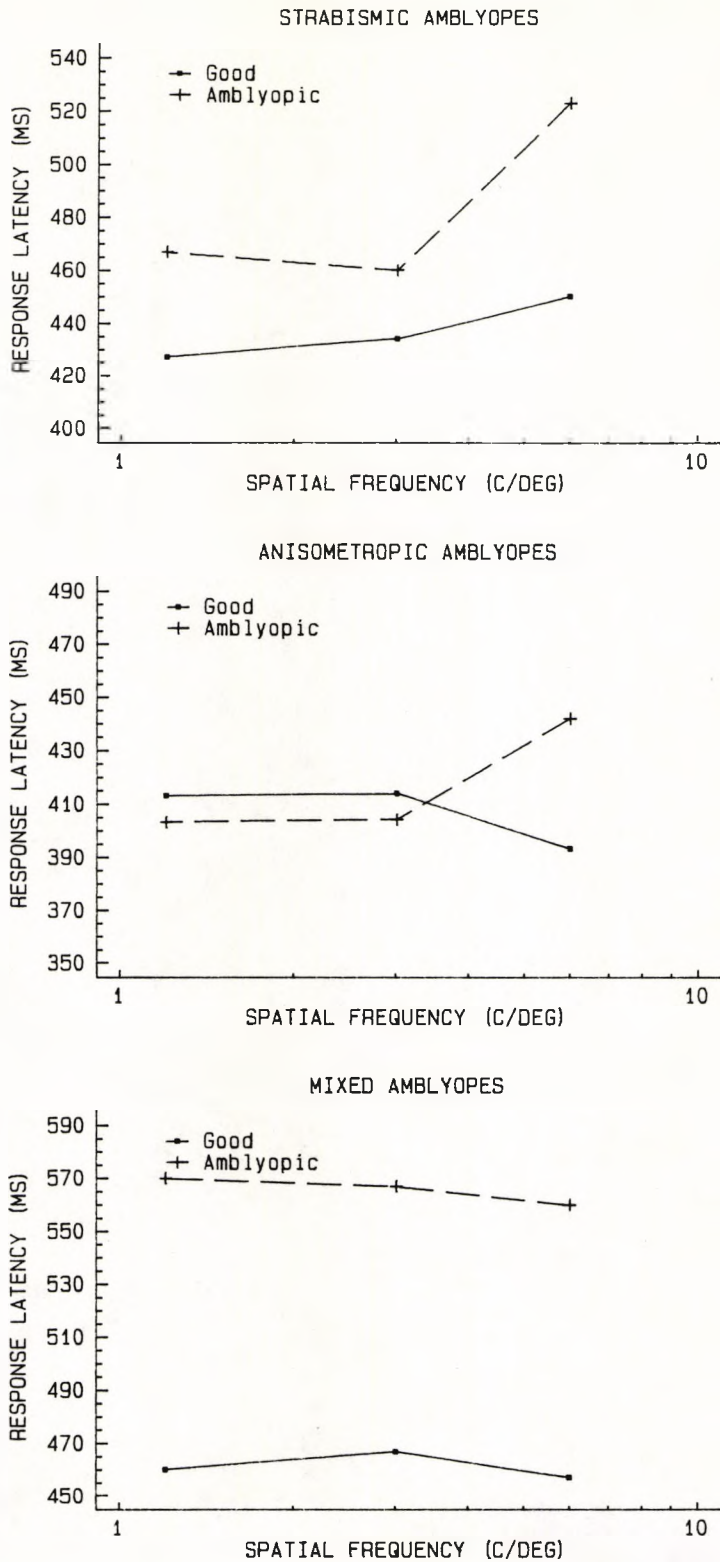


Figure 4.13. The average latency for the pupil grating response is plotted against grating spatial frequency for the normal and fellow amblyopic eyes for each amblyopic subgroup. Longer latencies are measured following stimulation of the amblyopic eye in each subgroup, but these differences are only significant at all spatial frequencies in the strabismic subgroup (see Figure 4.4).

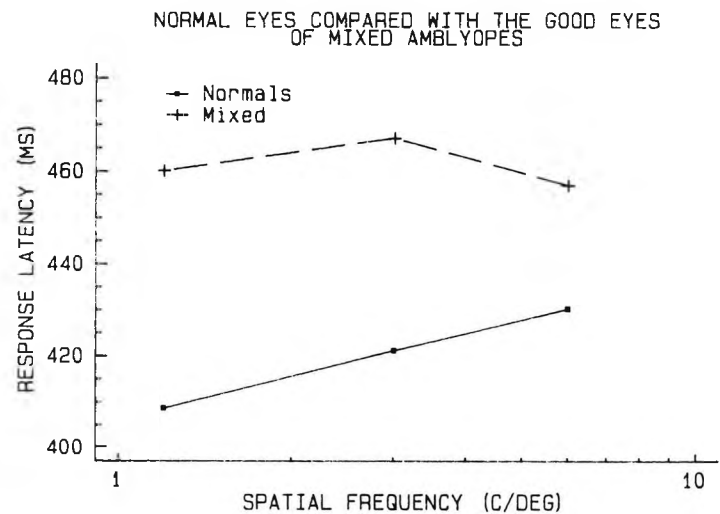
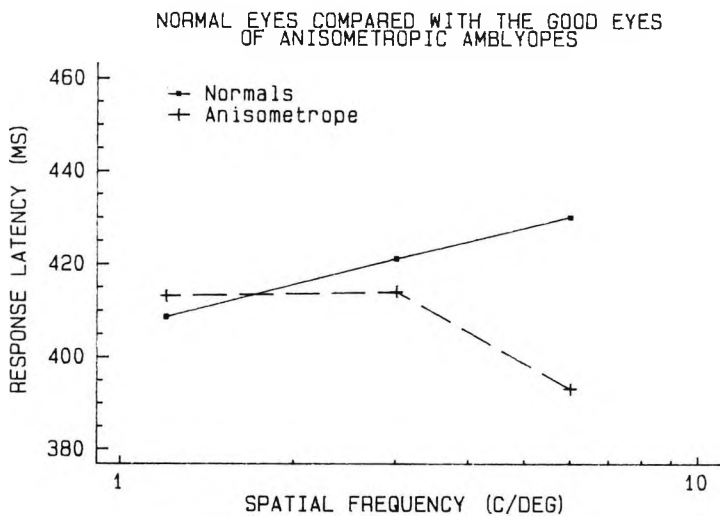
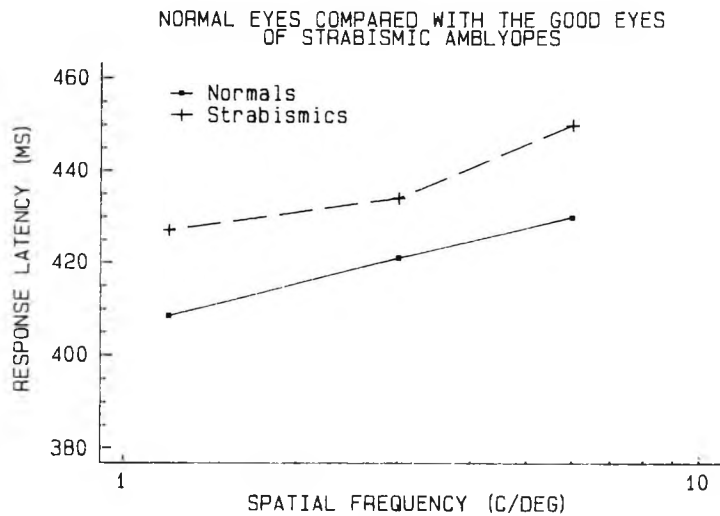


Figure 4.14. The average latency of the pupil grating response is plotted as a function of grating spatial frequency for a normal group of observers and for the fellow normal eyes of each amblyopic subgroup. The statistical analysis of results shows a significant difference between the normal subject group and the fellow normal eyes of amblyopes, but only for the strabismic and mixed subgroups (see Figure 4.4).

amplitudes, that is, the latency differences only proved significant at all spatial frequencies for the strabismic group, though the differences only become significant ($p < 0.05$) at a frequency of 6 c/deg for the anisometric group. On average, across all the frequencies tested, the amblyopic eyes of the strabismic group show a response latency increase of 46 ms compared to their fellow normal eyes. A comparison of pupil grating response latencies following stimulation of the normal eyes of the amblyopic groups with the mean response in the normal group shows statistically significant differences for all spatial frequencies, the only exception being the anisometric group (see Figures 4.4 and 4.14). Again no correlation ($r = 0.26$) was found to relate the magnitude of the deficit observed for amblyopic eyes with the corresponding Snellen visual acuity.

It would seem, therefore, that pupil grating responses are abnormal in amblyopic eyes, and furthermore that the magnitude of the abnormality is not related to the depth of the amblyopia as defined by the visual acuity. Perhaps the deficit measured by pupillometry is related to stimulus visibility? In order to investigate this hypothesis the pupil grating response was measured over a greater range of spatial frequencies and compared with the corresponding psychophysical contrast sensitivity function. The results of this experiment are presented for both the amblyopic eye and the fellow normal eye of three strabismic subjects (Figures 4.15, 4.16 and 4.17) and two anisometric subjects (Figures 4.18 and 4.19). Pupil traces, similar to those from which the previous figures were derived, are shown for one anisometric subject (N.L.) in Figure 4.20. For clarity, data are shown separately for the normal and amblyopic eye, and traces have been shifted vertically by an amount shown against each trace. In general it can be seen from the above figures that the way in which the contrast sensitivity abnormality varies with spatial frequency is similar to the way in which the pupillary amplitude and latency deficit varies with spatial frequency.

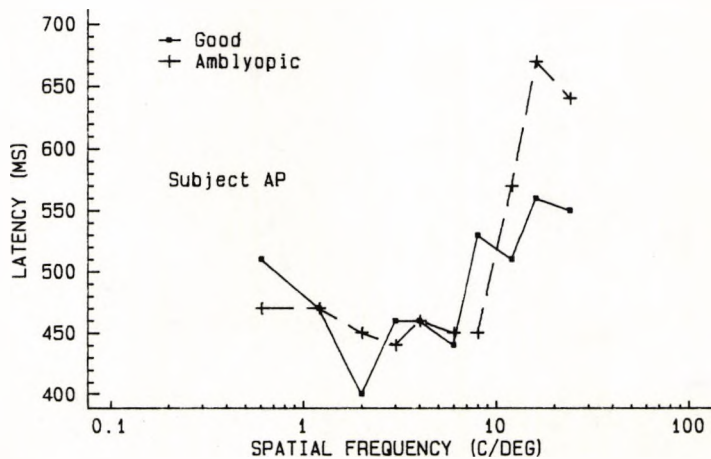
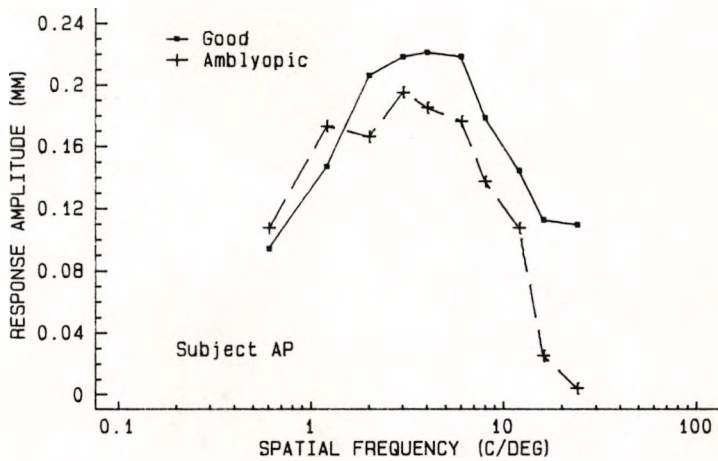
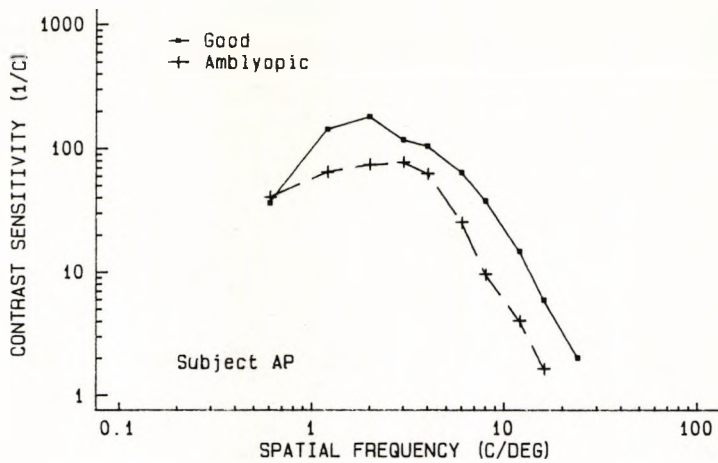


Figure 4.15. Psychophysical and pupillary deficits to the same grating stimuli presented monocularly to the good and amblyopic eye of an individual strabismic amblyope. **Upper figure:** contrast sensitivity is plotted as a function of spatial frequency. **Centre figure:** pupil response amplitude as a function of spatial frequency. **Lower figure:** pupil response latency as a function of grating spatial frequency. Gratings were of 60% contrast and the background luminance was 11.9 cd/m². Figures 4.16 - 4.19 are of similar format.

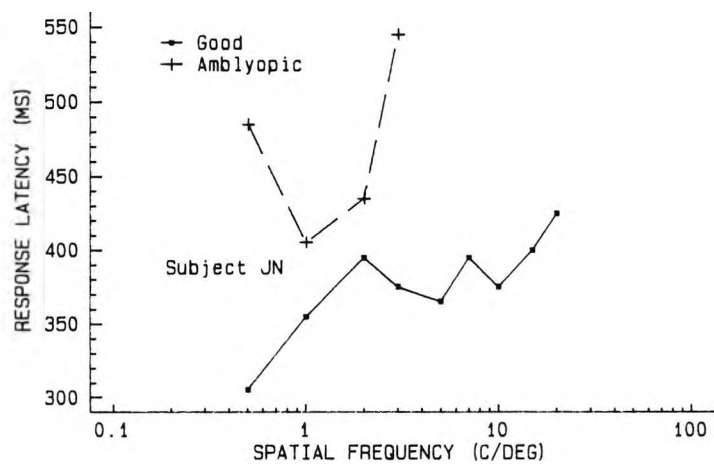
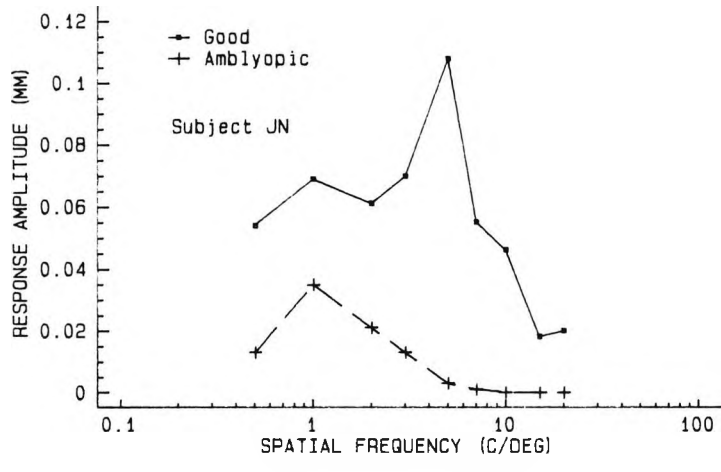
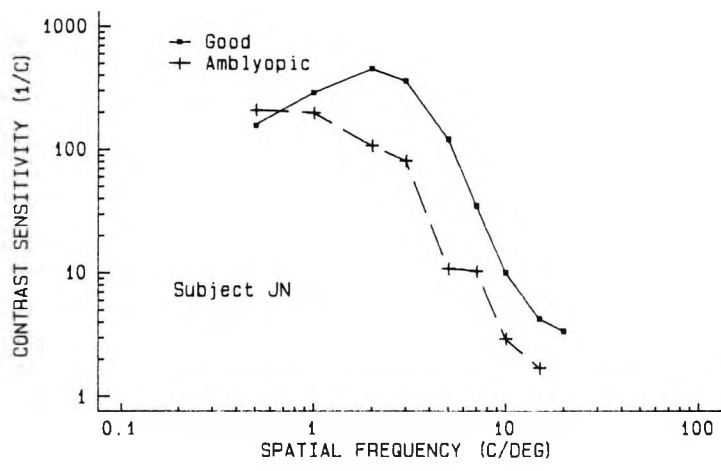


Figure 4.16. Format as for Figure 4.15. Data shown is for a strabismic amblyope.

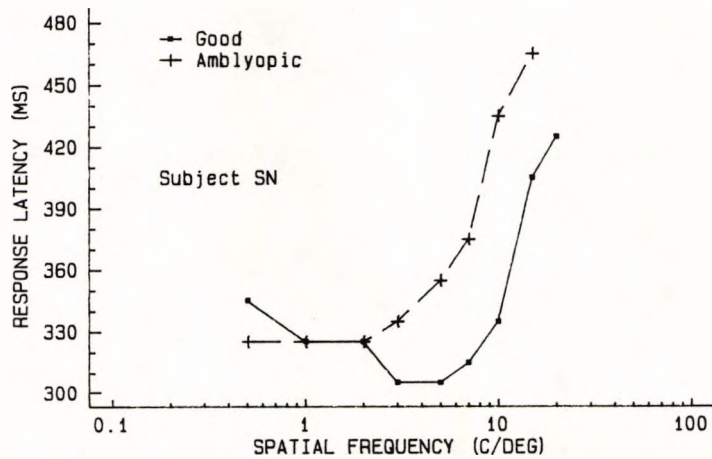
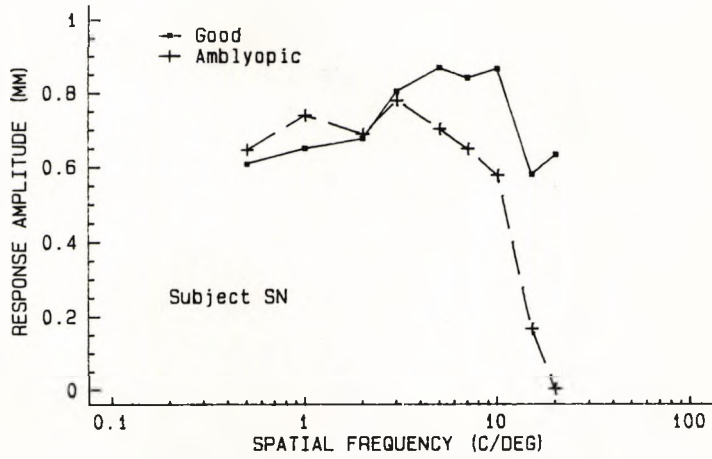
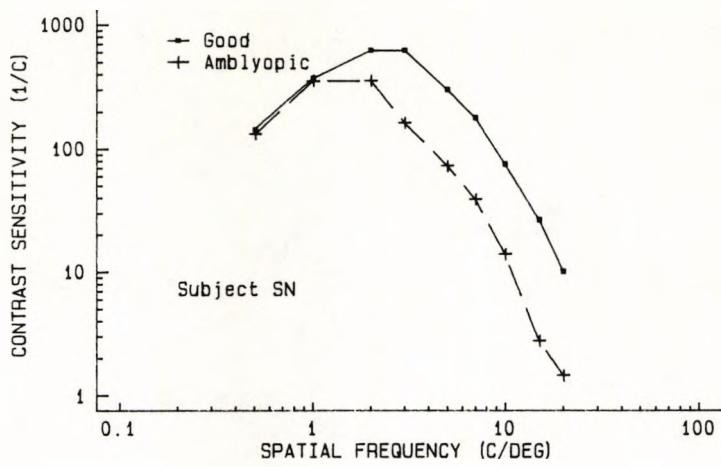


Figure 4.17. Format as for Figure 4.15. Data shown is for a strabismic amblyope.

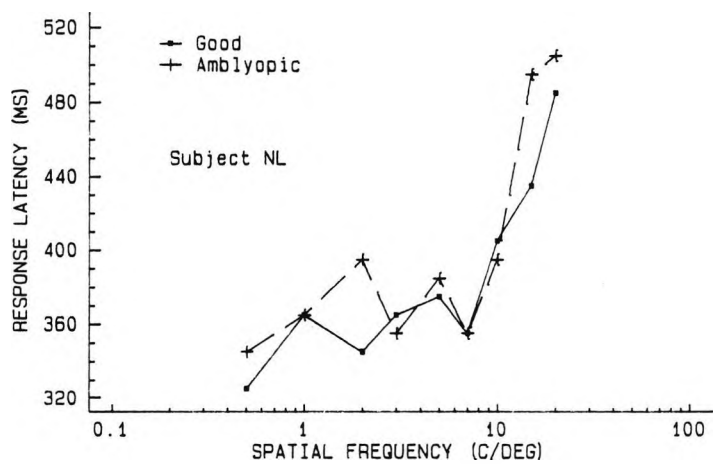
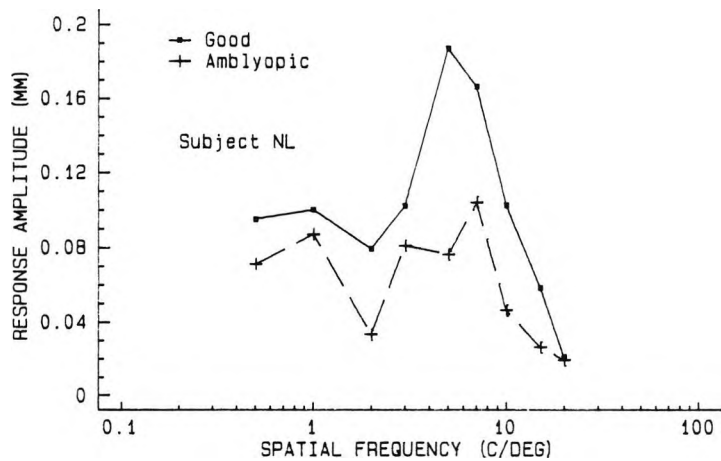
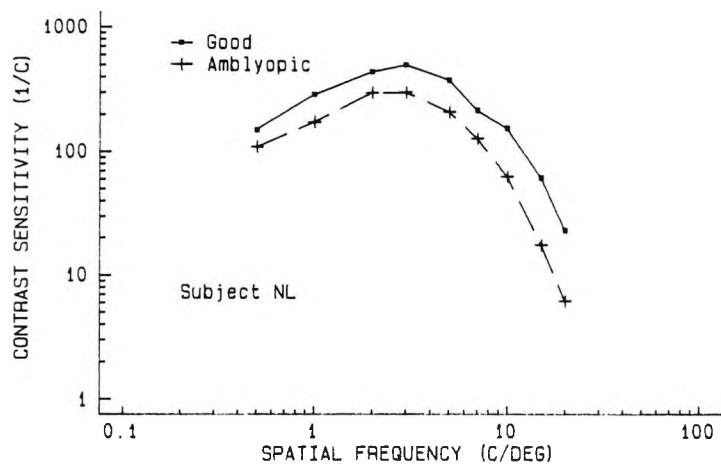


Figure 4.18. Format as for Figure 4.15. Data shown is for an anisometropic amblyope.

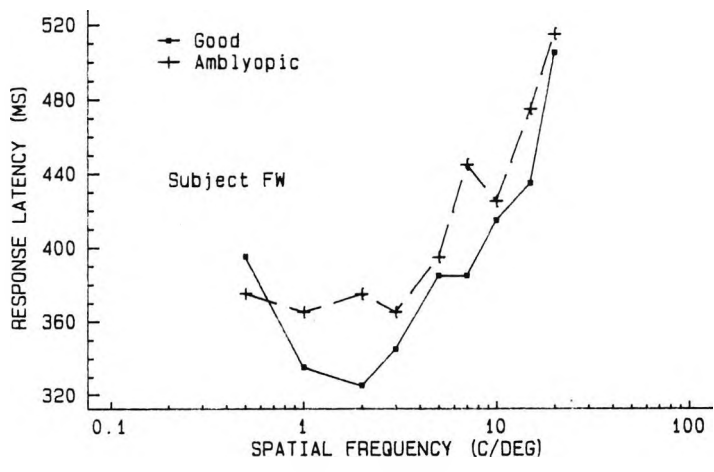
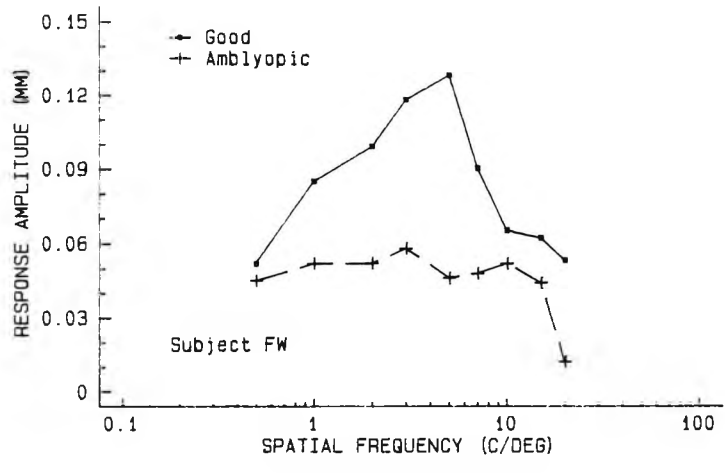
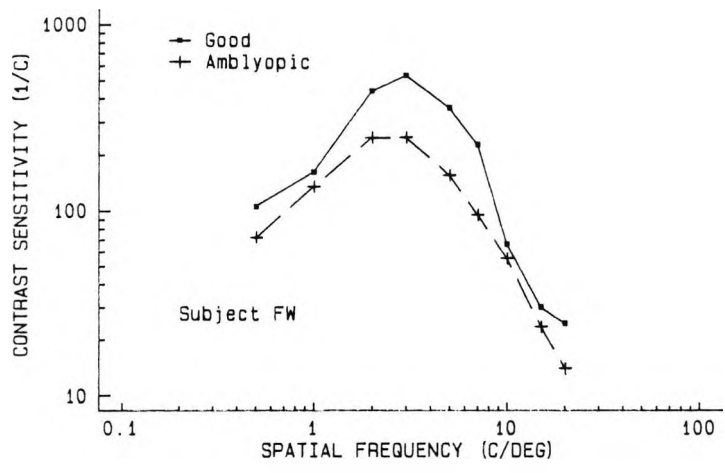


Figure 4.19. Format as for Figure 4.15. Data shown is for an anisometropic amblyope.

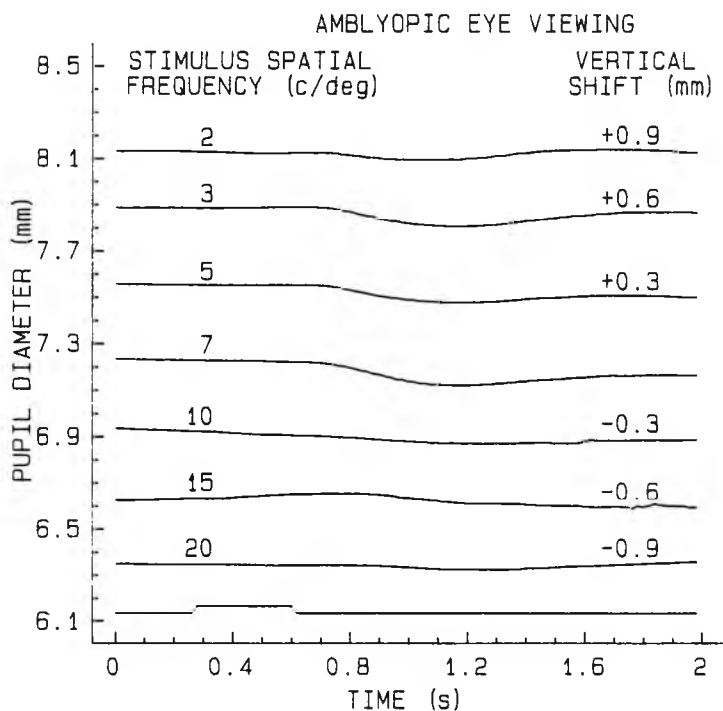
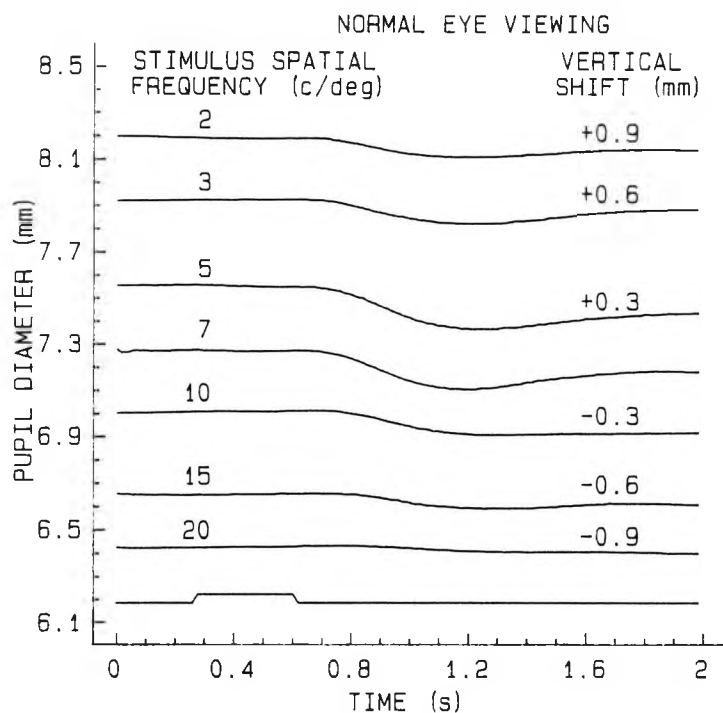


Figure 4.20. Typical pupil diameter traces obtained following stimulation with sinusoidal grating stimuli. Each trace represents the average of 15 separate recordings and the mean of the direct and consensual response. Data is presented for an individual anisometric amblyope (NL). **Upper figure:** responses recorded following stimulation of good eye. **Lower figure:** responses recorded following stimulation of amblyopic eye.

Pupil diameters recorded before stimulus presentation in the monocular viewing condition were averaged for the good and affected eyes of all participating amblyopic subjects. No significant differences were found between the resting state pupil size in the good and affected eyes of the amblyopic subjects as a whole ($p = 0.7$) or within any of the subject groups (see Figures 4.4 and 4.21). In fact for all the amblyopic subjects taken together, the average pre-stimulus pupil diameters differ by less than 0.1mm. Similarly no significant differences between good and amblyopic eyes ($p = 0.22$) were found for the binocular viewing condition.

The data representing measurements of the monocular and binocular resting state pupil diameter are shown in Figure 4.22. For comparison with previous studies, the results are plotted in bar chart form with the percentage pupil summation as ordinate. Summation is defined as the increase in pupil diameter from the binocular to the monocular viewing condition. The average percentage summation is displayed separately for the good and amblyopic eyes of 4 strabismics and 4 anisometropics, and for the right and left eyes of 4 normals. The differences observed between good and amblyopic, and between right and left eyes were not found to be statistically significant. Both amblyopic groups, however, showed significantly reduced binocular luminance summation when compared with the normal group (for strabismics $p = 0.028$, and for anisometropics $p = 0.075$, Student t-test). Differences between the strabismic group and the anisometropic group were not significant.

DISCUSSION AND CONCLUSIONS

The results of the present study indicate that the pupil light reflex is essentially of normal amplitude in amblyopic eyes. This finding is contrary to the reports of a number of previous studies (Krüger, 1961; Brenner et al., 1969; Portnoy et al., 1983) which have found that the amplitude of the pupil light reflex is grossly reduced in the majority of

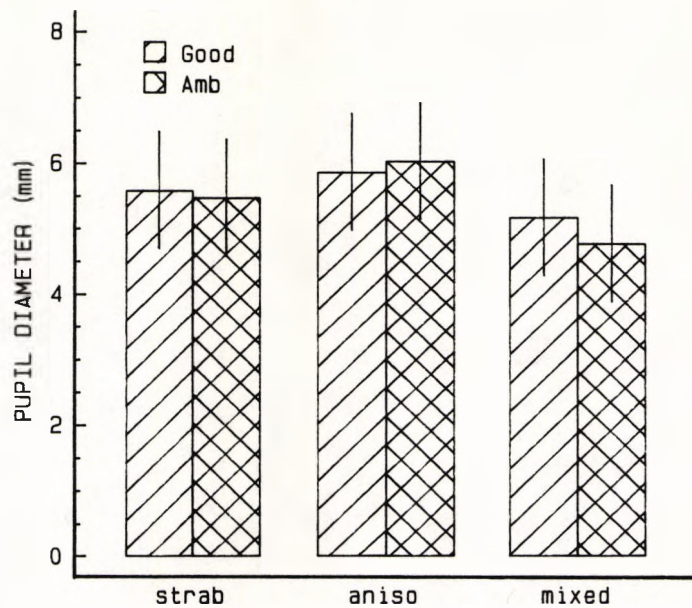


Figure 4.21. Pre-stimulus pupil diameters averaged for the good and amblyopic eyes of each amblyopic subgroup. Diameters were recorded in the monocular viewing condition. Amb, amblyopic; strab, strabismic; aniso, anisometric. Error bars represent ± 1 standard deviation. No significant differences in resting state pupil size were found between good and amblyopic eyes in any of the amblyopic subgroups.

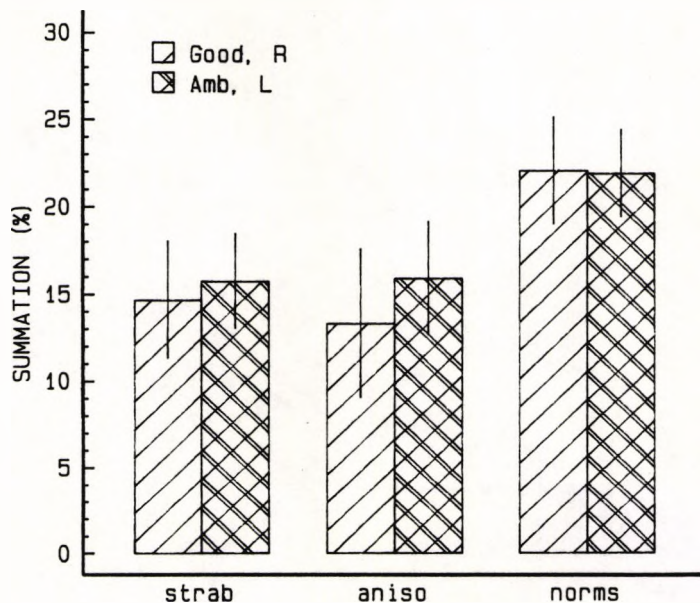


Figure 4.22. Percentage pupil summation is plotted for 4 strabismic (strab), 4 anisometric (aniso), and 4 normal (norms) observers. Data is displayed separately for the good and affected eyes of the amblyopic subgroups, and for the right and left eyes of the normal group. Both amblyopic subgroups showed significantly reduced binocular luminance summation when compared with the normal group.

amblyopic eyes. It is worth emphasising, however, that these previous studies have all employed very different techniques (usually the swinging flashlight test) and have probably all used stimuli of higher light flux levels than those used in the present study, although it must be said that Brenner et al. (1969) are the only authors to provide actual luminance data. In fact the mean stimulus light level used by these latter authors was of a luminance contrast approximately 180 times higher than the mean luminance contrast used in the present study. If for any reason a deficit in pupil response amplitude is apparent only at high stimulus light flux levels, then one would expect to see at least a trend to this effect in the data obtained in the investigation. Inspection of Figures 4.5, 4.9 and 4.10 show that no such trend is evident.

Whilst the data in this investigation has generally been presented as an average for each amblyopic category, response amplitudes were also analysed for each amblyopic subject individually. Of the 22 amblyopic subjects examined, 3 (i.e., 14%), comprising one amblyope from each category, did show significantly reduced response amplitudes in the amblyopic eye for each stimulus luminance level tested. This finding is in fairly close agreement with Greenwald and Folk (1983), who reported a "mild" afferent pupillary defect in 4 out of 45 (i.e., 9%) amblyopic patients.

A further finding of this study is the difference between the latency of the pupil light response for normal and fellow amblyopic eyes, a difference which is particularly evident at low stimulus luminance contrasts. Similarly Kase and his colleagues (Kase et al., 1984) found a pupil latency deficit for amblyopic eyes when using a low intensity (1 lux) stimulus. They measured this deficit at an average of 28 ms and could find no correlation between the magnitude of the deficit and subject visual acuity, findings which are supported by the present study. Interestingly, the magnitude of the latency deficit is similar to that found for amblyopic eyes in VEP studies (Yinon et al., 1974). In support of the results presented here, Kase and his

colleagues also found that pupil response amplitudes were not significantly different in amblyopic and normal eyes. The fact that the pupil latency deficit does not correlate with the low spatial frequency contrast sensitivity deficit suggests that reduced stimulus visibility is not responsible for the abnormality. Since there are no significant differences between the direct and consensual responses following stimulation of the normal eye in amblyopic subjects, then the increased response latency observed following stimulation of the amblyopic eye must involve the afferent fibres rather than the efferent fibres from this eye. The subtle abnormality of the pupil light reflex suggests that some retinal abnormality may exist in amblyopic eyes, though recent evidence of reduced light reflex responses in patients with damaged central visual pathways (Alexandridis et al, 1983; Keenleyside et al., 1988; and see also section 1.2 of this chapter) does not exclude a geniculo - striate influence on the pupillary light response. Perhaps also, since the latency deficit appears to be unrelated to the contrast sensitivity loss or reduction in visual acuity, the abnormality may reflect long - term secondary changes occurring as a consequence of a more centrally located deficit. Cowey and his colleagues (Cowey, 1974; Cowey et al., 1989) have provided evidence of such retinal changes occurring in monkeys as the result of transneuronal retrograde degeneration from an artificially induced cortical lesion. The observation that the pupil latency deficit is abolished for high luminance stimuli for strabismic, but not for anisometric amblyopes, adds further support to the theory that the two types of amblyopia are physiologically different (Hess and Pointer, 1985). Certainly it would appear that luminance levels have a more profound effect on visual function in strabismic amblyopia than in anisometric amblyopia (see also Hess and Howell, 1978; Hess et al., 1980; Hess and Bradley, 1980).

The results of this study show that the pupil grating response is abnormal in both amplitude and latency in the amblyopic eyes of strabismic and anisometric subjects. The averaged group data would seem to indicate that the

pupillary abnormality is restricted to high spatial frequencies for the anisometropic group, though this finding is not particularly noticeable in the responses of the two individual anisometropes for which a greater range of spatial frequencies were tested (see Figures 4.18 and 4.19). The similar characteristics of the contrast sensitivity function and the PGR function in amblyopes would seem to suggest that stimulus visibility is important in determining the amplitude and latency of the pupillary response to grating patterns. It follows, therefore, that stimulus contrast is likely to be an important parameter. Consequently an increase in the contrast of the grating presented to the amblyopic eye, thereby compensating for its increased contrast threshold, may have the effect of equalising the PGR's recorded from the good and amblyopic eyes. In order to investigate this hypothesis a further experiment was performed in which pupillary responses were measured for a range of grating contrasts. Contrast sensitivity functions for the two amblyopes who participated in this experiment are shown in Figure 4.23. Both amblyopes (S.R., strabismic, and T.O., anisometropic) display reduced contrast thresholds at all spatial frequencies, but for the pupillary measurements a grating spatial frequency of 2 c/deg was chosen since both amblyopes were clearly defective at this frequency. The results for each subject are displayed in Figure 4.24, in which pupil response amplitude (upper figure) is plotted as a function of grating contrast using a logarithmic scale for the contrast axis. As expected, response amplitude increases, with increase in grating contrast for both good and amblyopic eyes, but, again as expected, the amplitudes are smaller for the amblyopic eyes of each subject. By compensating for the contrast sensitivity deficit between the good and amblyopic eyes at 2 c/deg, the data for the amblyopic eyes may be replotted with suprathreshold grating contrast as abscissa as shown in the lower diagrams of Figure 4.24. In these figures therefore, the data for the amblyopic eye has been shifted along the contrast axis by an amount equal to the contrast sensitivity deficit. For subject T.O. it can be seen that this contrast correction tends to equalise the

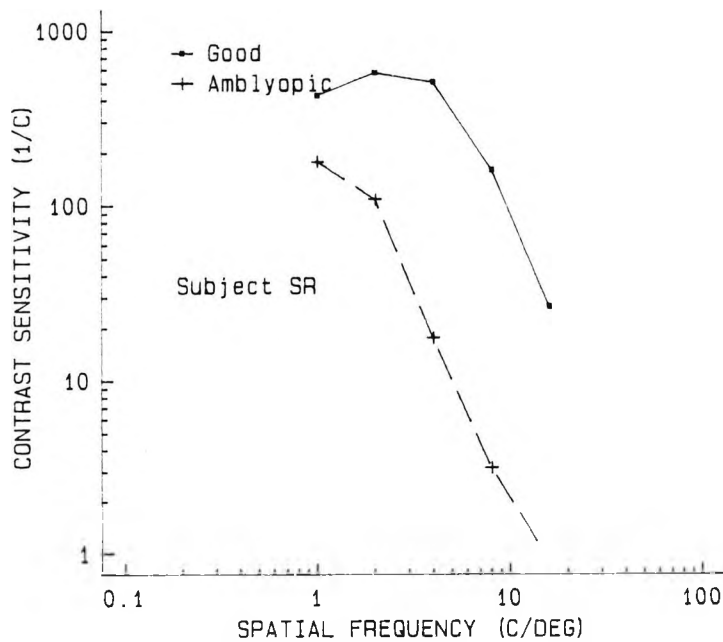
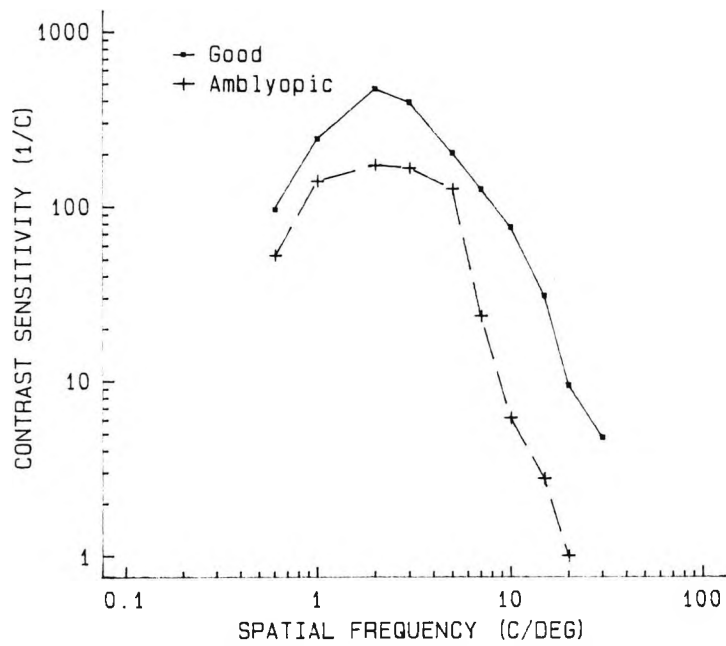


Figure 4.23. Psychophysical contrast sensitivity function for two amblyopic subjects. Data is shown for the good and amblyopic eyes viewing monocularly. **Upper figure:** anisometric subject (TO). **Lower figure:** strabismic subject (SR). Both subjects participated in the experiment to investigate the effect of grating contrast on pupil response amplitude (see text and Figure 4.24).

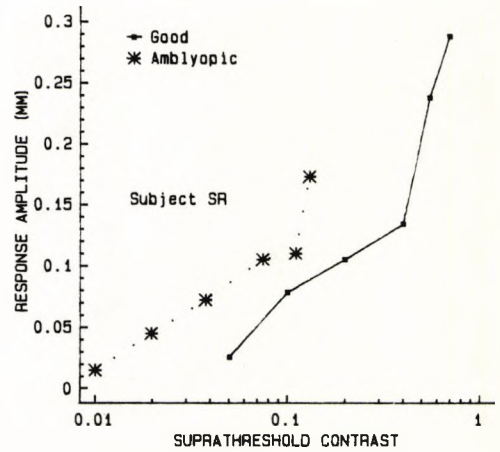
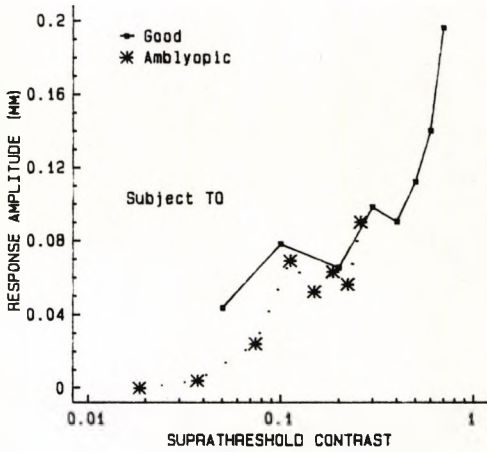
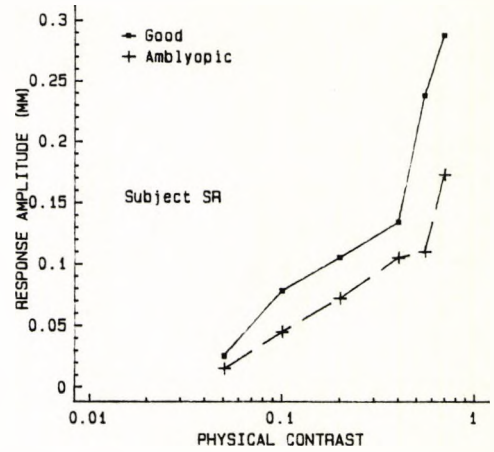
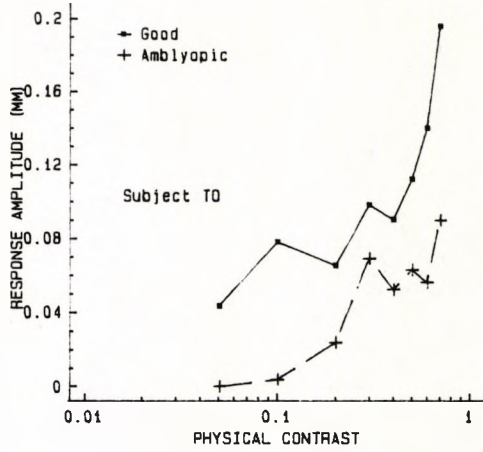


Figure 4.24. Upper figures: pupil response amplitude is plotted as a function of stimulus contrast for a sinusoidal grating of spatial frequency 2 c/deg. Data is presented for monocular stimulation of the good and affected eyes of two amblyopic subjects: T0 (an anisometric amblyope); and SR (a strabismic amblyope). **Lower figures:** pupil response amplitude for both subjects has been replotted against suprathreshold grating contrast i.e., the data for the amblyopic eyes has been shifted along the contrast axis by an amount equal to the contrast sensitivity deficit between good and amblyopic eyes at a spatial frequency of 2 c/deg.

pupil grating responses, whereas for subject S.R. the correction seems to over - compensate for the response deficit. Whatever the reason for these inter - subject differences, it is apparent that it is the suprathreshold contrast that determines the pupil grating response.

Whilst on the whole the contrast threshold versus spatial frequency abnormality in amblyopia is reflected in the pupillary response, it is interesting to examine the results of the strabismic subject J.N. (see Figure 4.16); at a spatial frequency of 0.5 c/deg the contrast thresholds appear normal, whereas the pupil grating response at this same spatial frequency is significantly lowered. Since the stimuli used to elicit pupillary responses are well above threshold, then, for this subject, it would seem that suprathreshold processing of visual information may be abnormal (see also Hess et al, 1978).

A novel, and perhaps somewhat unexpected, finding of the present study is that both the pupil light reflex and the pupil grating reflex are reduced in amplitude for the normal eye of amblyopic subjects when compared with the responses recorded from a group of normal, non - amblyopic, subjects. One possible explanation for this could again involve secondary changes occurring as the result of cortical or midbrain abnormalities.

Although the results of several studies (e.g., Barbur et al., 1987a; Keenleyside et al, 1988) indicate that central mechanisms are involved in the mediation of the PGR, the abnormality of the PGR in amblyopic eyes does not provide decisive evidence for a cortical anomaly in amblyopes since, analogous to the VEP, the response of the pupil may be affected by an anomaly sited anywhere along the pupillary nervous pathway. Thus, even though the PLR seems essentially normal (at least in terms of amplitude) it is impossible to rule out the possibility that abnormal spatial interactions at the retinal level contribute to the abnormality of the PGR in amblyopes.

Anecdotal reports among clinicians (personal communication with numerous optometrists and ophthalmologists) indicate that it is common for the pupil diameter of amblyopic eyes to be larger when compared with their fellow normal eyes. These observations suggest the existence of a resting state anisocoria in human amblyopes. Whilst individual subjects from each subgroup (including the normal subgroup) may exhibit an anisocoria, the results of this study (see Figure 4.21) do not support such observations. The inter - group differences found when comparing the pupil diameters of both eyes may be an artefact of a high degree of variability combined with the relatively small numbers within groups.

The finding that amblyopic subjects display less binocular pupil summation is in agreement with the work of Sireteanu (1987). Sireteanu found that the percentage summation for subjects with no functional binocularity was, on average, about 12%, which is very similar to the average of 14% measured in the present study (see Figure 4.22). The results for normal subjects differ somewhat more between the two studies, Sireteanu reporting an average luminance summation of 29% compared to the 22% found in this study. These differences, however, are unlikely to be statistically significant because of the relatively small numbers of normal subjects in the two studies and the large variances involved. Although the present results indicate that, on average, amblyopic eyes exhibit no pupillary amplitude abnormality for luminance modulation in the monocular viewing condition, the reduced binocular luminance summation does suggest abnormal input of the amblyopic eye under binocular conditions. The site of pupillary luminance summation is most likely to be at the level of the midbrain, where retinal afferents from each eye converge. However, since suppression in amblyopia is generally considered as being of a central nature (Pickwell, 1984), and since we observe less pupillary summation in amblyopic subjects, then the finding that summation is reduced in amblyopia may provide further evidence for the involvement of the cortex in the control of the pupil.

4.3 PUPILLARY RESPONSES TO CHROMATIC STIMULI

The pupil is known to respond systematically to changes in the chromatic content of the visual field, the amplitude of the response being dependent on the perceived chromatic difference between the stimulus and its immediate surround (see Chapter 1). The transient pupillary constriction observed may be related to the properties of the mechanisms involved in the processing of colour information in the human visual system. Several psychophysical studies have investigated spatio - chromatic properties in human vision with the aid of gratings which vary in chromaticity but not in luminance (Schade, 1958; van der Horst and Bouman, 1969; Granger and Heurtley, 1973; Mullen, 1985; Webster et al, 1990). Whilst isoluminant chromatic grating patterns have been shown to elicit responses in electrophysiological studies (Kulikowski and Russell, 1987; Murray and Parry, 1987; Murray et al., 1987), it is not known if the pupil can respond to such patterns. Furthermore, if pupillary responses can be elicited with chromatic gratings, then it is of interest to establish how the amplitude and the latency of such responses vary with the properties of the stimulus. Pupillary responses to chromatic gratings have therefore been investigated and the results are reported in this section.

4.3.1 PRELIMINARY EXPERIMENTS

It is of interest to establish how detection thresholds for chromatic gratings vary with spatial frequency, and to compare these psychophysical results with data obtained from pupillometric investigation. Chromatic grating stimuli were generated on the Ayadin 8886 colour monitor (see Chapter 2 section 2) by modulating sinusoidally the luminance of the red and green components of the "white" background field, with the red component being 180° out of phase with the green component. The gratings were presented on a uniform white (grey) background field of luminance 17 cd/m^2 . The red and green grating components were isoluminant with respect to each other (as computed from the CIE standard observer

data, see Wyszecki and Stiles, 1982) and with respect to the background field. Stimuli subtended a visual angle of $6 \times 6^\circ$ (at 1.25 m) and presentation time was fixed at 500 ms. Chromatic modulation thresholds were determined for a range of grating spatial frequencies between 0.6 and 6 c/deg. Viewing conditions were binocular and stimuli were presented both foveally and at an eccentricity of 6° in the periphery in two separate sessions. The experimental paradigm incorporated an adaptive staircase procedure with three reversals. Two subjects participated in this experiment (M.K. and D.W.), both were colour normal, had good visual acuity and were experienced observers. For this experiment and those to follow colour vision was assessed with the Ishihara and Farnsworth - Munsell 100 - Hue tests, and with the Nagel anomaloscope (see Birch, 1985).

RESULTS

Typical data showing the reciprocal of the threshold contrast for detection of the chromatic grating are plotted as a function of grating spatial frequency (M.K.) in Figure 4.25. The definition of chromatic contrast is often questionable, but for the purpose of this study, contrast has been computed on the basis of the red component only using the Michelson definition of contrast given by:

$$C = \frac{L_{\max} - L_{\min}}{L_{\max} + L_{\min}}$$

where L_{\max} and L_{\min} are the maximum and minimum luminances respectively. By convention, both axes in Figure 4.25 are logarithmic. The data points plotted represent the mean of nine individual determinations of the threshold contrast obtained in three separate experimental sessions.

The foveal measurements of chromatic contrast sensitivity indicate very little low frequency attenuation, but sensitivity falls off at spatial frequencies above 1 c/deg. The peripheral data show reduced sensitivity for detection of chromatic modulation. Interestingly there appears to be no further fall in sensitivity above frequencies of 2 c/deg.

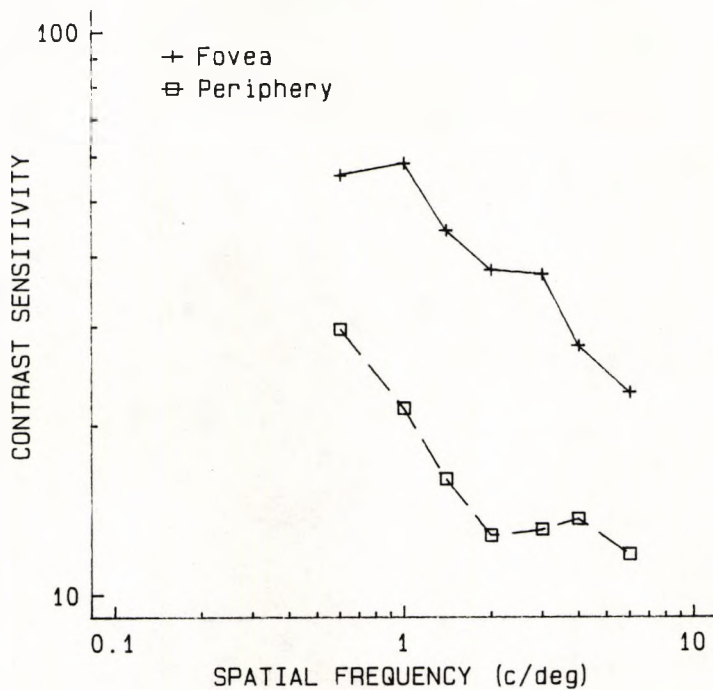


Figure 4.25. The contrast sensitivity for detection of an isoluminant red-green chromatic grating is plotted as a function of the grating spatial frequency (contrast was computed on the basis of the red component only). Data is presented for one subject (MK) for foveal observations, and also for observations made with the stimulus presented 6° in the periphery. Each data point represents the mean of nine observations made in three experimental sessions.

In spite of differences in the visual stimulus, the results of the present study to measure the detection thresholds of red - green chromatic gratings are in close agreement with data published previously for foveal observations (e.g., Granger and Heurtley, 1973; Mullen, 1985). Unfortunately, due to the limitations of the monitor used and also due to physical constraints, it was not possible to measure thresholds for stimuli with frequencies below 0.6 c/deg, or above 6 c/deg.

Measurements of chromatic contrast sensitivity in the periphery of the visual field are less common. At an eccentricity of 6°, cone density in the retina, and hence chromatic processing, is much reduced (see Figure 1.5, østerberg, 1935) and consequently it is not surprising that sensitivity falls off at lower spatial frequencies by comparison with foveal measurements. From these results it would appear that sensitivity does not fall for grating frequencies between 2 and 6 c/deg. This is a highly unlikely state of affairs and one questions if the threshold at these frequencies is determined by a possible luminance artefact, especially since the observers report that no colour is present in the gratings above frequencies of 2 c/deg. This possible luminance artefact may have two origins: (i) the computations used to generate the "isoluminant" gratings were based on foveal, and not peripheral, data for the CIE standard observer; (ii) chromatic aberrations may be more significant at higher spatial frequencies in the periphery, especially when the sensitivities involved are relatively low. Any luminance artefact produced in the generation of chromatic gratings would obviously corrupt the pupillary responses, and therefore, the method described in the following section was adopted to ensure that any possible luminance components were minimised.

4.3.2 PUPILLARY RESPONSES TO CHROMATIC GRATINGS AROUND ISOLUMINANCE

Chromatic grating stimuli were generated as described in the previous section but on this occasion the vertical red - green components of the grating were set at isoluminance by using an experimental paradigm similar to that proposed by Anstis and Cavanagh (1983). This procedure, known as "the minimum motion technique", capitalises on the fact that motion perception is impaired for patterns made up of equiluminant colours (Livingstone and Hubel, 1988). When the luminance - varying, red and green components of a chromatic grating are modulated in counter - phase, the grating pattern appears to move from side to side, but at equiluminance the perceived velocity of the grating is considerably slowed and the grating often appears to completely stop moving. In this way, by keeping the red contrast fixed, the isoluminant green contrast was determined by finding the green contrast component which yields minimum perceived grating movement. A temporal modulation frequency of 1.8 Hz was employed.

Preliminary experiments involved the measurement of pupillary responses to chromatic grating stimuli where the green component was varied around isoluminance. The red contrast was fixed in all presentations whilst five green contrast levels were chosen, two below isoluminance, two above isoluminance, and a contrast for which the green component was isoluminant with the red component. For all stimuli the space - averaged luminance of the gratings was equal to the luminance of the white background and measured 17 cd/m^2 . Particular attention was paid to ensuring that the stimulus luminance remained stable and to this end luminance measurements were made before each session. Grating spatial frequencies of 1 and 2 c/deg were used with a stimulus presentation time of 550 ms. Pupil diameter was recorded for 3 seconds with stimulus onset occurring 550 ms after the start of the recording period. Stimulus spatial frequency and contrast were randomly interleaved with 24 individual recordings for each stimulus condition. As for the

behavioural experiments described above, the gratings subtended a visual angle of $6 \times 6^\circ$.

Three observers participated in all these experiments, though the major findings were confirmed with several additional subjects. Two of the observers had normal colour vision (M.K. and D.W.) whilst the third (H.P.) was a protanope. All subjects had good visual acuity and wore the appropriate optical correction where necessary. Grating stimuli were viewed binocularly and were presented foveally for all subjects, and also at an eccentricity of 6° for subject M.K. Peripheral grating presentation was achieved by repositioning the subject's fixation target. The contrast of the red component was 20% for foveal, and 70% for peripheral, presentation.

RESULTS

It is first of interest to consider the isoluminant settings determined by each subject. For a red contrast of 20%, the two colour normal subjects adjusted the green contrast for minimum motion to very similar levels (see Table 4.2), whilst the protan subject (H.P.) required a very much lower

	<u>Subject</u>		
	M.K.	D.W.	H.P.
Green Contrast(%)	8.18	8.07	2.81

Table 4.2. Isoluminant green contrasts for a red contrast of 20%.

green contrast for isoluminance with the red. There were no differences in the isoluminant settings for the two spatial frequencies studied. All subjects experienced no difficulty using this technique and the end points were very repeatable.

Pupillary responses to chromatic grating stimuli presented foveally are shown for subject M.K. in Figure 4.26, similar responses were obtained for the second colour normal subject, D.W.. The upper (A) and lower (B) figures show

responses to the 1 and 2 c/deg grating respectively. In each figure the green contrast level decreases progressively from the upper to the lower trace with the centre trace representing responses to the isoluminant stimulus condition (indicated by "I"). For clarity of presentation responses have been shifted vertically and responses for right and left eyes paired. It may be seen that all stimulus conditions evoked significant pupillary responses of similar amplitude, though an analysis of the response latencies showed that responses to isoluminant stimuli displayed longer latencies (see Figure 4.27).

In Figure 4.28 response parameters are plotted for peripheral stimulus presentation (subject M.K.). The upper (A) and lower (B) figures display pupil response amplitude and pupil response latency respectively as a function of green grating contrast. Examination of the upper figure shows reduced amplitude responses at, and just around the isoluminance condition for both spatial frequencies investigated. Similar to the responses recorded for foveal grating presentation, the pupillary responses elicited by chromatic gratings presented in the periphery show relatively longer latencies at isoluminance.

Pupillary responses elicited by chromatic gratings for the protanopic observer are shown in Figures 4.29 (A) and (B). Whilst it may be seen that pupillary responses of similar amplitude to those observed in normal trichromats are obtained in this subject for gratings which have both luminance and chromatic contrast, responses to isoluminant grating stimuli are absent. Furthermore the overall response latencies for this colour defective subject appear to be much longer than those observed for colour normal subjects.

DISCUSSION

The preliminary finding that the isoluminant green grating contrast for the colour defective observer was less than for the colour normal observers was not entirely unexpected, since protanopes display reduced sensitivity to stimuli at

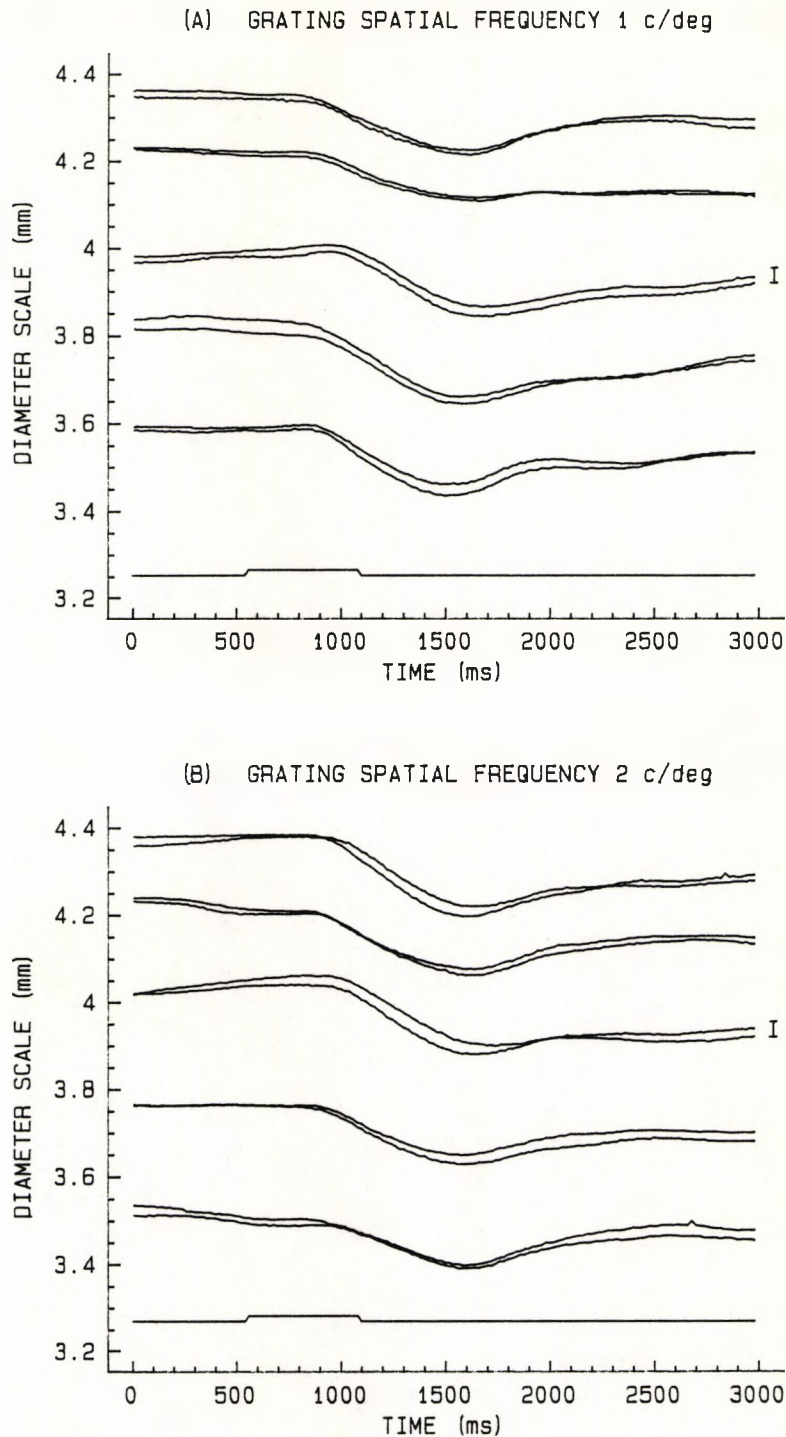


Figure 4.26. Pupillary response traces for stimulation with red-green chromatic gratings around isoluminance, subject MK (A) Shows data for a grating spatial frequency of 1 c/deg and (B) for 2 c/deg. Data is presented for 5 levels of green contrast representing equal increments around the red-green isoluminant point. Measurements were made binocularly and traces for right and left eyes are paired. For clarity, the traces have been shifted vertically in each figure, with the green contrast decreasing progressively from the upper trace to the lower trace. The centre traces (indicated with an "I") show responses to gratings which were judged to be isoluminant by the minimum motion technique (see text). All gratings were isoluminant with respect to the background.

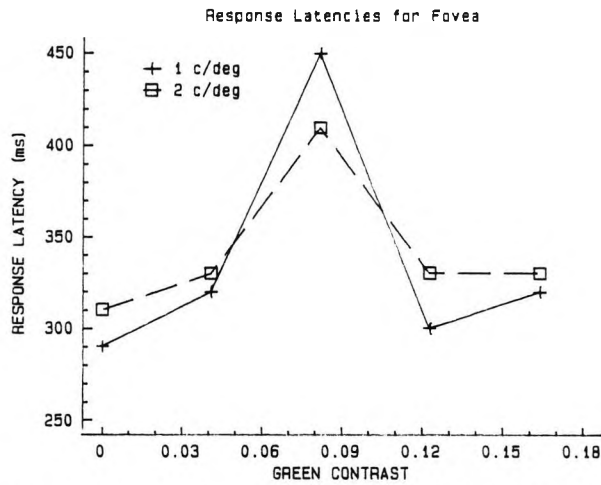


Figure 4.27. Pupil response latency plotted against the green contrast level of red-green chromatic gratings (subject MK). Data extracted from traces shown in Figure 4.26. The isoluminant green contrast is approximately 0.09.

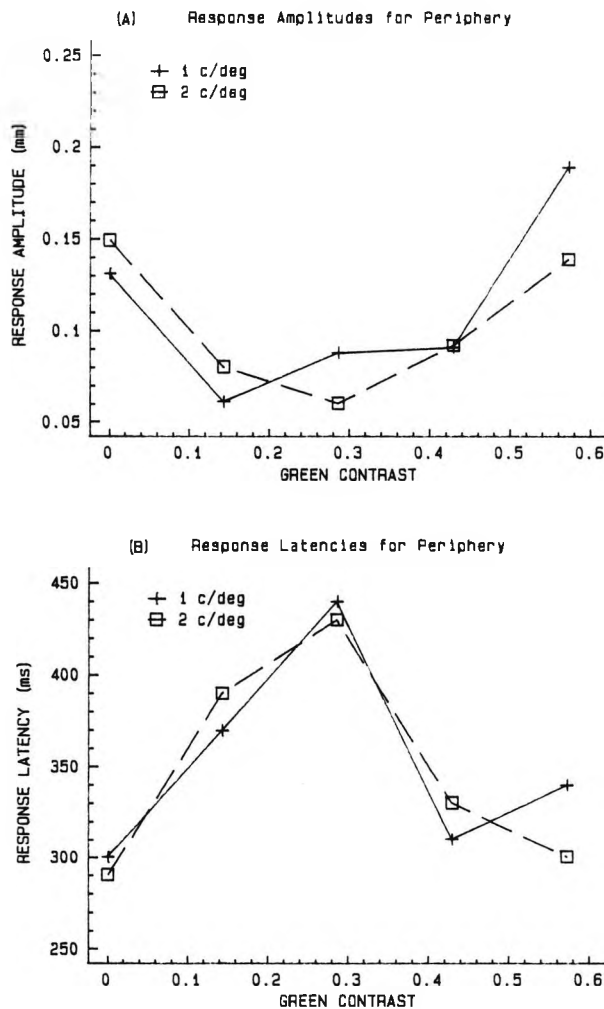


Figure 4.28. (A) Pupil response amplitude and (B) pupil response latency plotted as a function of the green contrast level of a red-green chromatic grating presented 6° in the periphery (subject MK). The red and green components of the grating were isoluminant with respect to each other when the green contrast level was approximately 0.3.

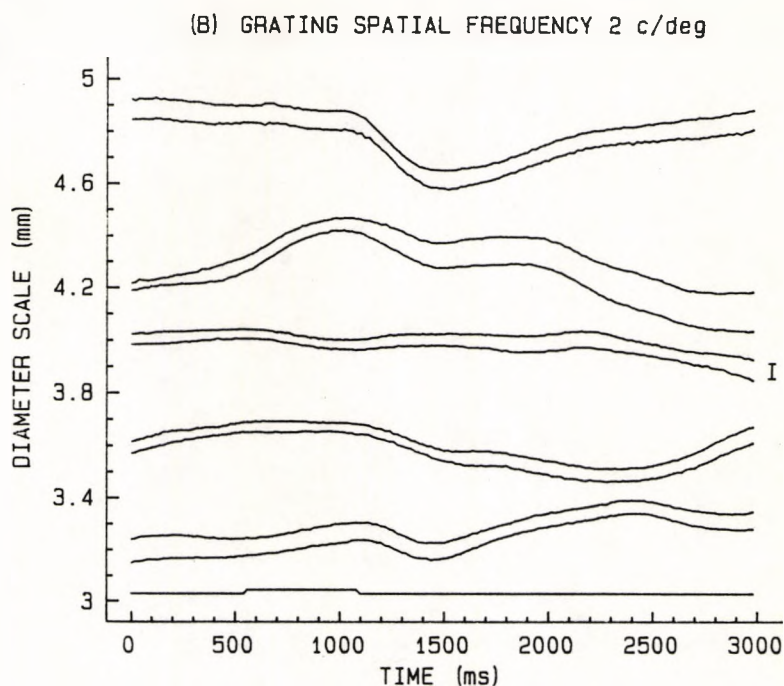
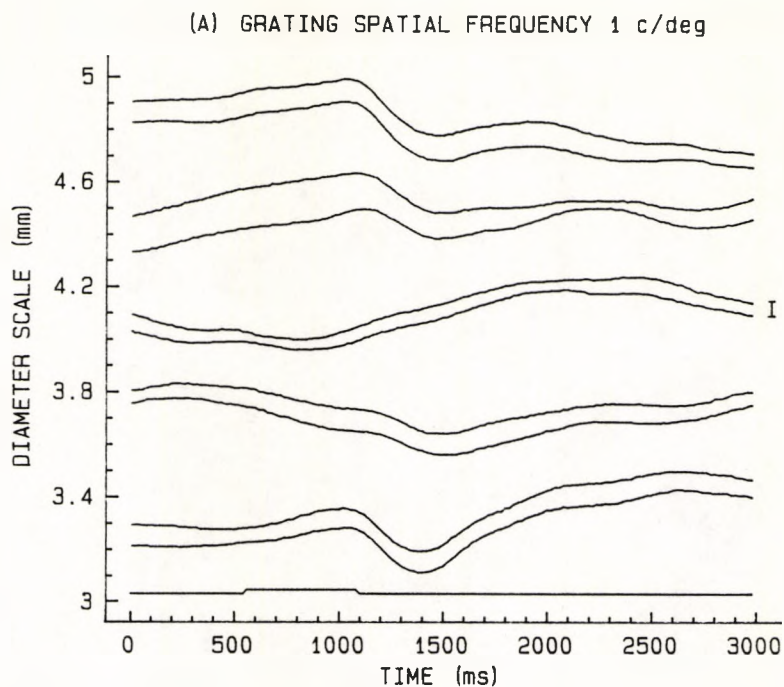


Figure 4.29. Pupillary response traces for stimulation with red-green chromatic gratings around isoluminance, subject HP, a protanope. (A) Shows data for a grating spatial frequency of 1 c/deg and (B) for 2 c/deg. Data is presented for 5 levels of green contrast representing equal increments around the red-green isoluminant point. Measurements were made binocularly and traces for right and left eyes are paired. For clarity, the traces have been shifted vertically in each figure, with the green contrast decreasing progressively from the upper trace to the lower trace. The centre traces (indicated with an "I") show that there are no responses to gratings which were judged to be isoluminant by the minimum motion technique (see text).

the "red end" of the visible spectrum (see Wyszecki and Stiles, 1982). Whilst the minimum motion technique was found to be a satisfactory method for determining red - green isoluminance at low contrast levels, most subjects found it impossible to stop the apparent movement of the grating when chromatic contrast levels were increased above about 20% (for the red component). This finding may suggest, therefore, that for high chromatic contrasts the red - green opponent mechanism can contribute to the detection of moving stimuli. An alternative explanation would be that some luminance artefact, only present for high chromatic contrasts, corrupted the results (though this is unlikely for reasons detailed below).

The results of the present study indicate that the pupil constricts transiently to an isoluminant, red - green chromatic grating stimulus. It may be argued, however, that uncorrected transverse and longitudinal chromatic aberrations may produce an unwanted luminance artefact which itself elicits the pupillary response. This problem has been addressed previously by Murray et al. (1987) in their work with VEP's. These authors found that VEP amplitudes were smaller when chromatic aberrations were eliminated than when they were not, but that qualitatively the results were the same with or without correction. In terms of the present study several other observations indicate that chromatic aberrations are not a significant factor in determining the response of the pupil. First, one would expect that if luminance artefacts are responsible for the pupillary constriction, then the resulting response latencies would be much shorter than those observed for the chromatic gratings. Secondly, any supposed luminance artefacts would be present for the protanopic subject and should still produce a response even when the gratings are isoluminant. It will be remembered that no pupillary responses were elicited in this subject for gratings which were isoluminant. Thirdly, the gratings used were of fairly low spatial frequencies and are consequently less likely to be affected by chromatic aberrations. Finally, any induced luminance variations must

be extremely small, and it is unlikely that these would be sufficient to evoke a pupillary response.

Having established that it is the chromatic content of the isoluminant grating that elicits the pupillary response, then the results suggest that responses to such stimuli are of longer latency than those observed for achromatic gratings. Young and Alpern (1980) found that longer response latencies were elicited by equiluminant heterochromatic stimuli when compared with the responses elicited by pure luminance stimuli. These authors found that the latency differences observed were of the order of 50 ms, though the results of the current study would indicate that the latency differences between chromatic and achromatic grating stimuli are nearer 80 to 100 ms (depending on spatial frequency). The discrepancy between the two studies is not entirely unexpected, however, since the stimuli used to elicit pupillary responses were vastly different, Young and Alpern using uniform, circular, monochromatic lights as stimuli. The additional spatial content of the gratings used in the present study, therefore, may account for these differences. Based on their findings of increased latencies for purely heterochromatic stimulus changes, Young and Alpern suggested that the cortex might be involved in the response of the pupil to chromatic stimuli. This hypothesis has found further support from the more recent finding that responses to uniform chromatic stimuli are absent when the stimuli are restricted to blind areas of the visual field in patients with geniculo - striate lesions (Keenleyside, 1989). Evidence from VEP studies (Murray et al., 1987; Kulikowski and Russell, 1987; Murray and Parry, 1987) suggests that isoluminant chromatic gratings may preferentially activate neurones in the parvo - cellular pathway, whilst achromatic gratings favour neurones in the magno - cellular pathways. The longer latencies observed for isoluminant chromatic gratings may therefore reflect the slower conduction velocities and processing that physiological studies have demonstrated for the parvo - cellular pathways.

The reduced pupil response amplitudes observed for the isoluminant stimuli presented in the peripheral visual field (see Figure 4.28) presumably reflect the lowered sensitivity to chromatic stimuli at this eccentricity. Similarly increased response latencies for the isoluminant stimuli as observed for foveal stimulation indicate that these responses are still mediated by chromatic processes.

The results of the present study indicate that deficiencies in the chromatic processing of protanopic subjects may be revealed by their anomalous pupillary responses. This finding is in good agreement with several earlier studies which have shown that pupillometry may provide a useful method for the objective assessment of colour vision defects (e.g., Young et al., 1987; Saini and Cohen, 1979; but see also Chapter 1). It is well - documented that protanopes show reduced sensitivity for stimuli of long wavelength. It follows, therefore, that the red - green opponent pathway must also show a reduced sensitivity to red - green isoluminant gratings. Along similar lines, Arden and his co-workers (Arden et al., 1988a, 1988b; Gündüz et al., 1988a, 1988b) have shown that detection thresholds for chromatic gratings are elevated in subjects with acquired colour vision defects. It is not surprising, therefore, that reduced pupillary responses are observed for the protanopic subject in the present study. The increased latencies relative to colour normal observers are likely to reflect the reduced signals generated in the chromatic pathway.

4.3.3 THE EFFECT OF CHROMATIC CONTRAST ON PUPILLARY RESPONSES

A natural extension of the above experiment was to investigate the effect of chromatic contrast on the response of the pupil to grating stimuli. Chromatic grating stimuli with red contrasts ranging from 2% to 70% were therefore generated and presented randomly at a fixed spatial frequency of 2 c/deg. The modulation of both the red and the green grating components was varied, but the green component was always made isoluminant with the red using the minimum

apparent motion technique. All other stimulus parameters, and the pupillometric methods used, were identical to those given in the previous section of this chapter when pupillary responses were determined for a range of contrasts around isoluminance.

RESULTS

The results of the experiment are shown for one subject (M.K.) in Figures 4.30 (A) and (B). Pupil response amplitude (A) and pupil response latency (B) are both plotted as a function of chromatic contrast. It can be seen that response amplitude initially increases with contrast, but for contrasts between about 5% and 50% the response amplitude remains fairly constant, only increasing again for gratings with a contrast in excess of 50%. Examination of the corresponding response latencies shows a more gradual decrease in latency with increasing contrast. The results suggest that the pupil response latency is minimal for grating contrasts of 50% and above.

CONCLUSIONS

A small, but significant pupillary response is measured for gratings with a chromatic contrast as low as 2%. This suggests that the psychophysical detection thresholds and pupillary response thresholds are very similar for red - green chromatic gratings. It would seem that once the contrast threshold is exceeded response amplitudes are almost invariant until contrasts increase beyond 50%. For these higher grating contrasts, the corresponding response latencies are relatively short and therefore it is difficult to rule out the possibility of an unwanted subjective luminance component producing the increased amplitudes responses.

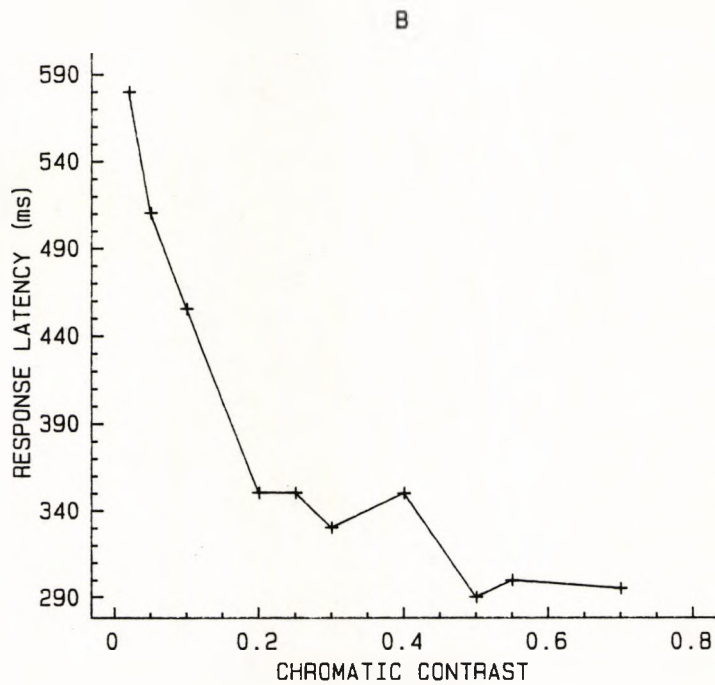
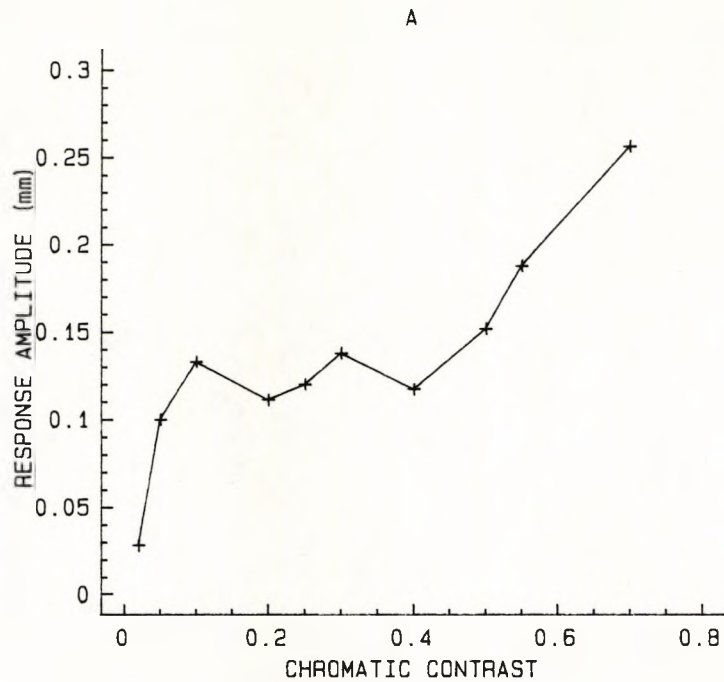


Figure 4.30. (A) Pupil response amplitude and (B) pupil response latency plotted as a function of the chromatic contrast of a red-green isoluminant grating of spatial frequency 2 c/deg. Data is shown for one subject (MK) for foveal stimulus presentation. Measurements were made binocularly and each data point represents the mean of right and left responses for 24 stimulus presentations.

4.3.4 PUPILLARY RESPONSES TO CHROMATIC GRATINGS. VARIATION WITH SPATIAL FREQUENCY

It has been shown previously that pupillary response amplitude and latency vary systematically with the spatial frequency of achromatic gratings (see section 2.2 of this chapter). Is the same true for pupillary responses to isoluminant chromatic gratings? In order to answer this question, pupillary responses were measured to chromatic gratings for stimulus spatial frequencies ranging from 0.6 to 6 c/deg. The contrast of the red component was fixed at 30%, while that of the green component was adjusted to be isoluminant with the red for each spatial frequency, again using the minimum apparent motion technique. The stimulus parameters and procedure were otherwise unchanged from the previous experiment described above. Three experienced, normal trichromats participated in the experiment (M.K., D.W., and J.B.) and measurements were made for gratings presented foveally and also at an eccentricity of 6° in the peripheral field.

RESULTS

Figures 4.31 (A) and (B) display the results for two observers (D.W. and M.K. respectively). Pupil response amplitude is plotted as a function of grating spatial frequency for both foveal and peripheral stimulation. In figure (C), comparative data are presented for foveal presentation of achromatic gratings using the same monitor to generate the stimuli. In general, for foveal measurements, pupil response amplitude was greatest for chromatic gratings with spatial frequencies between 1 and 2 c/deg, whereas for achromatic gratings the peak response occurs at a higher frequency of 5 c/deg. Above about 2 c/deg response amplitudes following stimulation with chromatic gratings decrease, reaching a minimum at 4 c/deg, and then increasing again for a spatial frequency of 6 c/deg. For peripherally presented chromatic gratings the results indicate that there is no low frequency attenuation to 0.6 c/deg, but again response amplitudes increase for

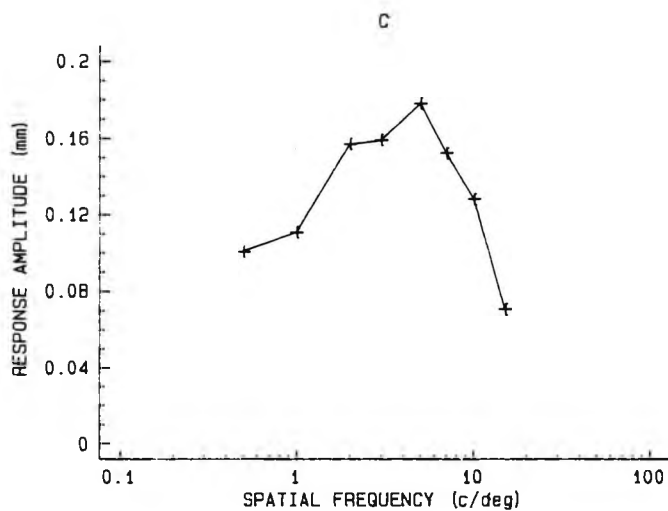
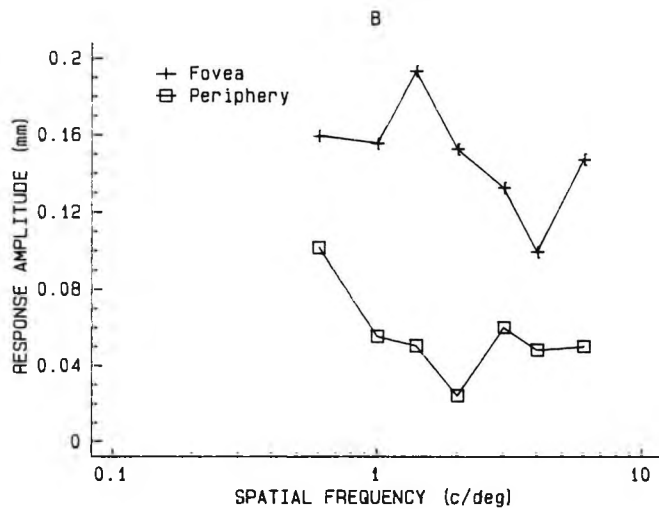
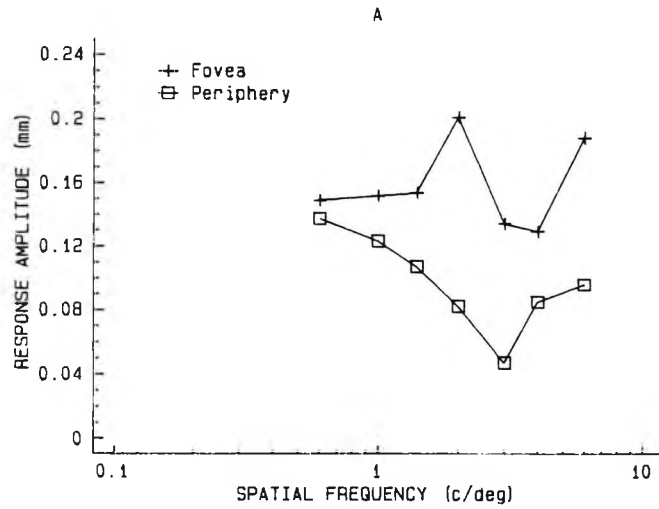


Figure 4.31. Pupil response amplitude is plotted as a function of the spatial frequency of a red-green isoluminant grating for two normal trichromats: (A) subject DW; (B) subject MK. The contrast of the red grating component was fixed at 30%, and the green component adjusted to isoluminance for each spatial frequency. Comparative data for an achromatic grating is shown in (C), note different x-scale.

stimuli of higher spatial frequencies, in this case above frequencies of 2 c/deg.

Pupil response latencies are plotted in Figures 4.32 (A) and (B) as a function of grating spatial frequency. The upper figure (A) displays the latencies recorded for subject D.W. for both foveal and peripheral chromatic grating presentation, whilst the lower figure (B) shows comparative latency data for achromatic and chromatic gratings presented foveally (subject J.B.). From figure (A) it may be seen that response latencies are longer for grating stimuli presented in the periphery and also that latencies increase with increasing grating spatial frequency. Figure (B) illustrates the increased pupil latencies for isoluminant chromatic gratings relative to achromatic gratings of the same space-averaged luminance as the background field.

CONCLUSIONS

The results suggest that the response of the pupil to isoluminant chromatic gratings correlates reasonably well with the psychophysical contrast thresholds determined for the same stimuli (see section 4.1 of this chapter). The increase in response amplitude for higher spatial frequency gratings is, however, somewhat unexpected, as one would have predicted a continuous reduction in response amplitude as frequency increases. The most likely explanation for this deviation from the predicted results is that the effect of chromatic aberrations becomes more marked for high spatial frequency stimuli thereby introducing a luminance artefact. Interestingly all subjects reported some difficulty in setting the isoluminant green contrast for minimum motion for the high spatial frequency grating stimuli, though the end point was not significantly different to that determined for the lower frequency stimuli. This difficulty, however, may simply reflect the reduced sensitivity of the chromatic pathway to high spatial frequency stimuli (see Chapter 1 section 4.4).

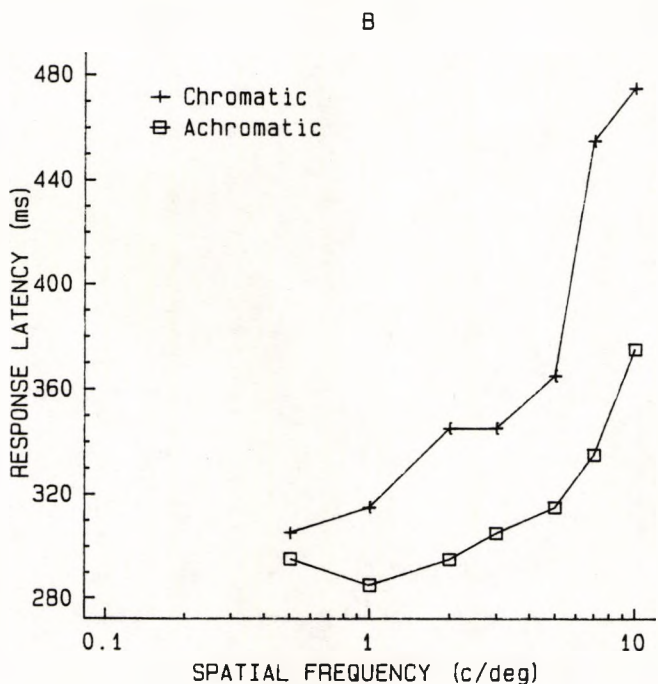
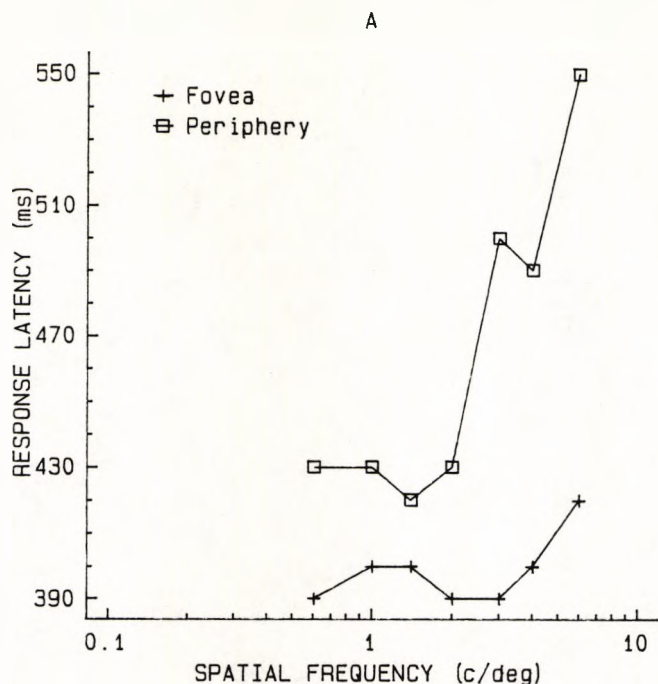


Figure 4.32. (A) Pupil response latency is plotted as a function of the spatial frequency of an isoluminant chromatic grating for stimuli presented foveally and at an eccentricity of 6° . Data is shown for subject DW and corresponds with the amplitude plot shown in Figure 4.31. (B) For comparison, pupil response latency is plotted against spatial frequency for both chromatic and achromatic gratings (subject JB). All gratings were isoluminant with respect to the background field, the contrast of the red component was 30%, and the contrast of the achromatic grating was 50%.

4.4 MEASUREMENTS OF ACCOMMODATION FOR CHROMATIC AND ACHROMATIC STIMULI

Many of the experiments reported in this chapter have involved the measurement of pupillary responses to chromatic and achromatic grating stimuli. It may be seen from these experiments that the response of the pupil varies systematically as a function of the spatial frequency of the grating stimulus. It has been proposed that these responses reflect the activity of central mechanisms which regulate the activity of the pupillomotor nucleus (e.g., Barbur and Forsyth, 1986; Barbur et al., 1992). It may be argued, however, that the observed pupillary responses occur as a result of synkinetic changes in accommodation and / or convergence associated with the near triad response (see Barbur, 1991; Alexandridis et al., 1991). The accommodation and pupillary systems certainly display some similarities in their response characteristics, for example, the latency of response to grating stimuli for both systems is usually between 0.3 and 0.4 s (Charman and Heron, 1988 and see also Figures 4.2 and 4.3), and both systems display micro - fluctuations about a steady - state position (though the frequency of accommodation oscillations is lower at 2 Hz) (Charman and Heron, 1988).

Several investigations have shown that the accommodative response, like the pupil response, varies as a function of target spatial frequency (Charman and Tucker, 1977, 1978; Owens, 1980; Ciuffreda and Hokoda, 1983; Ward, 1987a). The "contrast control" hypothesis of Owens (1980), for example, postulates that spatial frequencies around the peak of the contrast sensitivity function are most important as an aid to the control of accommodation. This in turn suggests that stimuli in the mid - spatial frequency range provide a better stimulus to accommodation and may possibly, therefore, produce an associated pupillary response of larger amplitude than for stimuli of higher or lower spatial frequencies. Charman and Tucker (1977, 1978) have, however, published conflicting results which indicate that high spatial frequency stimuli provide the best stimulus to

accommodation. If the "fine tune" accommodation hypothesis proposed by these authors is correct, then it would seem unlikely that the pupil grating response occurs as a consequence of changes in accommodation for stimuli of different spatial frequency. Interestingly, Ciuffreda and Hokoda (1985) have attempted to resolve these conflicting views on accommodation by showing that the differences between the two studies probably occurred as the result of different instructions given to the observers. In Owen's study (1980) the observers were instructed to view the targets without straining whereas, in Charman and Tucker's study (1977, 1978), the observers were instructed to maintain optimum target clarity.

Because of the possible correlation between accommodative responses and pupillary responses related above, attempts were made when designing the experiments to minimise changes in accommodation. Firstly, all experiments were conducted using a viewing distance of approximately 1 m, a distance which is known to correspond with the eye's resting, or dark, focus point (Leibowitz and Owens, 1975). Thus little accommodation was required to keep stimuli in focus. Furthermore, Owen's (1980) data indicates that at a distance of 1 m there is, in fact, little variation of accommodation as a function of target spatial frequency. Secondly, as suggested by the work of Denieul and Corno (1986), a high - contrast fixation target was visible throughout each experiment and all observers were instructed to keep it in focus, thereby encouraging steady accommodation and convergence. Thirdly, unwanted reflections which could provide secondary stimuli for accommodation were minimised by isolating the testing system and the observer with a blackened surround.

The effect of stimulus contrast on the accommodation response has been investigated in several studies (Charman and Tucker, 1978; Ciuffreda and Rumpf, 1985; Ward, 1987b) and the general consensus is that, for sinusoidal grating stimuli, contrast has little effect on steady - state accommodation, providing gratings are suprathreshold.

Analogous experiments have been carried out to investigate the response of the pupil to gratings of varying contrast (see Barbur et al., 1987a) but unlike accommodation responses, pupillary responses were found to increase in amplitude for stimuli of increasing contrast. If accommodation changes are responsible for the pupillary responses to sinusoidal grating stimuli, then one would expect that the two types of response would display a similar dependence on contrast, and this is clearly not the case.

Similarly, it may be argued that accommodation changes influence the pupillary response to chromatic stimuli. The fact that the eye suffers from longitudinal chromatic aberration is well known (e.g., Charman and Jennings, 1976) and means that the eye's refractive power varies as a function of wavelength. Consequently different amplitudes of accommodation are required to focus targets of different chromatic content positioned at the same distance. Charman and Tucker (1978), for example, used a laser optometer to measure accommodation while observers viewed Snellen letters of varying (narrow band) colours. Their results showed an increased accommodative response to red targets when compared with either yellow or green targets, and this finding has been confirmed by more recent studies (e.g. Lovasik and Kergoat, 1988). It has been shown that chromatic targets can serve as effective stimuli to accommodation (Murch, 1982; Lovasik and Kergoat, 1988), yet it is doubtful for a number of reasons whether accommodation influences the response of the pupil to chromatic stimuli. Firstly, Young and Alpern (1980) have reported that the systematic variation of pupil response amplitude with stimulus wavelength is not a consequence of chromatic aberration (or chromatic differences in magnification) because (i) an achromatising lens was used in the viewing system, and (ii) stimuli of equal chromatic aberration do not produce equal pupillary response in deuteranopes. Secondly, Charman and Tucker (1978) found that accommodation for two differently coloured targets could be stabilised by requesting the observer to maintain focus on only one of the targets. The

use of a fixation target in the experiments described in the present study should, therefore, minimise any accommodative changes occurring as a result of presentation of chromatic stimuli, since all subjects were required to maintain accurate focus on this target.

The factors discussed above suggest that the pupillary responses elicited following the presentation of chromatic or achromatic stimuli are not generated as a result of accommodation changes. An investigation was carried out, however, to measure the steady - state accommodation during the presentation of achromatic grating stimuli. At the time of this particular investigation the software required for the generation of isoluminant chromatic gratings had not been fully developed, and therefore accommodation to coloured targets was measured using isoluminant, uniform rectangular stimuli (see Barbur et al., 1987a).

PROCEDURE

All stimuli were generated on the Ayadin monitor described in Chapter 2. Achromatic gratings were presented at a fixed spatial frequency of 3 c/deg against a uniform grey background of 9 cd/m². The space - averaged luminance of the gratings was equal to that of the background. Stimuli were rectangular and subtended a visual angle of 5 x 5° at a viewing distance of 1.2 m. Two grating contrasts of 0.3 and 0.6 were used together with a control condition where no grating was presented. Stimulus conditions were randomly interleaved with each condition being presented a total of 24 times.

Measurements of accommodation were made with the Canon Auto Ref R-1 autorefractor, an instrument which has been used in numerous previous studies for the same purpose of measuring accommodation (Ward, 1987a, 1987b). This commercially available instrument allows the measurement of the refractive error of the eye using infra - red light and has a maximum sample rate of about one reading per second. This reading of refractive error can then be simply translated

into a measure of accommodation. The subject is positioned in a chin and forehead rest and the use of a large hot mirror allows an open binocular field of view (though measurements are monocular). Alignment is achieved and maintained with the aid of a joystick control. A small, adjacent CRT allows for the continuous monitoring of fixation. Normally the instrument is triggered using a button on the joystick control, but for the purpose of this study the autorefractor was interfaced to the computer allowing automatic computer - control. The manufacturer's specifications quote the measurement accuracy at ± 0.12 Dioptres (D).

Subjects viewed the stimuli binocularly through the autorefractor's large beamsplitter and measurements of accommodation were made at times equal to 0, 2, 4, and 6 s with respect to the onset of pupillary recording. Autorefractor and stimulus presentation were synchronised under computer control with each grating appearing at $t = 1$ s for a duration of 0.5 s. These timing parameters were designed such that a measurement of accommodative status was made at the time of maximal pupillary constriction when, if one assumes that accommodation is responsible for the pupillary response, the accommodative response should be present.

In a separate experiment, uniform red, green and blue rectangular stimuli replaced the gratings used above. Each stimulus was isoluminant with the background as determined by flicker photometry. The experimental conditions were otherwise identical to those given above for grating stimuli.

In order to directly compare pupillometric data with measurements of accommodation, the P_SCAN 100 system (described in Chapter 2) was used to obtain measurements of pupil size for identical stimulus conditions. Three experienced observers participated in these experiments, all had normal colour vision, uncorrected vision of 6/6 or

better, and spherical refractive error and astigmatism of less than 0.50 D.

RESULT AND CONCLUSIONS

The results of the experiment are presented for each subject in Figures 4.33 - 4.35 for grating stimuli, and in Figures 4.36 - 4.37 for chromatic stimuli. The uppermost diagram in each figure (A) presents pupil response data and it can be seen that all stimuli (apart from the control) elicit significant pupillary responses with maximal constriction occurring at time = 2 s.

Accommodation measurements are presented in the lower three diagrams of each figure (B - D), each diagram corresponds to a specific stimulus condition for a particular subject. The Canon autorefractor is principally a clinical instrument designed to measure refractive error in terms of a spherical and a cylindrical component. For clarity of presentation the results have been represented here by the dioptric value of the mean sphere plus cylinder combination. In this way no information is lost with respect to the meridional differences in accommodation which are known to occur (Arnulf et al., 1981). Each data point represents the mean of the 24 measurements taken for each stimulus condition, and the error bars drawn through each point represent ± 1 standard deviation. It may be seen that no systematic changes of accommodation occur for any of the stimulus conditions and that the averaged fluctuations of accommodation over the 6 s test period are generally less than 0.1 D. Similarly, accommodation fluctuations for specific test times (i.e., those represented by the error bars) are normally in the 0.10 - 0.15 D range. Multiple student t - tests on adjacent data points showed that there were no significant differences in accommodation for successive test times.

Eye position over a single 6 s recording period is displayed for each eye of one subject in Figure 4.38. Vertical and horizontal eye movements are shown on the ordinate and

Figures 4.33 - 4.35. These figures are all of the same format, each figure shows equivalent data for different subjects (DD, JB and MK respectively). In (A) averaged pupil response traces are shown for the three stimulus conditions employed: achromatic sinusoidal gratings of spatial frequency 3 c/deg presented at two contrast levels of 30% and 60%; and a control condition where no stimulus was presented. Diagrams (B), (C) and (D) show measurements of accommodation made at series of discrete times with respect to the specified stimulus. Each data point shows the mean of 24 observations and error bars represent ± 1 standard deviation.

Figures 4.36 - 4.37. Again these figures have the same format to that given above, but data are presented for uniform, rectangular, red, green and blue stimuli which were judged to be isoluminant with the background. Subjects DD and MK respectively.

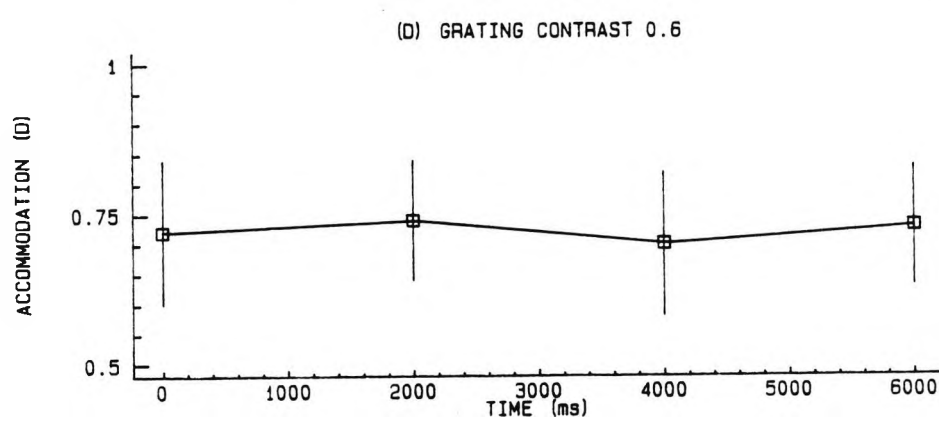
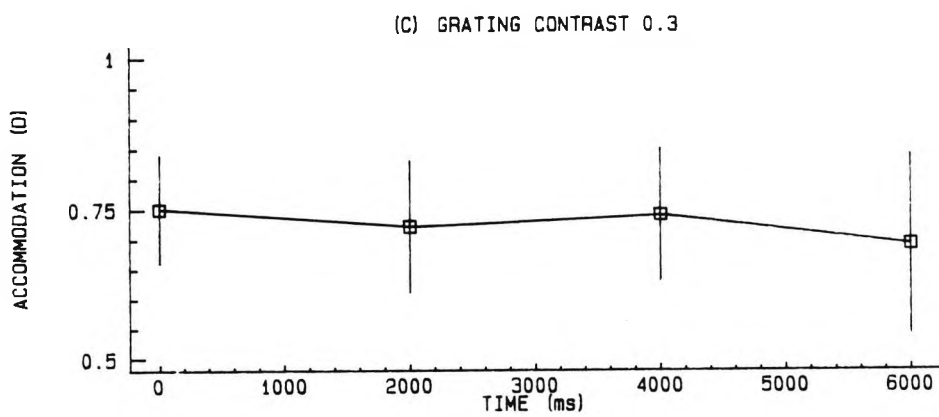
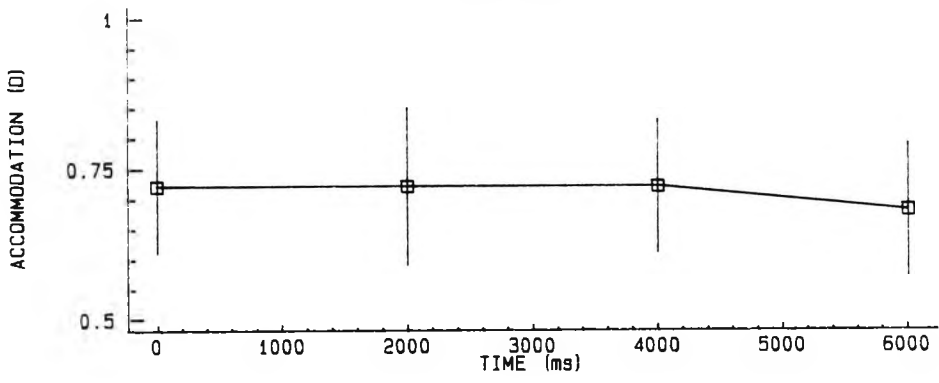
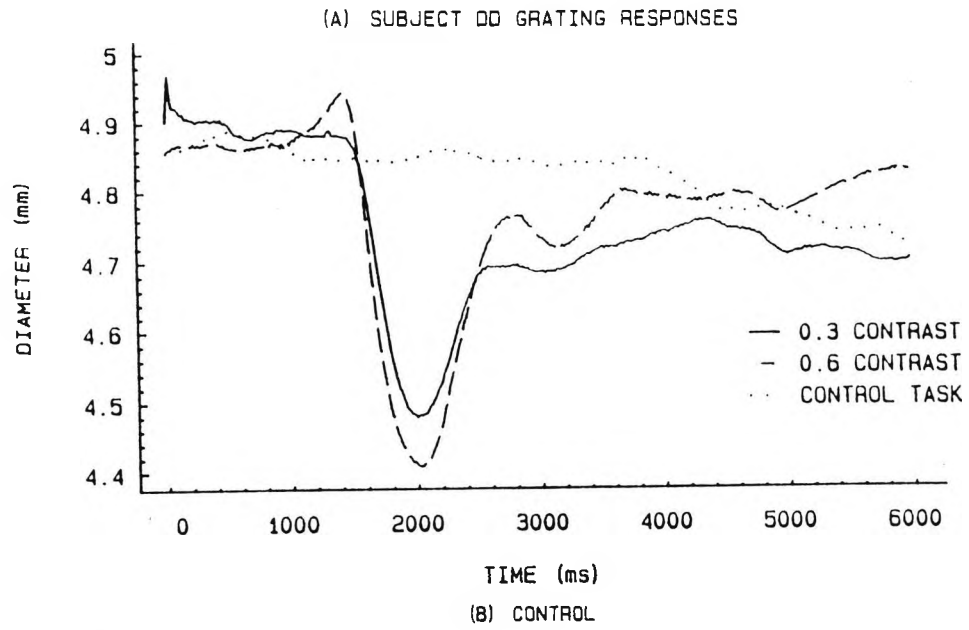


Figure 4.33.

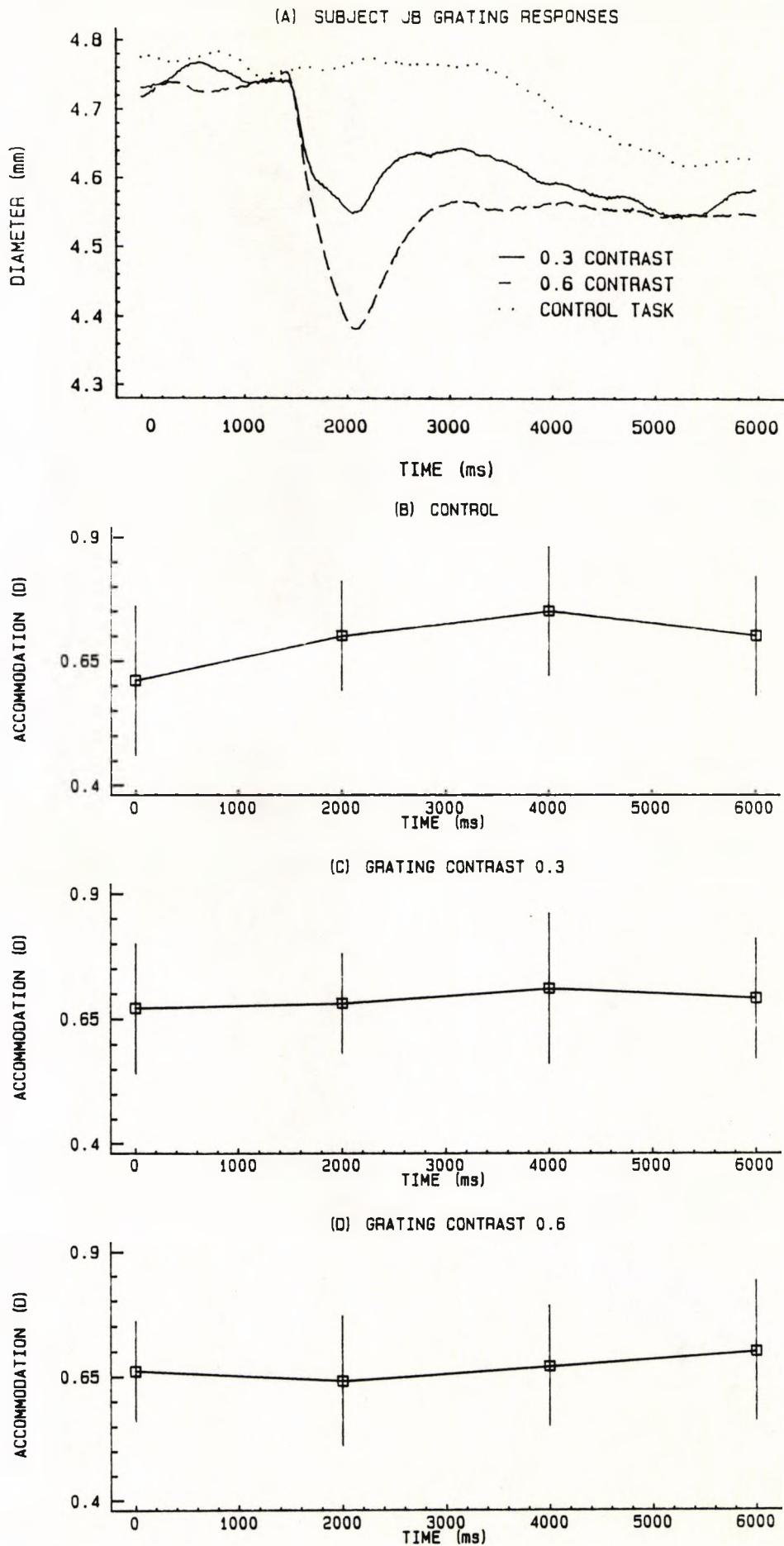


Figure 4.34.

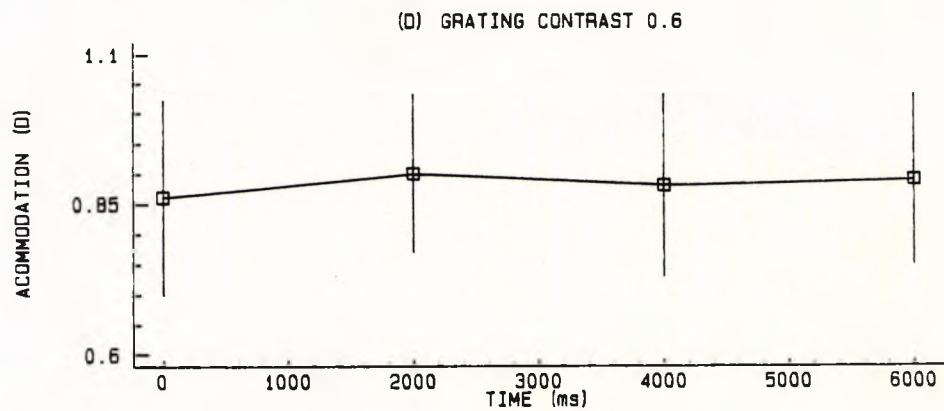
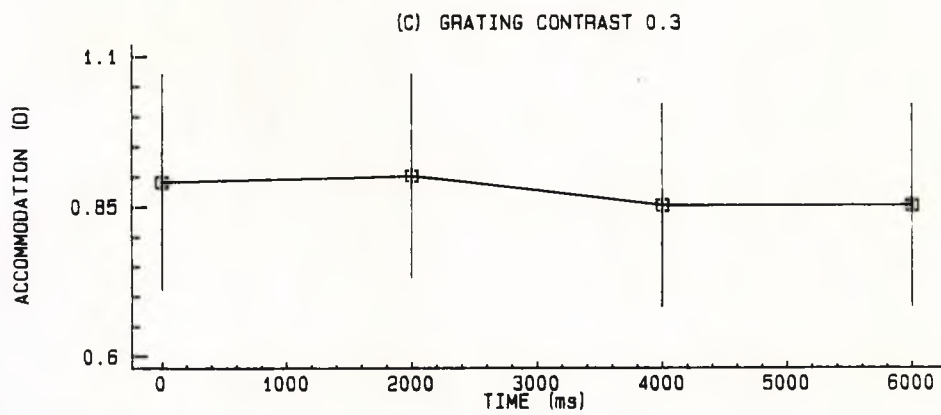
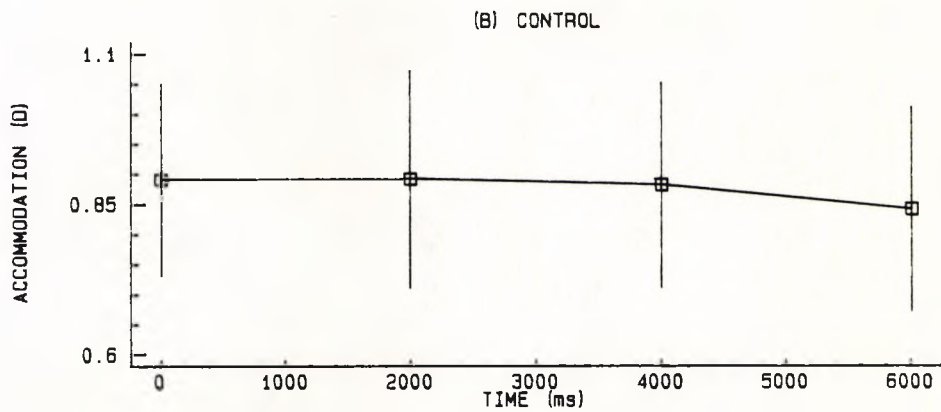
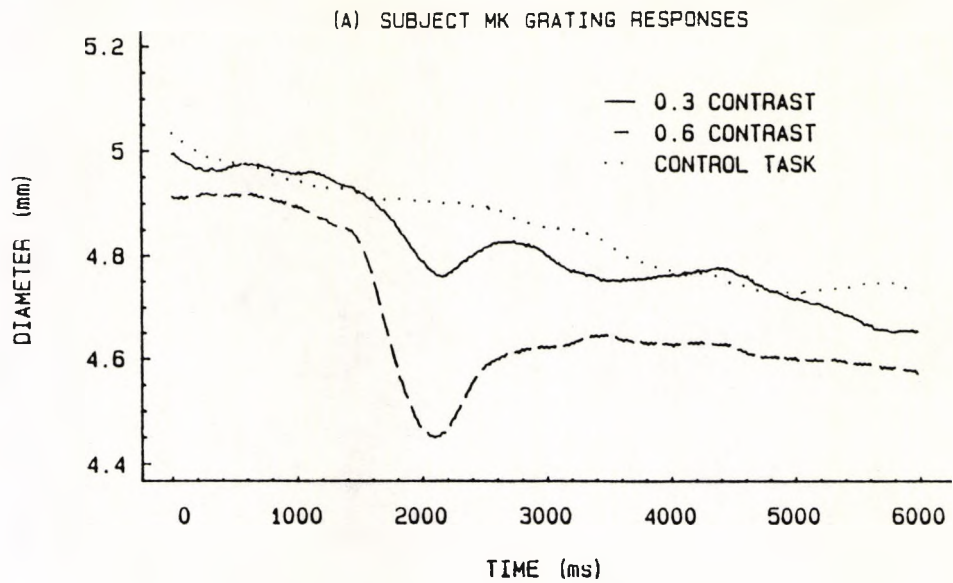
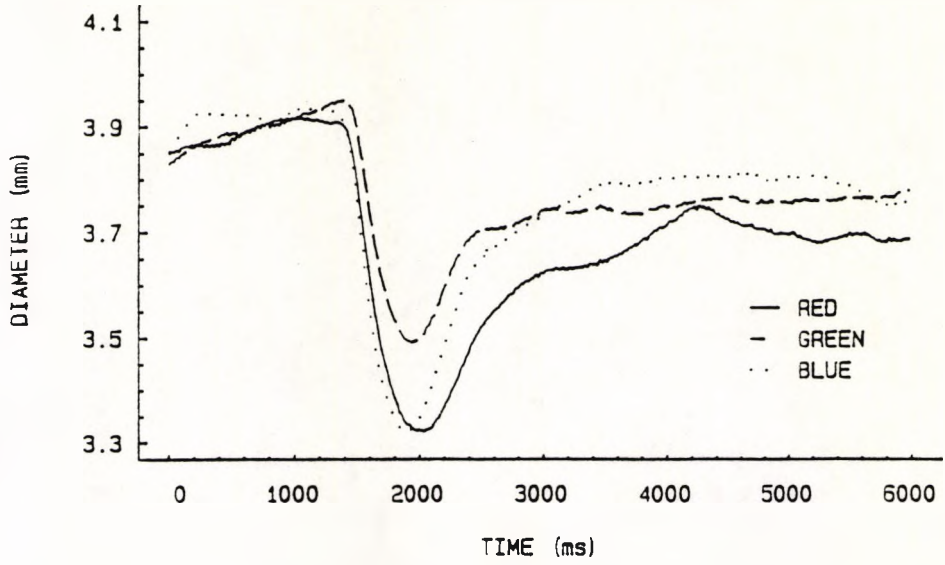
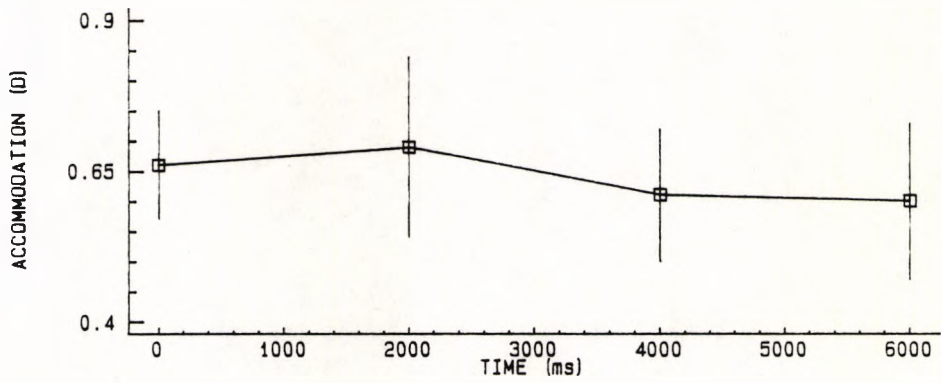


Figure 4.35.

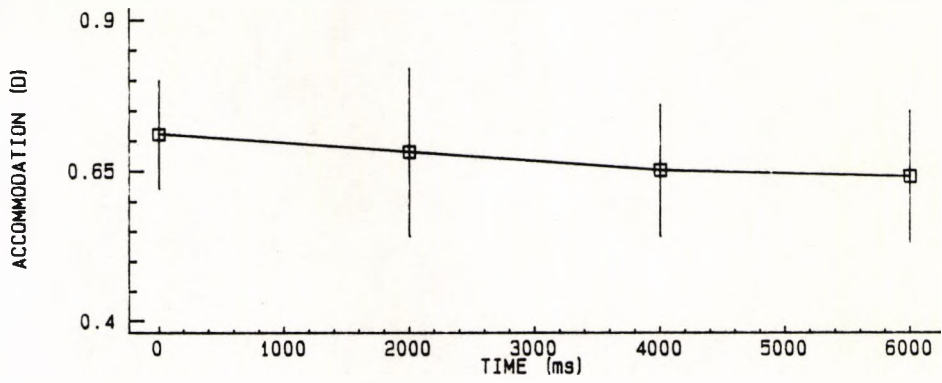
(A) SUBJECT DD COLOUR RESPONSES



(B) RED



(C) GREEN



(D) BLUE

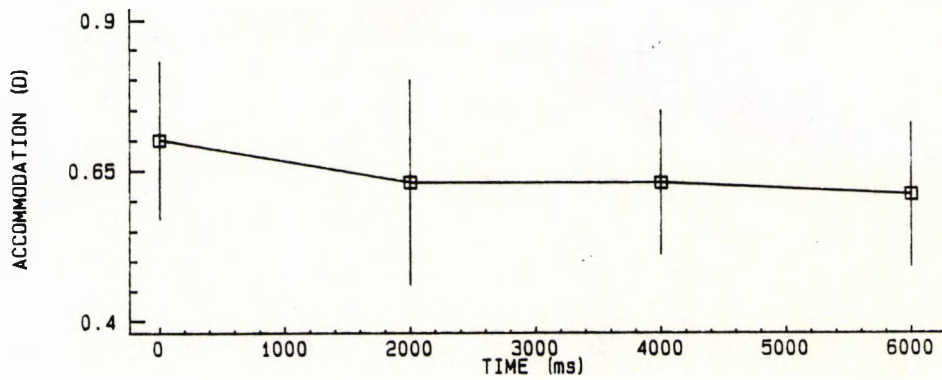


Figure 4.36.

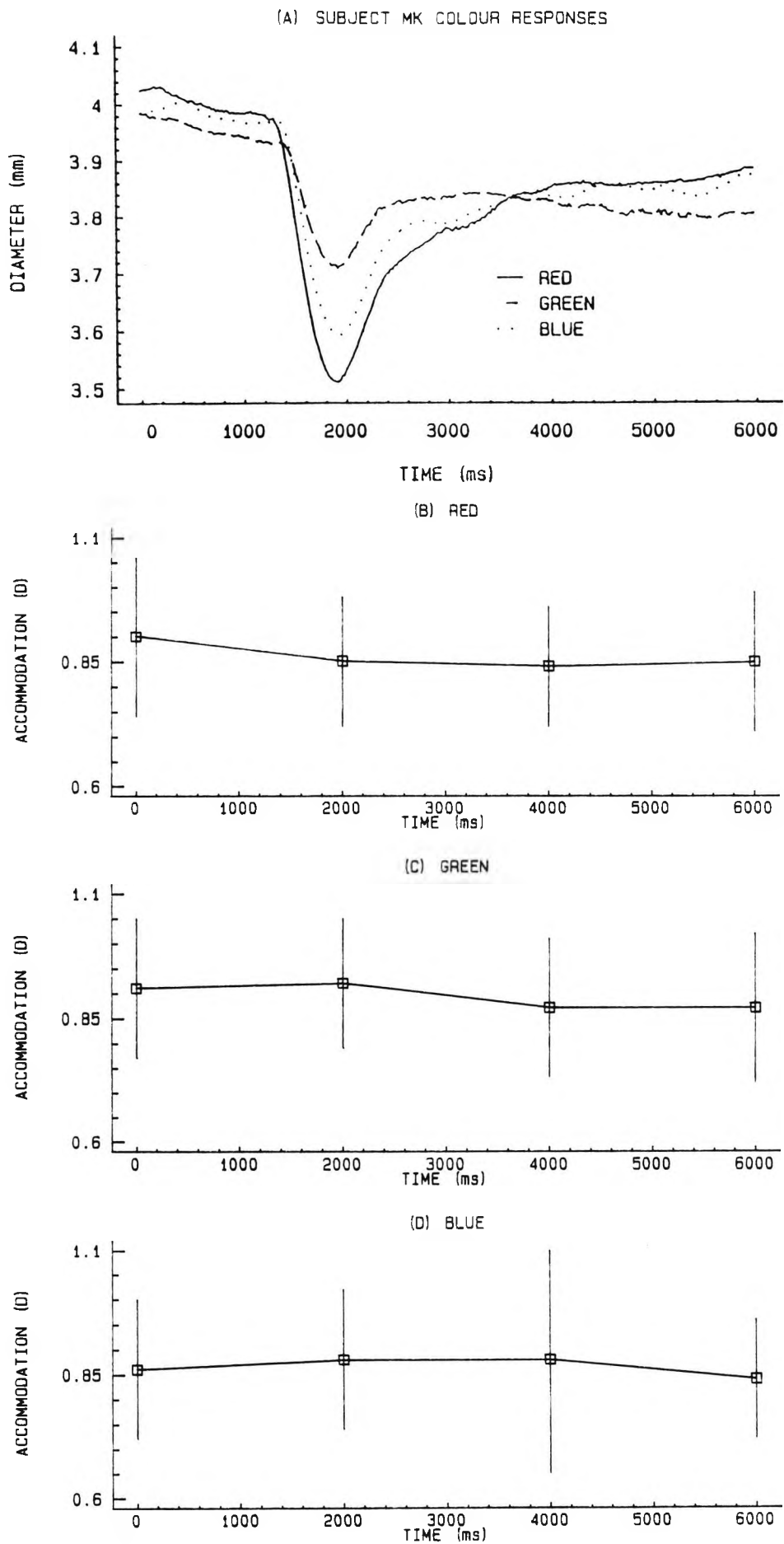


Figure 4.37.

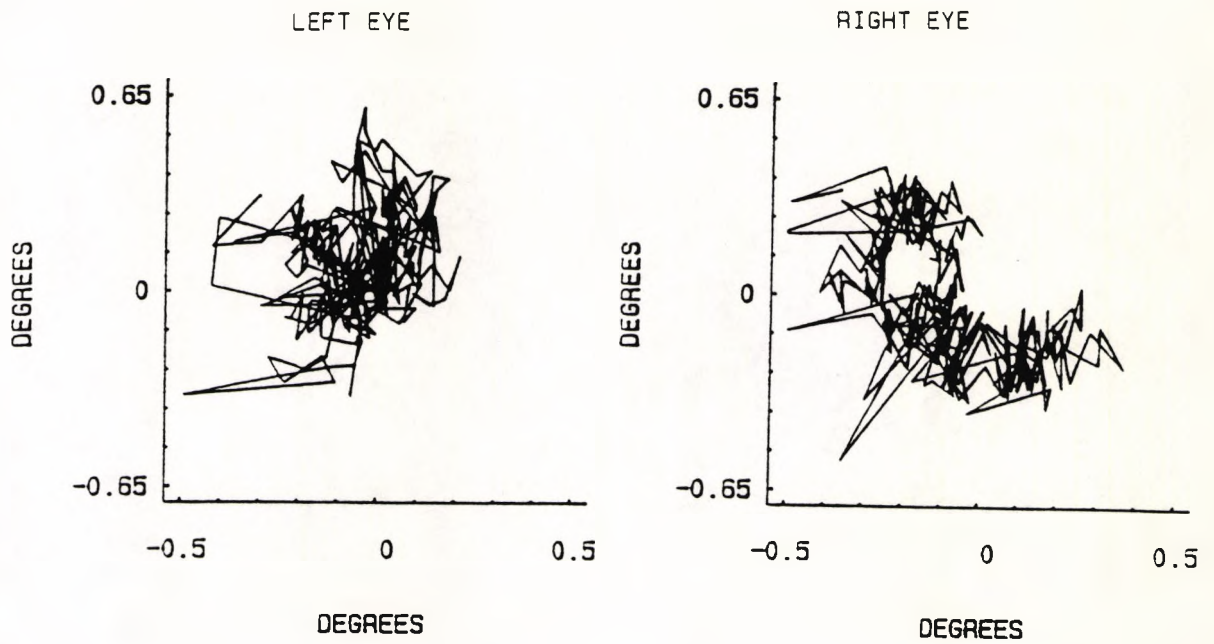


Figure 4.38. Typical eye movements measured over a period of 6 s during attempted binocular fixation. Vertical and horizontal angular displacements are shown on the ordinate and abscissa respectively. The data was recorded for subject JB for an achromatic grating stimulus of spatial frequency 3 c/deg, contrast 60%, and duration 500 ms.

abscissa, respectively. The magnitude of these observed eye movements is no greater than would be expected from a knowledge of the involuntary eye movements which necessarily occur when fixation is attempted (Padgham and Saunders, 1975).

The stimuli used in this investigation clearly elicit pupillary responses whilst measurements taken around the time of stimulus presentation indicate that any changes in accommodation are not significant. In summary, therefore, it would appear that fluctuations in accommodation or convergence triggered by the onset of the grating patterns or coloured stimuli cannot be used to explain the observed pupillary responses.

CHAPTER 5

PSYCHOPHYSICAL AND PUPILLOMETRIC METHODS FOR MEASURING CHROMATIC DISCRIMINATION THRESHOLDS

The results reported in the previous chapter suggest that pupillometry can be used to diagnose colour defective observers, although the success of the technique depends on the correct setting of isoluminance and the use of chromatic stimuli of low contrast. In order to avoid this difficulty, and to make possible the use of high chromatic contrast stimuli required to elicit measurable pupillary responses, a new stimulus has been developed which can be used with any class of colour defective observer in both threshold psychophysical tests and pupillometry.

Several previous studies have investigated the possibility of using computer - controlled raster display systems to test colour vision (King - Smith et al., 1983; Fallowfield and Krauskopf, 1984; Sellers et al., 1986; King - Smith et al., 1987; Heard et al., 1987; Arden et al., 1988a, 1988b). Generally such tests involve the measurement of detection thresholds for a chromatic target (e.g., a grating) which is equiluminant with its background. The chromaticity of this target can be modulated in specific directions in colour space chosen to coincide with the known colour confusion axes for colour defective observers (see Birch, 1985). Not only do computer - controlled display systems offer the means by which colour defective subjects may be identified and categorised, but also the ability to accurately grade the depth of an individual defect which is obviously a great advantage.

The problems of generating patterns which vary in chromaticity but not in luminance have been alluded to in the previous chapter and whilst raster display systems offer a great deal of flexibility in the generation of isoluminant chromatic patterns, at least two distinct disadvantages are evident. Firstly, displays offer only a limited gamut of higher luminances, and secondly, edge artefacts at chromatic

boundaries may be introduced by any slight misalignment of the electron guns, or simply from the organisation of the phosphor dots per se. Luminosity matches vary amongst both normal trichromats and colour defective subjects and therefore, in addition to the disadvantages which arise as a result of the physical limitations of the monitor, the need to ensure that any test patterns used are equiluminant for each individual, and also for each location in the visual field, necessitates the use of preliminary photometric procedures (e.g., the minimum apparent motion technique, or the more traditional minimum distinct border and minimum flicker techniques). Whilst this is not a major problem in the laboratory, in the clinical situation the additional time required to carry out such photometric procedures is often unacceptable and adds to the fatigue of the usually "naive" subject. Furthermore, elderly subjects, and subjects with abnormal visual function (e.g., optic neuritis), often have great difficulty in setting isoluminance.

Mollon and Reffin (1989) have attempted to overcome the problems described above by capitalising on techniques used by Stilling (1877) to solve similar problems encountered in the development of printed pseudo - isochromatic plates. Rather than attempting to create an equiluminant condition, the chromatic stimulus (in this case a Landolt C) is superposed onto a dark background composed of multiple discs which vary randomly in luminance. A more effective technique for eliminating luminance contrast cues involves the use of temporal, as well as spatial, luminance masking on a bright background field, when the subject becomes sensitive in discriminating small colour differences. In this chapter, therefore, a computer - controlled colour vision test is described in which chromatic discrimination thresholds are determined using a spatio - temporal luminance masking technique, the procedure being implemented on a high resolution, graphics display. Preliminary experiments to investigate pupillary responses to chromatic stimulus configurations identical to those used in the psychophysical experiments are also reported for both colour normal and colour defective subjects.

5.1 PSYCHOPHYSICAL METHODS TO DETERMINE CHROMATIC DISCRIMINATION THRESHOLDS

PROCEDURE

Stimuli were generated on a colour monitor similar to the Ayadin monitor described in chapter 2 section 2.2, but incorporating a higher screen resolution of 1280 by 1024 pixels. The monitor provided a large uniform background field of luminance 34 cd/m^2 and x,y - chromaticity co - ordinates of 0.305 and 0.323. The test pattern was presented at the centre of the background, and consisted of a rectangular array of individual square checks subtending a visual angle of $4 \times 4^\circ$ at a viewing distance of 1 m. Each of the checks comprising the test pattern subtended 12 minutes of arc and was separated from its neighbour by a gap of 4.5 minutes of arc. The luminance of each check changed randomly every 50 ms over a range of seven pre - determined values which were equal to, greater, or less than the luminance of the background. The amount of luminance masking produced was under the control of the experimenter and could be set at the beginning of each run by specifying the range, normally expressed as a percentage, of background luminance. For all settings the time - averaged luminance of the test pattern was always equal to that of the uniform background field. The chromatic component of the test pattern was composed of checks additionally modulated in colour space to form a series of vertical bars, the chromaticity of which could be adjusted under computer control with any chromatic displacement being completely independent of the random luminance modulation of the checks. Generally 12 directions in colour space were randomly interleaved, all radiating away from the background chromaticity point with equal angular separations.

A pilot run with each subject allowed the determination of approximate chromatic discrimination thresholds and familiarised the subject with the test pattern. An adjustment method was used with three separate estimates of

threshold for each angle of displacement. The subject simply used response buttons to either increase or decrease the chromatic displacement, pressing a third button when he perceived the stimulus to be close to threshold. The results of this pilot run were then input automatically into the experimental program proper which allowed the determination of discrimination thresholds using a procedure employing randomly interleaved staircases with variable step sizes. Each test pattern was presented for a duration of 1.65 s though the chromatic stimulus was only present for 550 ms following an initial 550 ms period of spatio - temporal dynamic noise. After the presentation of each stimulus, the subject responded by pressing one of two buttons to indicate the presence or absence of the vertical bars making up the chromatic component of the stimulus. Generally colour normal subjects perceived coloured bars when stimuli were above threshold for all angular displacements, though colour defective observers often failed to see any colour in the stimuli. A short inter - stimulus interval occurred following the subject's response to the previous pattern in which the uniform background filled the field of view.

The colour vision of participating subjects was assessed using conventional testing procedures incorporating the Ishihara and Farnsworth - Munsell 100 - Hue tests, and the Nagel anomaloscope (see Birch, 1985). In all, 13 subjects participated in the study. Of these, 3 subjects were normal trichromats, 2 were anomalous trichromats (1 protanomalous, 1 deuteranomalous), and 7 were dichromats (3 protanopes, 3 deuteranopes and 1 tritanope). Interestingly one subject gave mixed protanomalous / deuteranomalous responses in the colour vision tests used. All colour vision defects were known to be of congenital aetiology. Where necessary each subject wore the appropriate refractive correction.

RESULTS

Data are presented for one representative normal trichromat in Figure 5.1. The threshold chromatic displacement for detection of the stimulus is plotted as a function of the

displacement angle for a test pattern with a random luminance modulation of 8%. This data may be replotted in CIE x,y chromaticity space as shown in Figure 5.2 where, in order to obtain a reasonable representation, a small portion of the chromaticity diagram has been enlarged. The filled square drawn within the experimental data points represents the background chromaticity point. Data are also presented in this figure for two additional levels of random luminance modulation (i.e., 0% and 20%). The smooth continuous line represents the "best" ellipse fitted to the data points using a least squares algorithm. It may be seen that the size of the discrimination ellipse remains virtually invariant for different amplitudes of random luminance modulation.

Comparative data for three dichromats at several amplitudes of random luminance modulation are shown in Figures 5.3 (A), (B) and (C). For each dichromatic subject it is clear that the major axis of the discrimination ellipse elongates monotonically with the amplitude of the random luminance modulation applied. The orientation of the ellipse delimiting an individual's isochromatic zone is dependent on the type of dichromatism exhibited by the subject and correlates well with classical colour confusion lines. The same appears to be true for anomalous trichromats as shown in Figure 5.4. The upper diagram (A) in this figure displays the results obtained for a deuteranomalous subject, whilst the lower diagram (B) represents data obtained with a protanomalous subject. The axes of ellipse orientation shown for these anomalous trichromats closely resemble those obtained for the respective dichromats.

A summary of the three parameters which describe the best fit ellipse are displayed for each category of subject in Table 5.1 overpage. The major semiaxis and minor semiaxis refer to the longest and shortest dimension of the plotted discrimination ellipse respectively, and the orientation refers to the angle of inclination of the major semiaxis with the x - axis. The orientation axes for colour defective observers predicted on the basis of the classical colour

Subject JB

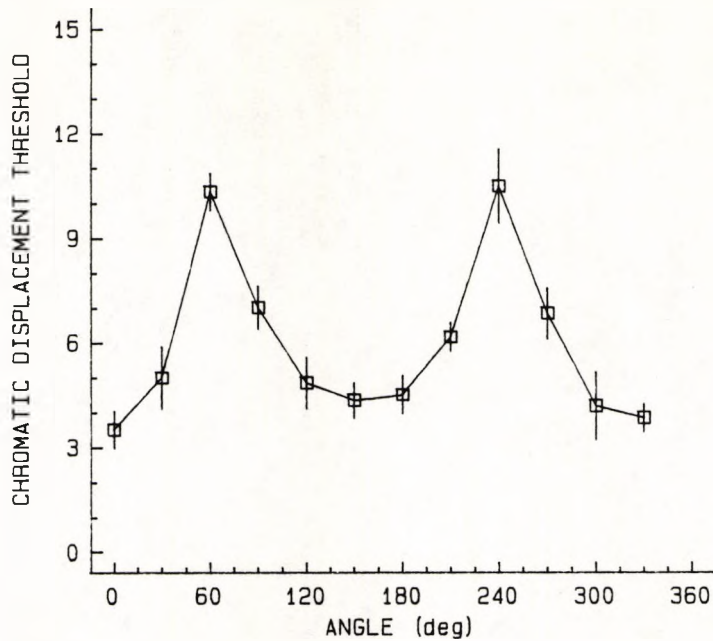


Figure 5.1. The threshold chromatic displacement for stimulus detection is plotted as a function of the displacement angle for a single representative normal trichromat (JB). Error bars show ± 1 standard error. The random luminance modulation (RLM) was fixed at 8%. These data are replotted in Figure 5.2 below.

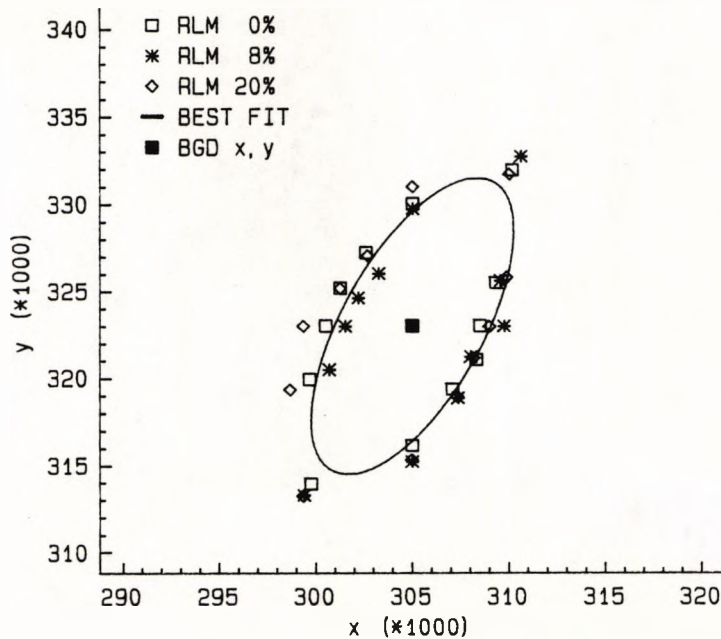
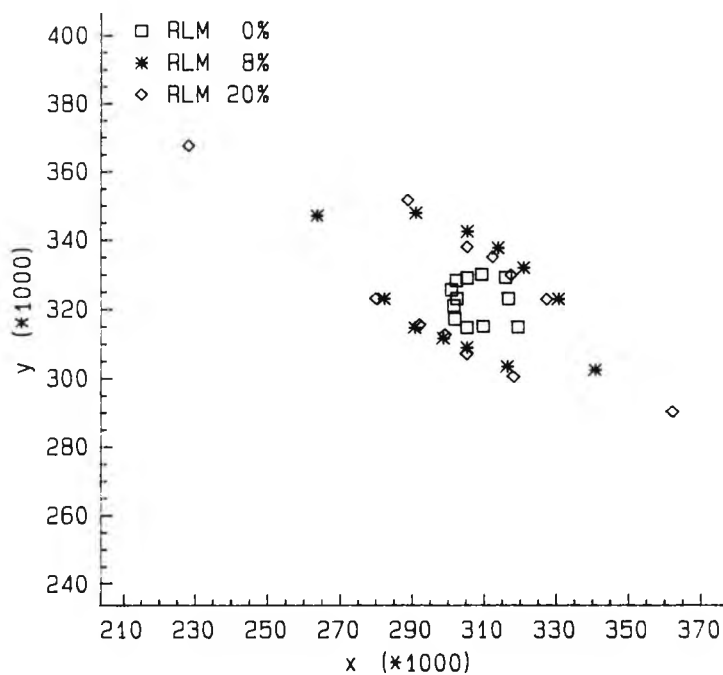


Figure 5.2. The effect of RLM amplitude on chromatic discrimination thresholds in a normal trichromat. Data are plotted in CIE x,y-chromaticity space. The luminance of the background field was 34 cd/m² and its chromaticity is shown by the central filled square. The results show that the RLM has little effect on chromatic discrimination thresholds. The smooth continuous line represents the "best fit" ellipse.

(A) Deuteranope AG



(B) Protanope HP

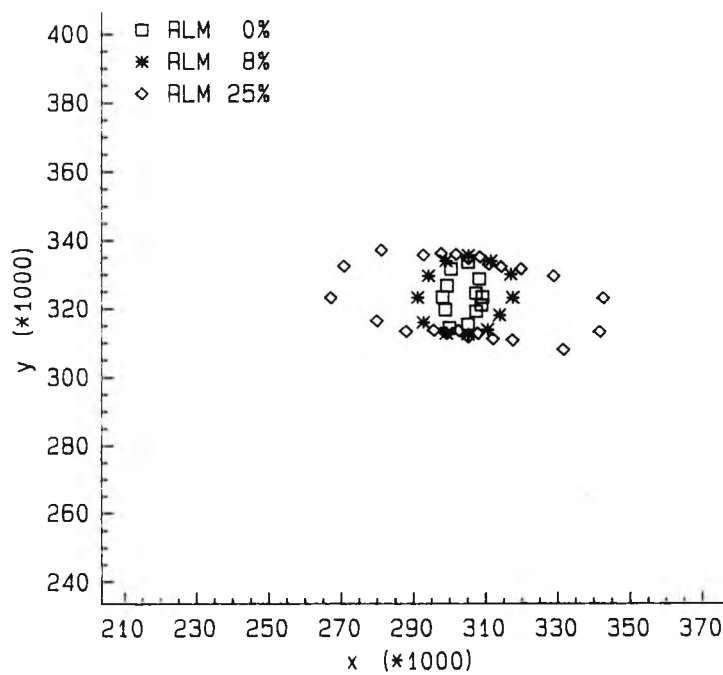


Figure 5.3. The effect of RLM amplitude on chromatic discrimination thresholds in dichromats. Data is presented for (A) a deuteranope, (B) a protanope and (C) a tritanope (overpage). The isochromatic regions revealed for the larger amplitudes of RLM correlate well with classical colour confusion lines. Continued

(C) Tritanope JF

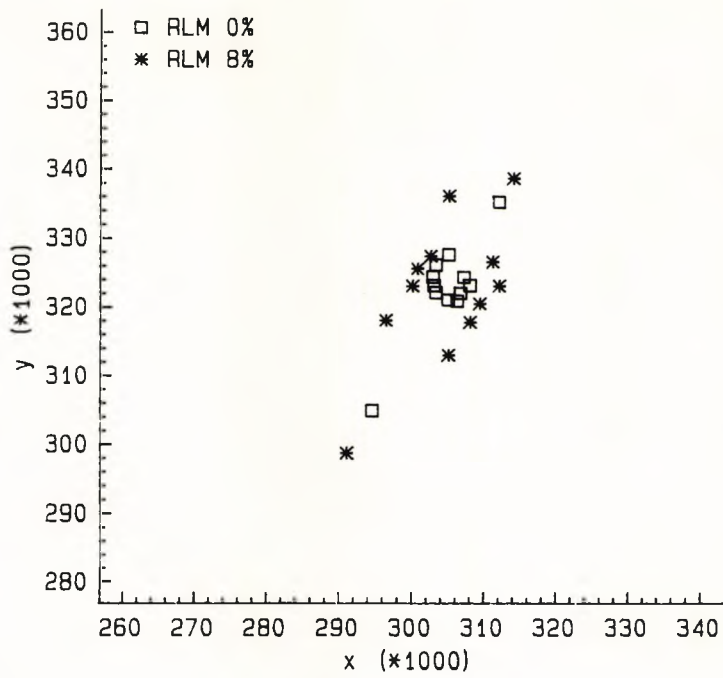
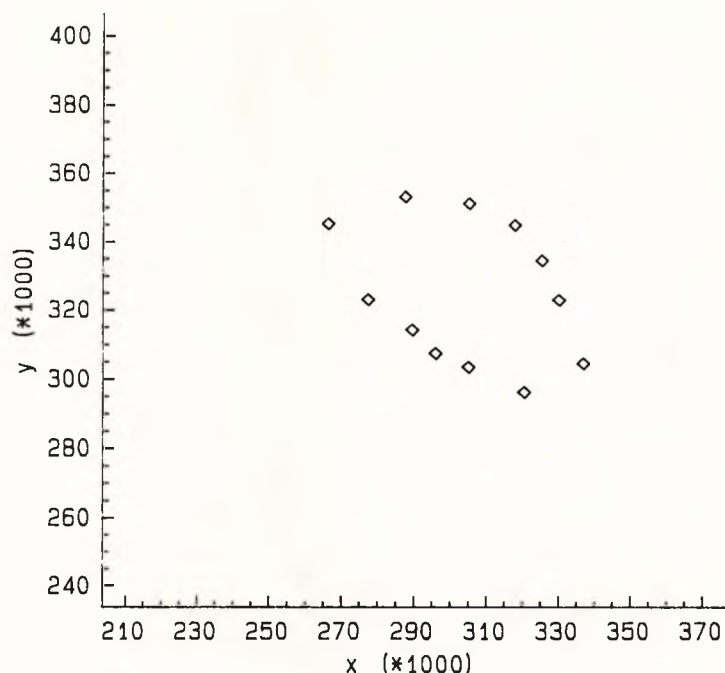


Figure 5.3. (C) The effect of RLM amplitude on chromatic discrimination thresholds in a tritanope.

(A) Deuteranomalous RP



(B) Protanomalous H0

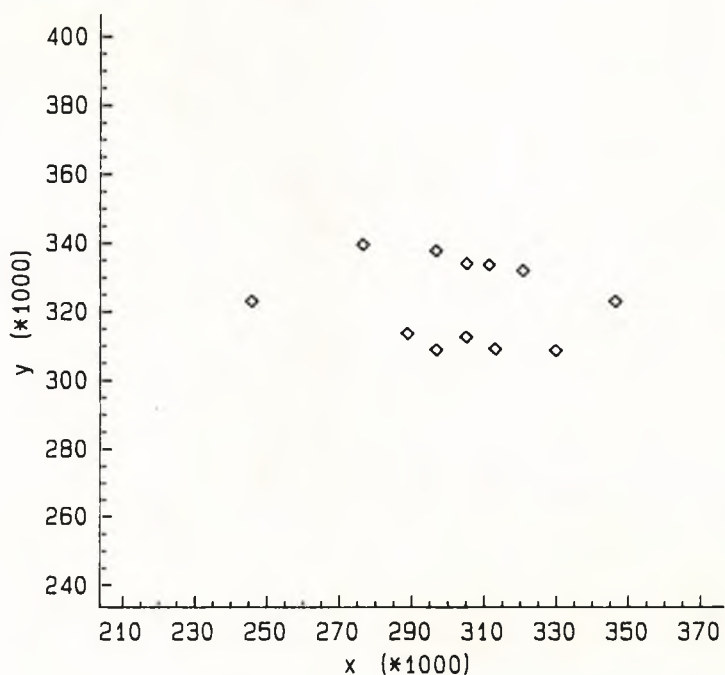


Figure 5.4. Chromatic discrimination thresholds in anomalous trichromats for a RLM amplitude of 20%. Data is presented for (A) a deuteranomalous subject, and (B) a protanomalous subject. The orientation of the ellipses which best fit the data points correlate well with the classical confusion lines.

confusion lines are 171° , 147° , and 67° for protan, deutan and tritan observers respectively (computed from data provided by Birch, 1985).

CLASS	SUBJECT	BEST FIT ELLIPSE PARAMETERS		
		Orientation	Major semi axis	Minor semi axis
Normal Trichromats	J.B.	64°	0.0093	0.0037
	M.P.	65°	0.0196	0.0055
	R.R.	65°	0.0070	0.0031
Deutans	A.G.	149°	0.0636	0.0133
	A.L.	149°	0.0298	0.0068
	G.C.	142°	0.0474	0.0221
	R.P.*	143°	0.0387	0.0184
Protans	H.P.	171°	0.0360	0.0136
	S.A.	177°	0.0320	0.0117
	D.B.	171°	0.0518	0.0151
	H.O.*	176°	0.0446	0.0112
Tritan	J.F.	61°	0.0170	0.0038
Mixed Protan/ Deutan	F.N.	166°	0.0365	0.0114

Table 5.1. Best fit ellipse parameters for each subject. Subjects marked with an asterix are anomalous trichromats.

DISCUSSION

The colour difference required to enable detection of a foveally located stimulus from its surroundings has been extensively studied by MacAdam (1942). MacAdam measured the standard deviations associated with repeated colour matches for numerous sample colours and showed that they could be related to the "Just Noticeable Difference" in colour (JND). In this way he found that thresholds for colour discrimination along a given direction in chromaticity space were about 3 to 5 times the measured standard deviation. Figure 5.5 displays MacAdam's original data representing colour discrimination thresholds on the 1931 CIE chromaticity diagram, for clarity the discrimination ellipses have been enlarged such that each semiaxis represents ten JND's. The results of the present study for

normal trichromats are consistent with MacAdam's findings (MacAdam, 1942), though the measured discrimination thresholds are somewhat higher than predicted. The stimulus configuration used by MacAdam was, however, different to that used in the current study and it was found that an increase in check size and background luminance level (from 34 to 48 cd/m²) to more nearly simulate MacAdam's (1942) paradigm, resulted in thresholds which were in closer agreement.

The finding that chromatic discrimination thresholds for normal trichromats remain invariant for different amplitudes of random luminance modulation indicate that dynamic luminance noise does not affect a subject's ability to detect chromatic modulation. The technique of spatio-temporal luminance masking may therefore be used provide an efficient way of negating the small luminance artefacts produced when chromatic patterns are generated on video displays (see Barbur et al., 1992).

The extent of the isochromatic regions in colour space can be, in theory, mapped out in traditional colour discrimination experiments, and these regions would be highly correlated with the direction of the classical colour confusion lines (Pitt, 1935; Wright, 1952). In practice, however, luminance contrast clues seen by colour defective subjects make conventional techniques difficult to implement. Using the present technique it is clear that the isochromatic zones are readily measurable. The isochromatic zone for colour defective subjects increases (i.e., the major axis of the discrimination ellipse elongates) with the amplitude of the random luminance modulation applied. Thus whilst the chromatic test pattern may be isoluminant for colour normal observers, colour defective observers must obviously use luminance contrast clues to detect the presence of the stimulus when there is no luminance masking since the discrimination "ellipses" are much smaller when no dynamic luminance noise is applied. Providing the level of masking is sufficient to eliminate luminance contrast clues in colour defective observers, then the isochromatic zone

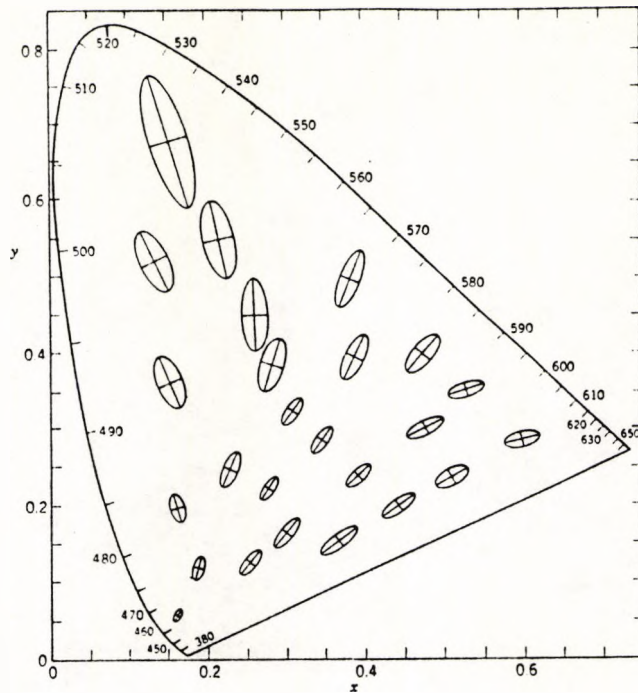


Figure 5.5. Statistical variation of chromaticity matches in different parts of the CIE x,y -chromaticity diagram. The elliptical loci correspond to chromaticities separated from the central point by the standard deviation of settings for chromaticity match. For clarity the axes of each ellipse have been enlarged 10 times. (After MacAdam, 1942).

Mixed Amblyope PD

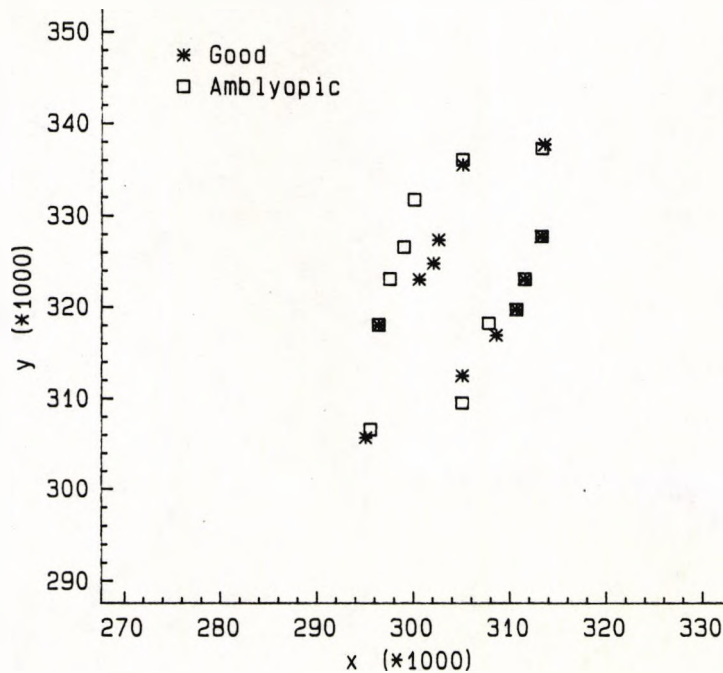


Figure 5.6. Chromatic discrimination thresholds in a mixed strabismic-anisometric amblyope with a VA of 6/24 in the affected eye. The RLM was equal to 8% of the background luminance (34 cd/m^2) and as before the background chromaticity co-ordinates were $x=0.305$, $y=0.323$. The small differences between the amblyopic eye and good eye were noted in two separate experimental sessions.

for each dichromat or anomalous trichromat may be defined by tangents to the normal discrimination ellipse in a direction corresponding to the classical colour confusion line. Whilst it was found difficult to classify one of the subjects (i.e., subject F.N.) using a battery of conventional testing procedures, this subject was more easily distinguishable as being protan using the present technique.

The technique described here may prove to be a valuable colour vision test since it allows the direct quantitative measurement of discrimination in various directions of colour space. The three parameters describing an individual's best fit ellipse may provide a useful means of accurately defining a colour vision anomaly. Whilst the time taken to determine a discrimination ellipse with 12 data points was not excessive, the procedure as it stands may still prove to be too time - consuming for certain clinical situations. An adaptation of the experimental procedure incorporating fewer test directions chosen to specifically lie on the protan, deutan and tritan confusion axes (similar to the technique used by Reffin et al., 1991) could, however, make this method particularly attractive to the clinician.

The opportunity also arose to use this technique to assess the colour vision of a colleague who was amblyopic. Using a combination of the clinical tests described in the previous chapter, this subject was diagnosed as a mixed strabismic - anisometropic amblyope, with a visual acuity of 6/24 in the affected eye and 6/5 in the normal eye. Fixation in the amblyopic eye was unsteady but foveal. Conventional colour vision testing procedures indicated that the subject had normal colour vision in each eye. Since the spatial frequency of the chromatic stimulus used was quite low, the subject had no difficulty performing the experiment when viewing with the amblyopic eye. The experiment was performed using a fixed random luminance modulation of 8% and the results obtained are presented in Figure 5.6. On the whole it would appear that chromatic discrimination in the amblyopic eye is normal but for certain angles of chromatic

displacement (between 120° and 180°), however, discrimination in the amblyopic eye is consistently, though only slightly, poorer than for corresponding angles in the normal eye. It seems unlikely that unsteady fixation was responsible for this deficit since if this were the case the expected result would have been increased discrimination thresholds for all angles of chromatic displacement.

The relatively few studies that have previously investigated chromatic processing in cases of human amblyopia have mainly been restricted to the measurement of increment threshold spectral sensitivity functions. Harwerth and Levi (1977), for example, have shown that anisometropic amblyopes exhibit reduced sensitivity in the yellow region of the visible spectrum when viewing with their amblyopic eyes. This loss of sensitivity, they proposed, reflects some dysfunction of the red - green opponent colour mechanism. Application of the subtractive interaction model proposed by Sperling and Harwerth (1971) to describe increment threshold spectral sensitivity data, led Harwerth and Levi to suggest that excessive inhibition of the green cones by the red cones was responsible for the lowered sensitivity observed for amblyopic eyes. A similar explanation could be pertinent to the results of the present study, since the observed reduction in chromatic discrimination occurs for stimuli of similar chromatic content. In addition to increment threshold measurements, Marré and Marré (1979) have compared spectral hue discrimination in the amblyopic eyes and fellow normal eyes of strabismic subjects. They found that the spectral sensitivity for hue discrimination was generally poorer for amblyopic eyes over the whole visible spectrum and that the extent of the deficit was dependent upon the magnitude of eccentric fixation, subjects with central fixation sometimes displaying normal hue discrimination functions. Data presented for one of their subjects with central fixation shows that sensitivity was particularly lowered for stimuli with wavelengths between about 530 and 560 nm, a finding which again is not inconsistent with the result of the present study. Inspection of Marré and Marré's data, however, does indicate a large degree of inter -

subject variability and this suggests that the examination of a large population of amblyopes is required before any conclusions about chromatic processes in amblyopia can be drawn.

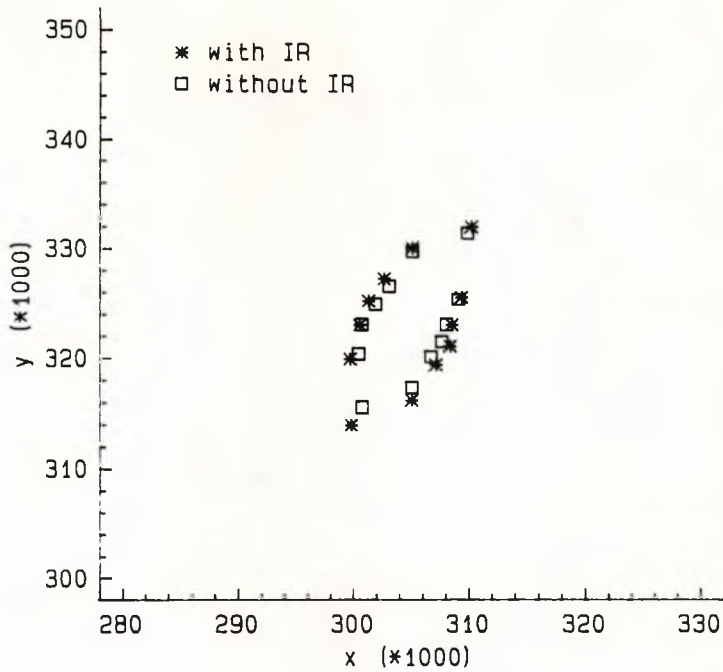
5.2 THE CHROMATIC PUPIL RESPONSE AND SPATIO - TEMPORAL LUMINANCE MASKING

The need to generate chromatic patterns without incurring luminance artefacts is even more important when such patterns are to be used to evoke pupillary responses, since the pupil is particularly sensitive to luminance modulation (see Chapter 4). It has already been shown in the previous section that, for psychophysical studies, spatio - temporal luminance masking provides an efficient way of eliminating unwanted luminance artefacts associated with the generation of chromatic stimuli. A preliminary investigation was therefore undertaken to determine the effectiveness of this masking technique in studies of the chromatic pupil response with a view to the development of an objective colour vision test.

PROCEDURE

The stimuli used to elicit pupil colour responses were identical to those described in the previous section where chromatic discrimination thresholds were measured psychophysically. The P_SCAN 100 pupillometer described in Chapter 2 was used to measure any pupillary responses elicited by the stimuli. It will be recalled from Chapter 2 that when using this system, the subject views the monitor through a large infra - red (IR) reflecting mirror. In order to verify that this mirror did not modify the spectral content of the stimulus, discrimination thresholds were determined for two subjects with, and without the mirror in place. The results of this preliminary experiment are shown for two subjects in Figure 5.7. It can be seen that the effect of the mirror is minimal with thresholds remaining virtually unaltered. This was also found to be the case for the second subject.

(A) Subject JB



(B) Subject HP

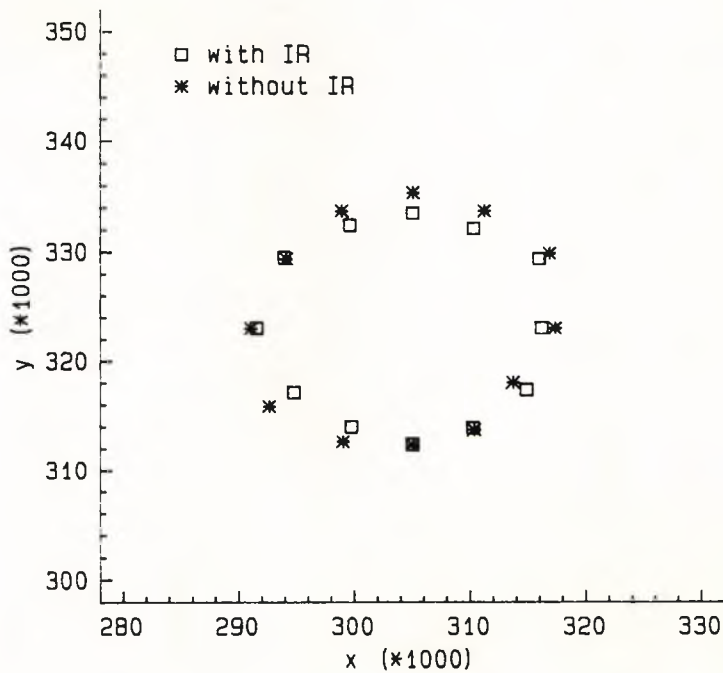


Figure 5.7. Chromatic discrimination thresholds plotted for observations made with and without the infra-red absorbing mirror required by the P_SCAN pupillometer. Data is shown for two subjects (A) JB, a normal trichromat, and (B) HP, a protanope. The results show that the mirror has little or no effect on the discrimination thresholds.

The amplitudes of pupillary constriction elicited by chromatic stimuli are generally quite small and therefore 64 responses to each stimulus condition were averaged. The parameter variable in each experiment was either the amplitude of chromatic displacement along a fixed direction in colour space, or the displacement angle for a fixed chromatic displacement.

RESULTS

Figure 5.8 displays pupil traces for a normal trichromat for a range of stimulus chromatic displacements from 0.01 to 0.06 at 0.01 intervals. Note that for clarity of presentation each trace has been separated vertically by 0.1 mm. The angular direction of chromatic displacement was fixed and was chosen to coincide with the deutan confusion line. Throughout the experiment the random luminance modulation was constant and equal to 20% of the background luminance. It is clear that pupillary constrictions are obtained for all stimulus conditions with an increase in response amplitude accompanying an increase in chromatic displacement. Similar results were obtained when the angle of chromatic displacement was changed so as to lie along other directions in colour space.

The pupil colour response was also investigated in a group of dichromats. For these subjects the amplitude of chromatic displacement was fixed (at a point well above threshold for the normal trichromat) and the angular direction of displacement was chosen to lie along each of the colour confusion lines determined from the previous psychophysical study. The depth of random luminance modulation was increased to 35% to ensure that any luminance contrast components in the chromatic pattern could not be detected. Typical results for each class of dichromat are presented in Figures 5.9 (A), (B) and (C). It would seem that when the chromatic displacement occurs along a direction in colour space which coincides with the colour confusion axis for a

Normal Trichromat JB

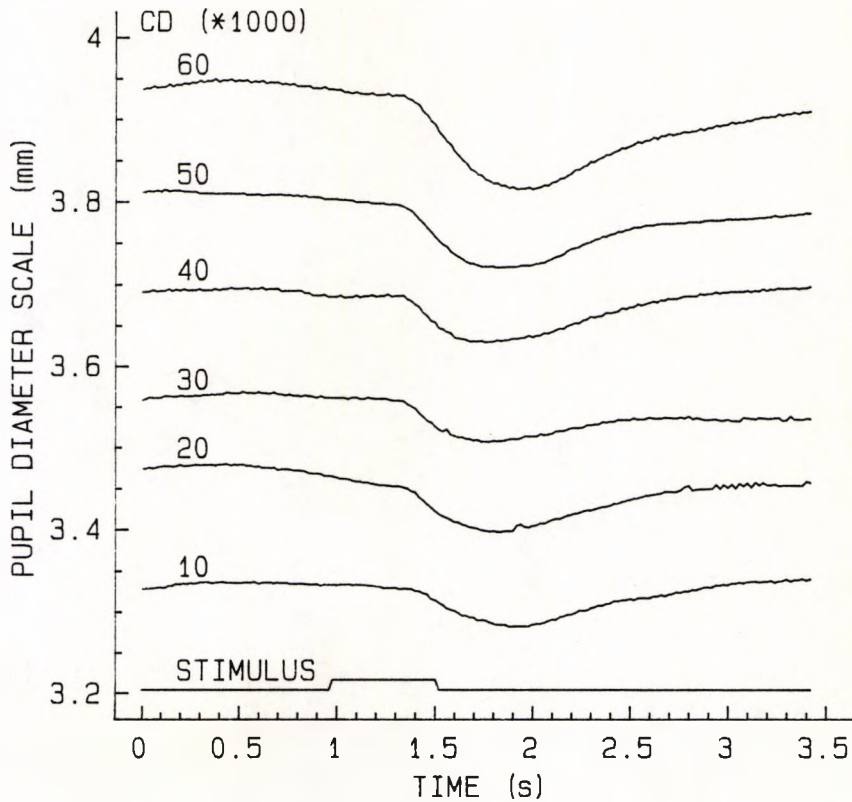


Figure 5.8. Pupil responses to the chromatic stimulus described in the text. Data are shown for a normal trichromat for several values of chromatic displacement (CD) along the deutan confusion line. The lowest trace shows the true pupil diameter (CD=10) whilst for clarity, the remaining traces have been shifted in 0.1 mm vertical steps. The RLM was constant at 20% of the background luminance (34 cd/m^2). The x,y-chromaticity co-ordinates of the background field were 0.305, 0.323.

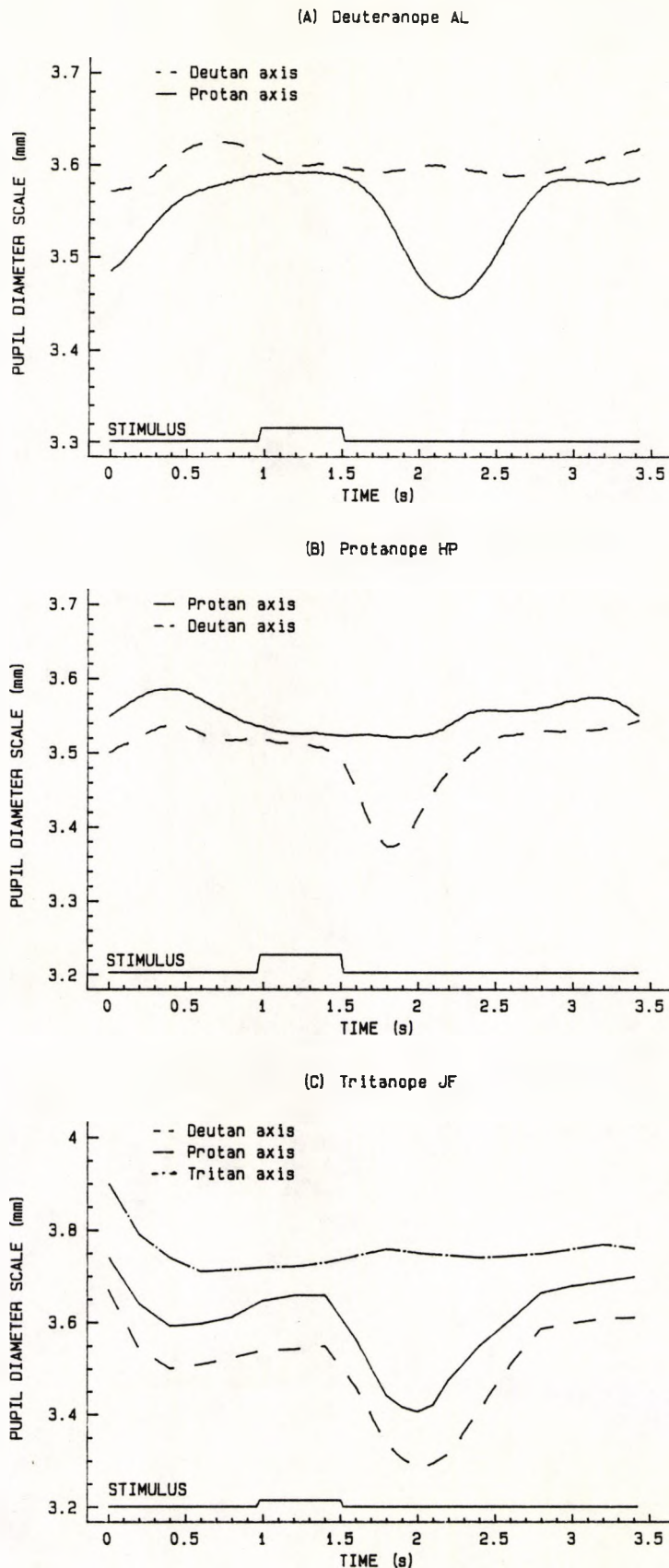


Figure 5.9. Measurements of pupillary responses to the luminance-masked chromatic stimulus described in the text. Data are shown for a representative deuteranope (A), protanope (B), and tritanope (C). The stimulus angular displacements were chosen to lie along the deutan, protan or tritan colour confusion lines. The RLM was fixed at 35%. For clarity traces have been shifted vertically.

particular class of dichromat, then the pupil of that particular dichromat fails to respond.

DISCUSSION

Pupillary responses to coloured grating patterns have been described in the previous chapter, and the requirement for true, isoluminant stimuli was stressed. The technique described here obviates the use of isoluminant chromatic stimuli and the need to make individual adjustments to set isoluminance. It has been shown that the response of the pupil to chromatic test patterns reflects psychophysical observations of the same patterns and that the definitive colour confusion axes of dichromatic subjects also apply to the pupillary reflex pathway.

The results of this preliminary pupillometric study are encouraging but a more detailed study incorporating a larger population of subjects and a greater number of stimulus parameters is required before the technique can be developed into a reliable and accurate objective colour vision testing procedure. Furthermore, the pupillometric test as it stands is still somewhat time - consuming when one envisages its use in the clinical environment for the assessment of non - verbal adults (often mentally handicapped) and infants. With the advent of faster processors and / or the development of specific hardware, the lengthy stimulus generation procedure could be shortened and this would help to reduce test - time considerably. It seems likely, however, that a large number of traces will always be required because the pupil colour response is small and has to be extracted from the much larger, random pupillary fluctuations (though this has never been a major setback in clinical electrophysiology).

CHAPTER 6

SOME MEASUREMENTS ON THE CHANGES IN VISUAL SENSITIVITY CAUSED BY INTENSE FLASHES OF LIGHT

INTRODUCTION

It is well - established that increment thresholds for detection of isolated light flashes depend largely on the background retinal illuminance level to which a subject is adapted. In the past a number of psychophysicists have investigated the relationship between the just - noticeable luminance change (δL), and the luminance of a large concentric background field (L). This relationship has been described by Weber (see Davson, 1980) who found that the increment threshold change is a constant percentage of the background luminance (i.e., the ratio $\delta L / L$ is a constant). Weber's law works well for an intermediate range of luminance levels and in the presence of steady background fields, but changes in visual sensitivity during flashes of light cannot be accounted for by a simple law and are more difficult to investigate experimentally.

Crawford (1947) was amongst the first to show convincingly that when the luminance of an adapting field is suddenly increased by the onset of a bright conditioning stimulus, the threshold of a superimposed test does not simply increase in proportion with the background, but rather changes in a much more complex manner. In fact, Crawford (1947) found similarly complex and unexpected changes to occur when the conditioning stimulus was switched off. Crawford's early observations were later confirmed, but little extended, by several other investigators including Baker (1953) and Boynton et al. (1954). In general these workers found that the sudden onset of a conditioning stimulus caused test threshold to increase rapidly to a level above that which is later achieved following a longer period of adaptation to the conditioning stimulus. After reaching a maximum value at, or around, the time of onset of the conditioning stimulus, the threshold for detection of

the test stimulus falls gradually and eventually reaches a steady - state value. Just before the time of offset of the conditioning stimulus, test threshold rises slightly, before falling to the final steady - state value which is largely determined by the background luminance level. The transient changes in test threshold which occur at the onset and offset of a conditioning stimulus have been referred to as "on responses" and "off responses" (Ikeda and Boynton, 1965) and the interaction between the two stimuli has become known as visual or "Crawford" masking (Alexander and Barry, 1981). Backward visual masking is said to occur when the masking stimulus (i.e., the conditioning stimulus) raises the detection threshold of a preceding test stimulus. The interval between the onsets of the test and conditioning stimuli is normally termed the "stimulus onset asynchrony" (SOA), with a negative SOA indicating that the test stimulus was presented before the conditioning stimulus. The effects observed by Crawford (1947) should be distinguished from the analogous phenomena of metacontrast (see Weisstein, 1972) and the contrast - flash effect (Alpern and Rushton, 1967). In metacontrast paradigms, the conditioning stimulus is spatially remote from the test stimulus. In the contrast - flash effect, the conditioning stimulus consists of a spatially - contiguous, but non - overlapping annulus. Both metacontrast and the contrast - flash effect are presumed to be mediated mainly by lateral inhibition at the retinal level (see also Breitmeyer and Ganz, 1976 and Breitmeyer, 1984, for a review of visual pattern masking).

In his early experiments, Crawford (1947) varied only the retinal illuminance level of the conditioning stimulus. The aim of the research described in this chapter was to extend Crawford's original findings by examining the effect of several other stimulus parameters on test thresholds using improved experimental equipment and techniques. To this end, thresholds were measured using a procedure which incorporated a series of randomly interleaved, multiple staircases (see Chapter 2 section 3), the staircase variable being one of the following: (i) the presentation time of the test stimulus with respect to the conditioning stimulus;

(ii) the spatial location of the test stimulus with respect to the centre of the conditioning stimulus; or (iii) the spectral wavelength of the test stimulus.

PROCEDURE

All measurements were carried out using the three - channel Maxwellian view optical system described in Chapter 2. Subjects viewed a small fixation target at the centre of a large, 44° diameter, uniform background field, the retinal illuminance of which was normally fixed at 2 log trolands. An adaptation period of at least 3 minutes was allowed before any measurements were taken. The stimulus configuration employed in most of the experiments to follow is illustrated schematically in Figure 6.1. The conditioning stimulus consisted of a uniform disc, the diameter and retinal illuminance of which could be varied by the manual insertion of the appropriate apertures and neutral density filters respectively (see Chapter 2). The duration of the conditioning stimulus was controlled by computer via a digitimer, and during the course of the experiments, was varied between 100 and 1000 ms. Increment thresholds for the detection of a small (0.5° diameter), brief (10 ms), test stimulus were measured at discrete times before, during, and after the presentation of the conditioning stimulus (see Figure 6.2). Up to 24 test stimulus presentation times were employed. To allow sufficient time for recovery to a steady - state of adaptation following the conditioning stimulus presentation, an 8 second delay between consecutive test stimulus presentations was employed. The geometric centres of the test and conditioning stimuli were spatially coincident with one another and also with the fixation target for foveal measurements. A typical experiment lasted approximately 60 minutes.

The effects of modifying certain parameters of the conditioning stimulus and background were investigated in a series of experiments. Thus, test increment thresholds were measured for a range of conditioning stimulus retinal illuminance levels (experiment 1), durations (experiment 2),

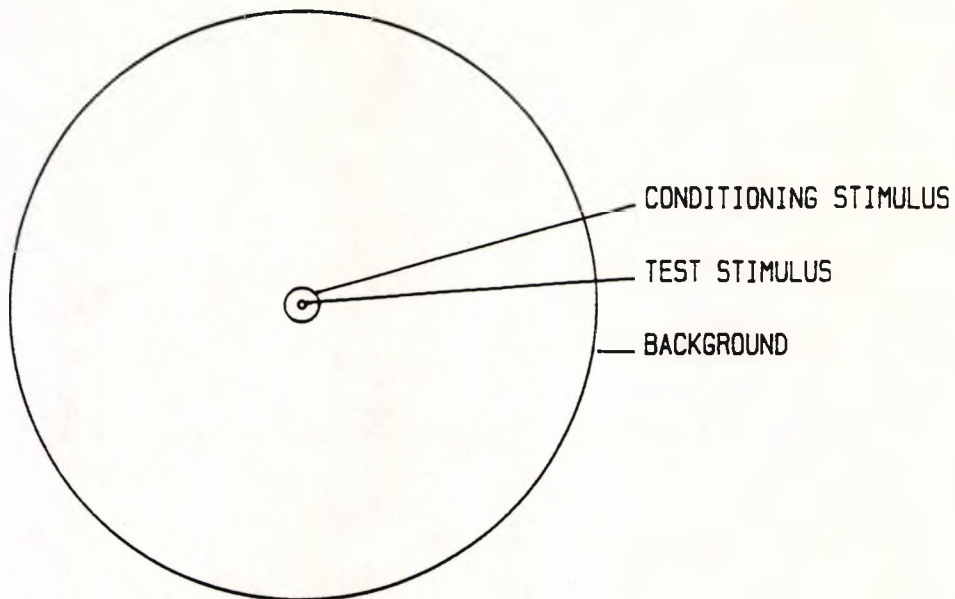


Figure 6.1. Representation of stimulus configuration. The test stimulus subtended a visual angle of 0.5° and was presented against a large uniform background field of 44° diameter. The conditioning stimulus consisted of a uniform disc, the diameter of which was under experimental control.

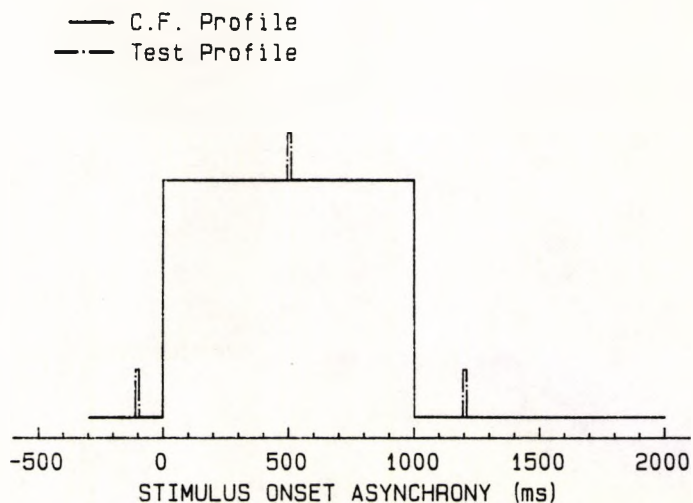


Figure 6.2. The diagram shows the temporal profile of the test and conditioning stimulus (C.F.). The 10 ms test stimulus was presented at discrete times before, during and after the conditioning stimulus. The stimulus onset asynchrony indicates time relative to conditioning stimulus onset. Both test and conditioning stimulus were presented against a background of fixed retinal illuminance level.

and sizes (experiment 3), both foveally and at an eccentricity of 6° in the nasal visual field (specific details of the parameters employed are given in the following results section). In order to investigate the importance of the level of steady - state adaptation, and also the significance of stimulus contrast, detection thresholds were measured for a range of background retinal illuminance levels using a conditioning stimulus of fixed intensity (experiment 4). Each stimulus condition in all the experiments was investigated in a separate session.

In order to determine the spatial extent of any sensitivity changes caused by the conditioning stimulus, increment thresholds for detection of a 0.33° , 10 ms test stimulus were measured at discrete spatial locations with respect to a 1° , 500 ms conditioning stimulus (experiment 5). Test thresholds were determined at 13 different eccentricities along the horizontal meridian up to 6° away from the centre of the conditioning stimulus. The conditioning stimulus was positioned either foveally or at an eccentricity of 6° and had a fixed retinal illuminance level of 4.6 log trolands. A test delay time (i.e., SOA) was designated at the beginning of each experimental session such that in any one session the test stimulus occurred at a single specific time relative to the conditioning stimulus. SOA's of -40, -20, 0, +20, +40, +200, +460, +480, +500, +520, and +540 ms were chosen, where conditioning stimulus onset and offset occurred at $t = 0$ and $t = +500$ ms respectively. Once again a randomly interleaved, multiple staircase procedure was used where test eccentricity was interleaved with test retinal illuminance level. For comparison purposes, measurements of detection thresholds as a function of eccentricity were also made in the absence of the conditioning stimulus. Threshold measurements taken with, and without the conditioning stimulus, were made in the same session and a typical experiment lasted approximately 80 minutes.

In the final experiment (experiment 6) to be reported here, the spectral wavelength of the test stimulus was interleaved with retinal illuminance level for a fixed test presentation

time and location. Since the maximum retinal illuminance level obtainable with the test channel was necessarily lowered by interposition of interference filters (see Chapter 2 section 3), a relatively low conditioning stimulus illuminance level of 2.5 log trolands was chosen for the experiment. Three SOA's were employed in three separate experimental sessions such that the test was presented at $t = 0, +500, \text{ or } +960 \text{ ms}$. In this way test spectral sensitivity could be measured in the presence of the conditioning stimulus, and also at the onset and offset of the conditioning stimulus.

The majority of experiments were carried out with at least two subjects (H.P. and J.B.), though the principle findings were confirmed with one of three other subjects (J.T., P.F., and A.W.). All subjects had normal colour vision (assessed using the Ishihara and Farnsworth - Munsell 100 - Hue tests) apart from one subject, H.P., who demonstrated protan defects. In addition one strabismic amblyope, subject H.H., participated in experiment 1. The subjects' ages ranged from 18 to 34 years, and H.P., and J.T., were myopic, whilst J.B., P.F., A.W. and H.H. were emmetropic. Suitable adjustment of the object plane position for each of the three channels allowed for the correction of any individual refractive error. Accordingly the resting state of accommodation was established for each subject. All measurements were carried out monocularly with the right eye viewing.

RESULTS

Figures 6.3 (A) and (B) show the results of the first of the above the experiments for a single representative subject, H.P.. In both figures, and in virtually all of those to follow in this section, the ordinate indicates the incremental test threshold retinal illuminance level (in log trolands) and the abscissa represents the test target SOA value (in milliseconds). The onset and offset of the 1.25° conditioning stimulus thus occurred at times $t = 0 \text{ ms}$ and $t = +1000 \text{ ms}$ respectively. Data are presented for four

conditioning stimulus retinal illuminance levels, for both foveal (Figure 6.3 A) and peripheral (Figure 6.3 B) locations in the visual field. In this experiment the test and conditioning stimulus were spatially coincident for both foveal and peripheral measurements. Note that the data plotted in the two figures refer to different conditioning stimulus retinal illuminance levels.

The data presented in these figures show that test thresholds begin to rise some 100 ms before the onset of the conditioning stimulus (this is backward masking), with the maximum increase in threshold generally occurring simultaneously with conditioning flash onset. The single subject data suggest that threshold maxima may occur at slightly earlier times relative to flash onset for conditioning stimuli of high retinal illuminance. This observation was confirmed for all other subjects who took part in the experiments. The peak thresholds tended to occur 20 ms before flash onset for conditioning stimuli with retinal illuminances greater than about 4.3 log trolands.

It may be seen from Figure 6.3 (A) that the peak threshold level, or on response, increases monotonically with the retinal illuminance level of the conditioning stimulus. Although it appears that the magnitude of the on response obtained with the 5.4 log troland conditioning stimulus is not as large as that predicted on the basis of the previous statement, it should be remembered (from the technical data presented in Chapter 2 section 3) that the maximum obtainable retinal illuminance level in the test channel was 5.95 log trolands. Consequently, for this particularly intense conditioning stimulus, the subject was unable to increase the test stimulus retinal illuminance level sufficiently for it to be detected clearly against the bright conditioning flash. Recovery to a steady - state of adaptation following the onset of the conditioning stimulus appears to be largely completed within about 500 ms. This observation was confirmed in a separate experiment using a long duration (6 second) conditioning stimulus in which the offset of the conditioning stimulus was less likely to

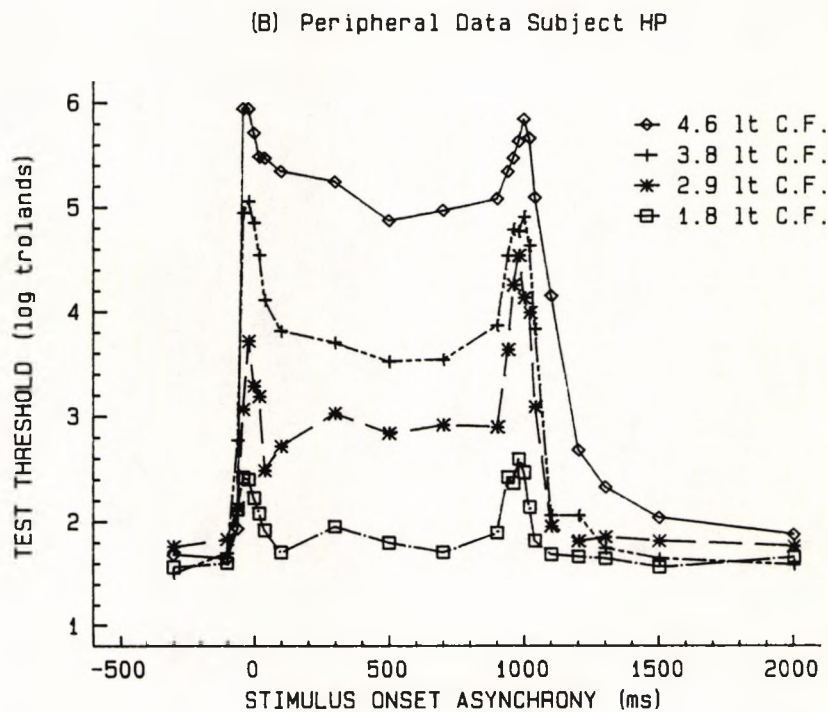
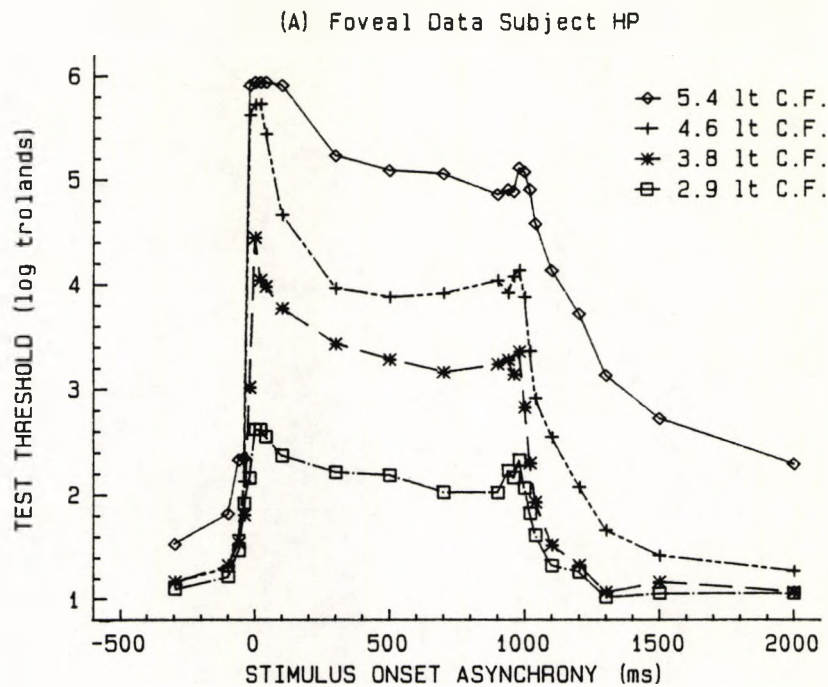


Figure 6.3. The increment threshold retinal illuminance for detection of a small (0.5°), brief (10 ms) test stimulus is plotted as a function of stimulus onset asynchrony for one representative subject HP. Data is presented for four conditioning stimulus (C.F.) retinal illuminance levels for measurements made (A) at the fovea and (B) at an eccentricity of 6° . The conditioning stimulus was 1.25° in diameter and 1000 ms duration and its onset and offset occurred at $t=0$ and $t=1000$ ms respectively. The geometric centres of test and conditioning stimulus were spatially coincident and both were presented against a background of retinal illuminance 2.0 log trolands.

influence the thresholds measured around flash onset (see below).

A small threshold rise, which peaks on average some 20 to 40 ms before the offset of the conditioning stimulus, is also seen to occur (see Figure 6.3 A). Unlike the on response, this off response, which measures about 0.2 log units in magnitude, does not appear to vary systematically with the retinal illuminance level of the conditioning stimulus. The return of the test threshold back to the background level of adaptation following the offset of the conditioning stimulus appears to be complete in approximately 300 ms for the two lower intensity stimuli. For the two high intensity conditioning stimuli (i.e., the 4.6 and 5.4 log troland flashes), however, extended recovery times are observed, neither threshold having returned completely to the background steady - state up to as much as one second after the extinction of the conditioning flash.

The observations made for foveal measurement of threshold increments also apply in general to the same measurements made in the periphery (see Figure 6.3 B). The most striking difference, however, relates to the magnitude of the peripheral off response, which is consistently much larger than that obtained at the fovea. For example, the magnitude of the off response for the 2.9 log troland conditioning stimulus measures about 1.5 log units, whereas for the same condition at the fovea, the off response measures only 0.2 log units. A comparison of measurements made for the 3.8 log troland conditioning stimulus at the fovea and at 6° in the periphery is shown in Figure 6.4. It may be seen that the on response for peripheral stimulus presentation differs only slightly from that obtained for the corresponding foveal presentation in that it generally peaks some 20 ms earlier. It is also clear from this figure that the overall threshold sensitivity for measurements made in the periphery is lower than for those made at the fovea. In order to verify that this was simply due to a difference in the absolute sensitivity of the fovea and the periphery, and not due to some long - lasting adaptation that occurs in the periphery

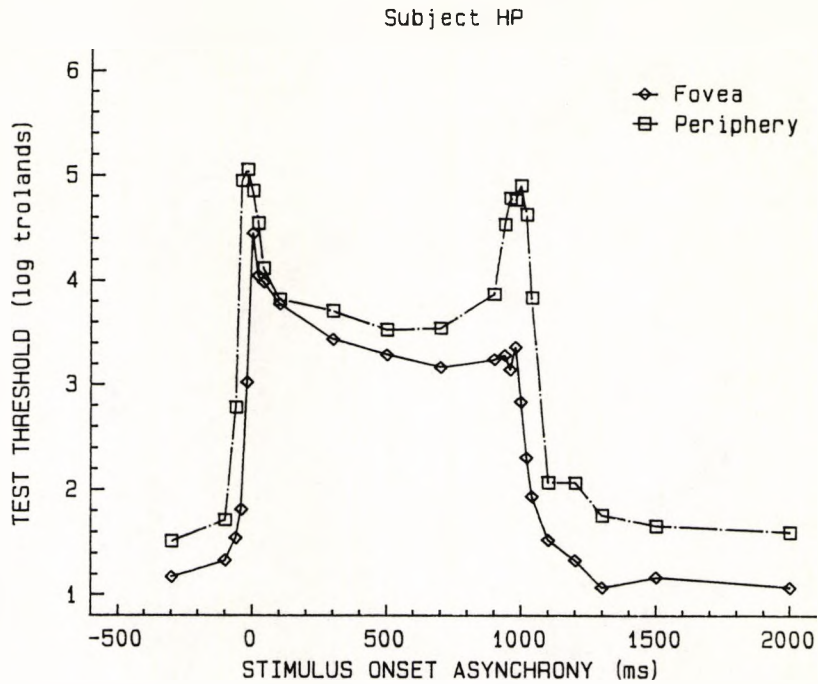


Figure 6.4. The increment threshold retinal illuminance for detection of a test stimulus plotted with respect to its onset asynchrony with a 3.8 log troland conditioning flash. A comparison of data is shown for one subject (HP) for measurements made at the fovea, and at an eccentricity of 6°. Stimulus parameters were as given in Figure 6.3.

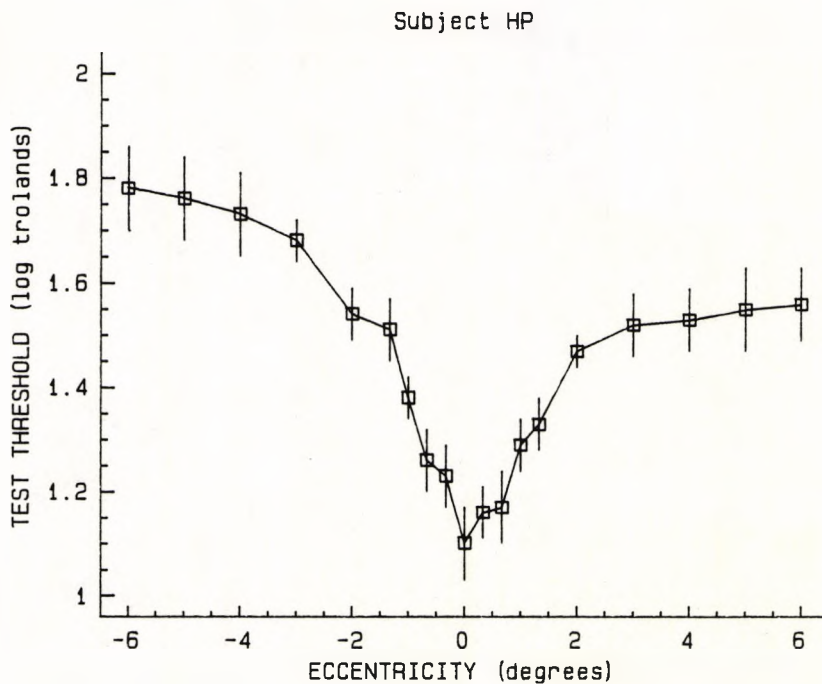


Figure 6.5. The increment threshold retinal illuminance for detection of a test stimulus plotted as a function of eccentricity. The 0.5°, 10 ms test stimulus was presented against a large uniform background field of diameter 44° and retinal illuminance 2.0 log trolands. Negative eccentricities indicate that the test was presented in the nasal visual field. Error bars represent ± 1 standard deviation.

with repeated presentations of the conditioning stimulus, test increment thresholds were determined in the absence of the conditioning stimulus for a series of retinal locations. The results of these measurements (see Figure 6.5) show that for a 0.5° test stimulus, the difference between threshold detection values at the fovea and at a location 6° in the periphery, can differ by as much as 0.6 log units (see also Barbur et al., 1986).

The corresponding data obtained with the amblyopic subject, H.H., are shown in Figure 6.6 for observations made 6° in the periphery using a 3.8 log troland conditioning stimulus. Comparative data are also shown for a non - amblyopic subject (A.W.) using identical stimulus parameters. It is evident that the on response is almost completely absent in the amblyopic subject, although the off response appears to be of normal magnitude.

The effect of shorter conditioning stimulus durations on detection thresholds is shown in Figures 6.7 (A) and (B) for subject H.P.. Foveal data are shown in Figure 6.7 (A) for a 4.9 log troland conditioning stimulus, and peripheral data are shown in Figure 6.7 (B) for a 4.3 log troland stimulus. The foveal data show a loss of the off response for flash durations less than 500 ms, though a small inflection at a time corresponding to flash offset may still be seen for the two shorter duration conditioning stimuli. The recovery rates following the offset of the conditioning stimulus appear to be independent of flash duration. Interestingly, the corresponding data for the periphery shows that the off response remains marked even for the shortest duration stimulus employed, although it can be seen that the temporal extent of the response is reduced for the shorter duration flashes. Furthermore, the magnitude of the off response for the periphery is greatest for the longest duration stimulus employed (i.e., 700 ms) and an inspection of Figure 6.3 (B) indicates that the magnitude of the off response is greater still for the 1000 ms conditioning stimulus used previously.

Figures 6.8 (A) and (B) show the results of experiment 3 for

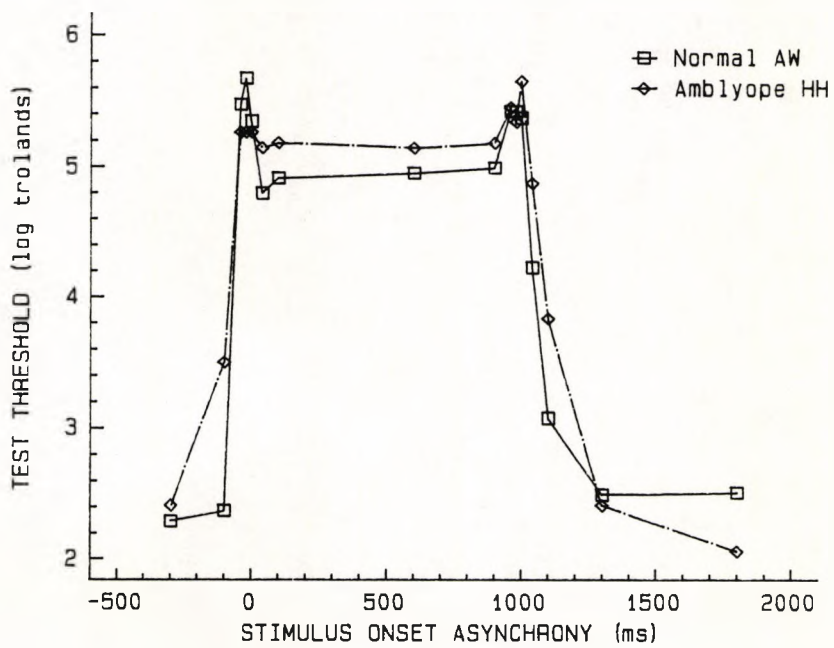
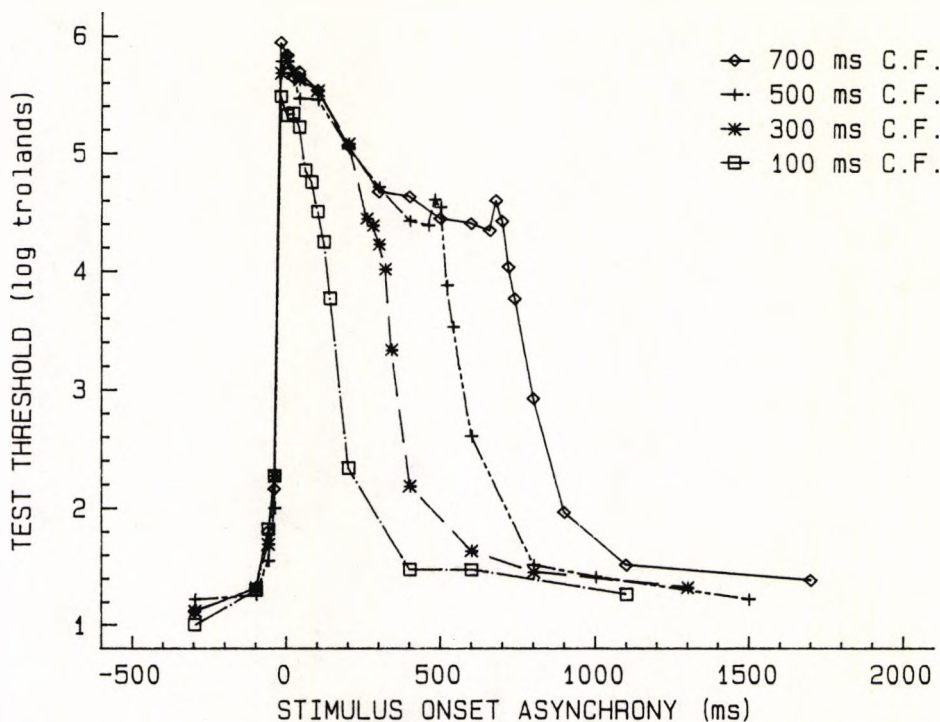


Figure 6.6. Test increment threshold is plotted as a function of stimulus onset asynchrony for a strabismic amblyopic (HH), and a normal subject (AW). Measurements were made at an eccentricity of 6° using a conditioning stimulus of retinal illuminance 3.8 log trolands. Stimulus parameters were otherwise as given in Figure 6.3.

(A) Foveal Data Subject HP



(B) Peripheral Data Subject HP

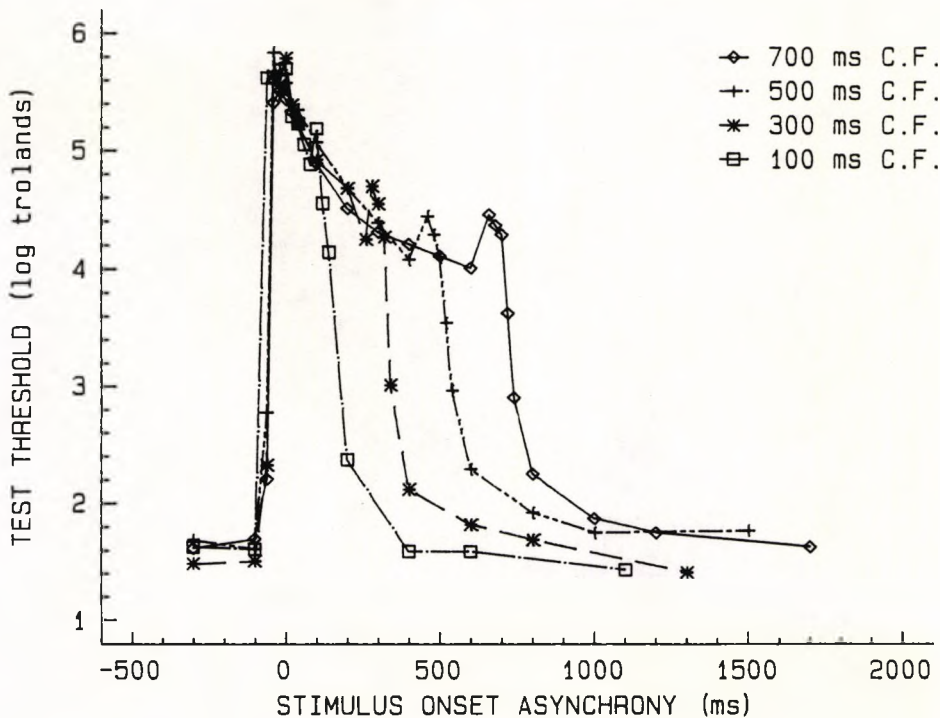


Figure 6.7. Test increment threshold is plotted as a function of stimulus onset asynchrony for four conditioning stimulus durations. Data are presented for (A) foveal measurements using a conditioning stimulus of 4.9 log tds and (B) measurements made at an eccentricity of 6° with a conditioning stimulus of 4.3 log tds. (Test 0.5° and 10 ms; conditioning stimulus 1.25° ; background 2.0 log tds).

a range of conditioning stimulus diameters from 0.8 to 4.8°. For both foveal and peripheral data, the retinal illuminance level of the conditioning stimulus was constant at 3.8 log trolands. The foveal data (Figure 6.8 A) show that detection thresholds in the presence of the conditioning stimulus are relatively elevated for smaller diameter stimuli. A small increase in the magnitude of the off response is seen for the smallest diameter conditioning stimulus used (i.e., 0.8°). The corresponding data for the periphery (Figure 6.8 B) similarly shows elevated thresholds for the smaller diameter conditioning stimulus, but the most striking feature of this figure is the markedly reduced off response for the largest diameter conditioning stimulus.

The results of experiment 4 for peripheral observations are displayed in Figure 6.9. Data are presented for four background illuminance levels ranging from 1.1 to 3.8 log trolands. Detection thresholds for test stimuli presented well before, or well after the conditioning stimulus, vary as predicted by Weber's law. The magnitude of the on response (relative to the adaptation level achieved shortly after in the presence of the conditioning stimulus) appears to be largely unaffected by the level of background illumination. In contrast, however, the magnitude of the off response is increased as the background retinal illuminance level approaches that of the conditioning stimulus.

The spatial extent of the desensitising effects of the conditioning stimulus investigated in experiment 5 is shown in Figures 6.10 and 6.11 for foveal and peripheral presentation of the conditioning stimulus, respectively. Detection thresholds are plotted as a function of test eccentricity with respect to the conditioning stimulus. The square symbols represent data obtained in the presence of the conditioning stimulus, whilst the diamonds show thresholds measured in the absence of the conditioning stimulus. Each graph displays the data obtained for a specific test presentation time, again with respect to the conditioning stimulus. Not unexpectedly, test threshold is always greatest when the test stimulus is spatially

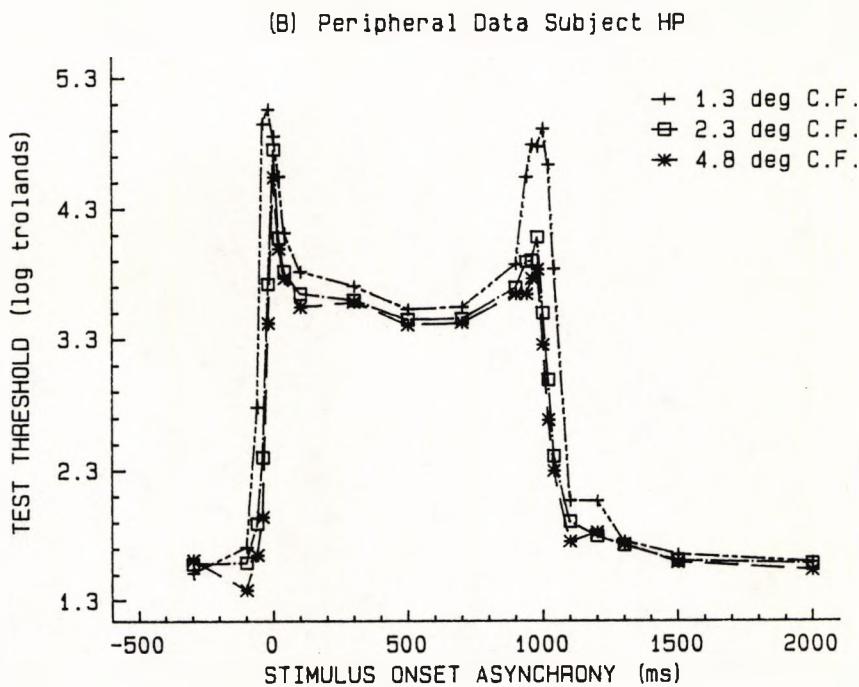
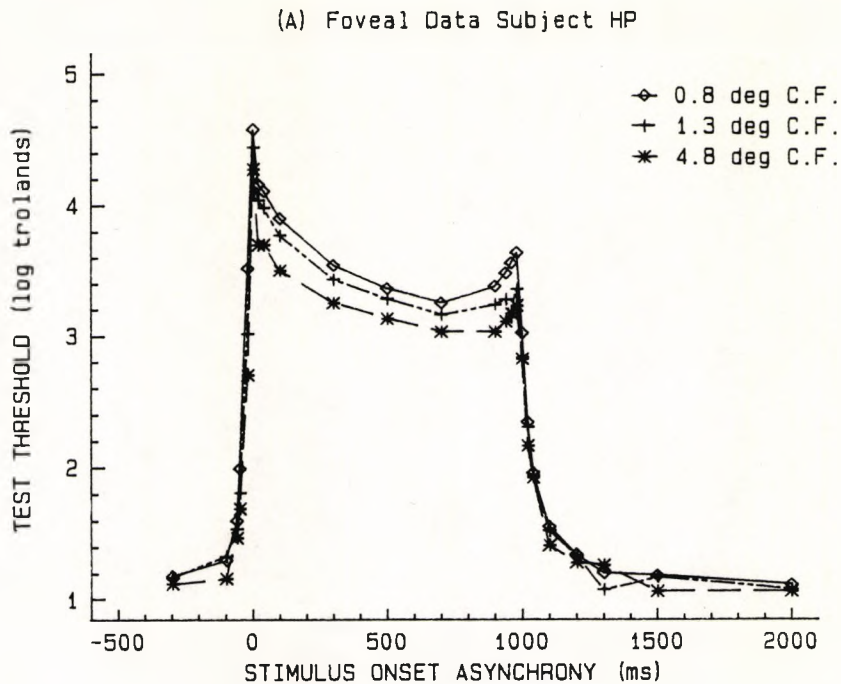


Figure 6.8. Test increment threshold is plotted as a function of stimulus onset asynchrony for three conditioning stimulus (C.F.) diameters. Data are shown for one representative subject for measurements made (A) at the fovea, and (B) at an eccentricity of 6° . Note that the diameters employed for foveal measurements differ from those employed for measurements made in the periphery. The conditioning stimulus retinal illuminance level was 3.8 log tds for both foveal and peripheral conditions. As before the test stimulus was of diameter 0.5° and duration 10 ms, and the retinal illuminance of the uniform background was constant at 2.0 log tds.

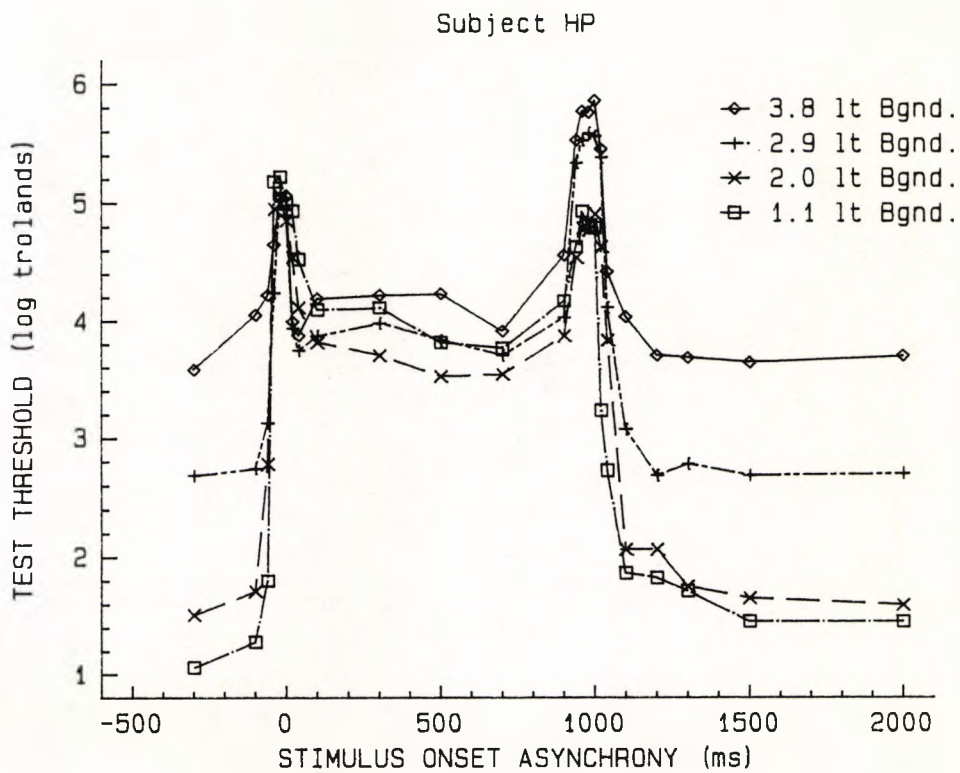


Figure 6.9. Test increment threshold is plotted as a function of stimulus onset asynchrony for four background retinal illuminance levels. Data are presented for measurements made at a retinal eccentricity of 6° for one representative subject HP. The retinal illuminance level of the conditioning stimulus was fixed at 3.8 log tds. The test stimulus was 0.5° in diameter and was presented for a duration of 10 ms. The conditioning stimulus was 1.25° in diameter and presented for a duration of 1000 ms.

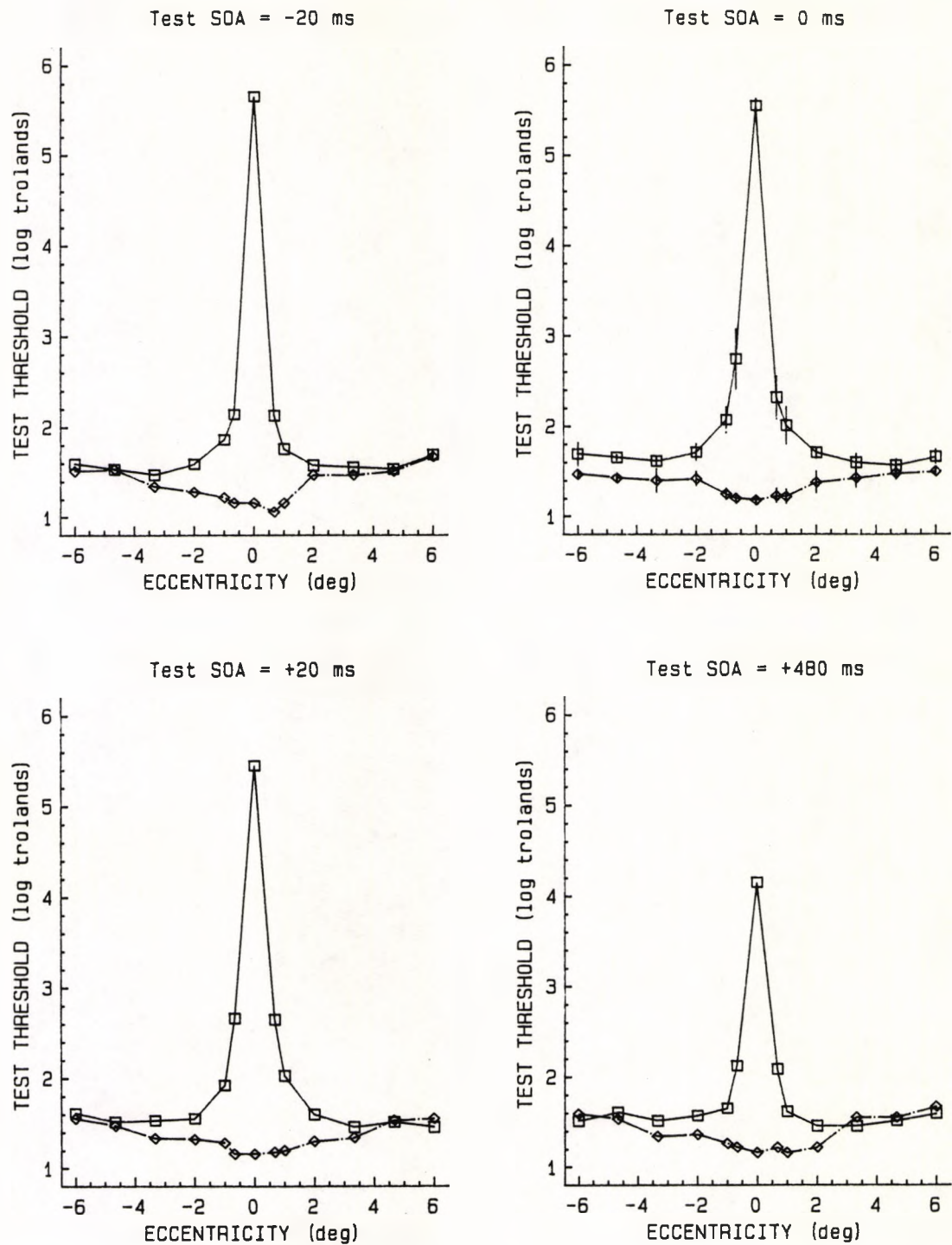


Figure 6.10. Test increment threshold is plotted as a function of eccentricity with respect to a conditioning stimulus centred on the fovea (subject PF). Data are shown for four specific values of stimulus onset asynchrony, and the appropriate values are given above each figure. The diamond symbols and discontinuous line indicate test thresholds measured in the absence of the conditioning stimulus and recorded in the same experimental session. The conditioning stimulus was 1° in diameter, 500 ms duration and 4.6 log tds. The test stimulus was 0.3° in diameter and of 10 ms duration. The background retinal illuminance was 2.0 log tds. Error bars shown for SOA=0 ms represent ± 1 se.

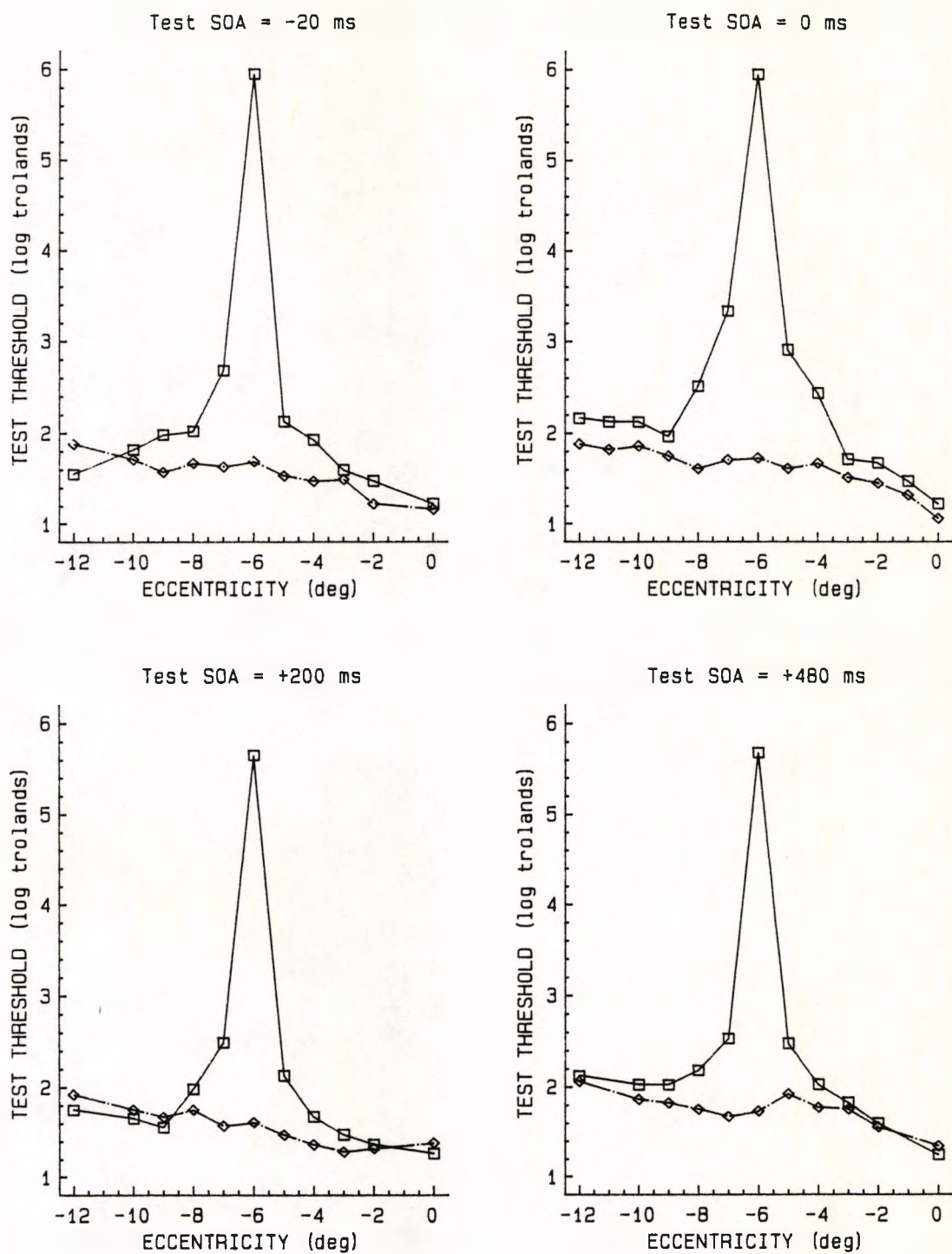


Figure 6.11. Test increment threshold is plotted as a function of eccentricity with respect to a conditioning stimulus centered 6° in the periphery (subject PF). Parameters are otherwise as given in the preceding figure.

coincident with the conditioning stimulus. It is also evident from both figures, however, that thresholds are elevated (for all presentation times) up to approximately 2° away from the conditioning stimulus. The function that describes the fall in test threshold with increasing distance from the conditioning stimulus correlates well with the known relationship between light scatter and eccentricity (see Fry and Alpern, 1953). Interestingly both foveal and peripheral data indicate that test thresholds are elevated by some 0.2 log units up to 6° away from the conditioning stimulus when the test presentation time is simultaneous with stimulus onset (i.e., SOA = 0). If this small, but repeatable, long - distance desensitisation was merely due to the effects of light scatter, then it should be apparent for each test presentation time, but the data presented in Figures 6.10 and 6.11 show that this is clearly not the case.

The results of experiment 6 are shown in Figure 6.12 where spectral sensitivity measurements are presented for three test presentation times. Data are shown for two subjects, J.T., a colour normal female and H.P., a protanopic male. By convention, the ordinate represents the logarithm of the test sensitivity, which is expressed as the reciprocal of the threshold irradiance level measured in watts / deg². Considering first the results of subject J.T., it may be seen that for a SOA of +500 ms (i.e., in terms of the time domain, the test stimulus is presented in the middle of the conditioning stimulus) the sensitivity - wavelength function shows at least two peaks at approximately 535 and 615 nm, and possibly a third, lower peak at about 445 nm. For the onset and offset conditions, the twin peaks at 535 and 615 nm appear to merge to a single peak at about 540 nm accompanied by an overall reduction in sensitivity. Sensitivity to test stimuli with wavelengths below about 460 nm shows less of a reduction than that seen at higher wavelengths. The three peaks of sensitivity measured in the normal trichromat at a SOA = +500 ms are replaced by only two peaks in the protanopic subject, occurring at wavelengths of about 440 and 550 nm . Not unexpectedly, this

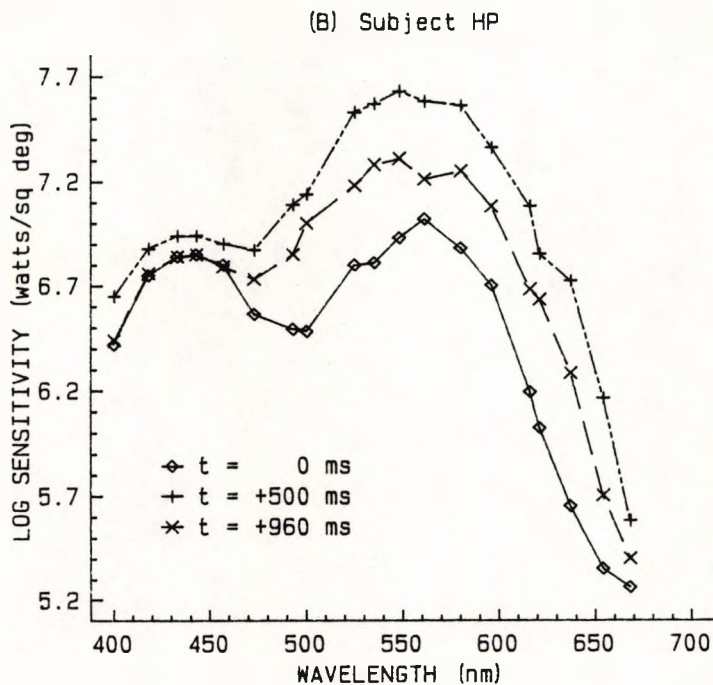
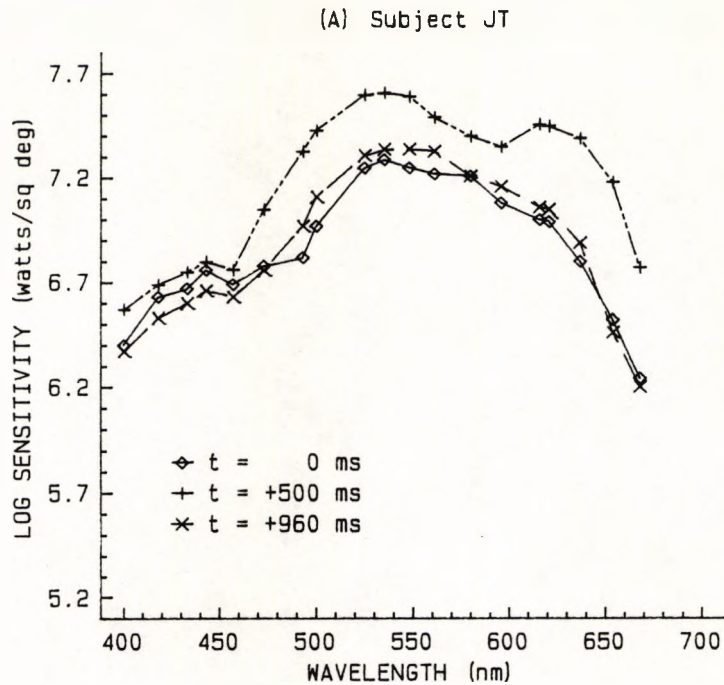


Figure 6.12. Spectral sensitivity measurements made for three discrete test presentation times for (A) a normal trichromat (JT) and (B) a protanope (HP). Data represent foveal measurements. The values given in the key for "t" refer to the stimulus onset asynchrony. The conditioning stimulus was 2.5 log trolands and 1.25° in diameter, and was presented for a duration of 1000 ms. The test stimulus was of diameter 0.5° and duration 10 ms. The retinal illuminance level of the background field was 2.0 log trolands.

subject also shows a large reduction in sensitivity for test stimuli with wavelengths greater than approximately 600 nm. Similar to the results obtained with subject J.T., however, sensitivity is clearly reduced at the onset and offset of the conditioning stimulus and also shows less of a reduction for test stimuli below 460 nm. The reduction in sensitivity for subject H.P. appears to be greater at the onset, compared to the offset, of the conditioning stimulus.

DISCUSSION AND CONCLUSIONS

The results of experiment 1 for foveal measurements are in excellent agreement with those published by Crawford (1947) for similar intensity conditioning stimuli (Crawford's data was, in fact, presented in units of cd / ft^2 , but use of the appropriate conversion factor reveals that his three conditioning stimuli were approximately equivalent to retinal illuminance levels of 3.7, 4.2 and 4.7 log trolands). In addition, the results of the present study indicate that the loss of sensitivity which occurs at the offset of the conditioning stimulus is about three fold greater for the periphery than for the fovea. The time course of the sensitivity changes following the offset of a conditioning stimulus was similar to that reported by Baker (1949; 1953), though it is clear that extended recovery times can occur following the offset of a particularly intense conditioning stimulus.

The results of experiment 2 show that the magnitude of the off response at the fovea decreases with a corresponding decrease in the duration of the conditioning stimulus. Ikeda and Boynton (1965) have similarly found that for short duration stimuli the on and off responses cannot be distinguished from one another, the off response being masked by the on response. Boynton (1972) has suggested that the transient sensitivity changes observed in such circumstances represent the on response only, since short flashes are fully integrated by the visual system and therefore do not produce distinct on and off responses. It seems more plausible, however, that the diminished off

response for short duration stimuli is related to the fact that thresholds are falling very rapidly at the time of flash offset and if we are to observe an off response then thresholds must be sampled at more frequent intervals. This explanation is supported by the finding that the off response is still quite marked for a 100 ms flash in the periphery, presumably because the magnitude of the off response is greater than for the corresponding foveal situation. The differences between foveal and peripheral data in terms of the effect of conditioning flash duration on the offset decrease in sensitivity, may be related to the relative distribution and frequency of sustained and transient neurones in the retina: sustained neurones are most frequently found in or near the fovea whereas transient neurones, which would be expected to generate larger signals at the time of flash offset, are more common in the peripheral retina (Ikeda and Wright, 1974).

The results of experiment 2 also indicate that the recovery rate of adaptation following the offset of the conditioning stimulus is independent of the latter's duration, which in turn suggests that the effects observed reflect rapid changes in retinal sensitivity which are determined by the incremental light intensity, and not by long term adaptation effects. That the magnitude of the on and the off response is largely independent of the contrast of the conditioning stimulus and the background is clearly demonstrated by the results of experiment 4 (see Figure 6.9).

The generally elevated test thresholds observed for conditioning stimuli of small diameter (see Figure 6.8 A and B) are reminiscent of the spatial sensitisation / desensitisation effects reported by Westheimer (1965; 1967; 1970) for both rod and cone mediated thresholds. Westheimer measured increment thresholds as a function of surround angular subtense and found that thresholds initially increased as the angular subtense of the surround was increased, but then, as the subtense of the surround was increased still further, thresholds began to fall. Subsequent studies (e.g., Markoff and Sturr, 1971) have

qualitatively confirmed Westheimer's findings and have also shown that both rod - cone (Latch and Lennie, 1977; Frumkes and Holstein, 1979), and cone - rod (Buck, 1985a; 1985b) interactions can be involved. (Buck and his co-workers (Buck et al., 1984) have shown specifically that rod - cone interactions can produce transient changes in sensitivity at both the onset and offset of a photopic background stimulus, the time course of the sensitivity changes being very similar to that found in the present study. Buck (1985a) also found that a transient cone - rod interaction occurred only at the onset of a scotopic background.) Spatial sensitisation has been explained in terms of a simple centre - surround receptive field model where, as originally proposed by Westheimer (1970), the effects are thought to involve lateral inhibition, in that when the test stimulus is viewed against a larger surround (in this case the conditioning stimulus), then the antagonistic effects of the surround aid the detection of the test (which stimulates the excitatory centre of the receptive field).

Electrophysiological studies have indicated that lateral inhibition, at least at the retinal level, is mediated largely by horizontal cells (Werblin and Dowling, 1969; but see also Gallego, 1986 for a review of horizontal cell function). The absence of the off response, but not the on response, for conditioning stimuli of large diameter suggests that different mechanisms may be involved in the mediation of the two types of response. The finding that an off response of larger magnitude can occur in foveal vision with a small diameter conditioning stimulus, and also that the magnitude of the off response is reduced for a large diameter conditioning stimulus in the periphery, implies that the off response is influenced by the relative stimulation of the centre and surround of the receptive field, the size of which is known to be smaller for foveal than for peripheral vision.

Electrophysiological recordings from the single optic nerve fibre of the horseshoe crab (Hartline et al., 1952) indicated that the intensity - increment threshold first rises just before the offset of an adapting field, and then

drops again into the classical dark adaptation curve. Baker (1953) was the first to correlate these early electrophysiological findings with his own, and Crawford's (1947), psychophysical observations. Refinement of electrophysiological techniques has more recently allowed recordings to be made specifically at the level of the photoreceptors in monkeys (e.g., Whitten and Brown, 1973) and lower vertebrates such as turtles (e.g., Baylor and Hodgkin, 1973). The time course of the cone response following an intense flash of light is often seen to be remarkably similar to the time course of the corresponding psychophysical thresholds measured in this study. Figure 6.13 illustrates some typical cone (and rod) late receptor potentials (see Whitten and Brown, 1973) for a series of stimuli of different wavelengths measured at two intensities. Whilst it is apparent that there exists an initial peak in receptor potential at stimulus onset, there is no obvious counterpart to the off response observed psychophysically. Werblin and Dowling (1969) however, found that the amacrine cells of the mudpuppy retina gave a transient response at both the onset and offset of a spot or annular stimulus, the off response being particularly marked for the latter stimulus configuration (see Figure 6.14). It is also possible that the long range, transient reduction in sensitivity observed for a spatially remote conditioning stimulus (experiment 5) may be mediated via these amacrine cells, the lateral inhibitions of which are known to extend over retinal distances of up to 800 μm (Vaney, 1985). Certainly at the ganglion cell level, on - centre and off - centre type cells which give preferential responses at the onset and offset of a stimulus have been identified (Cleland and Levick, 1974). Such ganglion cell responses are shown for the cat in Figure 6.15. In view of the known physiological differences between on - and off - centre cells in the vertebrate visual system (e.g., Cleland et al., 1973; Stone and Fukuda, 1974; see also Lennie, 1980), it is perhaps not surprising, therefore, that the corresponding psychophysical on and off responses observed in the present study should have different properties. Further evidence to support the hypothesis that the on and off responses are

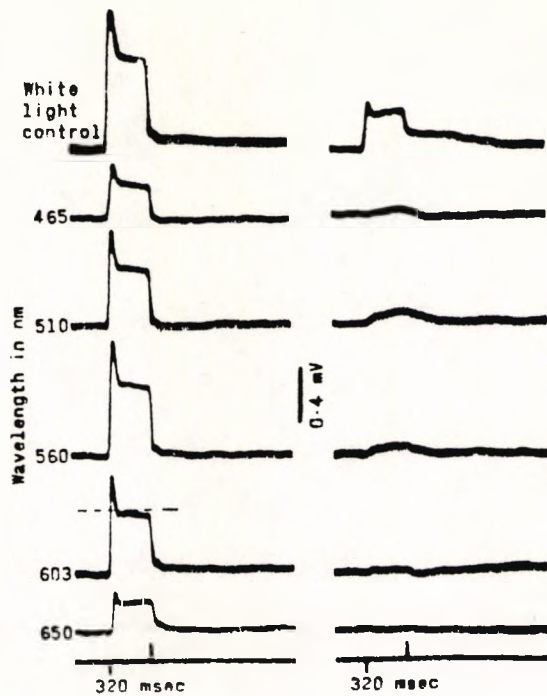


Figure 6.13. Late receptor potentials elicited from the parafovea of the monkey (from Whitten and Brown, 1973).

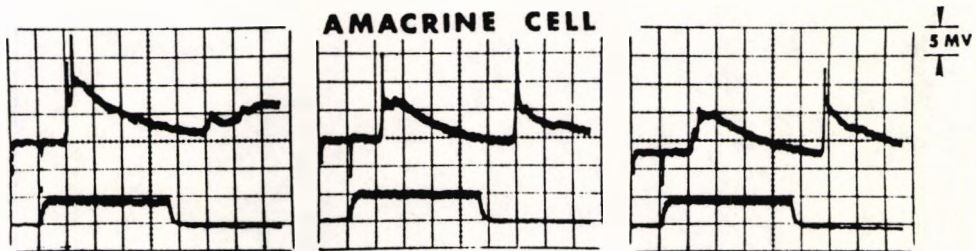


Figure 6.14. Amacrine cell responses for a spot stimulus in the mudpuppy retina (from Werbling and Dowling, 1969).

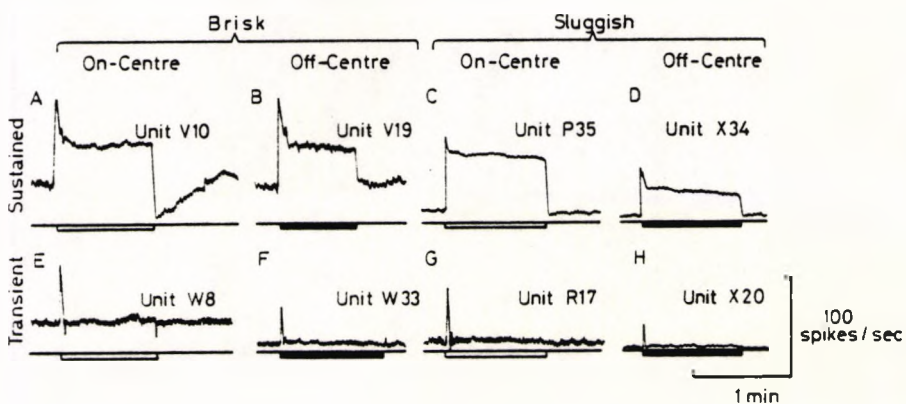


Figure 6.15. Ganglion cell responses in the cat retina. Responses are shown for the onset of a spot stimulus (A, E, G) or the unmasking of a contrasting disk. The dark and light bars below each diagram represent stimulus duration (darkening and brightening respectively). (From Cleland and Levick, 1974).

mediated by different mechanisms, derives from the finding that the on response, but not the off response, is absent for a strabismic amblyope (see Figure 6.6). Whilst it seems possible that the psychophysical on response relates to photoreceptor physiology, the absence of the on response in this amblyopic subject may indicate that spatial factors are also involved, since it is known that lateral inhibition is weaker in amblyopia (Lawwill et al., 1973). Interestingly, Baylor and his colleagues (Baylor et al., 1974) have shown that photoreceptor responses, like those illustrated in Figure 6.13, may in fact be influenced by feedback from horizontal cells. The experiment has been performed by only one amblyope and therefore, further experimentation with a larger group of amblyopes is required before any firm conclusions can be drawn.

It would seem that the sensitivity changes which have been shown to occur following exposure to a conditioning stimulus, may be accounted for, at least in part, by considering the spatial and temporal properties of cells at the retinal level. The increased recovery times observed for high intensity conditioning stimuli (see Figures 6.3 A and B) may also be directly related to the properties of cone photoreceptors. Three sensitivity regulating mechanisms have been proposed for cones: response compression (Boynton and Whitten, 1970), pigment bleaching (Boynton and Whitten, 1970) and cellular adaptation (Normann and Perlman, 1979). Response compression is caused by the non - linear, S - shaped, relation between stimulus and response (see Baylor et al., 1974 and also Figure 1.6) and it occurs when the operating point of the photoreceptor moves to a higher position on the response curve. Pigment bleaching causes desensitisation since fewer quanta may be absorbed by the cell. Cellular adaptation is an active mechanism in the receptor cell that adjusts its operating range so that it remains maximally sensitive with respect to the ambient level of illumination. Based on their study of cone responses in the rhesus monkey, Valeton and van Norren (1983) have shown that for stimulus intensities up to about 10^4 trolands, cellular adaptation and response compression

are responsible for photoreceptor sensitivity changes, but that above this intensity level, pigment bleaching occurs (in fact 20 years earlier in 1963, Brindley found similar results in that cone saturation occurred for intensities around 10^4 trolands). The recovery of photoreceptor sensitivity following a pigment bleach takes much longer than that following cellular adaptation and response compression, and probably contributes to the extended recovery times measured in the present study.

All the experiments in the present study were performed monocularly since it has been suggested previously that the dichoptic masking effect is relatively small (Boynton, 1972). More recently, however, Cogan (1989) has shown that this dichoptic effect can be much larger than initially proposed (though still not as large as that in the ipsilateral, monocular situation). These observations suggest that at least some small part of the observed changes in sensitivity associated with the onset and offset of a conditioning stimulus must involve processing at a more central level in the visual system. Cogan (1989) proposed that the transient loss of sensitivity at flash onset and offset may be thought of as the temporal analogue to the Mach band effect in which visual processing enhances border detection (Cornsweet, 1970).

The shape of the spectral sensitivity curves obtained in experiment 6 for a SOA of +500 ms is the same as would be expected for test detection in the absence of a conditioning stimulus i.e., for the colour normal subject there are three peaks of sensitivity, whereas for the colour defective subject only two peaks are evident. Previous studies have shown that the shape of the curve around 440 nm is well - matched by the sensitivity spectrum of the short - wavelength cones, whereas the shape of the curves at about 530 and 610 nm reflect opponent processing between the long - and middle - wavelength cones (Sperling and Harwerth, 1971). The relative insensitivity demonstrated for a short - wavelength test stimulus in the present study is related to the fact that the test stimulus employed was of short

duration only (10 ms), and consequently did not represent the optimum stimulus required for detection by short - wavelength cones (King - Smith and Carden, 1976; Finkelstein, 1988). Whilst the use of a test stimulus of longer duration would improve short - wavelength sensitivity, the temporal resolution of the technique would necessarily be impaired, and for this reason test duration was not changed. The finding that the reduced sensitivity at the onset and offset of the conditioning stimulus is mainly restricted to the middle and long wavelengths (see Figure 6.12), may be taken to suggest that the more transient, spectrally non - opponent pathway detects the test stimulus at these times, the short - wave cones contributing little to the detection of luminance change (Lennie and D'Zmura, 1988). The apparent fusion of the separate sensitivity peaks (at 535 and 615 nm) in the colour normal subject also supports this observation.

The results of this investigation reveal several interesting findings concerning the rapid changes in visual sensitivity which occur during flashes of light. Although the various experimental findings when considered in isolation relate well to the spatio - temporal and chromatic properties of photoreceptors and the various neural stages of the retina, it is not possible to make these findings more specific without additional experimental work.

CHAPTER 7

SUMMARY AND CONCLUSIONS

The technique described in Chapter 3 provides a quantitative method of measuring colour constancy, and the definition of the C_{index} simplifies the interpretation of the results. It is clear from the results presented that immediate (i.e., simultaneous) colour constancy is not perfect, and it follows therefore, that in normal everyday vision, other factors such as long term chromatic adaptation and memory must also play a part in colour constancy. Furthermore, the results show that the near surround is particularly important in determining the magnitude of the constancy effects observed, and more specifically, the presence or absence of a physical chromatic border between an object of interest and its surroundings is crucial. The results also suggest that the relative luminance of the test object and surround influences colour constancy; the values of the C_{index} were greater when the luminance of the test was below that of the surround. This finding provides evidence for the interaction between achromatic and chromatic visual mechanisms in colour constancy. Whatever the exact nature of the visual processes involved in colour constancy, any model developed to describe constancy in human vision should be able to predict colour appearance under all viewing conditions, including those for which colour constancy fails.

The technique should facilitate the future assessment of several other parameters of interest, including the spectral composition of the illuminant and the magnitude of illuminant changes. The results of the present study show that the complexity of the surround is apparently less important than its space - averaged chromaticity, however, in situations where an object is seen under various illuminants, pattern complexity must be an important factor in the determination of colour appearance (see Chapter 3 and also Arend et al., 1991). With this in mind, it would be interesting to see the results of analogous experiments

employing "real" scenes rather than the simplified centre - surround stimuli used in the present study. Some preliminary work has already been carried out to generate such scenes using digitised images (from a CCD colour camera) and a new graphics adaptor capable of providing a greater range of intensities per gun than the Vectrix adaptor used in the present study. These experiments require a considerable amount of programming work and unfortunately were not concluded in sufficient time to be presented in this thesis.

The results presented in the first section of Chapter 4 illustrate the response of the pupil to light flux change on the retina: the amplitude of the pupillary constriction increases, and its associated response latency usually decreases, as the luminance contrast of the stimulus is raised. These results are in close agreement with data published previously (e.g., Webster et al., 1968; Lee et al., 1969) and the current consensus is that the function of the PLR is to maximise acuity over a wide range of luminances (Woodhouse, 1975; Laughlin, 1992) and to facilitate dark adaptation by protecting the retina from excessive bleaching (Woodhouse and Campbell, 1975). Results were also presented in this section showing the response of the pupil to achromatic grating stimuli, the shape of the PGR function bearing a close resemblance to the corresponding psychophysical contrast sensitivity function. The latencies for the PGR were always longer than those for PLR's of similar amplitude but the absolute latency difference was found to depend on the spatial frequency of the grating stimulus used. The origin and function of the PGR is less clear, but it seems possible that, like the VEP, the PGR may occur as a consequence of increased cortical activity which subsequently influences the efferent pupillary pathways (see Barbur et al., 1992).

In the second section of Chapter 4, the PLR and PGR were examined for a group of amblyopic subjects. The results show that the PLR is essentially normal in amblyopia, although a subtle latency abnormality involving the afferent pupillary pathway does exist, and is apparent especially for stimuli

of low luminance contrast. The majority of previous studies have reported that the PLR is of reduced amplitude in between 9 and 93% of amblyopes (Krüger, 1961; Greenwald and Folk, 1983; Portnoy et al., 1983; Firth, 1990). It should be emphasised, however, that, as in these previous clinical studies, the results of the present investigation show that single amblyopic subjects may indeed display significantly reduced amplitude responses following stimulation of the amblyopic eye; three out of the 22 amblyopes (i.e., approximately 14%) showed significantly reduced constriction amplitudes. The analysis carried out in the present study differs to those reported previously by examining inter - group differences, and it is shown subsequently that the PLR following stimulation of good and amblyopic eyes compared within each of the three amblyopic subgroups is not statistically different. The reduced binocular summation exhibited by amblyopes in this study suggests, however, that the amblyopic eye provides an abnormal input under binocular viewing conditions.

Whilst the PLR seems essentially normal in amblyopia, there are clear pupillary anomalies for achromatic grating stimuli, and these anomalies closely parallel the psychophysical decrease in contrast thresholds observed for the same stimuli. This finding was not totally unexpected since it has been shown previously that the pathway for this reflex involves the striate cortex (see Barbur, 1988). Subtle differences may exist between strabismic and anisometropic amblyopes in terms of their respective responses to grating stimuli, but further work with a larger population of amblyopes is required before any firm conclusions can be drawn. The finding that the normal eyes of amblyopes can exhibit pupillary responses of reduced amplitude, and longer latency, when compared with those of normal observers is difficult to explain, but may be related to some long term, secondary cortical influence (see also Cowey et al., 1989).

The results of this investigation cannot be used to differentiate clearly between retinal and central

abnormalities of visual processing in amblyopia for a number of reasons. Firstly, there is no consistent abnormality in the PLR in amblyopia. This in itself would suggest, according to classical theories of the neural pathways involved in the control of the pupil, that the retino-tectal pupillary pathways are normal in amblyopes. Even if the PLR in amblyopes were grossly abnormal, studies in patients with damaged central visual pathways have demonstrated that the PLR is reduced in amplitude when the stimulus is restricted to blind areas of the visual field (e.g., Harms, 1951; Alexandridis et al., 1983). Secondly, the PGR reflects the activity of the pupillary pathway as a whole, and consequently abnormal spatial interactions at the retinal level could possibly contribute to the abnormality of the PGR in amblyopes.

Pupillary responses to isoluminant, red - green chromatic gratings were shown to have latencies approximately 80 ms longer than those recorded for equivalent achromatic grating responses. No pupillary responses were measured in a protanope when gratings were isoluminant with respect to the background. The results show that pupil response amplitude varied systematically as a function of grating spatial frequency, and, like similar measurements made with achromatic stimuli, the pupillometric function resembles the psychophysical contrast threshold function. In the final section of Chapter 4, evidence was obtained to show that the pupillary responses observed in the investigation could not be attributed to systematic changes in accommodation or convergence.

The generation of isoluminant chromatic gratings on a colour monitor is difficult if one wants to ensure that luminance artefacts are minimised. The technique described in Chapter 5 obviates the requirement of isoluminance by employing a new type of chromatic stimulus which is masked by both spatial and temporal random luminance noise. The experiments reported show that this stimulus can be used to determine chromatic discrimination thresholds in both normal and colour defective subjects, and is particularly useful

for the latter class of subjects where, unless appropriate adjustments are made specifically for each type of colour deficiency, luminance contrast clues often facilitate the detection of the stimulus. The larger the amplitude of the random luminance modulation applied, the more clearly defined the isochromatic region becomes for each group of colour defective subjects. The three parameters which describe the best ellipse fitted to the data points provide a means of identifying the class, and possibly the severity, of the colour deficiency. The stimulus design was also employed in some preliminary pupillometric experiments, and it was shown that no pupillary responses were elicited in dichromats when the chromatic displacement was confined to a direction in colour space which coincided with the confusion axis of the specific class of colour defective observer. The results presented demonstrate the possible use of the technique in the objective assessment of colour vision, although more fundamental work is first required to determine the variability of responses in both normal and colour defective subjects.

The time course of sensitivity changes which occur in relation to the onset and offset of a flash of light were investigated by measuring increment thresholds for a small, brief test stimulus. The results presented in Chapter 6 show that a rapid reduction in sensitivity occurs at both the onset and offset of a conditioning flash. For the fovea, the changes in sensitivity which occur at flash offset (the off response) are usually of a much smaller magnitude than those at flash onset (the on response), whereas in the periphery, the sensitivity changes are generally of similar magnitude. The magnitude of the on response was shown to increase with the retinal illuminance level of the conditioning flash, although the magnitude of the off response was largely independent of conditioning flash retinal illuminance level. The magnitude of the off response was highly dependent on the diameter of the conditioning flash, the larger the diameter of the conditioning flash, the smaller the size of the off response. This effect was particularly marked for measurements made in the peripheral visual field. It seems

likely that the greater number of transient neurones in the retinal periphery may explain the large off response observed for peripheral presentation of the conditioning flash, though the dependence of the sensitivity changes on the diameter of the conditioning flash suggests that certain spatial factors related to receptive field properties may also be important. Interestingly, a small, but repeatable, elevation of threshold was observed for test stimuli located up to 6° away from the conditioning flash, though the effect was apparent only when the onsets of the test and conditioning stimuli were simultaneous. Spectral sensitivity measurements made at the onset and offset of a conditioning flash show that the observed sensitivity changes are mainly restricted to the middle and long wavelengths of the visible spectrum. This finding was taken to suggest that transient, non - opponent neurones are responsible for the detection of the test stimulus during the onset and offset of the conditioning flash.

APPENDIX

DESCRIPTION OF COLORIMETRIC TRANSFORMATIONS DEVELOPED FOR USE IN THE COLOUR CONSTANCY STUDY

For the purpose of the study detailed in Chapter 3, it was necessary to reproduce accurately colours of specific chromaticity and luminance on the high resolution monitor. In the simplest case this involved adjustment of the phosphor radiances so as to reproduce a "white" under CIE Standard Illuminants D_{65} and A. Considering first the luminances we have

$$Y_{D65} = 683 * K_{D65} * \int D(\lambda) \bar{y}(\lambda) d\lambda$$

$$Y_A = 683 * K_A * \int A(\lambda) \bar{y}(\lambda) d\lambda$$

where $D(\lambda)$ and $A(\lambda)$ are the relative spectral power distributions of illuminants D_{65} and A respectively, and $\bar{y}(\lambda)$ is the CIE colour matching function (which is equivalent to $V(\lambda)$, the photopic spectral luminous efficiency function). In order to reproduce a "white" with the same luminance for each illuminant condition, then the appropriate constants must be derived

$$K_{D65} = \text{LUM} / Y_{D65} \quad \text{and} \quad K_A = \text{LUM} / Y_A$$

Each illuminant data file may now be reweighted with these constants such that

$$W_{D65}(\lambda) = D(\lambda) * K_{D65} \quad \text{and} \quad W_A(\lambda) = A(\lambda) * K_A$$

where W_{D65} and W_A are the weighted spectral power distributions of CIE Standard Illuminants D_{65} and A respectively.

The CIE tristimulus values for the white with each illuminant may now be computed as follows

$$X_{D65} = 683 * \int W_{D65}(\lambda) \bar{x}(\lambda) d\lambda \quad X_A = 683 * \int W_A(\lambda) \bar{x}(\lambda) d\lambda$$

$$Y_{D65} = 683 * \int W_{D65}(\lambda) \bar{y}(\lambda) d\lambda \quad Y_A = 683 * \int W_A(\lambda) \bar{y}(\lambda) d\lambda$$

$$Z_{D65} = 683 * \Sigma W_{D65}(\lambda) \bar{z}(\lambda) d\lambda \quad Z_A = 683 * \Sigma W_A(\lambda) \bar{z}(\lambda) d\lambda$$

Similarly, for a coloured patch of spectral reflectance $R(\lambda)$ the tristimulus values would be

$$X_{C_{D65}} = 683 * \Sigma W_{D65}(\lambda) R(\lambda) \bar{x}(\lambda) d\lambda$$

$$X_{C_A} = 683 * \Sigma W_A(\lambda) R(\lambda) \bar{x}(\lambda) d\lambda$$

$$Y_{C_{D65}} = 683 * \Sigma W_{D65}(\lambda) R(\lambda) \bar{y}(\lambda) d\lambda$$

$$Y_{C_A} = 683 * \Sigma W_A(\lambda) R(\lambda) \bar{y}(\lambda) d\lambda$$

$$Z_{C_{D65}} = 683 * \Sigma W_{D65}(\lambda) R(\lambda) \bar{z}(\lambda) d\lambda$$

$$Z_{C_A} = 683 * \Sigma W_A(\lambda) R(\lambda) \bar{z}(\lambda) d\lambda$$

The remaining problem is to compute the phosphor luminances required to produce the above tristimulus values. Let the CIE tristimulus values for each phosphor, as measured with the telespectroradiometer (see Chapter 2), be represented by

X_R, Y_R, Z_R (RED)
 X_G, Y_G, Z_G (GREEN)
 X_B, Y_B, Z_B (BLUE)

These may be used to compute the corresponding chromaticity co-ordinates e.g., for the red phosphor

$$x_r = x_r / (X_R + Y_R + Z_R)$$

$$y_r = y_r / (X_R + Y_R + Z_R)$$

$$z_r = z_r / (X_R + Y_R + Z_R) \quad (1)$$

The chromaticity co-ordinates for green and blue phosphors may similarly be calculated so that we have

x_r, y_r, z_r (RED)
 x_g, y_g, z_g (GREEN)
 x_b, y_b, z_b (BLUE)

Now let

$$\begin{aligned} x_r &= k'r \int \bar{x}(\lambda) PR(\lambda) d\lambda \\ y_r &= k'r \int \bar{y}(\lambda) PR(\lambda) d\lambda \\ z_r &= k'r \int \bar{z}(\lambda) PR(\lambda) d\lambda \end{aligned} \quad (2)$$

and similarly for x_g, y_g, z_g and x_b, y_b, z_b , where $PR(\lambda)$, $PG(\lambda)$ and $PB(\lambda)$ are the normalised phosphor spectral power distribution functions, \bar{x}, \bar{y} and \bar{z} are the CIE colour matching functions, and $k'r$ is a constant.

Consider an area which consists of RED, GREEN and BLUE radiances with corresponding luminances LR, LG, LB , then

$$\begin{aligned} K_r \int \bar{y}(\lambda) PR(\lambda) d\lambda &= LR \\ K_g \int \bar{y}(\lambda) PR(\lambda) d\lambda &= LG \\ K_b \int \bar{y}(\lambda) PR(\lambda) d\lambda &= LB \end{aligned} \quad (3)$$

and

$$\begin{aligned} X &= K_r \int \bar{x}(\lambda) PR(\lambda) d\lambda + K_g \int \bar{x}(\lambda) PG(\lambda) d\lambda + K_b \int \bar{x}(\lambda) PB(\lambda) d\lambda \\ Y &= K_r \int \bar{y}(\lambda) PR(\lambda) d\lambda + K_g \int \bar{y}(\lambda) PG(\lambda) d\lambda + K_b \int \bar{y}(\lambda) PB(\lambda) d\lambda \\ Z &= K_r \int \bar{z}(\lambda) PR(\lambda) d\lambda + K_g \int \bar{z}(\lambda) PG(\lambda) d\lambda + K_b \int \bar{z}(\lambda) PB(\lambda) d\lambda \end{aligned} \quad (4)$$

where $Y = LR + LG + LB$. K_r, K_g and K_b are constants.

From (2) above we have

$$\begin{aligned} y_r &= k'r \int \bar{y}(\lambda) PR(\lambda) d\lambda \\ \int \bar{y}(\lambda) PR(\lambda) d\lambda &= y_r / k'r \end{aligned} \quad (5)$$

and from (3) above

$$K_r = LR / \int \bar{y}(\lambda) PR(\lambda) d\lambda \quad (6)$$

Substituting (5) in (6)

$$\begin{aligned} K_r &= LR * k'r / y_r \\ K_g &= LG * k'g / y_g \\ K_b &= LB * k'b / y_b \end{aligned}$$

Using these constants in the equations in (4) above, we have

$$\begin{aligned}
 X &= \frac{LR}{y_r} * x_r + \frac{LG}{y_g} * x_g + \frac{LB}{y_b} * x_b \\
 Y &= \frac{LR}{y_r} * y_r + \frac{LG}{y_g} * y_g + \frac{LB}{y_b} * y_b \\
 Z &= \frac{LR}{y_r} * z_r + \frac{LG}{y_g} * z_g + \frac{LB}{y_b} * z_b
 \end{aligned}
 \tag{7}$$

and the chromaticity co - ordinates may now be calculated from the equations given in (1) above.

Thus, from a knowledge of the phosphor chromaticity co - ordinates and luminances, the equations given in (7), allow the computation of the chromaticity co - ordinates of a given area. The computation has been shown for the simplest case of reproducing a "white" patch, but may be easily augmented with the appropriate spectral reflectance functions.

$$\begin{aligned}
 \text{Let } x_r / y_r &= a_1 ; x_g / y_g = b_1 ; x_b / y_b = c_1 \\
 y_r / y_r &= a_2 ; y_g / y_g = b_2 ; y_b / y_b = c_2 \\
 z_r / y_r &= a_3 ; z_g / y_g = b_3 ; z_b / y_b = c_3
 \end{aligned}$$

Using determinants to solve linear equations in (7) above, then

$$\begin{aligned}
 \frac{LR}{\begin{vmatrix} X & b_1 & c_1 \\ Y & b_2 & c_2 \\ Z & b_3 & c_3 \end{vmatrix}} &= \frac{LG}{\begin{vmatrix} a_1 & X & c_1 \\ a_2 & Y & c_2 \\ a_3 & Z & c_3 \end{vmatrix}} = \frac{LB}{\begin{vmatrix} a_1 & b_1 & X \\ a_2 & b_2 & Y \\ a_3 & b_3 & Z \end{vmatrix}} = \frac{1}{\begin{vmatrix} a_1 & b_1 & c_1 \\ a_2 & b_2 & c_2 \\ a_3 & b_3 & c_3 \end{vmatrix}} = \frac{1}{D}
 \end{aligned}
 \tag{8}$$

$$\text{where } DR = \begin{vmatrix} X & b_1 & c_1 \\ Y & b_2 & c_2 \\ Z & b_3 & c_3 \end{vmatrix} \quad DG = \begin{vmatrix} a_1 & X & c_1 \\ a_2 & Y & c_2 \\ a_3 & Z & c_3 \end{vmatrix} \quad DB = \begin{vmatrix} a_1 & b_1 & X \\ a_2 & b_2 & Y \\ a_3 & b_3 & Z \end{vmatrix}$$

$$\text{and } D = \begin{vmatrix} a_1 & b_1 & c_1 \\ a_2 & b_2 & c_2 \\ a_3 & b_3 & c_3 \end{vmatrix}$$

$$D = a_1[b_2c_3 - b_3c_2] - a_2[b_1c_3 - b_3c_1] + a_3[b_1c_2 - b_2c_1]$$

from this

$$DR = X[b_2c_3 - b_3c_2] - Y[b_1c_3 - b_3c_1] + Z[b_1c_2 - b_2c_1]$$

$$DG = a_1[Yc_3 - Zc_2] - a_2[Xc_3 - Zc_1] + a_3[Xc_2 - Yc_1]$$

$$DB = a_1[b_2Z - b_3Y] - a_2[b_1Z - b_3X] + a_3[b_1Y - b_2X]$$

Since $LR = DR / D$; $LG = DG / D$; $LB = DB / D$, then the phosphor luminances LR, LG, LB required to reproduce tristimulus values X, Y, Z may be calculated.

REFERENCES AND BIBLIOGRAPHY

- Abrahamsson, M., Sjöstrand, J. (1988) Contrast sensitivity and acuity relationship in strabismic and anisometropic amblyopia. Brit. J. Ophthalmol., 72, 44-49.
- Alexander, K.R., Barry, S.H. (1981) Visual masking and the contrast-flash effect. Vis. Res., 21, 301-309.
- Alexandridis, E. (1968) Bestimmung der Dunkeladaptationsskurve mit Hilfe der Pupillenlichtreflexe. Ber. Dtsch. Ophthalmol. Ges., 274-277.
- Alexandridis, E. (1985) The Pupil. Springer-Verlag, New York.
- Alexandridis, E., Koeppe, E.R. (1969) Die spektrale Empfindlichkeit der für den Pupillenlichtreflex verantwortlichen Photorezeptoren beim Menschen. Albrecht Graefes Arch. Klin. Ophthalmol., 177, 136-161.
- Alexandridis, E., Krastel, H., Reuther, R. (1983) In wie weit sind die Pupillenlichtreflexe bei der kortikalen Amaurose gestört? Fortschr. Ophthalmol., 80, 79-81.
- Alexandridis, E., Leendertz, J.A., Barbur J.L. (1991) Methods for studying the behaviour of the pupil. J. Psychophysiology, 5, 223-239.
- Alpern, M. (1964) Relation between brightness and colour contrast. J. Opt. Soc. Am., 54, 1491-1492.
- Alpern, M., Campbell, F.W. (1962) The spectral sensitivity of the consensual light reflex. J. Physiol. Lond., 165, 478-507.
- Alpern, M., Ohba, N. (1972) The effect of bleaching and backgrounds on pupil size. Vis. Res., 12, 943-951.

Alpern, M., Ohba, N., Birndorf, L. (1974) Can the response of the iris to light be used to break the code of the second cranial nerve ? In: Pupillary Dynamics and Behaviour. Ed. Janisse, M.P. New York, Plenum Press.

Alpern, M., Rushton, W.A.H. (1967) The nature of the rise in threshold produced by contrast-flashes. J. Physiol., 189, 519-534.

Amos, J.F. (1978) Refractive amblyopia: a differential diagnosis. Optician, Nov. 17, 13-19.

Amsler, M. (1949) Amsler Charts Manual. Theodore Hamblin Ltd., London.

Anstis, S., Cavanagh, P. (1983) A minimum motion technique for judging equiluminance. In J.D. Mollon and L.T. Sharpe, Eds., Colour Vision: Physiology and Psychophysics, Academic, London.

Arden, G.B. (1985) Pattern ERG in amblyopia: clinical evidence of mode of generation. Invest. Ophthalmol. Vis. Sci., 26, 1649.

Arden, G.B., Wooding, S.L. (1985) Pattern ERG in amblyopia. Invest. Ophthalmol. Vis. Sci., 26, 88-96.

Arden, G.B., Carter, R.M., Hogg, C.R., Powell, D.J., Vaegan (1980a) Reduced pattern electroretinograms suggest a preganglionic basis for non-treatable human amblyopia. J. Physiol., 308, 82P.

Arden, G.B., Gündüz, K., Perry, S. (1988a) Colour vision testing with a computer graphics system. Clin. Vis. Sci., 2, 303-320.

Arden, G.B., Gündüz, K., Perry, S. (1988b) Colour vision testing with a computer graphics system: preliminary results. Doc. Ophthalmol., 69, 167-174.

Arden, G.B., Vaegan, Hogg, C.R., Powell, D.J., Carter, R.M. (1980b) Pattern ERGs are abnormal in many amblyopes. Trans. Ophthalmol. Soc. UK, 100, 453-460.

Arend, L., Reeves, A. (1986) Simultaneous color constancy. J. Opt. Soc. Am. A, 3, 1743-1751.

Arend, L., Reeves, A., Schirillo, J, Goldstein, R. (1991) Simultaneous color constancy: papers with diverse Munsell values. J. Opt. Soc. Am. A, 661-672.

Arnulf, A., Santamaria, J., Bescós, J. (1981) A cinematograph method for the dynamic study of the image formation by the human eye. Microfluctuations of the accommodation. J. Optics (Paris), 12, 123-128.

Ashworth, B., Isherwood, I. (1981) Clinical Neuro-ophthalmology. 2nd. Ed. Blackwell, London.

Baker, F.H. (1963) Pupillary response to double pulse stimulation; a study of nonlinearity in the human pupil system. J. Opt. Soc. Am., 53, 1430-1436.

Baker, F.H., Grigg, P., Noorden, G.K. von (1974) Effects of visual deprivation and strabismus on the response of the neurones in the visual cortex of the monkey, including studies on the striate and prestriate cortex in the normal animal. Brain Res., 66, 185-208.

Baker, H.D. (1949) The course of foveal light adaptation measured by the threshold intensity increment. J. Opt. Soc. Am., 39, 172-179.

Baker, H.D. (1953) The instantaneous threshold and early dark adaptation. J. Opt. Soc. Am., 43, 798-803.

Baker, H.D. (1963) Initial stages of dark and light adaptation. J. Opt. Soc. Am., 53, 98-103.

Bangerter (1950). Quoted by Muller (1951), Muller P. 1951, Uber das Sehen der Amblyopen. Ophthalmologica, 121, 143.

Barbur, J.L. (1988) Spatial frequency specific measurements and their use in clinical psychophysics. Clin. Vis. Sci., 2(3), 225-233.

Barbur, J.L. (1989) Sampling rates for the measurement of eye movements and pupillary responses in human vision. Poster Presentation at 5th European Eye Movement Conference, Pavia, Italy.

Barbur, J.L. (1991) Pupillary responses to grating stimuli. Journal of Psychophysiology, 5, 259-263.

Barbur, J.L., Forsyth, P.M. (1986) Can the pupil response be used as a measure of the visual input associated with the geniculo-striate pathway. Clin. Vis. Sci., 1, 107-111.

Barbur, J.L., Thomson, W.D. (1987) Pupil response as an objective measure of visual acuity. Ophthal. Physiol. Opt., 7, 425-429.

Barbur, J.L., Dunn, G.M., Wilson, J.A. (1986) The perception of moving comets at high retinal illuminance levels: a rod-cone interaction effect. Biol. Cybern., 55, 145-158.

Barbur, J.L., Harlow, A.J., Sahraie, A. (1992) Pupillary responses to stimulus structure, colour and movement. Ophthal. Physiol. Opt., 12, 137-141.

Barbur, J.L., Keenleyside, M.S., Thomson, W.D. (1987a) Investigation of central visual processing by means of pupillometry. In Seeing Contour and Colour. Eds. J.J. Kulikowski, C.M. Dickenson, and I.J. Murray. Pergamon Press, Oxford.

Barbur, J.L., Thomson, W.D., Forsyth, P.M. (1987b) A new system for the simultaneous measurement of pupil size and two-dimensional eye movements. Clin. Vis. Sci., 2, 131-142.

Barlow, H.B. (1972) Dark and light adaptation: Psychophysics. In: Handbook of Sensory Physiology, Vol VII/4 Eds. D. Jameson and L.M. Hurvich. Springer-Verlag, Berlin.

Barlow, H.B., Mollon, J.D. (1982) The Senses. Cambridge University Press.

Bartleson, C.J. (1979) Changes in color appearance with variation in chromatic adaptation. Color Res. Appl., 4, 119-138.

Baylor, D.A., Hodgkin, A.L. (1973) Detection and resolution of visual stimuli by turtle photoreceptors. J. Physiol., 234, 163-198.

Baylor, D.A., Hodgkin, A.L., Lamb, T.D. (1974) The electrical responses of turtle cones to flashes and steps of light. J. Physiol., 242, 685-727.

Baylor, D.A., Nunn, B.J., Schnapf, J.L. (1987) Spectral sensitivity of cones of the monkey *Macaca fascicularis*. J. Physiol., 390, 145-160.

Bedell, H.E., Flom, M.C. (1981) Monocular spatial distortion in strabismic amblyopia. Invest. Ophthalmol. Vis. Sci., 20, 263-268.

Bedell, H.E., Flom, M.C. (1983) Normal and abnormal space perception. Am. J. Optom. Physiol. Optics, 60, 426-435.

Benevento, L.A., Rezak, M., Santos-Anderson, R. (1977) An autoradiographic study of the projections of the pretectum in the rhesus monkey (*Macaca mulatta*): evidence for sensorimotor links to the thalamus and oculomotor nuclei. Brain Res., 127, 197-218.

Boynton, R.M., Bush, W.R., Enoch, J.M. (1954) Rapid changes in foveal sensitivity resulting from direct and indirect adapting stimuli. J. Opt. Soc. Am., 44, 56-60.

Boynton, R.M., Kaiser, P.K. (1968) Vision: the additivity law made to work for heterochromatic photometry with bipartite fields. Science, 161, 366.

Boynton, R.M., Whitten, D.N. (1970) Visual adaptation in monkey cones: recordings of late receptor potentials. Science, 170, 1423-1426.

Bradley, A., Freeman, R.D. (1981) Contrast sensitivity in anisometric amblyopia. Invest. Ophthalmol. Vis. Sci., 21, 467-476.

Brainard, D.H. (1989) Calibration of a computer controlled colour monitor. Color Res. Appl., 14, 23-34.

Breitmeyer, B.G. (1975) Simple reaction times as a measure of the temporal response properties of transient and sustained channels. Vis. Res., 15, 1411-1412.

Breitmeyer, B., Ganz, L. (1976) Implications of sustained and transient channels for theories of visual pattern masking, saccadic suppression, and information processing. Psychol. Rev., 83, 1-36.

Brenner, E., Cornellison, F.W., Nuboer, J.F.W. (1989) Some spatial aspects of simultaneous colour contrast. In Seeing Contour and Colour. Eds. J.J. Kulikowski, C.M. Dickenson, and I.J. Murray. Pergamon Press.

Brenner, R.L., Charles, S.T., Flynn, J.T. (1969) Pupillary responses in rivalry and amblyopia. Arch. Ophthalmol., 82, 23-29.

Brill, M.H., West G. (1986) Chromatic adaptation and color constancy: a possible dichotomy. Color Res. Appl., 11, 196-204.

- Brindley, G.S. (1957) Two theorems in colour vision. Q. J. Exp. Psychol., 9, 101-104.
- Brindley, G.S. (1963) Afterimages. Scient. Am., 209, 84-91.
- Brindley, G.S., Gautier-Smith, P.C., Lewin, W. (1969) Cortical blindness and the function of the non-geniculate fibres of the optic tracts. Journal of Neurology, Neurosurgery and Psychiatry, 32, 259-264.
- Brock, F.W. and Givnor, L. (1952) Fixation anomalies in amblyopia. Arch Ophthal, 47, 775-786.
- Bromley, J.M., Javadnia, A., Ruddock, K.H. (1987) Visual spatial filtering and pattern discrimination are abnormal in strabismic amblyopia. Clin. Vis. Sci., 1, 209-218.
- Brown, P.K., Wald, G. (1964) Visual pigments in single rods and cones of the human retina. Science, 144, 45-52.
- Buchsbaum, G. (1980) A spatial processor model for object colour perception. Franklin Inst., 310, 1-26.
- Buchsbaum, G. (1989) Personal communication.
- Buchsbaum, G., Gottschalk, A. (1983) Trichromacy, opponent colours coding and optimum information transmission in the retina. Proc. Soc. Roy. Lond. (B), 220, 89-113.
- Buck, S.L. (1985a) Cone-rod interaction over time and space. Vis. Res., 25, 907-916.
- Buck, S.L. (1985b) Determinants of the spatial properties of cone-rod interaction. Vis. Res., 25, 1277-1284.
- Buck, S.L., Stefurak, D.L., Moss, C., Regal, D. (1984) The time-course of rod-cone interaction. Vis. Res., 24, 543-548.

- Budge, J., Waller, A.V. (1852) Troisieme partie des recherches sur la pupille. CR Acad. Sci. (Paris), 34, 164-167.
- Burian, H.M. (1956) Thoughts on the nature of amblyopia ex anopsia. Am. Orthopt. J., 6, 5-12.
- Burian, H.M., Lawwill, T. (1966) Electroretinographic studies in strabismic amblyopia. Amer. J. Ophthalmol., 61, 422-430.
- Butler, S.R., Carden, D., Hilken, H., Kulikowski, J.J. (1988) Deficit in colour constancy following V4 ablations in rhesus monkeys. J. Physiol., 9, 72.
- Campbell, F.W. and Gregory, A.H. (1960) Effect of size of pupil on visual acuity. Nature. Lond., 187, 1121-1123.
- Charman, W.N., Heron, G. (1988) Fluctuations in accommodation: a review. Ophthal. Physiol. Opt., 8, 153-164.
- Charman, W.N., Jennings, J.A.M. (1976) Objective measurements of the longitudinal chromatic aberration of the human eye. Vis. Res., 16, 999-1005.
- Charman, W.N., Tucker, J. (1977) Dependence of accommodation response on the spatial frequency spectrum of the observed object. Vis. Res., 17, 129-139.
- Charman, W.N., Tucker, J. (1978) Accommodation as a function of object form. Am. J. Optom. Physiol. Opt., 55, 84-92.
- Chino, Y.M., Shansky, M.S., Hamasaki, D.I. (1980) Development of receptive field properties of retinal ganglion cells in kittens raised with a convergent squint. Exp. Brain Res., 39, 313-320.
- Cibis, G.W., Campos, E.C., Aulhorn, E. (1975) Pupillary hemiakinesia in supragenulate lesions. Arch. Ophthalmol., 93, 1322-1327.

Ciuffreda, K.J., Hokoda, S.C. (1983) Spatial frequency dependence of accommodation responses in amblyopic eyes. Vis. Res., 23, 1585-1594.

Ciuffreda, K.J., Hokoda, S.C. (1985) Effect of instruction and higher level control on the accommodation response spatial frequency profile. Ophthal. Physiol. Opt., 5, 221-223.

Ciuffreda, K.J., Kenyon, R.V., Stark, L. (1980) Increased drift in amblyopic eyes. Brit. J. Ophthalmol., 64, 7-14.

Ciuffreda, K.J., Rumpf, D. (1985) Contrast and accommodation in amblyopia. Vis. Res., 25, 1445-1457.

Cleland, B.G., Levick, W.R. (1974) Brisk and sluggish concentrically organized ganglion cells in the cat's retina. J. Physiol., 240, 421-456.

Cleland, B.G., Crewther, D.P., Crewther, S.G., Mitchell, D.E. (1982) Normality of spatial resolution of retinal ganglion cells with strabismic amblyopia. J. Physiol. (Lond.), 326, 235-249.

Cleland, B.G., Dubin, M.W., Levick, W.R. (1971) Sustained and transient neurones in the cat's retina and lateral geniculate nucleus. J. Physiol., 217, 473-496.

Cleland, B.G., Levick, W.R., Sanderson, K.J. (1973) Properties of sustained and transient ganglion cells in the cat retina. J. Physiol., 228, 649-680.

Cleland, B.G., Mitchell, D.E., Gillard-Crewther, S.G., Crewther, D.P. (1980) Visual resolution of retinal ganglion cells in monocularly-deprived cats. Brain Res., 192, 261-266.

Cogan, A.I. (1989) Anatomy of a flash. 1. Two-peak masking and a temporal filling-in. Perception, 18, 243-256.

- Cohen, G.H., Saini, V.D. (1978) The human pupil response as an objective determination of colour vision deficiency. Mod. Probl. Ophthalmol., 19, 197-200.
- Cole, R.B.W. (1959) The problems of unilateral amblyopia. Br. Med. J., 1, 202-206.
- Cornsweet, T.N. (1970) Visual Perception. Academic Press, London.
- Cowan, W.B. (1983) Discreteness artifacts in raster display systems. In J.D. Mollon and L.T. Sharpe, Eds., Colour Vision: Physiology and Psychophysics. Academic, London.
- Cowan, W.B. and Rowell, N. (1986) On the gun independence and phosphor constancy of colour video monitors. Color Res. Appl. Supplement, 11, S33-S38.
- Cowey, A. (1974) Atrophy of retinal ganglion cells after removal of striate cortex in a rhesus monkey. Perception, 3, 257-260.
- Cowey, A., Stoerig, P., Perry, V.H. (1989) Transneuronal retrograde degeneration of retinal ganglion cells after damage to striate cortex: evidence of a selective loss of P_{β} cells. Neuroscience, 29, 65-80.
- Cox, T.A., Parson-Drewes, C. (1984) Contraction anisocoria resulting from half field illumination. Am. J. Ophthalmol., 97, 577-582.
- Crawford, B.H. (1936) The dependence of pupil size upon external light stimulus under static and variable conditions. Proc. R. Soc. B, 121, 376-395.
- Crawford, B.H. (1947) Visual adaptation in relation to brief conditioning stimuli. Proc. Roy. Soc. B, 134, 283-302.

- Crawford, M.L.J. (1978) The visual deprivation syndrome. In "Symposium: current concepts of amblyopia." Ophthalmology, 85, 465-477.
- Crawford, M.L.J., Noorden, G.K. von (1979) The effects of short-term experimental strabismus on the visual system in Macaca Mulatta. Invest. Ophthalmol. Vis. Sci., 18, 496-505.
- Crewther, S.G., Cleland, B.G., Crewther, D.P. (1982) Is amblyopia a retinal ganglion cell phenomenon ? Perception, 11, 30A.
- Crewther, D.P., Crewther, S.G., Cleland, B.G. (1985) Is the retina sensitive to the effects of prolonged blur ? Exp. Brain Res., 58, 427-434.
- Cueppers, C. (1951) Eine neue Methode zur stetigen Registrierung der konsensuellen Pupillenreaktion. Klin. Monatsbl. Augenheilkd., 119, 411-417.
- Cynader, M.S. (1982) Competitive neuronal interactions underlying amblyopia. Human Neurobiol., 1, 35-39.
- Daniel, P.M., Whitteridge, D. (1961) The representation of the visual field on the cerebral cortex of monkeys. J. Physiol., 159, 203-221.
- Dannemiller, J.L. (1989) Computational approaches to color constancy: adaptive and ontogenetic considerations. Psychol. Rev., 96, 255-266.
- Dartnall, H.J.A., Bowmaker, J.K., Mollon, J.D. (1983) Human visual pigments: microspectrophotometric results from the eyes of seven persons. Proc. Roy. Soc. Lond. B., 220, 115-130.
- Davson, H. (1980) Physiology of the Eye. 4th. Ed., Churchill Livingstone, London.

Daw, N.W. (1984) The psychology and physiology of colour vision. Trends in Neurosci., 7, 330-335.

Dawson, G.D. (1951) A summation technique for detecting small signals in a large irregular background. J. Physiol., 115, 2.

Day, M.D. (1979) Autonomic Pharmacology. Experimental and Clinical Aspects. Churchill Livingstone, London.

Denieul, P., Corno, F. (1986) Accommodation et contraste. L'Optométrie, 32, 4-8.

De Valois, R.L., De Valois, K.K. (1988) Spatial Vision. Oxford psychology series. No. 14. Oxford University Press.

De Valois, R.L., Webster, M.A., De Valois, K.K., Lingelbach, B. (1986) Temporal properties of brightness and color induction. Vis. Res., 26, 887-897.

Doesschate, J. ten, Alpern, M. (1967) Influence of asymmetrical photo-excitation of the two retinas on pupil size. J. Neurophysiol., 30, 577-585.

Dowling, J.E. (1987) The Retina. Harvard University Press, London.

Dowling, J.E., Boycott, B.B. (1966) Organization of the primate retina: electron microscopy. Proc. Roy. Soc. B, 166, 80-111.

Dolének, A. (1960) Beitrag zur Pupillographie. Ophthalmologica, 139, 77-83.

Drews, R.C. (1962) The Gunn pupil sign. Am. J. Ophthalmol., 54, 1109-1113.

D'Zmura, M., Lennie, P. (1986) Mechanisms of color constancy. J. Opt. Soc. Am. A, 3, 1662-1672.

Eggers, H.M., Blakemore, C. (1978) Physiological basis of anisometropic amblyopia. Science, 201, 264-266.

Enroth-Cugell, C., Robson, J.G. (1966) The contrast sensitivity of retinal ganglion cells of the cat. J. Physiol., 187, 517-552.

Evans, R.M. (1948) An Introduction to Color. Wiley, New York.

Evans, R.M., Swenholt, B.K. (1967) Chromatic strength of colors: dominant wavelength and purity. J. Opt. Soc. Am., 57, 1319-1324.

Evans, R.M., Swenholt, B.K. (1969) Chromatic strength of colors III: chromatic surrounds and discussion. J. Opt. Soc. Am., 59, 628-634.

Fallowfield, L., Krauskopf, J. (1984) Selective loss of chromatic sensitivity in demyelinating disease. Invest. Ophthalmol. Vis. Sci., 25, 771-773.

Finkelstein, M.A. (1988) Spectral tuning of opponent channels is spatially dependent. Color Res. Appl., 13, 106-112.

Firth, A.Y. (1990) Pupillary responses in amblyopia. Brit. J. Ophthalmol., 74, 676-680.

Fishman, R.S., Copenhaver, R.M. (1959) Macular disease and amblyopia: the visual evoked response. Arch. Ophthalmol., 77, 718-725.

Fletcher, R., Voke, J. (1985) Defective Colour Vision. Bristol, Adam Hilger Ltd.

Flom, M.C., Bedell, H.E., Allen, J. (1982) Spatial distortions in strabismus, anisometropia and amblyopia. Invest. Ophthalmol. Vis. Sci. Suppl., 22, 160.

Frumkes, T.E., Holstein, G.R. (1979) Rod-cone inter-relationships at light onset and offset. J. Opt. Soc. Am., 69, 1727-1730.

Fry, G.A., Alpern, M. (1953) The effect of a peripheral glare source upon the apparent brightness of an object. J. Opt. Soc. Am., 43, 189-195.

Fuortes, M.G.F., Schwartz, E.A., Simon, E.J. (1973) Colour-dependence of cone responses in the turtle retina. J. Physiol., 234, 199-216.

Gallego, A. (1986) Comparative studies on horizontal cells. In Retinal Research, Vol.5, 166-206.

Glansholm, A., Hedin, A., Tengroth, B. (1974) Pupillography in colour normals and colour defectives with chromatic stimuli of equal physical power. Mod. Probl. Ophthalmol., 13, 185-189.

Gouras, P. (1968) Identification of cone mechanisms in monkey ganglion cells. J. Physiol., 199, 533-547.

Gouras, P. (1974) Opponent-colour cells in different layers of foveal striate cortex. J. Physiol. (Lond.), 238, 583-602.

Gouras, P., Zrenner, E. (1982) The neural organization of primate color vision. Color Res. Appl., 7, 205-208.

Graham, J., Lin, C.S., Kass, J.H. (1979) Subcortical projections of six visual cortical areas in the owl monkey, *Aotus trivirgatus*. J. Comp. Neurol., 187, 557-580.

Granger, E.M., Heurtley, J.C. (1973) Visual chromaticity-modulation transfer function. J. Opt. Soc. Am., 63, 1173-1174.

Green, D.G., Campbell, F.W. (1965) Effect of focus on the visual response to a sinusoidally modulated spatial stimulus. J. Opt. Soc. Am., 55, 1154-1157.

Greenwald, M.J., Folk, E.R. (1983) Afferent pupillary defects in amblyopia. J. Pediat. Ophthalmol. Strab., 20, 63-67.

Guillery, R.W. (1972) Binocular competition in the control of geniculate cell growth. J. Comp. Neurol., 144, 117-130.

Gündüz, K., Arden, G.B., Perry, S., Weinstein, G.W., Hitchings, R.A. (1988a) Colour vision defects in ocular hypertension and glaucoma. Arch. Ophthalmol., 106, 929-935.

Gündüz, K., Arden, G.B., Perry, S. (1988b) Colour contrast thresholds are elevated in mild disease though other colour tests give normal results. Invest. Ophthalmol. Vis. Sci. Arvo Suppl., 69.

Guth, S.L., Massof, R.W., Benzscharow, T. (1980) Vector model for normal and dichromatic vision. J. Opt. Soc. Am., 70, 197-212.

Hall, C. (1982) The relationship between clinical stereotests. Ophthalm. Physiol. Opt., 2, 135-143.

Hamasaki, D.I., Flynn, J.T. (1981) Amblyopic eyes have longer reaction times. Invest. Ophthalmol. Vis. Sci., 21, 846-853.

Harms, H. (1938) Ort und Wesen der Bildhemmung bei Schielenden. Albrecht v. Graefes Arch. Klin. Exp. Ophthalmol., 138, 149-210.

Harms, H. (1951) Hemianopische Pupillenstarre. Klin. Monatsbl. Augenheilkd., 118, 133-147.

Hartline, H.K., Wagner, H.G., MacNichol, E.F. (1952) The peripheral origin of nervous activity in the visual system. Cold Spring Harbor Symposia on Quantitative Biology, Vol.17, 125-141. Cold Spring Harbor Laboratory of Quantitative Biology, Cold Spring Harbor, L.I., New York.

- Harwerth, R.S. (1982) Glenn Fry Award Lecture: Behavioral studies of amblyopia in monkeys. Am. J. Optom. Pysiol. Optics, 59, 535-555.
- Harwerth, R.S., Levi, D.M. (1977) Increment threshold spectral sensitivity in anisometropic amblyopia. Vis. Res., 17, 585-590.
- Headon, M.P., Powell, T.P.S. (1973) The effects of unilateral eyelid closure upon the lateral geniculate nucleus of infant monkeys. J. Anat., 122, 714.
- Heard, P.F., Stone, C.J., Gregory, R.L., Marmion, V.J. (1987) A new computer graphics test for red/green colour anomaly. Doc. Ophthalmol. Proc. Ser., 46, 181-194.
- Hedin, A., Glansholm, A. (1976) Pupillary spectral sensitivity in normals and color defectives. Mod. Probl. Ophthalmol., 17, 231-236.
- Helmholtz, H.L.F. von (1867) Handbuch der physiologischen Optik 1st Ed., Voss, Hamburg.
- Helson, H. (1938) Fundamental problems in color vision. I. The principle in governing changes in hue, saturation and lightness of non-selective samples in chromatic illumination. J. Exp. Psychol., 23, 439.
- Helson, H. (1943) Some factors and implications of color constancy. J. Opt. Soc. Am., 33, 555-567.
- Hering, E. (1878) Zur Lehre vom Lichtsinne. Gerold's Sohn, Wien, 107-141.
- Hess, R.F. (1977a) Eye movements and grating acuity in strabismic amblyopia. Ophthal. Res., 225-237.

Hess, R.F. (1977b) On the relationship between strabismic amblyopia and eccentric fixation. Br. J. Ophthalmol., 61, 767-773.

Hess, R.F., Baker, C.L. Jr. (1984) The human pattern evoked electroretinogram. J. Neurophysiol., 51, 939.

Hess, R.F., Baker, C.L. Jr. (1985) Assessment of retinal function in severely amblyopic individuals. Vis. Res., 24, 1367-1366.

Hess, R.F., Bradley, A. (1980) Contrast perception above threshold is only minimally impaired in human amblyopia. Nature, 287, 463-464.

Hess, R.F., Howell, E.R. (1977) The threshold contrast sensitivity function in strabismic amblyopia: evidence for a two type classification. Vis. Res., 17, 1049-1055.

Hess, R.F., Howell, E.R. (1978) The luminance-dependent nature of the visual abnormality in strabismic amblyopia. Vis. Res., 18, 931-936.

Hess, R.F., Pointer, J.S. (1985) Differences in the neural basis of human amblyopia: the distribution of the anomaly across the visual field. Vis. Res., 25, 1577-1594.

Hess, R.F., Baker, C.L., Verhoeve, J.N., Tulunay Keeseey, U., France, T.D. (1985) The pattern evoked electroretinogram: its variability in normals and its relationship to amblyopia. Invest. Ophthalmol. Vis. Sci., 26, 1610-1623.

Hess, R.F., Campbell, F.W., Greenhalgh, T. (1978) On the nature of the neural abnormality in human amblyopia; neural aberrations and neural sensitivity loss. Pflugers Arch., 377, 201-207.

Hess, R.F., Campbell, F.W., Zimmern, R. (1980) Differences in the neural basis of human amblyopias: the effect of mean luminance. Vis. Res., 20, 295-305.

- Heywood, C.A., Cowey, A. (1987) On the role of cortical area V4 in the discrimination of hue and pattern in macaque monkeys. J. Neurosci., 7, 2601-2617.
- Hiltz, R., Cavonius, C.R. (1974) Functional organization of the peripheral retina. Vision Res., 14, 1333-1337.
- Horst, G.J.C. van der, Bouman, M.A. (1969) Spatio-temporal chromaticity discrimination. J. Opt. Soc. Am., 59, 1482-1488.
- Horton, J.C., Hubel, D.H. (1980) Cytochrome oxidase stain preferentially labels intersection of ocular dominance and vertical orientation columns in macaque striate cortex. Soc. Neurosci., Abstr. 6, 315.
- Hubel, D.H., Livingstone, M.S. (1982) Blobs and color vision. Can. J. Pharmacol., 61, 1433-1441.
- Hubel, D.H., Wiesel, T.N. (1962) Receptive fields, binocular interaction and functional architecture in the cat's visual cortex. J. Physiol., 160, 105-154.
- Hubel, D.H., Wiesel, T.N. (1965) Binocular interaction in striate cortex of kittens reared with artificial squint. J. Neurophysiol., 28, 1041-1059.
- Hubel, D.H., Wiesel, T.N. (1968) Receptive fields and functional architecture of monkey striate cortex. J. Physiol. (Lond.), 195, 215-243.
- Hubel, D.H., Wiesel, T.N. (1970) The period of susceptibility to the physiological effects of unilateral eye closure in kittens. J. Physiol., 206, 994-1002.
- Humphrey, A.L., Hendrickson, A.E. (1980) Radial zones of high metabolic activity in squirrel monkey striate cortex. Soc. Neurosci., Abstr. 6, 315.

Hunt, R.W.G. (1987) Measuring Colour, 1st. ed., Wiley, England.

Hurlbert, A. (1986) Formal connections between lightness algorithms. J. Opt. Soc. Am. A, 3, 1684-1693.

Hurvich, L.M., Jameson, D. (1955) Some quantitative aspects of an opponent-colors theory. II. Brightness, saturation, and hue in normal and dichromatic vision. J. Opt. Soc. Am., 45, 602.

Hurvich, L.M., Jameson, D. (1957) An opponent-process theory of color vision. Psychol. Rev., 64, 384-404.

Hutchins, B., Weber, J.T. (1985) The pretectal complex of the monkey: a reinvestigation of the morphology and retinal terminations. J. Comp. Neurol., 232, 425-442.

Ikeda, H., Wright, M.J. (1972) Differential effects of refractive errors and receptive field organisation of central and peripheral ganglion cells. Vis. Res., 12, 1465-1476.

Ikeda, H., Wright, M.J. (1974) Is amblyopia due to inappropriate stimulation of the "sustained" pathway during development? Brit. J. Ophthalmol., 58, 165-175.

Ikeda, H., Wright, M.J. (1976) Properties of LGN cells in kittens reared with convergent squint: a neurophysiological demonstration of amblyopia. Exp. Brain Res., 25, 63-77.

Ikeda, H., Tremain, K.E. (1978) Amblyopia resulting from penalisation: neurophysiological studies of kittens reared with atropinisation of one or both eyes. Brit. J. Ophthalmol., 62, 21-28.

Ikeda, H., Tremain, K.E. (1979) Amblyopia occurs in retinal ganglion cells reared with convergent squint without alternating fixation. Exp. Brain Res., 35, 559-582.

- Ikeda, M., Boynton, R.M. (1965) Negative flashes, positive flashes, and flicker examined by increment threshold technique. J. Opt. Soc. Am., 55, 560-566.
- Ingling, C.R., Martinez-Uriegas, E. (1983) The relationship between spectral sensitivity and spatial sensitivity for the primate r-g x-channel. Vis. Res., 23, 1495-1500.
- Ives, H.E. (1912) The relation between the color of the illuminant and the color of the illuminated object. Trans. Illum. Eng. Soc., 7, 62-72.
- Jameson, D., Hurvich, L.M. (1989) Essay concerning colour constancy. Ann. Rev. Psychol., 40, 1-22.
- Jampel, R.S. (1959) Representation of the near response on the cerebral cortex of the macaque. Am. J. Ophthalmol., 48, 573-582.
- Judd, D.B. (1940) Hue, saturation and lightness of surface colours with chromatic illumination. J. Opt. Soc. Am., 30, 2-32.
- Judd, D.B. (1960) Appraisal of Land's work on two-primary color projections. J. Opt. Soc. Am., 50, 254-268.
- Judge, S.J., Cumming, B.G. (1983) Brainstem neurons related to accommodation and vergence. Abstract Soc. Neurosci.
- Kase, M., Nagata, R., Yoshida, A., Hanada, I. (1984) Pupillary light reflex in amblyopia. Invest. Ophthalmol. Vis. Sci., 25, 467-471.
- Katz, D. (1935) The World of Colour. MacLeod, R.B., Fox, C.W. (transl.), Kegan Paul, Trench, Trubner, London.
- Keenleyside, M.S. (1989) Pupillometry and assessment of visual function. D. Phil. thesis: University of Oxford.

- Keenleyside, M.S., Barbur J.L., Pinney, H.D. (1988) Stimulus-specific pupillary responses in normal and hemianopic subjects. Perception, 17, 347.
- King-Smith, P.E., Carden, D. (1976) Luminance and opponent-color contributions to visual detection and adaptation, and to temporal and spatial integration. J. Opt. Soc. Am., 66, 709-717.
- King-Smith, P.E., Chioran, G.M., Sellers, K.L., Alvarez, S.L. (1983) Normal and deficient colour discrimination analysed by colour television. In J.D. Mollon and L.T. Sharpe, Eds., Colour Vision: Physiology and Psychophysics, Academic, London.
- King-Smith, P.E., Vingrys, A.J., Benes, S.C. (1987) Visual thresholds measured with color video monitors. Color Res. Appl., 12, 73-80.
- Kirschmann, A. (1890) Uber die quantitativ Verhältnisse des simultanen Heligkeits- und Farben-Contrastes. Philos. Stud. (Wundt) 6, 417-491.
- Kohn, M., Clynes, M. (1969) Color dynamics of the pupil. Ann. N.Y. Acad. Sci., 15, 931-950.
- Kraats, J. van der, Smit, E.P., Slooter, J.A. (1977) Objective methods by the pupil balance method. Doc. Ophthalmol. Proc. Ser., 14, 213.
- Krastel, H., Alexandridis, E., Gertz, J. (1985) Pupil increment thresholds are influenced by color opponent mechanisms. Ophthalmologica, 191, 35-38.
- Kratz, K.E., Spear, D.C. (1976) Postcritical period reversal of effects of monocular deprivation on striate cortex cells in the cat. J. Neurophysiol., 39, 501-511.
- Krauskopf, J. (1986) Computational approaches to color vision: Introduction. J. Opt. Soc. Am. A, 3, 1648.

Krauskopf, J., Zaidi, Q., Mandler, M.B. (1986) Mechanisms of simultaneous color induction. J. Opt. Soc. Am. A, 3, 1752-1757.

Kries, J. von (1905) Die Gesichtsempfindungen. In Nagel's Handuch der Physiologie des Menschen. Vol. 3, 205-240. Vieweg, Braunschweig.

Krishnan, V.V., Shirachi, D., Stark, L. (1977) Dynamic measures of vergence accommodation. Am. J. Optom. Physiol. Opt., 54, 470-473.

Krüger, K. (1961) Pupillenstörungen und Amblyopie. Ber Dtsch. Ophthalmol. Ges., 63, 275-278.

Kuffler, S.W. (1953) Discharge patterns and functional organization of mammalian retina. J. Neurophysiol., 16, 37-68.

Kulikowski, J.J., Russell, M.H.A. (1987) Electroretinograms and visual evoked potentials elicited by chromatic and achromatic gratings. In J.J. Kulikowski, C.M. Dickinson, and I.J. Murray Eds., Seeing Contour and Colour. Oxford, Pergamon Press.

Land, E.H. (1959a) Color vision and the natural image. Part I. Proc. Natl. Acad. Sci. USA., 45, 116-129.

Land, E.H. (1959b) Color vision and the natural image. Part II. Proc. Natl. Acad. Sci. USA., 45, 636-644.

Land, E.H. (1962) Colour in the natural image. Proc. R. Inst. Gt. Brit., 39, 23-58.

Land, E.H. (1964) The Retinex. Am. Sci., 52, 247-264.

Land, E.H. (1974) The Retinex theory of colour vision. Proc. R. Inst. Gt. Brit., 47, 23-58.

- Land E.H. (1986a) An alternative technique for the computation of the designator in the retinex theory of color vision. Proc. Natl. Acad. Sci. USA., 83, 3078-3080.
- Land E.H. (1986b) Recent advances in Retinex theory. Vis. Res., 26, 7-21.
- Land, E.H., Hubel, D.H., Livingstone, M., Perry, S., Burns, M. (1983) Color-generating interactions across the corpus callosum. Nature, 303, 616-618.
- Land, E.H., McCann, J.J. (1971) Lightness and Retinex theory. J. Opt. Soc. Am., 61, 1-11.
- Latch, M., Lennie, P. (1977) Rod-cone interaction in light adaptation. J. Physiol., 269, 517-534.
- Laughlin, S.B. (1992) Retinal information capacity and the function of the pupil. Ophthal. Physiol. Opt., 12, 161-164.
- Lawwill, T. (1973) Lateral inhibition in amblyopia: VER and metacontrast. Docum. Ophthalmol. (Den Haag), 34, 243-258.
- Lawwill T., Meur, G., Howard, C.W. (1973) Lateral inhibition in the central visual field of an amblyopic subject. Am. J. Ophthalmol., 76, 225-228.
- Lee, B.B., Pokorny, J., Smith, V.C., Martin, P.R., Valberg A., (1990) Luminance and chromatic modulation sensitivity of macaque ganglion cells and human observers. J. Opt. Soc. Am. A, 7(12), 2223-2236.
- Lee, H. (1986) Method for computing the scene-illuminant chromaticity from specular highlights. J. Opt. Soc. Am. A, 3, 1694-1699.
- Lee, R.E., Cohen, G.H., Boynton, R.M. (1969) Latency variation in the human pupil contraction due to stimulus luminance and/or adaptation level. J. Opt. Soc. Am., 59(1), 97-103.

Leibowitz, H.W., Owens, D.A. (1975) Anomalous myopias and the dark focus of accommodation. Science, 189, 646-648.

Lennie, P. (1980) Parallel visual pathways: a review. Vis. Res., 20, 561-594.

Lennie, P. (1984) Recent developments in the physiology of color vision. Trends in Neurosci., 7, 243-248.

Lennie, P., Sclar, G., Krauskopf, J. (1985) Chromatic sensitivities in neurons of striate cortex of macaque. Invest. Ophthalmol. Vis. Sci. Suppl., 26, 8.

Lennie, P., D'Zmura, M. (1988) Mechanisms of color vision. Critical Reviews in Neurobiol., 3, 333-400.

Levatin, P. (1959) Pupillary escape in disease of the retina or optic nerve. Arch. Ophthalmol., 62, 768-779.

Levi, D.M. (1975) Patterned and unpatterned visual evoked responses in strabismic and anisometric amblyopia. Am. J. Optom. Physiol. Optics, 51, 371-381.

Levi, D.M., Klein, S. (1982a) Differences in vernier discrimination for gratings between strabismic and anisometric amblyopes. Invest. Ophthalmol. Vis. Sci. Suppl., 22, 88.

Levi, D.M., Klein, S. (1982b) Differences in vernier discrimination for gratings between strabismic and anisometric amblyopes. Invest. Ophthalmol. Vis. Sci. Suppl., 23, 398-407.

Livingstone, M.S., Hubel, D.H. (1982) Blobs and color vision. The 11th J.A.F. Stevenson Memorial Lecture. Can. J. Physiol., 61, 1433-1441.

Livingstone, M.S., Hubel, D.H. (1984) Anatomy and physiology of a color system in the primate visual cortex. J. Neurosci., 4, 309-356.

Livingstone, M.S., Hubel, D.H. (1987) Connections between layer 4B of area 17 and the thick cytochrome oxidase stripes of area 18 in the squirrel monkey. J. Neurosci., 7, 3371-3377.

Livingstone, M.S., Hubel, D.H. (1988) Segregation of form, color, movement, and depth: anatomy, physiology, and perception. Science, 240, 740-749.

Lovasik, J.V., Kergoat, H. (1988) Accommodative performance for chromatic displays. Ophthal. Physiol. Opt., 8, 443-449.

Lowenfeld, I., Newsome, D. (1971) Iris mechanics - 1. The influence of pupil size on dynamics of pupillary movements. Am. J. Ophthalmol., 71, 247-262.

Lowenstein, O., Loewenfeld, I.E. (1958) Electronic pupillography. A new instrument and some clinical applications. Arch Ophthalmol, 59, 352-363.

Lowenstein, O., Loewenfeld, I.E. (1959) Influence of retinal adaptation upon the pupillary reflex to light in normal man. Am. J. Ophthalmol., 48, pt. 2, 536-550.

Lowenstein, O., Loewenfeld, I.E. (1969) The pupil. In The Eye, Vol. 3, 2nd Ed. Ed. H. Davson. Academic Press. London.

MacAdam, D.L. (1942) Visual sensitivities to colour differences in daylight. J. Opt. Soc. Am., 32, 247-274.

MacLeod, D.I.A. (1986) Computer controlled color displays in vision research: possibilities and problems. Color Res. Appl. Supplement, 11, S45-S46.

Mallett, R.F.J. (1970) Anomalous retinal correspondence - the new outlook. Ophthal. Optician, 10, 606-624.

- Mallett, R.F.J. (1975) Using after-images in the investigation and treatment of strabismus. Ophthalm. Optician, 15, 727-729.
- Maloney, L.T., Wandell, B.A. (1986) Color constancy: a method for recovering surface spectral reflectance. J. Opt. Soc. Am. A, 3, 29-33.
- Markoff, J., Sturr, J.F. (1971) Spatial and luminance determinants of the increment threshold under monoptic and dichoptic viewing. J. Opt. Soc. Am., 61, 1530-1537.
- Marré M., Marré, E. (1979) Das Farbsehen bei Schielamblyopie. Albrecht v. Graefes Arch. Klin. Exp. Ophthalmol., 210, 121-133.
- Mathes, K. (1941) Ueber die Registrierung von Bewegungsvorgängen mit dem lichtelektrischen Reflexionsmesser. Klin. Wochenschr., 20, 295-297.
- McCann, J.J., Houston, K.L. (1983) Color sensation, color perception and mathematical models of color vision. In J.D. Mollon and L.T. Sharpe, Eds., Colour Vision: Physiology and Psychophysics, Academic, London.
- McCann, J.J., McKee, S.P., Taylor, T.H. (1976) Quantitative studies in Retinex theory. A comparison between theoretical predictions and observer responses to the "color Mondrian" experiments. Vis. Res., 16, 445-458.
- McLaren, K. (1986) Edwin H Land's contributions to colour science. J. Soc. Dyers and Colourists, 102, 378-383.
- Michael, C.R. (1985) Laminar segregation of color cells in the monkey's striate cortex. Vis. Res., 25, 415-423.
- Miller, S.D., Thompson, H.S. (1978) Pupil cycle time in optic neuritis. Am. J. Ophthalmol., 85, 635-642.

Missotten, L. (1974) Estimation of the ratio of cones to neurones in the fovea of the human retina. Invest. Ophthalmol. Vis. Sci., 13, 1045-1049.

Mollon, J.D. (1982) Color vision. Ann. Rev. Psychol., 33, 41-85.

Mollon, J.D., Reffin, J.E. (1989) A computer-controlled colour vision test that combines the principles of Chibret and Stilling. J. Physiol., 414, 5P.

de Monasterio, F.M. (1978) Properties of concentrically organised X and Y ganglion cells of macaque retina. J. Neurophysiol., 41, 1394-1417.

de Monasterio, F.M., Gouras, P. (1975) Functional properties of ganglion cells of the rhesus monkey retina. J. Physiol., 251, 167-195.

Mullen, K.T. (1985) The contrast sensitivity of human colour vision to red-green and blue-yellow chromatic gratings. J. Physiol., 359, 381-400.

Munsell Book of Color - Matte Finish Collection (1976).
Munsell Color, Baltimore, MD, USA.

Murch, G.M. (1982) Visual accommodation and convergence to multichromatic information dispalys. Intern. Symp. Digest. Tech. Papers, 13, 192-193.

Murray, I.J., Parry, N.R.A. (1987) Generating VEPs specific to parvo- and magno-pathways in humans. In J.J. Kulikowski, C.M. Dickinson, and I.J. Murray Eds., Seeing Contour and Colour. Oxford, Pergamon Press.

Murray, I.J., Parry, N.R.A., Carden, D., Kulikowski, J.J. (1987) Human visual evoked potentials to chromatic and achromatic gratings. Clin. Vis. Sci., 1(3), 231-244.

- Myers, G.A., Stark, L. (1990) Topology of the near response triad. Ophthalm. Physiol. Opt., 10, 175-181.
- Naka, K.I., Rushton, W.A.H. (1966) S-potentials from colour units in the retina of fish (Cyprinidae). J. Physiol., 185, 536-555.
- Nawratski, I., Auerbach, E., Rowe, H. (1966) Amblyopia ex anopsia. Amer. J. Ophthalmol., 61, 430-435.
- Newsome, D.A., Milton, R.C., Gass, J.D.M. (1981) Afferent pupillary defects in macular degeneration. Am. J. Ophthalmol., 92, 396-402.
- Newton, I., (1704) Opticks: Or, a Treatise of the Reflexions, Refractions, Inflexions and Colours of Light. 1st Ed., Smith and Walford, London.
- Noorden, G.K. von (1973) Histological studies of the visual system in monkeys with experimental amblyopia. Invest. Ophthalmol., 12, 727-738.
- Noorden, G.K. von, Burian, H.M. (1959a) Visual acuity in normal and amblyopic patients under reduced illumination I. Behaviour of visual acuity with and without neutral density filters. Arch Ophthalmol., 61, 533-535.
- Noorden, G.K. von, Burian, H.M. (1959b) Visual acuity in normal and amblyopic patients under reduced illumination II. The visual acuity at various levels of illumination. Arch Ophthalmol., 62, 396-399.
- Noorden, G.K. von, Crawford, M.L.J. (1977) Form deprivation without light deprivation produces the visual deprivation syndrome in *Macaca Mulatta*. Brain Res., 129, 37-44.
- Noorden, G.K. von, Crawford, M.L.J., Middleditch, P.R. (1976) The effects of monocular visual deprivation: disuse or binocular interaction? Brain Res., 111, 277-285.

Noorden, G.K. von, Middleditch, P.R. (1975) Histology of the monkey lateral geniculate nucleus after unilateral lid closure and experimental strabismus: further observations. Invest. Ophthalmol., 14, 674-683.

Normann, R.A., Perlman, I. (1979) The effects of background illumination on the photoresponses of red and green cones. J. Physiol., 286, 491-507.

Ohba, N., Alpern, M. (1972) Adaptation of the pupil light reflex. Vis. Res., 12, 953-967.

Oliver, M., Nawratski, I. (1971) Screening of pre-school children for ocular anomalies. Br. J. Ophthalmol., 55, 462-467.

østerberg, G. (1935) Topography of the layer of rods and cones in the human retina. Acta Ophthalmol. Suppl., 6, 1-102.

Owens, D.A. (1980) A comparison of accommodative responsiveness and contrast sensitivity for sinusoidal gratings. Vis. Res., 20, 159-167.

Padgham, C.A., Saunders, J.E. (1975) The Perception of Light and Colour. G. Bell & Sons Ltd., London.

Parker, D.M., Salzen, E.A. (1977) Latency changes in the human visual evoked response to sinusoidal gratings. Vis. Res., 17, 1201-1204.

Perry, V.H., Cowey, A. (1984) Retinal ganglion cells that project to the superior colliculus and pretectum in the macaque monkey. Neuroscience, 12, 4, 1125-1137.

Perry, V.H., Cowey, A. (1985) The ganglion cell and cone distributions in the monkey's retina: implications for central magnification factors. Vis. Res., 25, 1795-1810.

- Perry, V.H., Oehler, R., Cowey, A. (1984) Retinal ganglion cells that project to the dorsal lateral geniculate nucleus in the macaque monkey. Neurosci., 12, 1101-1123.
- Pickwell, L.D. (1980a) Adaptations to squint. The Optician, Mar 7, 11.
- Pickwell, L.D. (1980b) Abnormal retinal correspondence. The Optician, May 2, 10-11.
- Pickwell, L.D. (1984) Binocular Vision Anomalies. Butterworths, London.
- Pierson, R.J., Carpenter, M.B. (1974) Anatomical analysis of pupillary reflex pathways in the rhesus monkey. J. Comp. Neurol., 158, 121-143.
- Pinney, H.D., Barbur, J.L., Saunders, J.E. (1989) A method for quantifying changes in colour appearance. Perception, 18, 530.
- Pitt, F.G.H. (1935) Characteristics of dichromatic vision. Medical Research Council Report Ser. 200.
- Pitt, I.T., Winter, L.M. (1974) Effect of surround on perceived saturation. J. Opt. Soc. Am., 64, 1328-1331.
- Polyak, S.L. (1941) The Retina. Chicago. University of Chicago Press.
- Polyak, S.L. (1957) The Vertebrate Visual System. Chicago. University of Chicago Press.
- Pöppel, E. (1986) Long-range colour-generating interactions across the retina. Nature, 320, 523-525.
- Portnoy, J.Z., Thompson, H.S., Lennarson, L., Corbett, J.J. (1983) Pupillary defects in amblyopia. Am. J. Ophthalmol., 96, 609-614.

Post, D.L. and Calhoun, C.S. (1989) An evaluation of methods for producing desired colors on CRT monitors. Color Res. Appl., 14, 172-186.

Reeves, P. (1918) Rate of pupillary dilation and contraction. Psychol. Rev., 25, 330-340.

Reffin, J.P., Astell, S., Mollon, J.D. (1991) Trials of a computer-controlled colour vision test that preserves the advantages of pseudoisochromatic plates. In B. Drum, J.D. Moreland and A. Serra, Eds., Colour Vision Deficiencies X, 69-76.

Rodieck, R.W. (1983) Raster-based colour stimulators. In J.D. Mollon and L.T. Sharpe, Eds., Colour Vision: Physiology and Psychophysics, Academic, London.

Rubinstein, M. (1984) Visual acuity and the crowding phenomenon. Ophthalm. Optician, September 15, 641-642.

Saini, V.D., Cohen, G.H. (1979) Using color substitution pupil response to expose chromatic mechanisms. J. Opt. Soc. Am., 69, 1029-1035.

Sakata, Shibutani, H., Kawano, K. (1980) Spatial properties of visual fixation neurons in posterior association cortex of the monkey. J. Neurophysiol., 43, 1654-1672.

Scalia, F. (1972) The termination of retinal axons in the pretectal region of mammals. J. Comp. Neurol., 145, 223-245.

Schade, O.H. (1958) On the quality of colour-television images and the perception of colour detail. J. Soc. Motion Pict. Telev. Eng., 67, 801-819.

Schiller, P.H., Malpeli, J.G. (1977) Properties and tectal projections of monkey retinal ganglion cells. J. Neurophysiol., 40, 428-445.

Schnapf, J.L., Kraft, T.W., Baylor, D.A. (1987) Spectral sensitivity of human cone receptors. Nature, 325, 439.

Schouten, J.F., Ornstein, L.S. (1939) Measurements of direct and indirect adaptation by means of a binocular matching method. J. Opt. Soc. Am., 29, 168-182.

Schweitzer, N.M.J. (1956) Threshold measurements on the light reflex of the pupil in the dark adapted eye. Doc. Ophthalmol., 10, 1-78.

Sellars, K.L., Chioran, G.M., Dain, S.J., Benes, S.C., Lubow, M., Rammohan, K., King-Smith, P.E. (1986) Red-green mixture thresholds in congenital and acquired colour defects. Vis. Res., 26, 1083-1097.

Shapley, R., Perry, V.H. (1986) Cat and monkey retinal ganglion cells and their visual functional roles. Trends in Neuro Sci., 9, 229-235.

Sireteanu, R. (1987) Binocular luminance summation in humans with defective binocular vision. Invest. Ophthalmol. Vis. Sci., 28, 349-355.

Sireteanu, R., Altmann, L. (1987) Binocular luminance summation in young kittens and adult strabismic cats. Invest. Ophthalmol. Vis. Sci., 28, 343-348.

Slooter, J. (1985) The Pupil, mirror of visual acuity. Ph.D. monograph. Catholic University of Nijmegen.

Slooter, J., Norren, D. van (1980) Visual acuity measured with pupil responses to checkerboard stimuli. Invest. Ophthalmol. Vis. Sci., 19, 105-108.

Smith, S.A., Smith, S.E. (1980) Contraction anisocoria; nasal versus temporal illumination. Brit. J. Ophthalmol., 64, 933-934.

- Smith, S.A., Smith, S.E. (1983) Reduced pupillary light reflexes in diabetic autonomic neuropathy. Diabetologia, 24, 330-332.
- Smith, S.A., Ellis, C.J.K., Smith, S.E. (1979) Inequality of the direct and consensual light reflexes in normal subjects. Brit. J. Ophthalmol., 63, 523-527.
- Smith, V.C., Pokorny, J. (1975) Spectral sensitivity of the foveal cone pigments between 400 and 500 nm. Vis. Res., 15, 161-171.
- Sokol, S., Nadler, D. (1979) Simultaneous electroretinograms and visually evoked potentials from adult amblyopes in response to a pattern stimulus. Invest. Ophthalmol. Vis. Sci., 18, 848-855.
- Sperling, H.G., Harwerth, R.S. (1971) Red - green cone interactions in the increment - threshold spectral sensitivity of primates. Science, 172, 180-184.
- Stone, J., Fukuda, Y. (1974) Properties of cat retinal ganglion cells: A comparison of W-cells with X- and Y-cells. J. Neurophysiol., 37, 722-748.
- Stephenson, G. (1971) Mathematical methods for science students. 2nd Ed., Longman, 276-296.
- Stiles, W.S. (1978) Mechanisms of Colour Vision. London: Academic.
- Stilling, J. (1877) Die Prüfung des Farbensinnes beim Eisenbahn- und Marinepersonal. 2nd Ed., Theodor Fischer. Cassel.
- Thomas, J. (1978) Normal and amblyopic contrast sensitivity functions in central and peripheral retinas. Invest. Ophthalmol. Vis. Sci., 17, 746-753.

Thompson, H.S. (1966) Afferent pupillary defects. Pupillary findings associated with defects of the afferent arm of the pupillary light reflex arc. Am. J. Ophthalmol., 62, 860-873.

Thorell, L.G., De Valois, R.L., Albrecht, D.G. (1985) Spatial mapping of monkey V1 cells with pure color and luminance stimuli. Vis. Res., 24, 751-769.

Tiplitz Blackwell, K., Buchsbaum, G. (1988a) Quantitative studies of color constancy. J. Opt. Soc. Am. A, 5, 1772-1780.

Tiplitz Blackwell, K., Buchsbaum, G. (1988b) The effect of spatial and chromatic parameters on chromatic induction. Color Res. Appl., 13, 166-173.

Tolhurst, D.J. (1975) Reaction times in the detection of gratings by human observers; probabilistic mechanisms. Vis. Res., 15, 1143-1149.

Troscianko, T.S. (1977) Effect of subtense and surround luminance on the perception of a coloured field. Color Res. Appl., 2, 152-159.

Troscianko, T.S. (1982) Saturation as a function of test-field size and surround luminance. Color Res. Appl., 7, 89-94.

Ukai, K. (1985) Spatial pattern as a stimulus to the visual system. J. Opt. Soc. Am., 2, 1094-1100.

Valberg, A. (1971) A visual tristimulus projection colorimeter. Applied Optics, 10, 8-12.

Valberg, A. (1974) Color induction: dependence on luminance, purity, and dominant or complimentary wavelength of inducing stimuli. J. Opt. Soc. Am., 64, 1531-1540.

Valberg, A., Lange-Malecki, B. (1990) "Colour constancy" in Mondrian patterns: a partial cancellation of physical chromaticity shifts by simultaneous contrast. Vis. Res., 30, 371-380.

Valeton, J.M., van Norren, D. (1983) Light adaptation of primate cones: an analysis based on extracellular data. Vis. Res., 23, 1539-1547.

Vaney, D. (1985) Fireworks in the retina. Nature, 314, 672-673.

Vassilev, A., Mitov, D. (1976) Perception time and spatial frequency. Vis. Res., 16, 89-92.

Vingrys, A.J., King-Smith, P.E., (1986) Factors in using color video monitors for assessment of visual thresholds. Color Res. Appl., 11 (Suppl.), S57-62.

Vos, J.J., Walraven, P.L. (1971) On the derivation of the foveal receptor primaries. Vis. Res., 11, 799-818.

Wagner, G., Boynton, R.M. (1972) Comparison of four methods of heterochromatic photometry. J. Opt. Soc. Am., 62, 1508-1515.

Wald, G., Burian, H.M. (1944) The dissociation of form vision and light perception in strabismic amblyopia. Am. J. Ophthalmol., 27, 950-963.

Walraven, J. (1973) Spatial characteristics of chromatic induction; the segregation of lateral effects from straylight artefacts. Vis. Res., 13, 1739-1753.

Walraven, J., Benzschawel, T.L., Rogowitz, B.E. (1987) Color-constancy interpretation of chromatic induction. Die Farbe, 34, 269-273.

Ward, P.A. (1987a) The effect of spatial frequency on steady - state accommodation. Ophthal. Physiol. Opt., 7, 211-217.

- Ward, P.A. (1987b) The effect of stimulus contrast on the accommodation response. Ophthalm. Physiol. Opt., 7, 9-15.
- Ware, C., Cowan, W.B. (1982) Changes in perceived color due to chromatic interactions. Vis. Res., 22, 1353-1362.
- Webster, J.G., Cohen, G.H., Boynton, R.M. (1968) Optimising the use of the criterion response for the pupil light reflex. J. Opt. Soc. Am., 58, 419-424.
- Webster, M.A., De Valois, K.K., Switkes, E. (1990) Orientation and spatial-frequency discrimination for luminance and chromatic gratings. J. Opt. Soc. Am. A, 7(6), 1034-1049.
- Weisstein, N. (1972) Metacontrast. In Handbook of Sensory Physiology. VII/4. Eds. D. Jameson and L.M. Hurvich. Springer-Verlag, Berlin.
- Weller, R.E., Kaas, J.H., Wetzell, A.B. (1979) Evidence for the loss of x-cells of the retina after long-term ablation of visual cortex in monkeys. Brain Res., 160, 134-138.
- Werblin, F.S., Dowling, J.E. (1969) Organisation of the retina of the mudpuppy, *Necturus maculosus*. II. Intracellular recording. J. Neurophysiol., 32, 339-355.
- Werner, J.S., Walraven, J. (1982) Effect of chromatic adaptation on the achromatic locus: the role of contrast, luminance and background colour. Vis. Res., 22, 929-943.
- West, G., Brill, M.H. (1982) Necessary and sufficient conditions for von Kries chromatic adaptation to give color constancy. J. Math. Biol., 15, 249-258.
- Westheimer, G. (1965) Spatial interaction in the human retina during scotopic vision. J. Physiol., 181, 881-894.

Westheimer, G. (1966) The Maxwellian view. Vis. Res., 6, 669-682.

Westheimer, G. (1967) Spatial interaction in human cone vision. J. Physiol., 190, 139-154.

Westheimer, G. (1970) Rod-cone independence for sensitizing interaction in the human retina. J. Physiol., 206, 109-116.

Westheimer, G., Blair, S.M. (1973) The parasympathetic pathways to internal eye muscles. Invest. Ophthalmol., 12, 193-197.

Wild, H.M., Butler, S.R., Carden, D., Kulikowski, J.J. (1985) Primate cortical area V4 important for colour constancy but not wavelength discrimination. Nature, 313, 133-135.

Whitten, D.N., Brown, K.T. (1973) Photopic suppression of monkey's receptor potential, apparently by a cone-initiated lateral inhibition. Vis. Res., 13, 1629-1658.

Wolff, E. (1976) Anatomy of the Eye and Orbit. 7th. Ed., Lewis, London.

Wood, I.C.J., Tomlinson, A. (1975) The accommodative response in amblyopia. Am. J. Optom. Pysiol. Opt., 52, 243-247.

Woodhouse, J.M. (1975) The effect of pupil size on grating detection at various contrast levels. Vis. Res., 15, 645-648.

Woodhouse, J.M., Campbell, F.W. (1975) The role of the pupil light reflex in aiding adaptation to the dark. Vis. Res., 15, 649-653.

Worthey, J.A. (1982) Opponent-colors approach to color rendering. J. Opt. Soc. Am., 72, 74-82.

Worthey, J.A. (1985) Limitations of color constancy. J. Opt. Soc. Am. A, 2, 1014-1026.

Worthey, J.A., Brill, M.H. (1986) Heuristic analysis of von Kries color constancy. J. Opt. Soc. Am. A, 3, 1708-1712.

Wright, W.D. (1952) The characteristics of tritanopia. J. Opt. Soc. Am., 42, 509-520.

Wyatt, H.J., Musselman, J.F. (1981) Pupillary light reflex in humans; evidence for an unbalanced pathway from nasal retina, and for signal cancellation in brain stem. Vis. Res., 21, 513-525.

Wyszecki, G. and Stiles, W.S. (1982) Colour Science. 2nd.ed., Wiley, New York.

Yinon, U., Jakobowitz, L., Auerbach, E. (1974) The visual evoked response to stationary checkerboard patterns in children with strabismic amblyopia. Invest. Ophthalmol., 13, 293-301.

Young R.S.L., Alpern M. (1980) Pupil responses to foveal exchange of monochromatic lights. J. Opt. Soc. Am., 70, 697-706

Young, R.S.L., Clavdetscher J.E., Teller D.Y. (1987) Screening of red-green color-deficient observers using the chromatic pupillary response. Clin. Vision Sci., 2, 117-122.

Young, T. (1802) On the theory of light and colours. Phil. Trans. R. Soc., 92, 12-48.

Zeki, S. (1977) Colour coding in the superior temporal sulcus of rhesus monkey visual cortex. Proc. R. Soc. Lond. B, 197, 195-223.

Zeki, S. (1980) The representation of colours in the cerebral cortex. Nature, 284, 412-418.

Zeki, S. (1983a) The distribution of wavelength and orientation selective cells in different areas of monkey visual cortex. Proc. R. Soc. Lond. B, 217, 449-470.

Zeki, S. (1983b) Colour coding in the cerebral cortex: the reaction of cells in monkey visual cortex to wavelengths and colours. Neurosci., 9, 741-765.

Zeki, S., Shipp, S. (1988) The functional logic of cortical connections. Nature, 335, 311-317.

Zihl, J. (1980) Blindsight: Improvement of visually guided eye-movements by systematic practice in patients with cerebral blindness. Neuropsychologia, 18, 71-77.

Zrenner, E. (1983) Neurophysiological aspects of colour vision mechanisms in the primate retina. In J.D. Mollon and L.T. Sharpe, Eds., Colour Vision: Physiology and Psychophysics, Academic, London.